The effects of the histone deacetylase inhibitor, LBH589, on breast cancer in bone and on physiological bone remodelling

Michelle Lee

A thesis submitted for the degree of Doctor of Philosophy of the University of Adelaide

May 2012

School of Medicine
Disciplines of Surgery and Orthopaedics
The University of Adelaide

Declaration

This work contains no material which has been accepted for the award of any other degree or diploma in any university or other tertiary institution to Michelle Lee and, to the best of my knowledge and belief, contains no material previously published or written by another person, except where due reference has been made in the text.

I give consent to this copy of my thesis, when deposited in the University Library, being made available for loan and photocopying, subject to the provisions of the Copyright Act 1968.

I also give permission for the digital version of my thesis to be made available on the web, via the University's digital research repository, the Library catalogue, the Australasian Digital Theses Program (ADTP) and also through web search engines, unless permission has been granted by the University to restrict access for a period of time.

Michelle Lee
School of Medicine
Disciplines of Surgery and Orthopaedics
The University of Adelaide

Acknowledgements

First and foremost, I would like to acknowledge my principal supervisor, Professor Andreas Evdokiou. His guidance and enthusiasm has encouraged the growth of strong professional foundations within me to persevere towards my career goals. I have been fortunate to have a supervisor who encourages individuality and personal growth during my candidature. His constant support during the past few years has been sincerely appreciated, and has shown me that a high standard of work ethic is required for this line of work.

To my co-supervisor, Professor David Findlay, your enthusiasm towards my research has been undeniable and I thank you for your critical eye for detail, especially during the thesis editing process. To the other members and fellow students of the Breast Cancer Research Unit and Bone Cell Biology Group, thank you for your advice, technical help, unrelenting support, laughter and your friendship. You have been paramount in developing my strength, motivation and determination throughout my PhD. I would like to extend a special thank you to my professional editor, Ted McMurchie from PhDex. Your eye for detail and constant encouragement has made the thesis editing process more enjoyable! I would also like to acknowledge the team from the *Endeavour Awards.* Receiving a Prime Minister's Australia Asia Endeavour Award was the highlight of my candidature. Not only was this award generous, but they were crucial in providing professional growth. Thank you for their constant personal and professional support whilst on Award, and their enormous networking opportunities for professional development are never-ending.

Some of the work in this thesis was made possible through the help of others. The teams from Adelaide Microscopy and the IMVS animal house have been fundamental

in the success of some of my experiments. I have the utmost respect for the work they do, and are grateful to them for sharing their time, expert technical advice and knowledge.

Finally, to my great friends and family. Your kindness, companionship, and entertainment have been undeniably cruicial to my achievements. Thank you for all your understanding, love and patience throughout my PhD.

Awards and publications arising from candidature

Awards

2011   **South Australian Young Woman of the Year Award Recipient**
South Australian Reunion Group of the Women of the Year Association

2010   **Prime Minister's Australia Asia Endeavour Award Recipient**
Department of Education, Employment and Workplace Relations, Australian Government

2009   **Millennium Sciences, 'Best Oral Presentation'**
Millennium Sciences, Adelaide, Australia

2009   **Faculty of Health Sciences Postgraduate Expo, 'Best Poster Presentation'**
University of Adelaide, Australia

Published abstracts from presentations to professional societies

M. Lee, G. Yue, E. Ko, V. Ponomarev, A. Evdokiou, P.C. Leung and C. Lau. *In vivo* investigation on the value of Chinese herbs in the management of bone metastasis. 2010 International Conference on Integrative Medicine Against Cancer cum The 6th Pong Ding Yuen International Symposium on Traditional Chinese Medicine, Nov. 26-28 2010, Hong Kong, SAR, China.

Lee M, Labrinidis A, Liapis V, Hay S, Zinonos I, Butler L, Findlay D, Evdokiou A. LBH589 inihibits osteoclastogenesis, enhances osteoblast activity and protects against breast cancer – induced bone destruction. Abstract #4556. AACR 100th Annual Meeting, April 2009, Denver, CO., U.S.A.

Lee M, Labrinidis A, Liapis V, Hay S, Zinonos I, Butler L, Findlay D, Evdokiou A. The histone deacetylase inhibitor, LBH589 blocks *in vitro* osteoclastogenesis and

reduces tumour burden *in vivo.* ANZORS 14th Annual Scientific Meeting, November 2008, Brisbane, Australia.

Lee M, Labrinidis A, Liapis V, Hay S, Vincent T, Atkins G, Butler L, Findlay D, Evdokiou A. The histone deacetylase inhibitor, LBH589 blocks osteoclastogenesis, promotes osteoblast maturation and reduces tumour burden *in vivo.* ASMR SA Meeting, June 2008, Adelaide, Australia.

Lee M, Labrinidis A, Liapis V, Hay S, Vincent T, Atkins G, Butler L, Findlay D, Evdokiou. The histone deacetylase inhibitor, LBH589 blocks osteoclastogenesis, promotes osteoblast maturation. 5th Clare Valley Bone Meeting, March 2008, Clare Valley, SA., Australia.

Publications in peer-reviewd journals

Lee M, Labrinidis A, Liapis V, Hay S, Zinonos I, Ponomarev V, Findlay DM, Evdokiou A. LBH589 inhibits osteoclastogenesis, enhances osteoblast maturation and protects against breast cancer-induced bone destruction. *Manuscript in preparation.*

Irene Zinonos, Agatha Labrinidis, **Michelle Lee**, Vasilios Liapis, Shelley Hay, Vladimir Ponomarev, Peter Diamond, David M Findlay, Andrew C.W. Zannettino and Andreas Evdokiou. Anticancer efficacy of Apo2L/TRAIL is retained in the presence of high and biologically active concentrations of osteoprotegerin *in vivo. J. Bone Mineral Res.,* 2010, 26 (3): 630-43.

Zinonos I, Labrinidis A, **Lee M**, Liapis V, Hay S, Ponomarev V, Diamond P, Zannettino ACW, Findlay DM, Evdokiou A. APOMAB, A Fully Human Agonistic DR5 Monoclonal Antibody, Exibits Potent Tumour Suppressive Activity in Murine Models of Primary and Metastatic Breast Cancer. *Molecular Drug Therapeutics,* 2009, 8 (10): 2969-80.

Abbreviations

μ-CT	micro-computed tomography
ALP	alkaline phosphatase
AR	androgen receptor
BFR	bone formation rate
BLI	bioluminescence
BV	bone volume
CTCL	cutaneous T-cell lymphoma
Dkk	dickkopf
FAT	factor acetyltransferases
GCT	giant cell tumour
HAT	histone acetyltransferases
HDAC	histone deacetylase
HDI	histone deacetylase inhibitor
MAR	mineral apposition rate
MM	multiple myeloma
MS	mineralising surface
NHB	normal human bone
OCN	osteocalcin
OPG	osteoprotegerin
PBMC	peripheral blood mononuclear cells
RANKL	receptor activator of nuclear factor-κB ligand
SEM	scanning electron microscope
SRE	skeletal related event
Tb.Th	trabecular thickness
Tb.N	trabecular number
Tb.Sp	trabecular separation
TRAP	tartrate-resistant alkaline phosphatase

List of figures

List of Tables

Abstract

Histone Deacetylase Inhibitors (HDIs) are emerging as an exciting new class of potential anticancer agents for the treatment of solid and haematological malignancies. Despite the infancy of the field, there is now an impressive body of data describing the ability of these molecules to modulate a wide variety of cellular functions, including cell differentiation, cell cycle progression, apoptosis, cytoskeletal modifications, and angiogenesis. Over the past few years, results obtained from clinical trials and pre-clinical animal experiments demonstrate the ability of HDIs to selectively kill cancer cells with limited or no toxicity to normal tissues and organs. Amongst the HDIs now in clinical trials, SAHA (Vorinostat) is the first of its class to get approval from the U.S.A. Food and Drug Administration (FDA) for the treatment of cutaneous manifestations in patients with cutaneous T-cell lymphoma (CTCL). Although a number of early-phase clinical trials using different HDIs have demonstrated promising antitumour responses for a variety of cancer types, the effect of HDIs on skeletal malignancies, or the consequence of HDI treatment on the bone microenvironment, and in the context of osteoclast and osteoblast function, has not been reported. The studies undertaken in this thesis aimed to:

1). Investigate the anticancer efficacy of the HDI LBH589 in animal models of primary breast cancer, and on bone destruction caused by breast cancer growth in bone.

2). Investigate the effects by which LBH589 regulates normal bone metabolism in the context of osteoclast and osteoblast function both *in vitro* and *in vivo*.

In vitro, LBH589 treatment resulted in a dose and time-dependent increase in apoptosis in a panel of well established breast cancer cell lines. This was associated with the processing and activation of caspases-8, and -3, concomitant with the

activation of the Bcl_2 family protein, Bid and cleavage of the apoptosis target protein, PARP. LBH589 treatment leads to a marked increase in acetylated histone-H3 and induction of the p21 protein.

The highly aggressive MDA-MB231-TXSA human breast cancer cell line was used to evaluate the antitumour activity of LBH589 in murine models of breast cancer development and progression at both the orthotopic site and in bone. MDA-MB231-TXSA cells form aggressive, rapidly growing tumours when injected into the orthotopic site of the mammary fat pad of nude mice, and stimulate the formation of osteolytic lesions when injected into the tibial marrow cavity of nude mice. MDA-MB231-TXSA breast cancer cells were tagged with a triple reporter gene construct, which allows real-time monitoring of tumour growth in live animals. Tumour progression with and without LBH589 treatment was monitored in live animals, and in real-time using bioluminescence imaging (BLI). The development of breast cancer-induced osteolysis was measured using high resolution µ-CT and histology.

In vivo, LBH589 had no effect on tumour growth in the mammary fat pad or in bone, as demonstrated by BLI and histology. However, high resolution µ-CT analyses of the tibiae demonstrated significant protection from breast cancer-induced osteolysis with LBH589 treatment, associated with a marked reduction in the number of $TRAP^{+}$ osteoclasts lining the trabecular bone surface. Furthermore, the bone volume of the contralateral, non-tumour bearing tibiae was significantly increased with LBH589 treatment compared to the vehicle-treated group of animals. This effect was also seen in the tibiae of mice bearing mammary tumours, suggesting potential anabolic actions of LBH589.

The effect of LBH589 on osteoclast differentiation and bone resorption was then evaluated using three independent *in vitro* models of osteoclastogenesis. When human peripheral blood mononuclear cells and the RAW264.7 murine monocytic cells were cultured with the receptor activator of nuclear factor kappa B-ligand (RANKL), both formation of TRAP$^+$, multinucleated cells and bone resorption were increased compared with control cells that were cultured in the absence of RANKL. When added in combination with RANKL, LBH589 dose-dependently inhibited RANKL-induced osteoclastic differentiation and bone resorption. Similarly, bone resorption by mature osteoclasts that were isolated from human Giant Cell Tumours of bone was also inhibited by LBH589 treatment. The effect of LBH589 was selective for osteoclast differentiation and bone resorption since cell viability was not affected. The effect of LBH589 on osteoblast function was also investigated by using mineralised bone forming primary human osteoblast cultures. When osteoblasts harvested from normal human bone donors were cultured under osteogenic conditions, LBH589 significantly enhanced the ability for these cells to produce mineral. The enhanced mineralisation was associated with significant increases in Runx2, OPG and RANKL mRNA expression. The effects of LBH589 treatment on normal bone metabolism were further investigated in animals with an intact immune system and in the absence of tumours. In these experiments, the rate of new bone formation and bone remodelling *in vivo* was investigated using the fluorescent calcium-binding dye, calcein. Longitudinal live µ-CT analysis of the tibiae in these animals showed an increase in bone volume with LBH589 treatment. The increase in bone volume was attributed to an inhibition of the number of TRAP$^+$ osteoclasts lining the trabecular bone surface, and also, to an increase in the activity of osteoblastic cells. The observed increase in bone formation rate (BFR) was

attributable to an enhanced mineral apposition rate (MAR), suggesting that the effect of LBH589 was most likely appositional, with little evidence for new bone formation.

The data presented in this thesis demonstrate a lack of anticancer efficacy of LBH589 against breast cancer growth in the mammary tissue and in bone. However, the ability of LBH589 to modulate bone metabolism by regulating osteoclast and osteoblast function indicate new and previously unrecognised osteotropic properties of LBH589. Taken together, these results suggest that LBH589 can inhibit the activities of osteoclasts, whilst promoting osteoblast activity, with limited toxic side effects, therefore potentially providing a new avenue for the treatment of skeletal conditions in which bone loss is significant.

Table of contents

Chapter 1. Literature review

1.1   Introduction

The skeleton is the organ system most commonly affected by metastatic cancer, with breast cancer frequently establishing as metastatic lesions in bone (Liao and McCauley, 2006). Breast cancer is the most common cancer among women, and causes the greatest morbidity and mortality. Around 30% of patients with early disease will relapse with distant metastases, and a number of treatment modalities exist, with most patients needing surgery and radiation (Drabsch and Ten Dijke, 2011, Gonzalez-Suarez, 2011, Iwata, 2011, WHO). This reflects both the high incidence as well as the relatively long clinical course of these tumours. The variation between patterns of metastasis is influenced by cellular and molecular characteristics of both the tumour cells, and of the tissues to which they spread (Coleman, 2001). The capillary structures and blood flow are important in the establishment of bone metastases, and physical properties within the bone marrow compartment promote the establishment of secondary cancers (Coleman, 1997). In support of this notion, an elegant cadaver experiment demonstrated that venous blood flow from the pelvis and breast flowed into the vertebral-venous system of blood vessels extending from pelvic structures throughout the epidural and perivertebral veins and into the thoraco-abdominal wall, head and neck. Therefore, this pathway offers a low-pressure system for blood flow to be continually subjected to arrest and reversal of direction of flow, as intrathoracic and abdominal pressures change during normal physiological processes (Batson, 1942).

Cancer has classically been viewed as a disease of genetic defects, including gene mutation or chromosomal abnormalities that result in the loss of tumour suppressor genes and/or activation of oncogenes (Bolden *et al*., 2006). However, there is increasing evidence that gene expression governed by external or epigenetic changes is also a factor in the development, progression and metastatic spread of cancer, mediated

by DNA methylation and histone modifications (Baylin and Ohm, 2006, Lund and van Lohuizen, 2004). In recent years, there has been a heightened level of understanding of epigenetics and cancer, which has lead to the development of anticancer therapeutics that target the post-translational modification of the genome in a variety of solid and haematological malignancies (Liu *et al.*, 2006). This review aims to develop an understanding of the actions of opposing enzymes; histone acetyltransferases (HATs), and histone deacetylases (HDACs). Their respective influences on chromatin structure and gene expression, as well as an overview of their role in the development of cancers, will be discussed. Specifically, this chapter will focus on the approach in targeting the HDAC enzymes, using Histone Deacetylase Inhibitors (HDIs) in the treatment of cancer-induced bone disease.

1.2   Normal bone metabolism and metastatic bone disease

Maintenance of bone integrity depends on constant remodelling by a dynamic balance between bone resorption by osteoclasts and bone formation by osteoblasts (Mundy, 1987). As these processes are coupled, there is a quantitative relationship between the amount of bone lost and formed, which in healthy maturity maintains a skeletal balance close to zero. A number of mediators have been identified, which contribute to this renewal process by creating several signalling pathways that include endocrine, autocrine and paracrine factors (Salari Sharif *et al.*, 2010). The central inflammatory cytokine in bone remodelling is the receptor activator of nuclear factor-κB ligand (RANKL), which is expressed on the surface of osteoblasts and osteocytes. Binding of RANKL to its cognate receptor, RANK, on myeloid osteoclast precursors, promotes osteoclast differentiation and bone resorbing activity (Atkins *et al.*, 2003,

Manolagas and Jilka, 1995, Sankar *et al*., 2004, Boyce and Xing, 2008, Jakob *et al*., 2008). When cancer cells invade and establish growth within the bone microenvironment, the normal process of bone turnover is interrupted, which may lead to the uncoupling of the dynamic balance between osteoclast and osteoblast function. This imbalance can weaken and destroy the bone architecture, hence decreasing the resistance of the skeleton to compressive and bending forces (Kanis *et al*., 1991). Therefore, the most common complications of skeletal malignancies are fractures, spinal cord compression, bone pain and hypercalcaemia, all of which severely reduce the patients quality of life (Araujo and Logothetis, 2008).

When tumour cells invade the bone microenvironment, interactions occur between the cancer and the bone cells that have been described as a 'vicious cycle' of cancer-induced bone destruction. Osteolysis is a common feature of many types of bone cancers, and is predominantly the result of a net increase in osteoclastic activity. However, different forms of bone lesions tend to predominate in certain types of advanced cancer, and these vary depending on the nature of the primary cancer. For example, multiple myeloma is associated with purely osteolytic lesions, whereas bone lesions in prostate cancer patients are predominantly osteoblastic, due to the heightened activity of osteoblasts. These lesions tend to produce a non-uniform growth of extra bone surrounding the existing bone structure. However, bone lesions in primary osteosarcoma or breast cancer, patients can show osteolytic, osteosclerotic or mixed lesions. Multiple forms of bone lesions may even be present in the same patient with varying radiological appearance (Coleman and Rubens, 1987, Dorfman and Czerniak, 1995). Figure 1-1 represents radiographic bone lesions associated with different cancer types often seen in the clinical setting. Tumour cells associated with osteolytic lesions secrete various factors including tumour necrosis factor (TNF), parathyroid hormone

related protein (PTHrP), RANKL, IL-8 and IL-1, all of which can enhance resorption while suppressing bone formation (Mundy, 1991). This in turn causes the release of factors such as transforming growth factor-β (TGF-β) from the bone matrix, that further stimulate tumour growth by additional PTHrP production (Coleman, 2001, Kiriyama *et al*., 1993), (as depicted in figure 1-2). It is recognised that enhanced expression of PTHrP is frequently identified in tumours with bone metastasis and associated bone lesions (Liao and McCauley, 2006, Martin, 2002). It has been hypothesised that PTHrP can facilitate bone metastasis by enhancing the metastatic potential of malignant cells through both autocrine and paracrine mechanisms (Bryden *et al*., 2002, Downey *et al*., 1997). Patients with tumours demonstrating purely osteolytic lesions are more prone to pathological fractures than those with lesions having a sclerotic phenotype (Mercadante, 1997). The resulting sclerotic lesions are less prone to fractures, probably because factors such as TGF-β, bone morphogenic protein (BMP) and fibroblast growth factor (FGF) secreted by the tumour cells, stimulate new bone formation (Koutsilieris *et al*., 1987). A comparative study of patients with bone metastases arising from primary prostate or breast cancers showed that osteoblastic lesions are associated with significantly higher levels of both bone resorption and bone formation markers than those observed in patients with osteolytic or mixed lesions (Demers *et al*., 2003). Furthermore, many studies have shown that osteoblastic lesions are normally associated with a strong osteolytic component and that osteogenesis must be preceded by local osteolysis, resulting in decreased bone integrity at the site of tumour growth (Berruti *et al*., 2000).
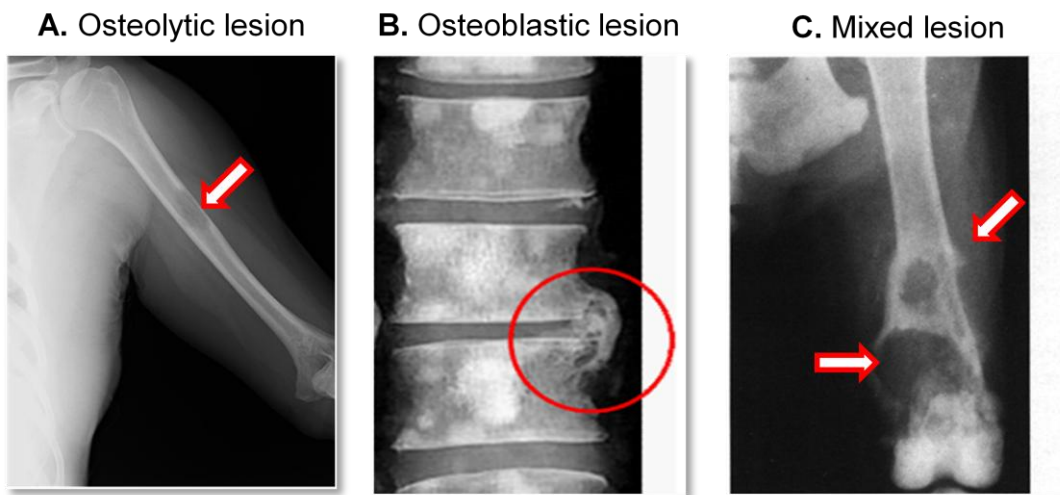
Figure 1-1. Radiographic representation of morphological features of cancer-induced bone destruction.

A). Osteolytic lesions, **B**). Osteoblastic lesions and **C**). Mixed lesions.
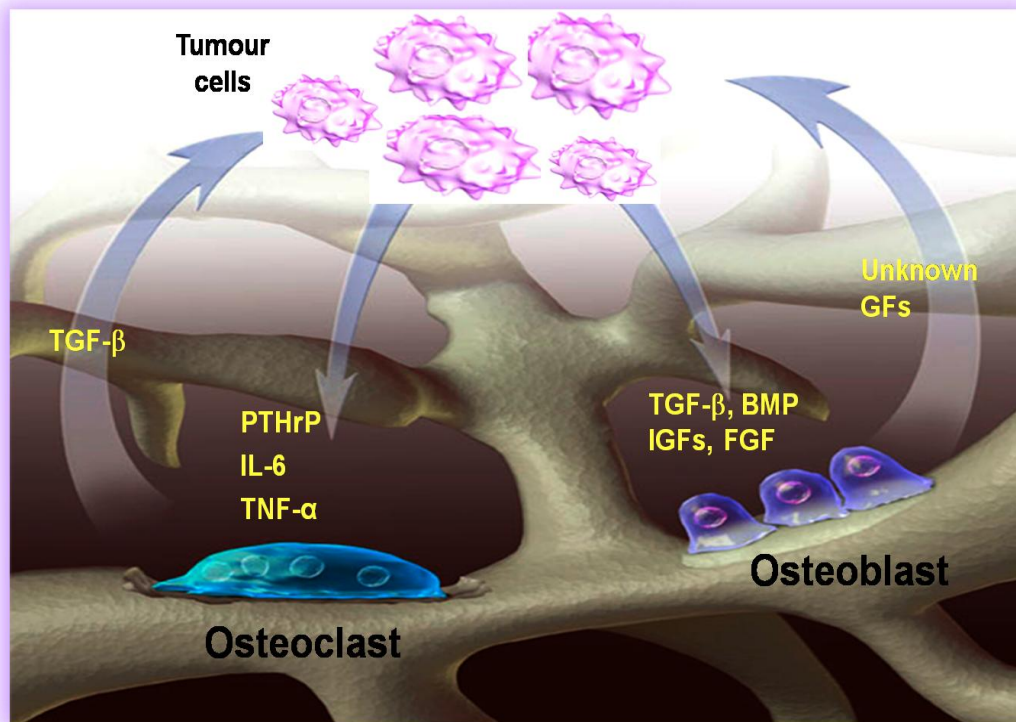
Figure 1-2. The 'vicious cycle' of cancer-induced bone destruction.

Osteolytic bone lesions: Tumour cells from breast cancer can secret factors (PTHrP, IL-6, TNF-α), which stimulate osteoclasts and pre-osteoclasts to develop and mature, to increase its resorptive activity. This in-turn causes a release of growth factors, such as TGF-β, into the bone matrix, which further stimulates tumour growth.

Osteoblastic bone lesions: Similar to osteolytic bone lesions, tumour cells from prostate cancer can secret factors (TGF-β, BMP, IGFs, FGF), which stimulate the osteoblasts to increase its osteogenic activity. This in-turn causes a release of growth factors (currently unknown) into the bone matrix to further stimulate tumour growth. In both instances, a heightened activity of bone cells further increases the tumour load within the bone, contributing to the 'vicious cycle' of cancer-induced bone destruction.

1.3 General introduction to bisphosphonates, clinical applications and their limitations

Conventional approaches to treating patients with skeletal metastases include chemotherapy or biological therapies, which may be given together with additional supportive or palliative therapies. Severe bone pain is normally treated with radiotherapy, which can also stabilise bone lesions and may prevent further or impending fractures. Orthopaedic surgery is used to treat existing fractures or to reduce the risk of further fractures and/or spinal cord compression (Coleman, 2004b). In addition to these palliative interventions, bisphosphonate therapy has emerged in recent years as a highly effective therapeutic option for the prevention of skeletal complications associated with metastatic bone disease, and has been the standard of care worldwide. Clinical trials have investigated the effects of several bisphosphonates on typical end point analyses, termed skeletal-related events (SRE) or bone events. These include pathological fractures, spinal cord compression, hypercalcaemia of malignancy, or the requirement for radiation or surgery to bone (Coleman, 2004b). Bisphosphonate therapy has been shown to significantly reduce the incidence of these events in patients with bone metastases arising from several solid and haematological tumours including breast, prostate, multiple myeloma and in lung cancers (Saad, 2002, Body *et al.*, 1998).

The evolution of bisphosphonates began in the 19th century when they were termed diphosphonates. These compounds were used in the textile, fertilizer and oil industries because of their property of inhibiting calcium carbonate precipitation (Fleisch, 2002). This property eventually prompted investigations into the biological characteristics of bisphosphonates, with the first being reported in 1968 (Fleisch *et al.*, 1968). Bisphosphonates are synthetic analogues of inorganic pyrophosphates (PPi),

characterised by two phosphonate groups linked by two non-hydrolysable phosphoether bonds to a central carbon atom (P-C-P). This structure enables bisphosphonates to bind strongly to divalent metal ions, such as calcium (Ca^{2+}) (Rogers, 2003). Therefore, this molecular P-C-P backbone structure allows a number of structural variations, and small changes in the structure can lead to extensive alterations of the physicochemical, biological, therapeutic and toxicological characteristics of this class of therapeutics (Fleisch, 2002). Currently, eight bisphosphonates are commercially available for the treatment of osteolytic bone disease and these are summarised in figure 1-3.
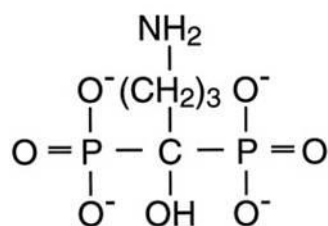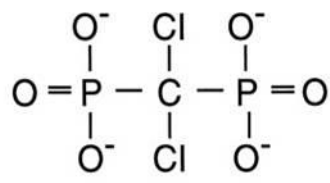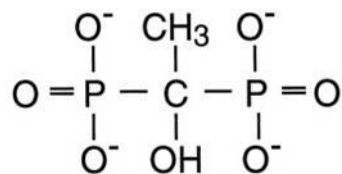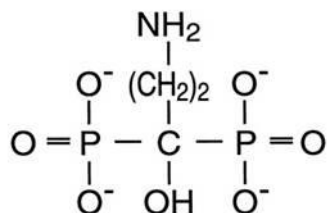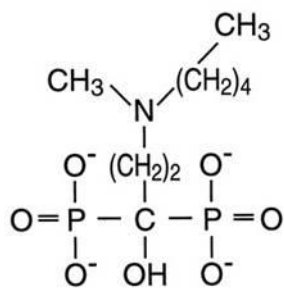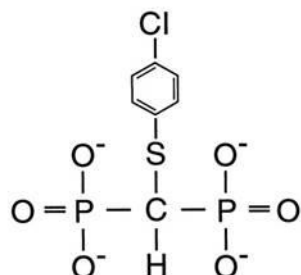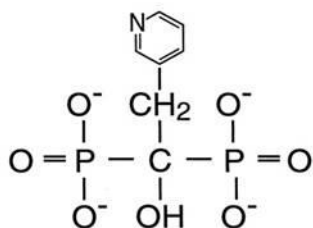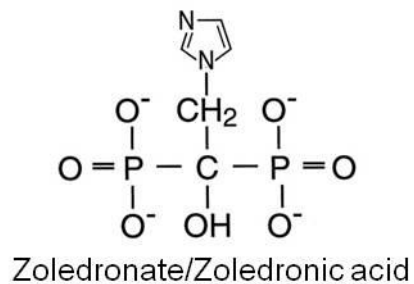
Figure 1-3. Structures of the eight current bisphosphonates used for the treatment of human bone cancers.

Bisphosphonates can be separated into two groups according to their molecular modes of action. Bisphosphonates that bear a close resemblance to PPi, such as clodronate and etidronate, are metabolised intracellularly into analogues of adenosine triphosphate (ATP). These metabolites or analogues accumulate in the cytoplasm of osteoclasts during active resorption and induce death of the osteoclasts through a series of events that inhibit ATP-utilising enzymes. This eventually permeates the mitochondrial membrane, and therefore releases cytochrome c, inducing apoptosis (Coxon *et al*., 2006, Lehenkari *et al*., 2002, Rogers, 2003). Alternatively, nitrogen-containing bisphosphonates inhibit resorption by disrupting the localisation and function of small GTPases (eg. Ras, Rho and Rab families), that are essential for osteoclast function, including cytoskeletal arrangement, membrane integrity, trafficking of intracellular vesicles and cell survival (Rogers, 2003, Coxon and Rogers, 2003). These types of bisphosphonates are characterised by a nitrogen moiety either in an alkyl chain (aledronate and ibandronate) or within a heterocyclic structure (risedronate and zoledronic acid) (refer to figure 1-3). Nitrogen-containing bisphosphonates act by inhibiting an enzyme of the mevalonate pathway (farnesyl diphosphate [FDP] synthase), thereby depriving cells of the key lipid proteins (FDP and GGPP), which are required for the post-translational prenylation of small GTPases, involved in osteoclast activity and survival (Dunford *et al*., 2001, van Beek *et al*., 1999, Coxon *et al*., 2006).

The use of bisphosphonates or bone modifying agents in metastatic breast cancer therapy have not changed since the 2003 guidelines, with regard to dose, dose interval, or duration of therapy (Hillner *et al*., 2003, Van Poznak *et al*., 2011). Several bisphosphonates have been approved in the U.S.A. and Europe for the treatment of breast cancer patients with bone metastases. These include, oral clodronate, administered as a daily dose of 1600 mg (approved in Europe), and the more potent

nitrogen-containing bisphosphonates that are administered via i.v. infusions. For example; pamidronate is given at a dose of 90 mg over 2 hours, every 3-4 weeks for 2 years; ibandronate is given at a dose of 6 mg, infused for an hour every 3-4 weeks for 2 years; whereas zoledronic acid is infused for 15 minutes at a dose of 4 mg, every 4 weeks for 1 year (Coleman, 2004b). Only i.v. pamidronate and zoledronic acid have been approved by the Food and Drug Administration (FDA), in the U.S.A., and are recommended for the treatment of breast cancer patients with bone metastasis by the American Society of Clinical Oncology (ASCO) (Van Poznak et al., 2011). Extensive placebo-controlled trials assessing the safety and efficacy of pamidronate and zoledronic acid have shown a significantly lower percentage of patients with SRE, longer median time to first SRE, longer time to increase of pain level, lower risk of developing a SRE, and higher performance status scores than patients given placebo (Hultborn et al., 1999, Rosen et al., 2003, Theriault et al., 1999, Van Poznak et al., 2011, Coleman, 2004a, Lipton et al., 2000). Both pamidronate and zoledronic acid have demonstrated the most consistent clinical benefit across multiple end-point analyses, when compared to other bisphosphonates, including i.v. ibandronate and oral clodronate (Coleman, 2004a, Van Poznak et al., 2011). Of note, patients receiving zoledronic acid appeared to have achieved a better clinical outcome than patients receiving pamidronate (Coleman, 2004a, Rosen et al., 2004). Although bisphosphonate therapy for bone metastases secondary to breast cancer demonstrated significantly greater clinical benefit, these did not translate into a greater survival advantage compared to placebo-treated patients (Guise et al., 2010).

Based on extensive clinical experience, bisphosphonates appear to be well tolerated in patients with metastatic breast cancer, and adverse effects were not different to those of placebo-treated patients (Coleman, 2004a). Some common adverse

events associated with pamidronate and zoledronic acid includes fatigue, pyrexia and acute-phase infusion-related reactions (Coleman, 2004a, Guise *et al*., 2010). Moreover, intravenous bisphosphonates (pamidronate and zoledronic acid), are primarily excreted by the kidneys, and therefore can be associated with renal deterioration. This is particularly evident for patients with pre-existing renal impairment and in those who receive multiple cycles of bisphosphonate therapy. Consequently, it is now recommended, at least for zoledronic acid, that for patients with pre-existing renal conditions, a lower initial dose be given (ranging from $3.0 - 3.5$ mg), or complete cessation of therapy, depending on the estimated creatinine clearance (Van Poznak *et al*., 2011). In addition, rare incidences of osteonecrosis of the jaw (ONJ) have been reported in patients receiving oral or i.v. bisphosphonates. Necrotic jawbones can present with pain, soft-tissue abscesses, and sinusitis, which can impair the patient's quality of life (Balla *et al*., 2012). Whilst the incidence, prevalence and pathogenesis of ONJ remain unknown, the risk factors are thought to include bisphosphonate type and duration of exposure; with an increased risk of ONJ with the higher potency drugs (e.g. zoledonic acid) and a longer duration of exposure (Guise *et al*., 2010, Van Poznak *et al*., 2011).

Many lines of pre-clinical evidence, including reports by this laboratory, have demonstrated the significant protection of cancer-induced bone disease by bisphosphonates, in particular, zoledronic acid. These included osteolytic lesions in rat (Heymann *et al*., 2005) and mouse (Dass and Choong, 2007), and more recently, osteosarcoma-induced osteolytic and osteoblastic lesions in both mouse (Labrinidis *et al*., 2009b) and rat (Labrinidis *et al*., 2010), orthotopic transplant models. While a reduction in resorption has been reported, there is evidence for bisphosphonate suppression of osteoblast maturation and bone formation in several pre-clinical studies

(Huja *et al*., 2009, Lloyd *et al*., 2008), resulting in complications for bone healing. Although treatment with bisphosphonates offered considerable protection against cancer-induced osteolytic and osteoblastic lesions, their direct effect on cancer cells and on metastatic spread is debatable. Many studies have provided *in vitro* data to suggest that bisphosphonates have a direct effect on tumour cells, as they inhibited tumour cell proliferation, promoted cell cycle arrest and induced apoptosis (Aft *et al*., 2011, Green and Guenther, 2011, Matsumoto *et al*., 2005, Sawada *et al*., 2002, Senaratne and Colston, 2002, Singh *et al*., 2011). However, these effects often have not translated into *in vivo* efficacy. Early studies involving myeloma tumour-bearing mice demonstrated that oral pamidronate reduced bone resorption, but failed to produce any significant anti-myeloma activity (Radl *et al*., 1985). Subsequently, a study showed that long-term pamidronate treatment significantly prolonged survival of mice bearing myeloma tumours, although no anti-myeloma effect was observed (Croese *et al*., 1991). The more potent nitrogen-containing bisphosphonate, ibandronate, was also reported to have no significant anticancer activity (Shipman *et al*., 2000). Conversely, animal models have reported the pro-apoptotic and anti-metastatic effects of zoledronic acid in animal models of neuroblastoma (Peng *et al*., 2007), osteosarcoma (Dass and Choong, 2007), and breast cancer (Ottewell *et al*., 2009). Recently, a mouse study by this laboratory demonstrated that treatment with zoledronic acid had no anticancer efficacy, and that lung metastases were not reduced and may even have been promoted (Labrinidis *et al*., 2009b). The reasons for these different observations are not clear, but may relate to cell type, animal model, dose, treatment schedule and type of bisphosphonate used.

While bisphosphonate therapy is highly effective for palliative treatment, in real terms, there is minimal improvement in the long-term survival of patients with bone

metastases. It is also inadequate to inhibit bone resorption without addressing the over-suppression of bone formation, and the lack of efficacy towards tumour growth. Therefore, there is a need for the evaluation and development of new agents, which may be efficacious in treating the 'vicious cycle' of cancer-induced bone destruction.

1.4   Introduction to the chromatin, nucleosomes and histones

The human genome is assembled into chromatin, consisting of histones, non-histone proteins and DNA, compacted into functional units known as nucleosomes (Cho *et al*., 2004, Grunstein, 1997). These are approximately 200 base pairs of DNA wound twice around a histone core of 8, formed by a tetramer of H3-H4 and two H2A-H2B dimers (Jenuwein and Allis, 2001), with each nucleosome linked by the "linker" DNA, histone-H1 (figure 1-4), (Kornberg and Lorch, 1999). These histones were once thought to be the genetic material itself due to their abundance being roughly equal to that of the DNA. However, they were later proved to be diverse proteins, which function as gene regulators (Kornberg and Lorch, 1999). All histones are small basic proteins, consisting of a globular domain and containing 15-30 residues at the amino termini that are unstructured, flexible and commonly referred to as the histone "tail" that protrudes from the nucleosome (Jenuwein and Allis, 2001, Kornberg and Lorch, 1999). These protruding tails appear to promote fibre formation, possibly by contact with adjacent nucleosomes or by influencing the position or arrangement of the linker DNA (Luger *et al*., 1997). Thus, post-translational modification of the histone tails by acetylation, methylation, phosphorylation and ubiquitination may support or disrupt these contacts, thereby influencing chromatin formation and structure, and hence modulating the accessibility of gene transcription (Tse *et al*., 1998).
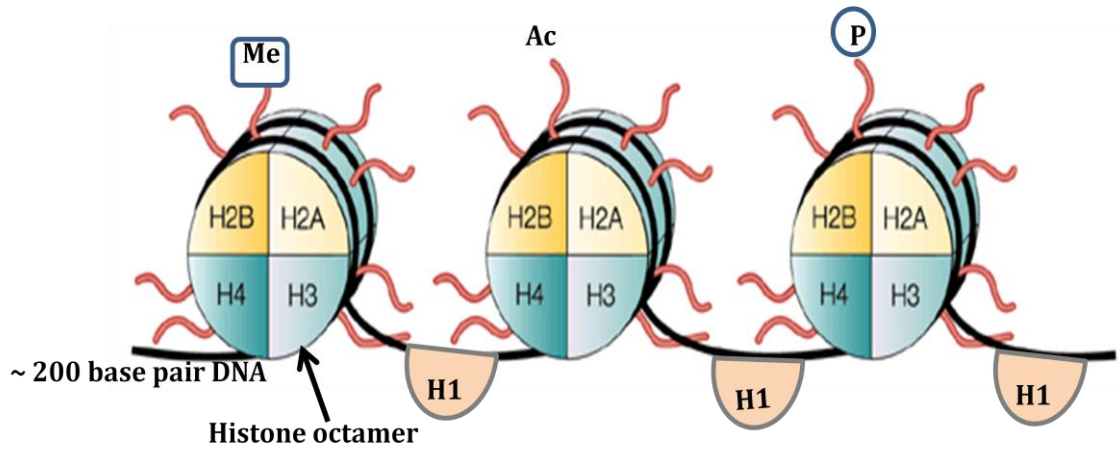
Figure 1-4. The Nucleosome.

Animated schematic diagram displaying the nucleosome, which is composed of approximately 200 base pairs of DNA (black line), wrapped around a histone octamer. Each histone octamer consists of a histone H3-H4 tetramer and two H2A-H2B dimers. Nucleosomes are linked by histone-H1. Post-translational modification of histone tails by methylation (Me), acetylation (Ac), or phosphorylation (P), can alter the higher-order nucleosome structure.

1.5   Modification of histones by histone acetyltransferases (HATs)

The chromatin is a dynamic structure because the histone tails are exposed to the environment outside of the chromatin polymer. This provides an attractive signalling complex, which can then modulate critical interactions with proteins or other complexes, leading to remodelling of the chromatin. Acetylation of histones refers to the addition of an acetyl group to conserved lysine residues on the histone tails. This results in the neutralisation of the charge on the histones, resulting in altered interactions between neighbouring nucleosomes, and/or interactions between histones and regulatory proteins (Luger *et al*., 1997). This leads to a more open and free chromatin conformation for gene transcription (Roth *et al*., 2001). Various polypeptides have been identified, which are responsible for acetylation of histones by histone acetyltransferases (HATs), and these have been grouped into two general classes depending on their cellular location and function. Type A HATs are classed as 'nuclear', as they are likely to catalyse the acetylation of histones related to transcriptional activity (Brownell and Allis, 1996). Type B HATs are 'cytoplasmic', as they are likely to catalyse acetylation events associated with the transport of fresh histones synthesised from the cytoplasm to the nucleus for deposition onto newly replicated DNA (Ruiz-Carrillo *et al*., 1975). There are 3 main HAT families, which display several highly conserved acetylation-related structural and functional domains, from yeast to human (Roth *et al*., 2001). Table 1-1 outlines the basic characteristics of the 3 main HAT families.

HAT Family	HAT (and complexes associated with it)	Histones acetylated by HAT complex	Interactions with other HATs
GNAT	GCN5 (SAGA, ADA, A2)	H3, H2B	p300, CBP
	PCAF (PCAF)	H3, H4	p300, CBP
	Hat1 (HatB)	H4, H2A	
	Elp3 (Elongator)	H2A, H3	
	Hpa2		
MYST	Esa1 (NuA4)	H2A, H4	
	MOZ (MSL)	H3	P300, CBP
	Sas2	H2A, H3	
	Sas3 (NuA3)	H3	
	MORF	H2A, H3, H4	P300, CBP
	Tip60	H2A, H3, H4	
	Hbo1 (ORC)		
P300/CBP	p300	H3, H4	PCAF, GCN5
	CBP	H2A, H2B	MORF

Table 1-1. Characteristics of the three main HAT families.

HATs are classified into different subfamilies, and have defined specificities for histones.

Although HATs, by definition, are able to acetylate histones, they are also capable of acetylating non-histone proteins, previously described as Factor Acetyltransferases (FATs), (Gu and Roeder, 1997). Of note, GCN5, p300/CBP and PCAF have been identified as HATs with FAT activities, and have been implicated in different cancer types. These include transcriptional activators such as, p53 (Gu and Roeder, 1997), GATA1 (Boyes *et al*., 1998), some structural proteins such as tubulin (MacRae, 1997), angiogenesis substrates (Qian, 2006), apoptotic or cell arrest substrates, such as heat-shock protein 90 (Hsp90), (Zhou *et al*., 2008), p21 (Prystowsky *et al*., 2009) and ubiquitin B (Wu *et al*., 2009).

1.6   HATs and cancer

HATs are important for normal cellular functions, including proliferation and differentiation, and abnormal HAT activities have been associated with disease states. Many lines of evidence suggest that HAT functions are linked to tumour suppression, and that loss, misregulation, or gene mutation involving HAT functions may contribute to the development of cancer (Davie *et al*., 1999). It was first discovered that viral oncoproteins, such as E1A, were reported to bind to and disrupt the functions of p300/CBP (Eckner *et al*., 1994). This binding results in the inactivation of the retinoblastoma (Rb), and p53 tumour suppressor functions, leading to increased cell proliferation and tumorigenesis (Arany *et al*., 1994, Gu and Roeder, 1997). Similarly, mice heterozygous for the CBP null allele (CBP$^{+/-}$), developed spontaneous tumours of the haematopoietic origin (Kung *et al*., 2000). Various lines of evidence clearly indicate the tumour suppressor function of p300, as mutations to p300 are associated with an

increase in human malignancies, including glioblastomas, colorectal cancers, epithelial and breast cancers (Gayther *et al*., 2000).

In contrast, a gain of function of HATs is also associated with certain leukemias due to chromosomal translocations (Davis and Brackmann, 2003). A recurrent translocation associated with acute myeloid leukemia (AML) involves the fusion of two HAT domains (CBP and MOZ), leading to inappropriate HAT activity by the recruitment of cofactors by CBP or MOZ to target exposed promoter regions (Ayton and Cleary, 2001, Roth *et al*., 2001). In addition, two inversions [inv(8)(p11q13)] within chromosome 8, associated with leukaemia, also involve the fusion of MOZ to another HAT, TIF2 (Carapeti *et al*., 1999). Moreover, HAT over-expression may also contribute to the development of cancers. In oestrogen receptor-positive (ER$^+$) breast and ovarian cancers, AIB1, a nuclear hormone cofactor is over-expressed, leading to an increase in transcriptional activity (Anzick *et al*., 1997). Collectively, these studies identify the connection between HATs and cancer, irrespective of whether altered HAT activity is caused by chromosomal abnormalities or altered expression levels, resulting in aberrant histone acetylation and consequently abnormal gene expression.

1.7   Histone deacetylases (HDACs)

To date, 18 human histone deacetylases (HDACs) have been identified, and their activities have been reported to influence transcription, cell cycle progression, differentiation and DNA replication (Wang *et al*., 2001, Won *et al*., 2002, Zhang *et al*., 2002). The role of HDACs is to regulate gene transcription by catalysing the removal of acetyl groups by HATs on lysine residues from histones and deacetylation of non-

histone proteins (Johnstone, 2002), resulting in chromatin condensation and suppression of transcriptional activity (Bolden *et al*., 2006). The HDACs can be separated into 4 classes based on their homology to yeast HDACs, their cellular location, and their enzymatic activity. Class I HDACs (1, 2, 3 and 8) all share a high degree of homology with the yeast RPD3 gene. These are predominantly located within the nucleus, are approximately 400-500 amino acids in length, and are ubiquitously expressed in various human cell lines and tissues. Class II HDACs (4, 5, 6, 7, 9 and 10) share a certain degree of homology to the yeast deacetylase Hda1, and are twice as long (approximately 1000 amino acids), and localised to the cytoplasm, but can shuttle to the nucleus as required. These are also differentially expressed in human tissues, with the highest levels being found in the heart, brain and skeletal muscle. The third family of HDACs are also known as Sirtuins (SIRT1, 2, 3, 4, 5, 6 and 7), because of their homology to the yeast Sir2 gene. The catalytic activity of this class of HDACs is dependent upon NAD^+, and regulates gene expression in response to redox status. HDAC 11 was recently cloned and characterised as a member of the Class IV enzymes. This characterisation was based on the fact that it was approximately the size of class I enzymes, but also shared similar sequences with the catalytic core of regions in both class I and II enzymes. HDAC 11 is differentially expressed in the heart, brain and skeletal muscle, which is typical of class II, but is predominately a nuclear protein, and therefore does not have a strong enough identity to be placed in either class (Bolden *et al*., 2006, Marks *et al*., 2001, Thiagalingam *et al*., 2003). Table 1-2 summarises the HDAC classes.

Table 1-2. Human histone deacetylases sensitive to HDAC inhibition.

Class	Localisation	HDAC	Amino Acids	Homology with yeast
Class I	Nuclear	1, 2, 3, 8	377 - 488	RPD3 deacetylase
Class II	Nuclear/cytoplasm	4, 5, 6, 7, 9, 10	669 - 1215	HDA1 deacetylase
Class III	Nucleus	SIRT 1-7	310 - 747	SIRT2 family
Class IV	Nuclear	11	~ 347	

Source: (Voelter-Mahlknecht *et al*., 2005)

1.8   HDACs and cancer

Chromosomal translocation is a key factor in aberrant recruitment of HDACs to promoter regions, which contributes to gene silencing and cancer development. Over-expression of transcription factors, which interact with HDACs, can also result in atypical repressive activities. For example, this is well documented for acute promyelocytic leukaemia (APL) and AML, where the oncogenic PML-RARα, PLZF-RARα and AML1-ETO factors are fused together by translocation, thus recruiting HDAC-containing co-repressors, and resulting in constitutive expression of specific target genes involved in proliferation and differentiation (Lin *et al*., 2001, Pandolfi, 2001). Diffuse large B-cell lymphoma (DLBCL) is a form of non-Hodgkin's lymphoma, which stems from the chromosomal translocation affecting band 3q27. This abnormality results in B-cell lymphoma 6 (BCL6) being constitutively expressed, where normally its down-regulation allows for normal B cell activity and function. As a consequence, BCL6 actively recruits HDAC2 to repress apoptotic target genes, such as CDKN1A encoding p21 (Pasqualucci *et al*., 2003).

Altered expression of individual HDACs has also been reported in various tumour types. For example, HDAC1, which is involved in the control of cell proliferation and differentiation, is over-expressed in prostate (Halkidou *et al*., 2004), and human gastric cancers (Choi *et al*., 2001), whereas HDAC2 is over-expressed in cervical carcinomas, and knockdown of HDAC2 resulted in an increase in apoptosis associated with p21 upregulation (Huang *et al*., 2005). HDAC3 expression is increased in colon tumours, and silencing of this gene resulted in growth inhibition and apoptosis of cancer cells (Wilson *et al*., 2006). In contrast, over-expression of certain HDAC enzymes may serve as a protective role in human breast cancer in response to drug treatment. Of note, HDAC1 and HDAC6 protein levels are highly expressed in invasive

$ER\alpha^+$ and progesterone receptor positive (PR^+) breast cancer samples, and this is thought to correlate with increased responsiveness to drug therapy compared with other breast cancer types expressing lower levels of these enzymes. Furthermore, this enhanced expression was statistically correlated to a better prognosis and disease-free survival (Zhang *et al*., 2005b, Zhang *et al*., 2004). In a recent study, HDAC8 was implicated in tumourigenesis of neuroblastoma, a common childhood tumour originating from the neural crest. High levels of HDAC8 correlated with markers of the advanced stage of the disease, poor prognostic outcome and survival. Interestingly, down-regulation of HDAC8 was observed in stage 4S of neuroblastoma, associated with spontaneous tumour regression (Oehme *et al*., 2009). Taken together, these data support the role of HDACs in tumour onset and progression and highlight HDACs as an appropriate therapeutic target.

1.9   HATs and HDACs in normal bone biology

Little is known about the effects of epigenetic remodelling through the actions of HATs and HDACs on normal bone biology. However, what is clear is that for normal skeletal development and function, these two opposing enzymes play a critical role, and inappropriate activity of either generally gives rise to disease states (Haberland *et al*., 2009). For example, Gcn5, a HAT, was shown to be a critical player in normal patterning of mouse skeletal development, as deletions or mutations of this gene generated severe defects in the thoracic and lumbar regions of mouse vertebrae (Lin *et al*., 2008). In addition, MEF2C is a transcription factor responsible for the control of bone development in mice, which is involved in chondrocyte hypertrophy. Gene deletion or mutation to MEF2C gives rise to mice with functional impairment of
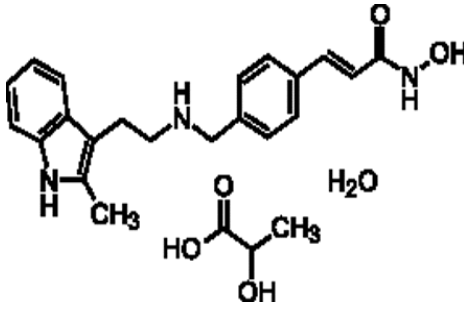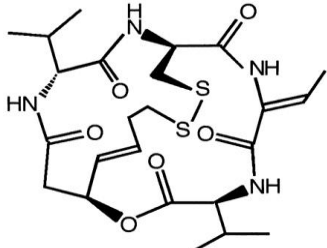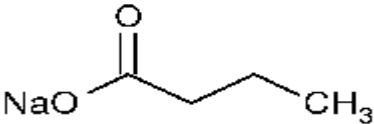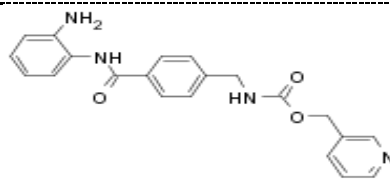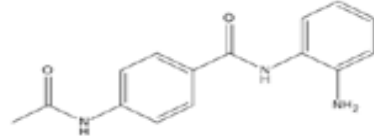
hypertrophy, ossification, cartilage angiogenesis and long bone formation. This was associated with an increase in HDAC4 activity, as subsequent mutations to HDAC4 demonstrated that the bone phenotype could be rescued (Arnold *et al*., 2007). In contrast, down regulation of expression of the HDAC8 gene was responsible for impaired development of the skull in mice, with death occuring shortly after birth. HDAC8 is therefore thought to control the patterning of the skull by inhibiting the abnormal expression of certain transcription factors (Otx2 and Lhx1), in cranial neural crest cells (Haberland *et al*., 2009).

1.10 Histone deacetylase inhibitors

Histone deacetylase inhibitors (HDIs) are a new class of anticancer agents for the treatment of solid and haematological malignancies. These agents are attractive in the treatment of cancers because they were shown to be potent inducers of growth arrest, differentiation and apoptosis of cancer cells *in vitro* and *in vivo*, while exhibiting little or no toxicity to normal cells (Bolden *et al*., 2006, Johnstone, 2002). Several natural and synthetically derived HDIs have been developed and many have advanced to clinical trials. These compounds can be divided into six groups based on their structure: 1). Hydroxamic acid-derived compounds, 2). Cyclic tetrapeptides, 3). Short-chain fatty acids, 4). Synthetic pyridyl carbamate derivatives, 5). Synthetic benzamide derivatives and 6). Ketones (Summarised in table 1-3). These inhibitors exert their effects in one of two ways; firstly some inhibitors have polar ends, which bind to the zinc ion of the catalytic pocket of HDAC enzymes, whereas other HDIs physically bind to the HDACs active site, hence producing a stronger inhibitory effect (Finnin *et al*., 1999). For example, the more potent complex hydroxamic acids (e.g. SAHA), contains a 5-6

carbon aliphatic chain, which mimics a lysine side chain, a functional group that interacts with the zinc ion of the HDAC, and a hydrophobic cap moiety, which interacts with the catalytic pocket (figure 1-5), (Bieliauskas and Pflum, 2008). On the other hand, the less potent HDIs from the short-chain fatty acids group (e.g. valproic acid or sodium butyrate), cannot make significant contact with the catalytic pocket due to their short side chains, but are still able to interact with the catalytic zinc ion (Johnstone and Licht, 2003).

Table 1-3. Diverse structures of HDAC inhibitors.

Group	Examples	Structure example
Hydroxamic acid-derived compounds	Trichostatin A	
	SAHA	
	LBH589	
	LAQ824	
	Pyroxamide	
	M-carboxycinnamic acid bis-hydroxamide	**LBH589**
Cyclic tetrapeptides	Depsipeptide (FK228)	
	Apicidine	
	Trapoxin	
	HC-toxin	
	CHAPS	**FK228**
Short-chain fatty acids	Valproic acid	
	Sodium butyrate	
	Phenyl butyrate	**Sodium butyrate**
Synthetic pyridyl carbamate derivative	MS-275	
Synthetic benzamide derivatives	CI-994	
Ketones	Trifluoromethyl ketone	
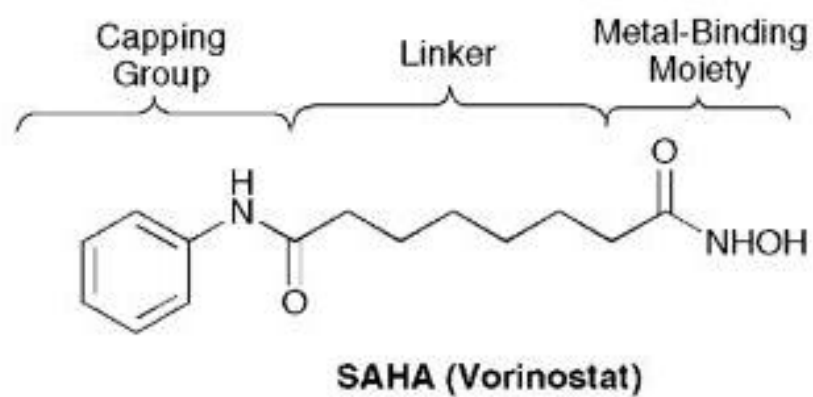
Figure 1-5. Chemical structure of SAHA (Vorinostat).

Taken from (Bieliauskas and Pflum, 2008)

The evolution of HDIs stem from the first confirmed inhibitor, sodium butyrate, which belongs to the natural short-chain fatty acids group, and is produced as a result of fermentation of dietary fibres by bacterium in the colon. However, sodium butyrate is a weak, non-specific HDAC inhibitor, producing large toxic side effects *in vivo* (Joseph *et al*., 2005). Another HDI from the same class of compounds, valproic acid (VPA), was once used to treat clinical epilepsy and mental disease. At therapeutic levels, VPA exerts its inhibitory actions on class I HDAC enzymes (Phiel *et al*., 2001), however as this drug has a short plasma half-life, relatively high concentrations (millimolar), are necessary for it to be effective (Johnstone, 2002). The hydroxamic acid, Trichostatin A (TSA), was derived in the late 1980s from the culture broths of *Streptomyces platensis*, and at therapeutic levels (micromolar ranges), TSA generally targets class I HDACs, and has a longer *in vivo* half-life and bioavailability than the short-chain fatty acids (Chen *et al*., 2004b, Yoshida *et al*., 1987, Johnstone, 2002). Interestingly, cyclic hydroxamic acid-containing peptide (CHAP) compounds appear to have substrate specificity, with a preference for HDAC1 and HDAC4 over HDAC6. These compounds are derived from hybrid structures of hydroxamic acids and cyclic tetrapeptides, and structure-function analyses of various CHAPs have identified reversible compounds that can induce gene expression at nanomolar concentrations (Komatsu *et al*., 2001).

1.11 Biological effects of histone deacetylase inhibitors on cancer

HDIs have now emerged as a potent class of anticancer agents for treating various malignancies with high efficacy and with little or no toxicity to normal cells. These agents provide a continuous open DNA reading frame for gene transcription and expression of target genes. The most extensively studied HDIs are those that target

class I, II and/or IV HDACs, and a separate set of inhibitors that target class III HDACs (sirtuins). Although the exact mechanisms of action of HDIs are unclear, there is nonetheless a large amount of evidence demonstrating that HDIs have the ability to influence cell cycle, differentiation, apoptosis, angiogenesis and inflammation-enhanced immune response (Kouraklis and Theocharis, 2006, Liu *et al*., 2006, Haefner *et al*., 2008). To explain the biological effects of HDIs, earlier studies focused on the direct hyperacetylation of histones at specific gene loci, inducing altered gene expression. Around 2-10% of genes were altered in their expression levels following treatment with HDIs, and many of these genes have been shown to be directly involved in the biological effects of HDIs (Bolden *et al*., 2006, Johnstone, 2002). However, it is now understood that a number of non-histone proteins are also targeted by HDIs and show regulated activity depending on their acetylation status (Johnstone and Licht, 2003, Ellis *et al*., 2009a), thus indirectly regulating gene expression. These protein targets include transcription factors such as p53, NF-κB and E2F1, which play important roles in tumourigenesis and anti-tumour responses (Johnstone and Licht, 2003, Johnstone *et al*., 2002). In addition, proteins that have no direct role in regulating gene expression can also be directly acetylated. For example, Hsp90 and α-tubulin can be acetylated to regulate cellular processes such as stabilisation and cell motility. Therefore, HDIs may influence the function of these proteins, resulting in decreased tumour growth or increased cell survival (Bolden *et al*., 2006, Rodriguez-Gonzalez *et al*., 2008). The role of HDIs in tumour angiogenesis, metastasis and invasion has been well demonstrated in numerous *in vitro* and *in vivo* studies. The anti-angiogenic properties of various HDIs, including SAHA, LAQ826 and LBH589 are associated with their ability to regulate genes directly involved in angiogenesis. These include decreased expression of vascular endothelial growth factor (VEGF) and its associated

receptors (Park *et al*., 2008), hypoxia inducible factor-1α (HIF1α), (Semenza, 2003), and endothelial nitric oxide synthase (eNOS), (Qian *et al*., 2006, Qian *et al*., 2004). In addition, HDIs downregulate the chemokine CXCR4, which is important in the chemotaxis or "homing" of various haemopoietic progenitor cells to the bone marrow, in particular osteoclast precursors (Crazzolara *et al*., 2002). Recently, it was demonstrated by both *in vitro* and *in vivo* experiments that the SDF1α/CXCR4 axis plays a key role in the survival and progression of both primary solid tumours and their metastases including, breast, prostate, pancreatic cancers, as well as osteosarcomas and rabdomyosarcomas (Koshiba *et al*., 2000, Libura *et al*., 2002, Perissinotto *et al*., 2005, Taichman *et al*., 2002).

While the molecular mechanisms, by which HDIs suppress tumour growth are not fully understood, nonetheless the regulation of histone function and subsequent effects on gene expression, together with their effects on non-histone proteins, appear to be the dominant approach to target tumour cell apoptosis. Anticancer efficacy of HDIs can proceed via two functionally distinct, yet molecularly linked pathways; the 'extrinsic' death receptor pathway, or the 'intrinsic' mitochondrial pathway. Despite the difference in initiating apoptotic stimuli, a number of downstream molecular events are mediated by common activators such as caspase-3, indicating that both pathways share common biochemical and morphological events during apoptosis (Johnstone *et al*., 2002, Johnstone *et al*., 2008). (Note that the mechanisms relating to the extrinsic and intrinsic apoptotic pathways will be explained in detail in section 3.4, following experimental outcomes). The involvement of the death receptor pathway in mediating apoptosis induction by HDIs originated from earlier studies, in which neutralising antibodies and siRNA that target death receptors and/or ligands were shown to protect cells from apoptosis following to HDI treatment (Insinga *et al*., 2005, Frew *et al*., 2009). In

addition, Nebbioso *et al.* (2005) demonstrated that MS275, SAHA and VPA could strongly induce the expression of TNFSF10 mRNA, the gene encoding TRAIL, as well as the TRAIL protein (and to a lesser extent, the TRAIL pro-apoptotic receptors). This results in cell death, as evident from *in vitro* studies and from *in vivo* models of AML. RNA interference or knockdown of TRAIL abrogated the HDI-induced apoptosis (Nebbioso *et al.*, 2005). Furthermore, TSA, sodium butyrate and SAHA were shown to markedly induce protein expression of the DR5 TRAIL death receptor and activity in a number of human acute lymphoblastic leukemia (ALL) cell lines (Nakata *et al.*, 2004), as well as in mouse breast cancer. This affect was concomitant with a down-regulation of the intracellular inhibitor of apoptosis protein, c-FLIP (Frew *et al.*, 2008), contributing to the sensitisation of TRAIL-induced apoptosis. In addition, osteosarcoma-bearing mice treated with FR901228 demonstrated that apoptosis was caused by an induction of expression of Fas ligand (FasL) mRNA, resulting in the expression of membrane-bound FasL, followed by activation of caspase-8 and -3, leading to apoptosis. By blocking the downstream activation of the Fas/FasL signal, or over-expression of the inhibitory protein, FADD or neutralising anti-FasL antibody, the level of HDI-mediated apoptosis was markedly reduced (Imai *et al.*, 2003). While it is evident that HDIs can induce cell death through the extrinsic death receptor pathway, the signals that are necessary through death receptors and their ligands appear to be cell-type dependent. Moreover, HDIs that act via the extrinsic apoptotic death receptor pathway may also affect downstream signals that link together with the intrinsic apoptotic pathway, therefore enhancing HDI-mediated apoptosis (Frew *et al.*, 2008, Imai *et al.*, 2003). Whilst the mechanisms are still unclear, a common feature amongst HDI-mediated intrinsic apoptotic cell death appears to involve altered differential gene expression of pro-apoptotic (including BH3-only genes, Bax and Bak), and anti-

apoptotic (including Bcl_2 and Bcl_{XL}), genes, to favour apoptosis (Bolden *et al*., 2006, Lindemann *et al*., 2007, Newbold *et al*., 2008). Studies involving the silencing of RNAs of genes including Bim, Bmf and Noxa, have implicated these molecules in explaining the reduced efficacy of various HDIs (Inoue *et al*., 2007, Zhang *et al*., 2006a, Zhang *et al*., 2006b, Zhao *et al*., 2005). Additionally, hydroxamic acids, such as SAHA and oxamflatin, cannot overcome the acquired protection from the over-expression of Bcl_2 and Bcl_{XL} in murine breast cancer cells and lymphoma (Frew *et al*., 2008, Newbold *et al*., 2008). Furthermore, the HDI romidepsin (from the cyclic tetrapeptide class), was found to be redundant when Bcl_{XL} was over-expressed in lymphomas. However, romidepsin could induce apoptosis when Bcl_2 was over-expressed (Newbold *et al*., 2008), highlighting that HDI-mediated apoptosis is triggered through the intrinsic pathway. These data provide considerable support for the notion that HDIs of different chemical classes have subtle differences in their molecular and biological activities, which may be important in their therapeutic outcomes.

In the search for more efficient treatments for cancer, combinations of agents with synergistic or additive activity are attractive because they enable the use of lower drug doses and potentially reduce toxic side effects (Boumber and Issa, 2011, Deleu *et al*., 2009). Cell death induction by HDIs and conventional chemotherapeutic drugs may induce apoptosis of cancer cells through different but perhaps overlapping signalling pathways. Therefore combinatorial approaches may facilitate killing of tumour cells that resist death induction through either one of the apoptotic pathways, in addition to reducing the probability of acquired resistance to either therapy. Therefore, combining new cancer therapeutics with approved anticancer modalities is a well established approach to developing new therapeutic regimens. Significant co-operative and synergistic activity has been observed in a number of combinations of HDIs with

standard chemotherapeutics (Frew *et al*., 2009). Various studies have demonstrated apoptotic synergism when combining current chemotherapeutics with one of the classic and representative drugs of HDIs, the FDA approved SAHA. SAHA or Vorinostat, was the first HDI of its class to gain approval from the FDA, for the treatment of cutaneous T-cell lymphoma (CTCL), (Mann *et al*., 2007). In several recent *in vitro* and *in vivo* studies, SAHA in combination with doxorubicin or the topoisomerase I inhibitor, topotecan or the selective antagonist of the 26S proteasome, bortezomib, significantly enhanced apoptosis compared to monotherapy, in multiple myeloma (Cheriyath *et al*., 2011), renal cancer (Sato *et al*., 2011) and in human cervical HeLa cells (Jiang *et al*., 2010). Furthermore, a triple combination of SAHA, bortezomib and gemcitabine was more potent in antitumour efficacy of pancreatic xenografts than either agent alone, or as a double combination (Lee *et al*., 2011).

The mechanisms, by which HDIs may sensitise tumour cells to the cytotoxic effects of other drugs, have been widely explored. A simplistic explanation for the potentiated activity is that HDIs modify chromatin structure such that the open-conformation state allows access of DNA damaging drugs to their targets, thus enhancing cytotoxicity (Frew *et al*., 2009). In addition, it is thought that HDIs may mimic the response to ionising radiation by inducing DNA strand breaks through the activation of the DNA damage kinase, *ATM* (Bakkenist and Kastan, 2003). Simultaneously, HDIs may also act to inhibit the DNA repair process (Adimoolam *et al*., 2007), thereby potentiating further cellular death. This is because the regulation of phosphorylation/dephosphorylation of histone H2AX at the site of DNA damage is important for DNA strand repair, and HDIs can induce the persistent phosphorylation of H2AX, suggesting a decrease in the cells' ability to repair itself from DNA strand breaks (Adimoolam *et al*., 2007). HDIs are able to induce apoptosis through the death

receptor pathway and enhance pro-apoptotic thresholds by engaging the intrinsic apoptotic pathway. In this context, combinations with death receptor agonists have shown increased efficacy in cancer treatment. Specifically, murine models of breast cancer have demonstrated that SAHA, in combination with an anti-TRAIL receptor antibody, induced regression of established tumours (Frew *et al*., 2008), as well as re-sensitising breast cancer cells to TRAIL-induced apoptosis (Butler *et al*., 2006). The mechanisms supporting the observed synergism may be related to a redistribution of TRAIL receptors, resulting in enhanced formation of the death-inducing signal complex (DISC), down-regulation of inhibitors involved in the extrinsic pathway (e.g. survivin, c-FLIP), and up-/down-regulation of pro-/anti-apoptotic proteins involved in the intrinsic pathway including the Bcl_2 family proteins (Bolden *et al*., 2006, Butler *et al*., 2006, Frew *et al*., 2009). In a recent study by Marrocco and colleagues (Marrocco *et al*., 2007), the combination of SAHA and an androgen receptor (AR) antagonist was shown to reduce the expression of AR-regulated genes, *PSA* and *kallikrein 2*, thereby reducing AR signalling for prostate cancer growth and survival. Moreover, a number of studies using HDIs in combination with proteosomal inhibitors have established a role for targeting proteosome degradation pathways for the treatment of cancer. For example, the inhibitor of the chaperone protein Hsp90, 17-AAG, in combination with HDIs, resulted in enhanced degradation of Hsp90 client oncoproteins (George *et al*., 2005, Rao *et al*., 2008). One possible explanation for this synergistic activity may be related to the inhibition of HDAC6, leading to the hyperacetylation of Hsp90. Hyperacetylation decreases the affinity of co-chaperone binding to Hsp90 and acts to enhance the affinity of Hsp90 for 17-AAG, resulting in Hsp90 client oncoproteins for proteosomal degradation and ubiquitination, and subsequent death of cancer cells (Rao *et al*., 2008). An impressive body of evidence demonstrates beneficial effects of HDIs

and cancer, although it is not clear whether there is one dominant mode of HDAC inhibition alone or in synergism with cytotoxic drugs or DNA damaging agents. However, it is apparent that the combined effects of cytotoxic drugs and HDIs have effects in impairing the DNA repair processes, enhancing DNA damaging responses, and triggering cell death pathways.

It is clear that HDIs are emerging as an exciting new class of anticancer agents for the treatment of solid and haematological malignancies. Despite the infancy of the field of HDIs, an impressive body of data describes the ability of these molecules to modulate a wide variety of cellular functions, including cell differentiation, cell cycle progression, apoptosis, cytoskeletal modifications and angiogenesis. Over the past few years, results obtained from clinical trials and pre-clinical animal experiments demonstrate the ability of HDIs to selectively kill cancer cells, with limited or no toxicity to normal tissues and organs. Amongst the HDIs now in clinical trials, SAHA is the first of its class to gain approval from the U.S.A. FDA for the treatment of cutaneous manifestations in patients with CTCL, who have progressive, persistent or recurrent disease (Carafa *et al*., 2010). Although a number of early-phase clinical trials using different HDIs have demonstrated promising anti-tumour responses for a variety of cancer types (de Bono *et al*., 2008, Giles *et al*., 2006, Duvic *et al*., 2007, Atadja, 2010), the effect of HDIs in metastatic bone disease has not been reported.

1.12 Biological effects of HDIs on bone biology

Despite an impressive collection of data describing the effects of HDI treatment on cancer cells, there is very little information on the effects of HDIs on cells within the bone microenvironment. The molecular mechanisms of action by HDIs on osteoclast and osteoblasts are unclear and there have been few studies which have attempted to explore these. RANKL is expressed on the surface of osteoblasts, stromal cells and osteocytes, and is the key regulator of osteoclast differentiation and bone resorption. RANKL regulates osteoclastogenesis through its receptor RANK, expressed on osteoclasts and osteoclast progenitors. Upon binding, a series of downstream signalling events occur to induce osteoclastogenesis, including the activation of p38-MAPK, NF-κB and the master transcription factor, NFATc1. Inhibitors specific for these molecules were shown to suppress osteoclastogenesis (Jimi *et al*., 2004, Matsumoto *et al*., 2000, Takayanagi *et al*., 2002). Various HDIs, including TSA and sodium butyrate were shown to specifically inhibit the differentiation of rat and mouse bone marrow cells into pre- and fully functional osteoclasts, but not macrophages, suggesting that HDIs have specific effects in this cell lineage (Rahman *et al*., 2003).

Despite the efficacy of HDIs on cancer cells, there has been minimal information regarding its effects on cells within the bone microenvironment. However, one study recognised the effects of SAHA on abolishing murine osteoclastogenesis by suppressing NF-κB activation. This was associated with a decrease in expression of several NF-κB-dependent reporter genes, including TNFs, TRADD and TRAF2, responsible for osteoclast differentiation and function (Takada *et al*., 2006). Furthermore, treatment with TSA on mature osteoclasts isolated from mouse bone marrow cells induced apoptosis, associated with an induction of p21 (Yi *et al*., 2007). A recent study demonstrating the effects of the HDI, JNJ-26481585, on a mouse model of

multiple myeloma (MM) bone disease, confirmed that in combination with the second-line treatment for MM, bortezomib (Velcade), resulted in an augmentation of the balance of osteoclasts and osteoblasts, to favour bone formation (Deleu *et al*., 2009).

Bone loss associated with osteoporosis or cancer-induced bone loss is commonly associated with heightened osteoclast activity, with insufficient compensatory bone formation. Runx2 is known as the master transcription factor for osteogenesis and osteoblast activity. Earlier studies have shown that TSA increases transcriptional activity of Runx2 in MC3T3-E1 murine pre-osteoblast cells and a concomitant increased in matrix mineralisation by these cells. This activity was also correlated with an increase in other key osteogenic markers, including alkaline phosphatase (ALP), osteopontin, bone sialoprotein and osteocalcin (Schroeder and Westendorf, 2005). In a similar study, the same authors showed that HDAC3 was responsible for the repression of the Runx2-targeted genes. By interfering with the activity of this HDAC enzyme using RNA interference or HDIs in MC3T3-E1 cells, these authors found that the mechanisms, by which osteoblast maturation could be enhanced was at least, in part by promoting the Runx2-dependent transcriptional process (Schroeder et al., 2004a). More recently, gene profiling analysis of the same murine pre-osteoblast cells in response to HDIs revealed 9 genes that were differentially regulated. Of note, a gene known as NHERF-1, previously shown to be required for optimal bone density and bone homeostasis, was significantly up-regulated following HDI treatment (Schroeder *et al*., 2007). NHERF-1 is a membrane phosphoprotein that links membrane proteins with cytoplasmic proteins to regulate actin cytoskeletal reorganisation (Bretscher *et al*., 2000). Mice rendered deficient in this gene have a significant reduction in bone mineral density and a decrease in bone mineral content, presenting with multiple fractures

(Shenolikar *et al*., 2002). In summary, the full potential of these inhibitors, remain to be determined.

1.13 Current treatments for non-cancerous conditions that affect bone loss

People over the age of 50 are at a 55% increased risk of osteoporosis, 80% of which occurs in women (Nanes and Kallen, 2009). Recently, the definition of osteoporosis was re-defined as a "skeletal disorder characterised by compromised bone strength, predisposing a person to an increased risk of fracture" (Hosoi, 2010). This definition encompasses multiple factors that contribute to the pathogenesis of osteoporosis, including low bone mineral density, genetic and environmental factors (Richards *et al*., 2008, Styrkarsdottir *et al*., 2008). Common therapeutic options include anti-resorptive agents such as, bisphosphonates, hormone replacement therapy and calcitonin. Anabolic agents such as, parathyroid hormone (PTH) and strontium ranelate (SR), are used to increase the number of osteoblast precursors, stimulate osteoblast maturation, and alter osteoblast function and survival (Brennan *et al*., 2009, Trivedi *et al*., 2010). For the majority of the drugs currently available, there are concerns about their side effects, safety and efficacy for long term treatment (Antoniucci *et al*., 2007, Cramer *et al*., 2007, Rossouw *et al*., 2002). To date, there is no single treatment option that is completely safe for the treatment of patients with osteoporosis (Hosoi, 2010), and further studies into the pathogenesis and the identification of new therapeutic strategies are required for the advancement of osteoporosis therapy.

1.14 LBH589 (Panobinostat)

LBH589 or Panobinostat, developed by Novartis Pharmaceuticals, is classed as a pan-DAC inhibitor, which simply means an inhibitor of class I, II and IV HDAC enzymes, and it is classed as a hydroxamic acid-derived compound. The IC_{50} of LBH589 on all HDAC enzymes, was reported to be either in the low ($\leq$ 13.2 nM), or mid (203-531 nM), nanomolar range, which was consistently lower than other pan-DAC inhibitors, such as SAHA (Vorinostat) and Belinostat (Shao *et al*., 2008), and therefore LBH589 is at least 10-fold more potent than the above.

There is a plethora of *in vitro* studies that have demonstrated the potency of LBH589 on tumour cell growth. At low nanomolar concentrations, LBH589 induced growth arrest, differentiation and/or cell apoptosis in a variety of haematological malignancies, including chronic myeloid luekemia (CML), AML, non-Hodgkin's lymphoma (Gupta *et al*., 2009) and CTCL (Atadja, 2010). Similar results were also observed in other cancer cell lines, including, breast (Zhou *et al*., 2008), head and neck squamous cell carcinoma cells (Prystowsky *et al*., 2009), pancreatic cancer (Haefner *et al*., 2008) and colon cancer (Beckers *et al*., 2007). It was also reported that LBH589 can synergistically enhance the effects of other chemotherapeutic agents. For example, MM cells that was ensitive or rendered resistant to Dexamethasone therapy, co-treatment with Bortezomib, generated bundles of hyperacetylated α-tubulin and histones. Hyperacetylation was concomitant with caspase and PARP cleavage, and up-regulation of p21, consistent with cell death (Catley *et al*., 2006). In a similar study of freshly isolated MM cells that were resistant to conventional chemotherapeutic agents, resistance was reversed by co-treatment with LBH589. This effect was associated with down-regulation of Bcl_2, Bcl_{XL}, up-regulation of p21, p53, and increased mitochondrial outer membrane permeability (Maiso *et al*., 2006). More recently, LBH589 enhanced

the effects of Decitabine-mediated de-repression of JunB, resulting in apoptosis of AML cells. This effect was associated with depletion of DNMT1, responsible for the epigenetic modification of DNA methylation (Fiskus et al., 2009). Furthermore, LBH589 can impede the actions of non-histone products associated with tumour angiogenesis, cell cycle arrest and cell proliferation (Qian, 2006) of breast and prostate cancers, both *in vitro* and *in vivo* (Qian *et al*., 2006). In addition, LBH589 inhibited the chaperone, hsp90, therefore, sensitizing $ER\alpha^+$ breast cancers to polyubiquitination (Fiskus *et al*., 2007). Therefore, the attractiveness of LBH589 is in part due to its potent actions in the nanomolar range (compared to other HDIs at micromolar ranges), as well as its selectivity to target cancer cells with virtually no toxicity to normal cells (Shao *et al*., 2008).

Currently, LBH589 is in Phase I/II clinical trials for a number of diseases, including CTCL, Hodgkin's lymphoma (HL), AML and MM, in all of which has demonstrated promising anti-tumour efficacy (Atadja, 2010). Several phase I studies have been conducted to evaluate the safety, maximum tolerated dose (MTD) and efficacy of LBH589. In general, Panobinostat was well tolerated and objective clinical responses were observed in several clinical trials in patients with various solid tumours (Fukutomi *et al*., 2011, Jones *et al*., 2011, Prince *et al*., 2009). The MTD in western polulations was determined to be 20 mg (oral) given 3 times per week, regardless of tumour type (Ellis *et al*., 2008, Fukutomi *et al*., 2011, Prince *et al*., 2009). However this dose was reduced to 10 mg in the Japanese population (Fukutomi *et al*., 2011). Recently the MTD of LBH589 was reviewed to a lower dose of 10 mg when combined with gemicitabine (Jones *et al*., 2011). The most common adverse effects across the board were fatigue, nausea, diarrhea and thrombocytopenia, with no cases of grade 3/4 QTc prolongation being observed (Buglio and Younes, 2010, Fukutomi *et al*., 2011).

Therefore, LBH589 has promising clinical activity with a good safety profile, hence combination studies with LBH589 are ongoing, including the testing of combination therapy in patients with relapsed HL (Buglio and Younes, 2010).

1.15 Aims

The current course of treatment for metastatic bone disease relies on a therapy, which aims to alleviate the complications associated with bone disease as a palliative measure. Therefore, there is a need for research into new agents which could potentially act on the bone resorbing osteoclasts and the bone forming osteoblasts as well as tumour growth within the bone, to inhibit the 'vicious cycle' of cancer-induced bone destruction. In comparison with genetic mutations, most epigenetic changes are reversible and some preventable. Thus the reorganisation of aberrant epigenetic status, in particular histone acetylation in tumourigenic cells, is now given more attention as a therapeutic approach to treat or prevent cancer. The growing number of investigations into the actions of HDIs on cancer and in bone is a testament to their promising potential as therapeutic agents.

The studies undertaken in this thesis aimed to build on the body of research performed over the years on the effects HDIs on cancer and on bone cells. In particular, these studies sought to elucidate the effects of LBH589 on breast cancer in bone. To achieve this aim, *in vitro* and *in vivo* studies were conducted in a coordinated approach to elucidate step-by-step the actions of LBH589 on breast cancer and/or on bone. Specifically, the aims and hypotheses of this project were to:

AIM 1: To investigate the effects of LBH589 on human breast cancer cells *in vitro.*

HYPOTHESIS 1: Treatment with LBH589 induces apoptosis of human breast cancer cells.

AIM 2: To assess the anticancer efficacy of LBH589 in murine models of primary and metastatic breast cancer, and on breast cancer-induced osteolysis.

HYPOTHESIS 2: LBH589 treatment reduces tumour growth *in vivo* and protects the bone from breast cancer-induced osteolysis.

AIM 3: To investigate the effects of LBH589 on osteoclast development and on bone resorption, using *in vitro* models of osteoclastogenesis, namely:

Murine RAW264.7 cell line

Human peripheral blood mononuclear cells (PBMC)

Human giant cell tumours (GCT) of bone

HYPOTHESIS 3: LBH589 is a potent and selective inhibitor of osteoclastogenesis and bone resorption.

AIM 4: To investigate the actions of LBH589 on human osteoblast function.

HYPOTHESIS 4: LBH589 increases osteoblast activity.

AIM 5: To investigate the effects of LBH589 on normal bone metabolism *in vivo*.

HYPOTHESIS 5: LBH589 enhances osteoblast activity, while simultaneously reduces osteoclast activity *in vivo*, to favour bone formation.

Chapter 2. Materials and methods

In vitro cancer-related studies

2.1   Breast cancer cell lines

The MDA-MB231, MDA-MB453, MDA-MB468, ZR-75, MCF-7 and T47D human breast cancer cell lines were obtained from the American Tissue Culture Corporation (ATCC, Manassas, VA, U.S.A.). The MDA-MB231 derivative cell line, MDA-MB231-TXSA, was kindly provided by Dr Toshiyuki Yoneda (University of Texas Health Sciences Centre, San Antonio, TX, U.S.A.). All cell lines were cultured in Dulbecco's Minimal Essential Media (DMEM), supplemented with 2 mM glutamine, 100 IU/ml penicillin, 160 μg/ml gentamicin, HEPES (20 mM) and 10% (v/v) fetal bovine serum (FBS, Biosciences, Sydney, Australia), in a 5% CO_2-containing humidified atmosphere.

2.2   Reagents

The histone deacetylase inhibitor, LBH589, was kindly provided by Novartis Pharma (Boston, MA, U.S.A.). For *in vitro* studies, LBH589 was dissolved in DMSO as a stock solution of 1 mM and then divided into 10 μl aliquots and stored in -80ºC. Only aliquots that had been through one freeze-thaw cycle were used. For all *in vitro* experiments, the final concentration of DMSO was < 0.05% v/v, which was found not to interfere with cell viability.

Monoclonal antibodies (mAb) against caspase-8 and polyclonal antibodies (pAb) against caspase-9, survivin and VDAC were purchased from Cell Signalling

Technology (Beverly, MA, U.S.A.); mAb anti-caspase-3 was from Transduction Laboratories (Lexington, KY, U.S.A.); pAb anti-Bid was from Chemicon International (Temecula, CA, U.S.A.), and pAb anti-PARP was from Roche Diagnostics (Mannheim, Germany). P21, Bcl_2, Bcl_{XL} and Bax were all purchased from Santa Cruz Biotechnology Inc. (CA., U.S.A.), whilst cytochrome c was purchased from BD Pharmingen (NSW, Australia). The pro-apoptotic proteins Bmf was purchased from Alexis Laboratories (Alexis, NC, U.S.A.), and AIF was from Merck Millipore (Darmstadt, Germany).

2.3 Generation of Luciferase expressing MDA-MB231-TXSA breast cancer cell line

Luciferase expressing MDA-MB231-TXSA cells were generated using the retroviral expression vector SFG-NES-TGL, which gives rise to a single fusion protein encoding herpes simplex virus thymidine kinase (TK), green fluorescence protein (GFP), and firefly luciferase (Luc) (Ponomarev *et al*., 2004). Virus particle-containing supernatants were generated and filtered to remove any cellular debris and then used to infect cells, as described previously (Labrinidis *et al*., 2009a, Zannettino *et al*., 1996, Ponomarev *et al*., 2004). The retrovirally transfected cells were grown in culture for 48 hours and subsequently sorted to enrich for positive GFP expression. This was performed by using 2 cycles of fluorescence-activated sorting (FACS), (Aria BD Biosciences, Franklin Lakes, NJ, U.S.A.), collecting only the 10% most strongly GFP expressing cells. This cell line, MDA-MB231-TXSA was used for subsequent *in vitro* and *in vivo* experiments.

2.4   Determination of cell viability

The viability of cells from various cancer cell lines was measured using the CellTiter-Blue cell viability reagent (Promega, Madison, WI, U.S.A.). This assay provides a homogeneous, fluorometric method for determining the number of viable cells present in multiwell plates by measuring the metabolic capacity of cells. Viable cells retain the ability to reduce resazurin into its fluorescent end product, resorufin, thus generating a fluorescent signal directly proportional to cell viability. Non-viable cells lose metabolic capacity and therefore do not reduce the indicator dye, nor generate a fluorescent signal. The CellTiter-Blue reagent is a buffered solution containing the highly purified redox dye, resazurin, and is added directly to the wells containing cells cultured in serum-supplemented media, at a ratio of 20 μl of reagent to 100 μl of cell solution. An incubation time of 4 hours in a humidified incubator at 37ºC, with 5% CO_2 was optimised to ensure an adequate response. Quantitation of the fluorescent signal was achieved by using a fluorescent plate reader at $560_{ex}/590_{em}$ wavelengths.

2.5   Measurement of the effect of LBH589 on breast cancer cell lines

A panel of human breast cancer cell lines was examined for sensitivity to LBH589. MDA-MB231, MDA-MB453, MDA-MB468, ZR-75, MCF-7, T47D and MDA-MB231-TXSA were seeded (in triplicate) into 96-well multiwell plates at 1 x 10^5 cells/ml, and allowed to adhere overnight before commencing treatment with LBH589 at a dose range of 0 – 500 nM. In order to determine the cytotoxic effect of LBH589 on these cell lines, CellTiter-Blue reagent was added to each well 48 hours after treatment, and cells were incubated at 37ºC with 5% CO_2 for 4 hours, before the fluorescent signal was determined. This experiment was repeated at least 3 times, prior

to determining the IC_{50} for each cell line against LBH589. Representative experimental results are expressed as mean ± SD.

2.6 Measurement of DEVD-caspase-3 activity

To verify cell death by apoptosis, each cell line was seeded into 96-well multiwell plates in triplicate, as described above. Caspase activity was determined for each cell line after exposure to its respective IC_{50} value for LBH589, over a 48 hour period. Caspase activity was assayed by cleavage of zDEVD-AFC (z-asp-glu-val-asp-7-amino-4-trifluoro-methyl-coumarin), a fluorogenic substrate based on the peptide sequence at the caspase-3 cleavage site of poly (ADP-ribose) polymerase. Cells were lysed in 20 μL of NP40 lysis buffer containing 1 mM Tris-HCl, 1 mM EDTA and 10% (v/v) NP40, at pH 7.6, for 15-20 minutes on ice. Triplicate sets of cells were pooled and transferred into an Eppendorf tube and centrifuged at 15,000 x g for 10 minutes and the supernatant was collected. Aliquots of the lysate were analysed for caspase-3 activity. For each 20 μl of cell lysate, 8 μM of the fluorogenic substrate (zDEVD-AFC) was added in 1 ml of flurometric protease buffer (50 mM HEPES, 10% (w/v) sucrose, 10 mM DTT and 1% (w/v) CHAPS, pH 7.4), and incubated for 4 hours at room temperature, in the dark. Fluorescence activity ($400_{ex}/515_{em}$) was quantified using a Perkin Elmer LS50 spectrofluorimeter. The response to LBH589 by this panel of human breast cancer cell lines was measured at 0 (baseline, control), 6, 12, 24 and 48 hours after treatment commenced.

Prior to commencement of the *in vivo* studies, further *in vitro* characterisation of the human MDA-MB231-TXSA breast cancer cell line was performed. The caspase

activity of the MDA-MB231-TXSA breast cancer cell line was determined with respect to the dose and time response to LBH589. These cells were seeded at 1×10^5 cells/ml in 96-well multiwell plates and were treated with LBH589 in various concentrations (5, 25, 50, 100 and 200 nM), and caspase-3 activity was measured at 0, 6, 12, 24 and 48 hours. Results were expressed relative to the protein concentration of the sample, determined using a commercial BCA^{TM} protein assay reagent. The above experiments were repeated three times, and each representative experiment is presented as the mean of triplicates ± SD.

2.7 Measurement of cell viability after treatment with the pan-caspase inhibitor, ZVAD-fmk

MDA-MB231-TXSA cells were seeded in 96-well multiwell plates at 1×10^5 cells/ml and allowed to adhere overnight. The pan-caspase inhibitor, ZVAD-fmk, was resuspended in DMSO at a concentration of 50 mM and added to the cells at a final concentration of 50 μM, either alone, or in combination with LBH589 at 5, 25, 50, 100 or 250 nM. Cell viability was analysed by CellTiter-Blue. All treatments were conducted in quadruplicate and repeated 3 times. Representative experiments are presented as the mean of quadruplicates ± SD.

2.8 DAPI and Phalloidin staining of MDA-MB231-TXSA breast cancer cell line

In order to visualise the apoptotic effect of LBH589 on the MDA-MB231-TXSA cancer cell line, cells were seeded (1×10^5 cells/ml) on plastic chamber slides and

allowed to adhere overnight in a 5% CO_2-containing humidified atmosphere. The medium was changed to contain 50 nM LBH589 and cells were treated under this condition for 48 hours. Upon completion of the treatment protocol, cells were fixed with 4% (w/v) paraformaldehyde for 5 minutes at room temperature. To permeabilise the cells, saponin (0.1% w/v) with HHF buffer (HANKS media, 10 mM HEPES and 5% (v/v) FBS), was added to the cells for 10 minutes. Thereafter, the cells were rinsed twice with PBS containing 0.1% v/v Tween-20. Non-specific sites were blocked with blocking buffer (5% (v/v) goat serum, 0.1% (w/v) sodium azide and 1% (w/v) BSA), for 5 minutes at room temperature. To observe morphological changes, the cytoskeletal stain, Phalloidin, was incubated at room temperature with cells kept in the dark at a concentration of 100 µg/ml in blocking buffer, for 1 hour. After two washes with HHF buffer, 1 µg/ml DAPI-methanol was gently placed onto the cells for 5 minutes to stain the nuclei of cells. After several gentle washes with HHF buffer and PBS, the chamber slides were fixed with FACS Fix solution (including DAPI anti-fade mounting media; Invitrogen Australia, Vic, Australia), for 10 minutes, and the gasket removed and the slide was allowed to air dry. Once dried, coverslips were placed onto the dual-labelled slides and air bubbles removed. Slides were stored at 4ºC until visualisation by confocal microscopy.

2.9   Confocal Microscopy

Confocal microscopy is an imaging technique which allows for high resolution visualisation of fluorescent cellular structures on different planes. Confocal microscopy optically sections cellular structures in different planes and then removes the scattered light from each plane to produce 3D structural representations of intact samples. The

images were produced using the Nikon C1-Z Confocal Microscope (at Detmold Imaging Core Facility, Hanson Institute, Adelaide, SA, Australia), equipped with three solid lasers; Sapphire 488 nm, Compass 532 nm, Compass 405 nm, and a Nikon E-2000 inverted microscope. The objective used was a Nikon 20x UAPO (NA= 0.70). The dual-labelled samples were imaged with three separate channels using Photo Multiply Tubes. Wavelengths of 405 nm and 532 nm were used to excite DAPI and Phalloidin, respectively.

Detection of protein expression

2.10 Preparation of whole cell lysates

MDA-MB231-TXSA cells were seeded at 1×10^6 cells/T25 flask and allowed to adhere overnight. Media containing 50 nM LBH589 were replaced, and cell lysates were collected in a time-dependent manner (0 (baseline, control), 6, 12, 24, 48 hours). Cells were removed from the flasks using a cell scraper and lysed in protein lysis buffer containing 10 mM Tris HCl, pH 7.6, 150 mM NaCl, 1% (v/v) Triton X-100, 0.1% (w/v) sodium dodecyl sulphate (SDS), 2 mM sodium vanadate and a protease inhibitor cocktail (Roche Diagnostics, Mannheim, Germany), and kept on ice for 20 minutes. The cell solution was then transferred into a 1.5 ml Eppendorf tube and centrifuged at 1000 x g at 4°C for 3 minutes and the supernatant collected. The samples were stored at -80oC until ready to quantify.

2.11 Protein concentration determination

The amount of protein in each sample was quantified using the BCA Protein Assay Reagent, according to the manufacturer's instructions. Briefly, various amounts of BSA protein were loaded into 96-well multiwell plates incubated with the BCA protein Assay Reagent for 30 minutes at 37ºC in 5% CO_2, to produce a concentration gradient. At the same time, 5 µl of each protein sample (in duplicate), was incubated with the BCA reagent. The protein concentration in each sample was determined from a standard curve.

2.12 Western blot analysis

Protein extracts were mixed with 4x Nupage LDS Sample Buffer (Invitrogen Australia, Vic, Australia), 1M DTT, and milli-Q (MQ) water in an amount according to the protein determination, with a total of 30 µL per sample. Protein samples were then heated at 70ºC for 10 minutes and loaded into 4-12% polyacrylamide gels (Invitrogen Australia, Vic, Australia), for electrophoresis under reducing conditions. Separated proteins were electrophoretically transferred to PVDF transfer membranes (GE Healthcare, Buckinghamshire, UK), kept at 4ºC. The SNAP ID system (Invitrogen Australia, Vic, Australia), was employed for rapid detection of proteins, which draws fluid via a vacuum pump through the membrane to allow rapid binding of antibodies. The membranes were loaded into the vacuum chamber and blocked in water containing 0.5% (v/v) blocking reagent (GE Healthcare, Buckinghamshire, UK), for 10 minutes. Primary immunodetection was performed in MQ/BSA containing 0.1% (v/v) Tween-20 for 10 minutes, rinsed 3x in PBS containing 0.1% (v/v) Tween-20, with the secondary antibodies performed in 0.5% (v/v) blocking buffer for 10 minutes. All antibodies were

used at dilutions that were 3x more concentrated than recommended by the manufacturer to allow for rapid binding under vacuum conditions. Actin was detected using anti-actin mAb (Sigma-Aldrich, St. Louis, MO, U.S.A.) to control for loading variance. After washing the membranes, they were incubated with a 1:2000 dilution of anti-mouse, anti-goat, or anti-rabbit alkaline phosphatase-conjugated secondary antibodies (Pierce Chemical Co., Rockford, IL, U.S.A.) for a further 10 minutes. Visualization and quantification of protein bands were performed using the Attophos substrate (Promega, Madison, WI, U.S.A.) on the Typhoon FluorImager (Molecular Dynamics Inc., Sunnyvale, CA, U.S.A.).

2.13 *In vitro* histone-H3 acetylation detection

Cells were seeded (8 x 10^5 cells) into T25 flasks and allowed to attach for 24 hours before addition of LBH589 (50 nM). Isolation of histones was performed as described previously (Yoshida *et al*., 1990). Briefly, cells were harvested and washed in ice-cold PBS at various time points (0 (baseline, control), 6, 12, 24, 48 hours). Nuclei were isolated by Dounce homogenisation with 1 ml of ice-cold lysis buffer containing 10 mM Tris-HCl (pH 6.5), 50 mM sodium bisulphite, 1% (v/v) Triton X-100, 10 mM $MgCl_2$ and 8.6% (w/v) sucrose. Histones were then isolated from the nuclear fraction by acid extraction, as described previously (Yoshida *et al*., 1990). Briefly, the nuclear pellet was resuspended in 100 μl of ice-cold MQ water and 2.3 μl of 17.6N H_2SO_4 (to give a final concentration of 0.4N), was added to the mixture and vortex mixed for 15 seconds, followed by incubation on ice for 1 hour. The mixture was centrifuged at 14,000 x g for 5 minutes at 4ºC, and the supernatant collected. 1 ml of acetone was added and the sample was incubated overnight in -20ºC. The solution was then

centrifuged at 14,000 x g for 10 minutes at 4ºC, and the pellet was air-dried. Once dried, the pellet was resuspended in 50 µl of MQ water and stored at -20ºC.

2.5 µg of histone lysates were separated on 4-12% SDS-PAGE gels (Invitrogen Australia, Vic., Australia) and transferred onto nitrocellulose membranes (Amersham, Buckinghamshire, UK). Rabbit polyclonal anti-acetylated-H3 (Upstate Biotechnology, Temecula, CA, U.S.A.) antibody (1:1000), was used to detect acetylated-H3 histones. The secondary antibody used for detection of the primary signal was goat anti-rabbit IgG, alkaline phosphatase conjugated at a dilution of 1:5000 in 0.5% (w/v) milk in MQ water. Membranes were then visualised with the Attophos substrate on a FluorImager immediately after addition. Gels were stained for 1 hour with gelstain solution (Invitrogen Australia, Vic., Australia), and destained with MQ water, to control for protein loading.

Osteoclast-related studies

2.14 Osteoclast differentiation of the murine RAW264.7 cell line

The mouse RAW264.7 cell line was obtained from the ATCC and cultured in DMEM, supplemented with 2 mM glutamine, 100 IU/ml penicillin, 160 µg/ml gentamicin, 100 µg/ml streptomycin and 10% (v/v) FBS in a 5% CO_2-containing humidified atmosphere. Cells were seeded into 96-well multiwell plates at 1 x 10^5 cells/ml in triplicates, and allowed to adhere overnight. Treatment with or without LBH589 in the presence or absence of the osteoclastic stimuli, 100 ng/ml RANKL, was continued over 5 days. The medium was refreshed on day 3. All treatments were

conducted in triplicates and repeated at least 3 times. Representative experiments are presented as the mean of triplicates ± SD.

2.15 Osteoclast differentiation and bone resorption by human peripheral blood mononuclear cells (PBMC)

The following experiments were designed to determine the ability for the human PBMC to differentiate into osteoclasts, as well as assessing their bone resorbing activities. Peripheral blood mononuclear cells (PBMC) were isolated from human blood obtained from the Australian Red Cross Blood Bank donors. The procedure employed was based on the Ficoll-Hypaque gradient, as described previously (Fuss *et al*., 2009). This concept is based on the fact that the Ficoll-Hypaque solution has a specific gravity of 1.077, which is denser than lymphocytes, monocytes and platelets, but less dense than granulocytes and red blood cells. This allows successful separation of these respective cell populations by centrifugation, such that the granulocytes and red blood cells sediment to the bottom layer, whilst the lower density lymphocytes, monocytes and platelets are retained at the interface between the plasma and the Ficoll-Hypaque solution. To ensure that the purest population of PBMC were harvested, the monocytic cell layer was collected and another centrifugation process with the Ficoll-Hypaque solution was repeated once more.

The purified PBMC were then cultured in two ways. Firstly, these cells were seeded at a density of 2.5 x 10^5 cells/well (quadruplicates) into 96-well multiwell plates. Secondly, the cells were seeded directly onto whale dentine slices (quadruplicates), which were cut into small (3 x 3 mm) squares and placed inside 96-

well multiwells. Cells were allowed to adhere overnight, prior to the commencement of treatment. Treatment consisted of 50 ng/ml RANKL, 25 ng/ml macrophage colony stimulating-factor (MCS-F), 10^{-8} M dexamethasone and 10^{-8}M 1,25 (OH)$_2$ vitamin D3 in DMEM media. Cells were treated over a 9 day period, with or without LBH589 (0 – 2.5 nM), and the medium was refreshed every 3 days. These experiments were repeated using cells from at least 4 donors, with representative experiments presented as the mean of quadruplicates ± SD.

2.16 Osteoclast function by human giant cell tumours (GCT) of bone

Highly active mature osteoclasts were isolated from Giant Cell Tumours (GCT) of bone to assess the activity of LBH589 against the bone resorbing activities of mature osteoclasts, independently of osteoclast formation. Tissue samples were digested in 2 mg/ml Collagenase (Sigma-Aldrich, St. Louis, MO, U.S.A.), and kept in a humidified incubator at 37ºC with 5% CO_2. Digested cells were then seeded into 96-well multiwell plates (triplicates), at a density of 4 x 10^6 cells/ml, with or without whale dentine slices. Cells were maintained in complete DMEM supplemented with 10% (v/v) FBS, in the presence or absence of LBH589 (0 – 10 nM), over a 5 day period. Culture medium was refreshed on day 3. All treatments were conducted in triplicates and repeated at least 3 times. Representative experiments are presented as the mean of triplicates ± SD.

2.17 Detection of tartrate-resistant acid phosphatase positive (TRAP⁺) osteoclasts in cell cultures

Osteoclastic cells were defined as multinucleated cells with 3 or more nuclei, and those staining for the osteoclast marker, tartrate-resistant acid phosphatase (TRAP). To detect the osteoclast marker, TRAP, a staining kit was used (Sigma-Aldrich, St. Louis, MO, U.S.A.). At the end of each experiment, the supernatant was removed and the cells in each well were fixed in 10% (v/v) buffered formalin for 15 minutes and then washed twice in PBS. Freshly made TRAP stain according to the manufacturer's kit instructions, was filtered using Whatman filter paper, and 50 µl of the filtered TRAP solution was placed into each well. The plate was covered and incubated at 37ºC for approximately 40 minutes. TRAP solution was removed from each well and cells were then gently washed 3x with PBS and allowed to dry overnight. The number of purple-stained osteoclasts with 3 or more nuclei in each well was then counted.

2.18 Detection of resorption pits on whale dentine slices

At the completion of each experiment, the supernatant was removed from each well, leaving only dentine slices, which were washed with extran detergent. After rinsing several times with MQ water, ammonium hydroxide (NH_4OH) was added to each well for 5 minutes to completely rid bone slices of any cell remnants. After several washes with MQ water, the dentine was dehydrated with ethanol, starting at 50%, 70%, 90% then finally 100% (all v/v) ethanol in MQ, for 3 minutes each. Bone slices were left to dry overnight before mounting onto stubs for viewing by scanning electron microscopy (Semenza). Photos were also taken by SEM and the resorption pits counted. Representative experimental results are expressed as mean ± SD.

Osteoblast-related studies

2.19 Preparation of osteoblasts from bone

Normal human bone (NHB; osteoblast-like) cells were cultured as described previously (Atkins *et al*., 2003). Briefly, normal trabecular bone fragments were obtained from patients (70-80 years old), during joint replacement surgery in the Department of Orthopaedics and Trauma at the Royal Adelaide Hospital. All patient sample collections were approved by the Royal Adelaide Hospital Institutional Ethics Committee and informed patient consent was obtained. These fragments were cut into small pieces and placed into 75 cm^2 tissue-culture flasks in complete α-minimal essential medium (α-MEM), supplemented with 10% (v/v) FBS, 100 µg/ml ascorbic acid and 2 mM l-glutamine. Once the flask was confluent with cells from the primary cultures of NHB fragments, single cell suspensions were obtained by enzymatic digestion with 2 mg/ml collagenase for 1.5 hours at 37ºC. Cells were used immediately after digestion.

2.20 Determination of cell density

The crystal violet method was used for detection of normal human bone cell density during mineralisation experiments. The supernatant was gently removed from the cells using a pipette tip and 10% (v/v) buffered formalin was added to the cells for 20 minutes. Wells were washed 3x with PBS and stained with crystal violet. Wells were washed several times with MQ water and allowed to dry overnight before dissolving in acetic acid. The dissolved violet colour was quantitated using an

absorbance reader at a wavelength of 570 nm. This reagent was also used as a co-stain for cell visualisation under light microscopy for the set of experiments, as referred in sections 2.14 – 2.16: Osteoclast related studies.

2.21 Normal human bone (NHB) cell mineralisation

Cells obtained from enzymatic digestion described in section 2.19 were plated at 1×10^5 cells/ml into 96-well multiwell plates (in quadruplicate), and at 1×10^6 cells/ml into 6-well multiwell plates (in duplicate). To induce osteoblast differentiation, the medium was changed 3 days after seeding to complete α-MEM, also containing 10^{-8} M dexamethasone and 1.8 mM potassium phosphate, with or without 2.5 nM LBH589. The medium was replaced every 3 days over a 21 day period. The cell layer-associated calcium levels deposited by these cells were quantified using a calcium kit (Sigma-Aldrich, St. Louis, MO, U.S.A.). At various time points (days 0 (baseline), 1, 3, 7, 14 and 21), the cells in the 96-well plates were washed with PBS and the mineral layer was dissolved in 0.6 M hydrochloric acid (HCl). Calcium content was normalised to BCA^{TM} protein standard (Pierce Chemical co., Rockford, IL, U.S.A.), and absorbance was read at a wavelength of 570 nm. This experiment was repeated at least 8 times using different cells from different donors. Results of representative experiments are expressed as the mean of quadruplicate results ± SD.

2.22 Isolation of RNA

NHB cells were plated into 6-well multiwell plates (in duplicate). At days 0 (baseline), 1, 3, 7, 14 and 21, total RNA was isolated from the cells using 1 ml of Trizol reagent (Life Technologies, Gaithersburg, MD, U.S.A.), per Eppendorf tube (per treatment condition). Tubes were then incubated for 5 minutes at room temperature to allow for further cell lysis. 0.2 ml of chloroform per 1 ml of Trizol was added to each tube, and tubes were capped and vortexed for 15 seconds, then allowed to stand for 5 minutes at room temperature. The tubes were then centrifuged in a refrigerated centrifuge at 4ºC for 15 minutes at 12,000 x g. The upper aqueous phase was transferred to a fresh 1.5 ml Eppendorf tube, and RNA was precipitated by adding 2 µl of glycogen and mixing with 0.5 ml of isopropanol as a co-precipitant, and stored at -20ºC overnight. The samples were then centrifuged at 12,000 x g for 30 minutes at 4ºC. The supernatant was removed and the pellet was washed once with 750 µl of 75% (v/v) ethanol. The tubes were then centrifuged at 12,000 x g for 10 minutes at 4ºC, and the supernatant removed to allow the pellet to dry for 5 minutes. The pellet was then resuspended in 15 µL of RNase-free, diethylpyrocarbonate (DEPC)-treated MQ water (0.1% v/v), and then incubated at 68ºC for 5 minutes to completely dissolve the RNA. The RNA samples were then quantified and stored at -80ºC prior to their use for the preparation of cDNA.

2.23 RNA quantification and cDNA synthesis

RNA samples were allowed to thaw on ice and 2 µl of each sample were used to measure the concentration of RNA per treatment condition using the Nanodrop Bioanalyser. To validate the RNA, ethidium bromide-stained formaldehyde gels were

conducted to confirm that there was no evidence of any significant degradation of the RNA. First-strand complementary DNA (cDNA) was synthesized from 1 µg of total RNA isolated from the NHB cells, using the Superscript kit III (Promega Corp., Madison, WI, U.S.A.), and random primers (Bresagen, Inc., Adelaide, SA, Australia), as per manufacturer's instructions. The RNA was subjected to 3 heat cycles (25ºC, 42ºC and 95ºC), to complete the transcription to cDNA.

2.24 Real-Time PCR

cDNA was then amplified by the polymerase chain reaction (PCR) to generate products corresponding to mRNA encoding human osteoprotegerin (OPG), Runx2, RANKL, alkaline phosphatase (ALP), osteocalcin (OCN), Type-1 collagen and the housekeeping gene, glyceraldehyde-3-phosphate dehydrogenase (GAPDH). mRNA expression of these genes was analysed by real-time PCR using the SYBR Green incorporation technique. Samples were amplified using the SYBR Green Supermix (Bio-Rad Laboratories, Cambridge, MA, U.S.A.), on a Rotor-Gene Thermocycler (Corbett Research, NSW, Australia). GAPDH was chosen as the reference gene to ensure that the various mRNA levels were normalized against the total mRNA content in the samples, as described previously (Atkins *et al*., 2007). PCR was performed for 40 cycles for GAPDH and 45 cycles for each of the other genes, and the PCR reactions were validated by the presence of a single peak in the melt curve analysis. The amplification of OPG, Runx2, RANKL, ALP, OCN and Type-1 collagen mRNA are represented as the ratio of the respective PCR product to the GAPDH PCR product, and the relative expression between samples was calculated as previously described (Atkins

et al., 2007). To show that there were no false-positive results, PCR reactions were also performed using mixtures with no RNA added. The primers used were;

GAPDH: 5'- ACCCAGAAGACTGTGGATGG -3' and

5'- CAGTGAGCTTCCCGTTCAG -3',

Runx2: 5'- CCAAGATCTCCAACATGACT -3' and

5'- TACACCATTAGTTGAAGATACT -3',

OPG: 5'- GCTCACAAGAACAGACTTTCCAG -3' and

5'- CTGTTTTCACAGAGGTCAATATCTT -3'

RANKL: 5'- CCAAGATCTCCAACATGACT -3' and

5'- TACACCATTAGTTGAAGATACT -3'

ALP: 5'- TGCTCCCACGCGCTTGTGCCTGGA -3' and

5'- CTGGCACTAAGGAGTTAGTAAG -3

OCN: 5'- ATGAGAGCCCTCACACTCCTCG-3' and

5'- GTCAGCCAACTCGTCACAGTCC-3'

Type-1 collagen: 5'- AGGGCTCCAACGAGATCGAGATCCG -3' and

5'- TACAGGAAGCAGACAGGGCCAACGTCG -3'

In vivo-related studies

2.25 Reagents

For all *in vivo* use of LBH589, a maximum of 2 mg/ml of LBH589 was dissolved in a 5% (w/v) anhydrous glucose solution (Pfizer Pty. Ltd., WA, Australia) by sonication (water bath at room temperature for 25 minutes), as instructed by the manufacturer. Once formulated, the solution is stable at room temperature for one week. Fresh LBH589 solutions were made weekly. D-Luciferin substrate for live animal monitoring of tumour growth was purchased from Xenogen (Alameda, CA, U.S.A.). Aliquots were stored at -20ºC, and dissolved into 30 mg/ml calcium and magnesium-free PBS immediately before use. The double label reagent, calcein was purchased from Sigma-Aldrich (St. Louis, MO, U.S.A.). 10% (w/v) calcein reagent was prepared into 0.9% (w/v) saline solution buffered with 10% (w/v) sodium bicarbonate, for a final concentration of 10 mg/ml, and stored at 4ºC until use. A dose of 10 mg/kg body weight per mouse was used.

2.26 Animals

Female athymic nude mice at 4 and 8 weeks old, and normal 6 week old balb/c mice (Institute of Medical and Veterinary Services Division, Gilles Plains, SA, Australia), were acclimatized under pathogen-free conditions in the animal housing facility for a minimum period of 1 week prior to the commencement of the experimentatal protocol. The general physical well-being and weight of animals were monitored continuously throughout the experiments. All of the experimental procedures

on animals were carried out with strict adherence to the rules and guidelines for the ethical use of animals in research, and were approved by the Animal Ethics Committees of the University of Adelaide, and the Institute of Medical and Veterinary Science, Adelaide, SA, Australia.

2.27 *In vivo* histone-H3 acetylation detection

6 week old balb/c *nu/nu* mice were injected i.p. with 30 mg/kg of LBH589 and after 4 hours the mice were euthanized by cervical dislocation. The spleen and marrow were isolated for detection of histone acetylation. Bone marrow from the hind legs was collected by flushing with PBS and suspended to a final volume of 10 ml. The spleen was Dounce homogenised briefly (at least 3 strokes) and both the marrow and spleen were centrifuged for 5 minutes at 1000 x g, and the supernatant discarded. The pellet was then resuspended in 1 ml of histone lysis buffer (10 mM Tris-HCl [pH 6.5], 50 mM sodium bisulfite, 1% (v/v) Triton X-100, 10 mM $MgCl_2$ and 8.6% (w/v) sucrose), and homogenised using at least 3 strokes in a Dounce homogeniser. Lysates were centrifuged at 1000 x g for 5 minutes and the nuclear pellet was washed 3 more times by centrifugation with histone lysis buffer and once with 10 mM Tris-HCL with 13 mM EDTA (pH 7.4). Histones were isolated by the acid extraction process, as described previously (Yoshida *et al.*, 1990). Western blot analysis was used to detect the level of histone acetylation of the spleen and marrow. Histone protein determination was measured against the BCA^{TM} Protein Assay Reagent, and 2.5 µg of histone lysate was loaded onto 4-12% SDS-PAGE gels and transferred onto nitrocellulose membranes. Rabbit polyclonal anti-acetylated-H3 antibody (1:1000) was used to detect acetylated-H3 histones. The secondary antibody used for detection of the primary signal was goat

anti-rabbit IgG, alkaline phosphatase conjugated at a dilution of 1:2000 in 0.5% (w/v) milk in MQ water. Membranes were then visualised on a FluorImager immediately after addition with an Attophos substrate. Gels were incubated for 1 hour with Gelstain solution and destained with water, as a control for protein loading.

2.28 The effect of LBH589 on orthotopic breast cancer

MDA-MB231-TXSA human breast cancer cells were cultured as described in section 2.1, until they reached 60-70% confluency. Adherent cells were removed from flasks with 2 mM EDTA and resuspended in 1 x PBS at $1x10^6$ cells/10 µl and kept on ice in an Eppendorf tube. An equal volume of Matrigel™-HC (BD Biosciences, Bedford, MA, U.S.A.), was added to the resuspended cells. A total of thirty 8 week old mice were anaesthetised with Isoflurane (Faulding Pharmaceuticals, SA, Australia), and the mammary fat pad area of the mice was wiped with ethanol and the skin was lifted over the left outermost nipple. Finally, a 26 gauge needle was inserted, and 20 µl of cells were injected into the mammary fat pad. Mice were allowed to recover under the heat lamp before being transferred into three cages at random with 10 mice per cage. Treatment commenced 1 week post cancer cell transplantation with either vehicle, 15 mg/kg of LBH589 (i.p.), or 50 mg/kg of SAHA (i.p.).

2.29 The effect of LBH589 on breast cancer-induced bone destruction

Cells were prepared for injections as described above. Cells were resuspended at $1x10^8$ cells/ml in 1 x PBS, and kept on ice until inoculations. To reduce air bubbles,

cells were drawn up with a Hamilton syringe (Alltech Associates, NSW, Australia), without the needle attached, then a 26 gauge needle was attached to the syringe and finally the cells were slowly pushed down into the needle. This process was repeated to allow 10 µl of cells to be injected below the knee. The tibiae were wiped with ethanol and the cells were injected into the left tibial marrow cavity of 4 week old athymic nude mice, anaesthetised with isoflurane. Mice were allowed to recover under the heat lamp before being randomised into four cages of 10 animals. Treatment with the vehicle, 15 or 30 mg/kg of LBH589 (i.p.), or 50 mg/kg of SAHA (i.p.), commenced 4 days post cell transplantation.

2.30 *In vivo* bioluminescent imaging (BLI)

Non-invasive, whole body imaging to monitor luciferase-expressing MDA-MB231-TXSA cells in mice was performed weekly using the IVIS 100 Imaging system (Xenogen, Alameda, CA, U.S.A.). Thirty minutes before analysis, mice were injected with 100 μl (i.p.) of the D-Luciferin solution at a final dose of 3 mg/20g mouse body weight, and then gas-anaesthetized with isoflurane. Images were acquired for 1-30 seconds from the front angle (mammary fat pad injections), and side angle (intratibial injections), and the photon emission transmitted from mice was captured and quantitated in photons/sec/cm^2/sr using the Xenogen Living image software (Igor Pro version 2.5).

2.31 Ex-vivo micro-computed tomography (μ-CT)

High-resolution μ-CT was used to assess the extent of bone destruction caused by intratibial transplants of breast cancer cells. Tibiae were surgically resected into 10% (v/v) buffered formalin. For scanning, each tibia was secured in a specimen tube and placed into the tube holder of the SkyScan-1072 X-Ray μ-CT scanner (SkyScan, Kontich, Belgium). Scanning of each tibia was performed at the highest resolution of 5.2 microns/pixel, with scanning parameters 0.5 mm aluminium filter, 80 kV, 120 mA, 0.8 rotation step, with 4 images taken per 1 second. Imaging time per tibiae was approximately 2 hours.

2.32 Bone volume analysis

The tibial bone cross sections were reconstructed using a cone-beam algorithm (software cone reconstruction, SkyScan, Kontich, Belgium). Image files were converted from TIFF to BMP files using the NRecon software at optimum image quality. Using the 2D images obtained, 730 slices, starting from the growth plate/tibial interface and moving down the tibia were selected for bone volume analysis, using the CTAn software (SkyScan, Kontich, Belgium). For quantification, all data sets were acquired by selecting 2 seperated regions of interest, one for total bone and another for analysing trabecular structures, to determine 3D bone morphometric parameters. Graphs representing total bone and trabecular bone volumes were generated and compared to the contralateral, non-tumour bearing tibiae. 3D images of representative tibiae were generated using ANT software (SkyScan, Kontich, Belgium).

2.33 Histology

Tibiae were fixed in 10% (v/v) buffered formalin (at least 7 days at 4°C), followed by 10-12 weeks of decalcification in 0.5 M EDTA/0.5% (v/v) paraformaldehyde in PBS, pH 8.0 at 4°C. Complete decalcification was confirmed by radiography and tibiae were then paraffin embedded and H&E stained (by the Pathology Division, IMVS, Hanson Institute, SA Pathology, Adelaide, Australia). Five micron longitudinal sections were prepared in paraffin and stained with the TRAP reagent kit (Sigma-Aldrich, St. Louis, MO, U.S.A.). The corresponding H&E and TRAP stained slides were imaged at 40x magnification on the NanoZoomer C9600. Analysis was performed using the software; the NanoZoomer digital Pathology Scanner (NDP) system (Hamamatus Photonic K.K, Systems Division, Japan), and TRAP$^+$ cells were manually counted.

2.34 The effect of LBH589 on normal bone metabolism

To determine its effects on normal bone metabolism, 30 mg/kg LBH589 was injected (i.p.) into 6 week old balb/c mice for 5 consecutive days, with 2 days break, for a period of 4 weeks. Vehicle-treated mice were injected with 5% (w/v) glucose solution only. Animals were anaesthetised with isoflurane. High-resolution, live animal μ-CT (SkyScan 1076 live μ-CT, Belgium), scanning of the left tibiae was performed 1 day prior to commencement of treatment, and at 2 weeks after the commencement of treatment. Scanning of each tibia was performed at the highest resolution of 9 microns/pixel, with scan parameters of 1 mm Aluminium filter, 60 kV, 100 mA, 0.8 rotation step with 1 image taken per second. These settings allowed for the minimum amount of radiation exposure to the animals, with a scanning time of approximately 20

minutes. All animals were labelled with 10 mg/kg calcein (i.p.) at 6 and 2 days prior to euthanasia, to determine osteoblastic bone formation. Upon completion of the experiment, both the hind legs (femur and tibia) were resected for each animal and stored in 10% (v/v) buffered formalin at 4ºC for 7 days, then transferred into PBS ready for histomorphometric analysis using resin embedded sections.

2.35 Histomorphometric analysis of tibiae and femurs

Processing of bones for polymerisation in resin was kindly performed by Ms. Rebecca Sawyer from the Endocrine Bone Research Laboratory, Chemical Pathology, SA Pathology (SA, Australia). Briefly, the required section of each bone was cut using a diamond edged slow speed saw, and dehydrated in ethanol (with successive changes of 70, 80, 90, then 100% [v/v]) for 1 hour each. Bones were then placed at 4ºC in a softening solution of methyl methacrylate (MMA) and polyethylene glycol for 14 days, prior to polymerisation with peroxydicarbonate in a heated water bath at 37ºC for 24 hours. Resin blocks were mounted onto aluminium blocks using Araldite glue and cut into 5 micron sections on the Polycut instrument (Hanson Institute, SA Pathology, Adelaide, Australia). Each section was gently placed onto glass slides for visualisation of dynamic measures of the double-labelled calcein using a UV-fluorescent microscope (Hanson Institute, SA Pathology, Adelaide, Australia). Images were captured at 40x magnification and each double-labelled section of the trabeculae was manually quantitated.

2.36 Statistical analysis

Experiments were performed in triplicate unless otherwise stated, and data presented as mean ± SD. All statistical analysis was performed using SigmaStat for Windows version 3.0 (Systat Software, Inc., Port Richmond, CA, U.S.A.) using a two-tailed distribution, unpaired Student's t-test. In all cases, $p < 0.05$ was considered statistically significant.

Chapter 3. The effects of LBH589 on human breast cancer cells *in vitro*

3.1 Introduction

Breast cancer is the most common malignancy in women, and for Australia, it is estimated that approximately 36 women are diagnosed with breast cancer every day (BCS, 2011). About $70 - 80\%$ of breast cancers are $ER\alpha^+$, therefore offering clinicians first-line treatments that modulate oestrogen signalling, such as Tamoxifen (anti-oestrogen), or more recently, aromatase inhibitors, such as Letrozole or exemestane (Abo-Touk *et al*., 2010, EBCTCG, 2001). The effectiveness of hormonal therapy relies on the expression of the $ER\alpha$. Several studies, including clinical trials, have demonstrated that patients expressing both the $ER\alpha$ and PR have improved clinical outcomes compared with patients with low expression of both receptors (Bardou *et al*., 2003). However, patients treated long-term with hormonal therapy can develop resistance, described as "endocrine-resistant disease". Moreover, patients lacking the $ER\alpha$ ($ER\alpha^-$) are non-responsive to hormonal manipulation (Massarweh and Schiff, 2007). Hormone therapy is dependent upon optimum intrinsic cell signalling. For example, processes involving cell survival, signal through molecules such as Bad or Bcl_2, while those involving cell proliferation, signal through the epidermal growth factor receptor type 2 (HER2). Both signalling pathways are important in determining the efficacy of hormone therapy (Brodie and Sabnis, 2011). It has been proposed that aberrant intrinsic cell signalling events, and/or polymorphisms in drug metabolising enzymes, may contribute to the resistance to the therapeutic benefits from hormonal therapy (Riggins *et al*., 2007, Yue *et al*., 2007, Hoskins *et al*., 2009), which is well documented for the hepatic CYP2D6 (Hoskins *et al*., 2009). In addition, up-regulation of the $ER\alpha$ transcription factors (such as, NF-κB, AP1), or mutations to the $ER\alpha$, and truncated $ER\alpha$-variant ($ER\alpha36$), have also been reported to confer resistance to hormone therapy (Zhou *et al*., 2007b, Ring and Dowsett, 2004, Musgrove and

Sutherland, 2009). Therefore, there are many challenges associated with mammary cancer research. The development of more specific markers to predict responses to hormonal therapy, together with the development of new combined targeted therapies towards hormone-insensitive tumours, are of the highest priority.

In recent years, epigenetic modulation by HDIs in breast cancer cells has gained greater attention due to the findings of increased HDAC expression in early tumour development and the hypoacetylation status of histone-H4 in breast cancer, compared to normal mammary epithelial cells (Suzuki *et al*., 2009). In the context of tumour progression, the same authors also demonstrated a decrease in HDAC1, HDAC2 and HDAC6 protein levels in breast cancer. However, this reduction was not correlated with a decrease in histone acetylation, suggesting that the expression of other HDACs (not analysed in the study), may be increased during breast cancer development, leading to the global reduction in histone acetylation. Several authors have correlated the expression of HDAC1, HDAC3 and HDAC6 to ERα$^+$ invasive breast tumours, and the expression of HDAC1 and HDAC6, in early, less aggressive tumours, is associated with a better prognosis, but not necessarily a better overall survival (Krusche *et al*., 2005, Zhang *et al*., 2005b, Zhang *et al*., 2004). In summary, the data suggest a potential role for HAT and HDAC deregulation in breast cancer progression, with the possibility that modulation through HDAC inhibition may offer new therapeutic approaches.

In breast tumour models, HDIs were shown to induce potent anti-proliferative and cytotoxic effects *in vitro* and *in vivo* (Margueron *et al*., 2004, Vigushin *et al*., 2001, Bolden *et al*., 2006). The anti-proliferative effects of pan-DAC inhibitors were found to be more potent in ERα$^+$ mammary cells than ERα$^-$ cells, and such effects were likely to be associated with a more pronounced induction of the cell cycle inhibitor, p21 (Margueron *et al*., 2004, Ocker and Schneider-Stock, 2007). This may, in part, explain

the difference in HDI-mediated anti-proliferation according to the ER status. Furthermore, apoptosis induction of cell lines, including MDA-MB231 (ERα^-), MCF-7 (ERα^+) and BT-474 (ERα^+), by VPA, MC1568, MC1575 and SAHA, was associated with a reduction in the cell survival proteins, survivin, Bcl$_2$, and induction of pro-apoptotic proteins, Bak and Bim, and p21 (Bali et al., 2005, Duong et al., 2008, Zhang et al., 2011). In addition to the intrinsic modulation by HDIs, apoptosis of breast cancer cells can also be induced by extrinsic signalling, observed through the up-regulation and engagement of death receptors (Chopin *et al.*, 2004), as well as synergistic co-operation and enhancement of cytotoxicity with chemotherapeutic agents (Ranney *et al.*, 2007, Linares *et al.*, 2011). In addition to direct anticancer effects, VPA was shown to induce expression of the ERα and its function in the ERα^- cell line, MDA-MB231, therefore restoring its sensitivity to Tamoxifen (hormonal) therapy (Fortunati *et al.*, 2010). Additionally, LBH589, LAQ824 and SAHA were shown to re-sensitise ERα^+ breast cancer cells to ERα antagonists by hyperacetylation of Hsp90, leading to the depletion of ERα through polyubiquitination (Fiskus *et al.*, 2007, Yang *et al.*, 2008). Specifically, with regards to LBH589 and breast cancer, the literature describes the potent anti-tumour activity, as well as synergistic efficacy when combined with breast cancer-targeted drugs. It was shown that LBH589 targets different pathways and signalling cascades that contribute to breast cancer cell death, including GRP78 acetylation, through the inhibition of HDAC6, leading to endoplasmic reticulum stress, thus inducing cell death (Rao *et al.*, 2010). Furthermore, induction of pro-apoptotic proteins, such as, Bak, Bim and Bak have also been implicated in LBH589-mediated breast cancer cell death (Linares *et al.*, 2011, Rao *et al.*, 2010). Sensitisation to Tamoxifen therapy in MDA-MB231 cells was achieved by inducing the mRNA and protein expression of the ERα without altering the DNA promoter hypermethylation

(Zhou *et al*., 2007a). In particular, with hormone-dependent breast cancers, LBH589 (at 25 nM) was shown to be a potent inhibitor of aromatase expression through its promoter-specific region (Chen *et al*., 2010). Aromatase is an enzyme that converts androgens to oestrogens, and pharmacological inhibition of aromatase (through aromatase inhibitors such as Letrozole), is associated with severe oestrogen deprivation, leading to a loss of bone density (Tomao *et al*., 2011). The authors in this study reported that only one-fifth of the amount of Letrozole was required when used in combination with LBH589 to generate a similar anti-proliferative response in breast cancer cells. This suggested a synergistic relationship, and a need for further clinical evaluation for the use of HDIs in hormone-dependent breast tumours (Chen *et al*., 2010).

Taken together, the literature demonstrates that HDIs have potent anti-tumour effects in breast cancer, targeting both ERα^+ and ERα^- cells, and this presents potential avenues for further investigation and clinical trials using HDI therapy. Therefore, the work described in this chapter aimed to determine the effects of LBH589 using a panel of human breast cancer cell lines. As a prelude to the subsequent *in vivo* experiments to assess the anticancer efficacy of LBH589, the cell line MDA-MB231-TXSA was fully characterised to develop an understanding of the molecular events governing LBH589-induced cytotoxicity.

3.2   Results

3.2.1 The effect of LBH589 on the viability of human breast cancer cells *in vitro*

A panel of 7 human breast cancer cell lines was examined for their sensitivity to the cytotoxic effects of LBH589. As shown in figure 3-1, LBH589 induced a dose-dependent decrease in cell viability after 48 hours of treatment in all cell lines tested. The concentration of LBH589 that induced 50% loss of viability (IC_{50}) was determined for each cell line, and is summarised in Table 3-1. The cell lines that were most sensitive to LBH589 appear to be MDA-MB453, with an IC_{50} of 7 nM and T47D, (IC_{50} 25 nM), followed by MDA-MB231-TXSA and MDA-MB231, both with an IC_{50} of 50 nM. MDA-MB468 (IC_{50} 75 nM) and MCF-7 (IC_{50} 85 nM) were less sensitive to the effects of LBH589, with ZR75 being the least sensitive, with an IC_{50} of 250 nM.

To investigate whether LBH589 was mediating its effects by inducing apoptotic cell death, DEVD-caspase-3 activity was also measured for each cell line after 48 hours exposure to the same doses. Figure 3-2 shows a dose-dependent increase in caspase-3 activity to LBH589 for all cell lines after 48 hours of treatment. In cell lines MDA-MB231-TXSA, MDA-MB453, ZR75 and MDA-MB231, caspase-3 induction was associated with the dose at which cell death had commenced. For the remaining cell lines, induction of significant caspase-3 activity was related to the corresponding IC_{50}, or occurred at higher doses, suggesting that other mechanisms may be responsible for LBH589-induced apoptotic cell death.

Figure 3-1. The viability of human breast cancer cells against LBH589. Seven human breast cancer cell lines were seeded into 96-well multiwell plates at 1×10^{4} cells/well, and treated with increasing doses of LBH589, as indicated. Cell viability was assessed by CellTitre-Blue reagent 48 hours after treatment. LBH589 reduced cell viability in all cell lines tested, with IC_{50} values ranging between 7-250 nM. Data bars (± SD) show means of triplicate results from a representative experiment, each repeated at least 3 times. Error bars are within the dimensions of the respective data bars.

Breast cancer cell line	IC_{50} (nM)
ZR75	250 ± 31
MDA-MB453	7 ± 0.4
T47D	25 ± 0.7
MDA-MB231	50 ± 10
MCF-7	85 ± 9
MDA-MB468	75 ± 2
MDA-MB231-TXSA	50 ± 4

Table 3-1. The IC_{50} of LBH589 generated against a panel of human breast cancer cell lines. Values are expressed $\pm$ SD of the means of the IC_{50} obtained from triplicates of each experiment, repeated 3 times.
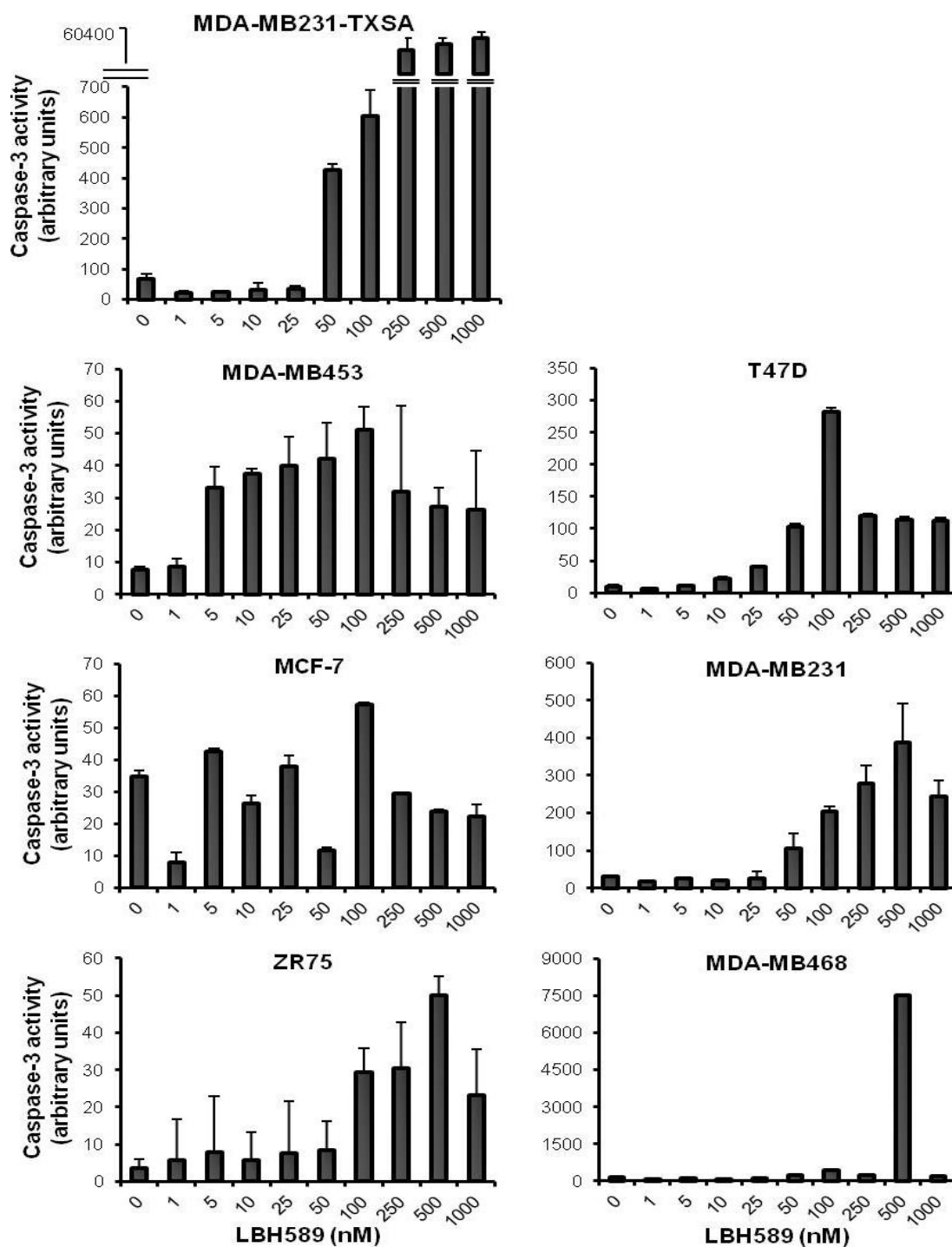
Figure 3-2. Caspase-3 activity of human breast cancer cells induced by LBH589. Cells were treated with increasing doses of LBH589, as indicated. Cell lysates were used to determine caspase-3 activity using the caspase-3 fluorogenic substrate, zDEVD-AFC, as described in the Materials and methods. Data bars (± SD) show means of triplicate results from a representative experiment, each repeated at least 3 times. Error bars are within the dimensions of the respective data bars.

To examine the time-dependency of the response to LBH589, cells were treated over a 48 hour period using the corresponding IC_{50} doses of LBH589 (as indicated in table 3-1). Cell viability and DEVD-caspase-3 activity were measured at times 0 (baseline, control), 6, 12, 24 and 48 hours after treatment. Figure 3-3 depicts the decrease in viability during the course of LBH589 treatment, observed from 24 hours onwards in all cell lines except MDA-MB231-TXSA, where a reduction in viability was evident by 12 hours. This compares to each untreated controls, which demonstrates the steady increase in viability when cultures were left untreated over the same period, indicating the apoptotic effects of LBH589. Concomitant with the loss of cell viability, there was a time-dependent increase in DEVD-caspase-3 activity with LBH589 treatment in all cell lines. Figure 3-4 shows the time-dependent caspase-3 activity of each cell line when treated with LBH589 at its corresponding IC_{50}, expressed as a percentage of control. Consistent with figure 3-2 (dose-response curves after 48 hours treatment), the MDA-MB231-TXSA, MDA-MB453, MDA-MB468 and MDA-MB231 cell lines exhibit the most pronounced increase in caspase-3 activity starting from 12 hours after treatment. ZR75, T47D and MCF-7 demonstrate a later caspase-3 response starting from 24 hours after treatment.
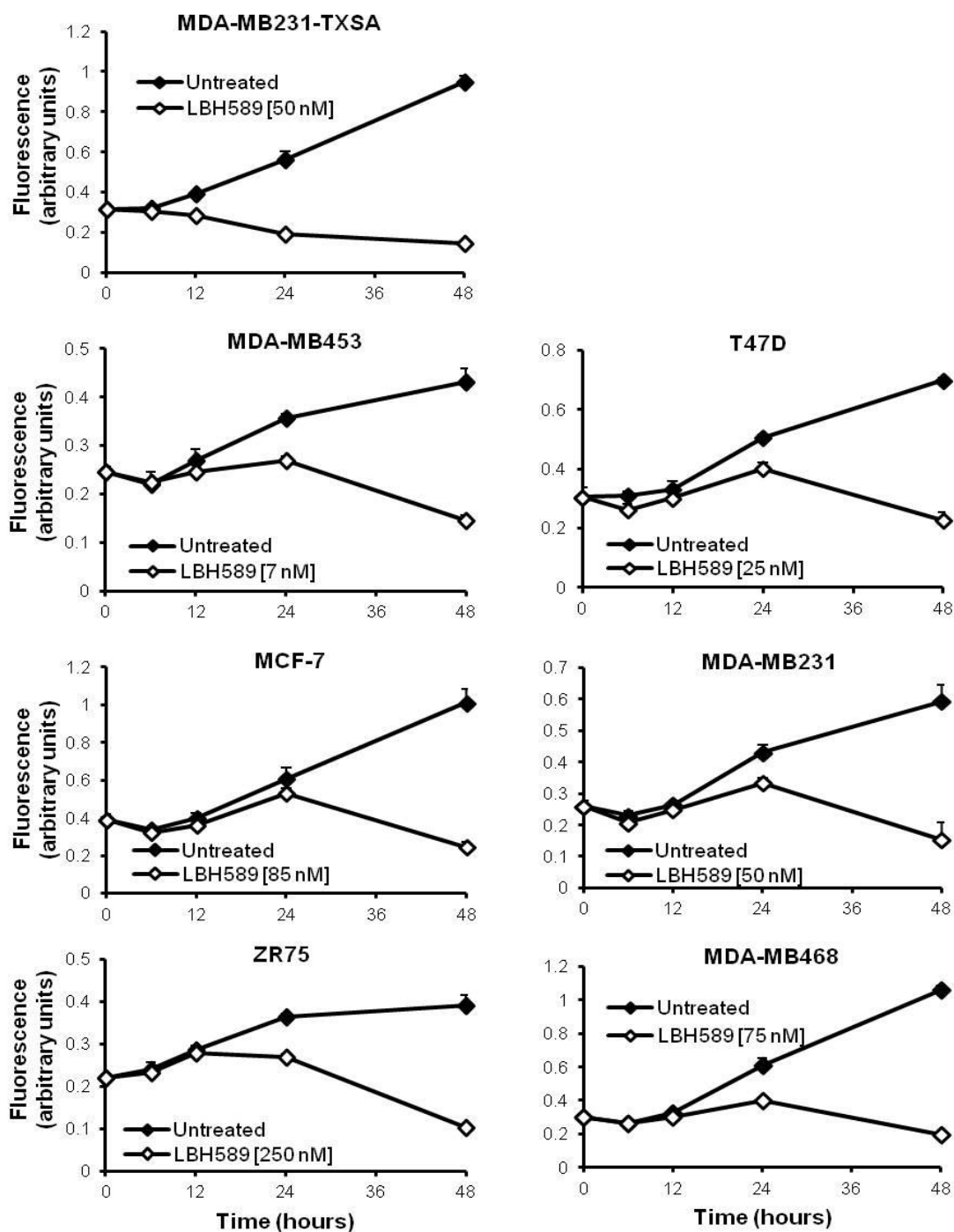
Figure 3-3. Time-dependent activity of LBH589 against human breast cancer cell viability. Cells were left untreated or treated with the IC_{50} of LBH589, as indicated in Table 3-1 for each cell line. Cell viability was determined with CellTitre-Blue reagent at times 0, 6, 12, 24 and 48 hours after treatment. Data points ($\pm$ SD) show means of triplicate results from a representative experiment, each repeated at least 3 times. Error bars are within the dimensions of the respective data points.
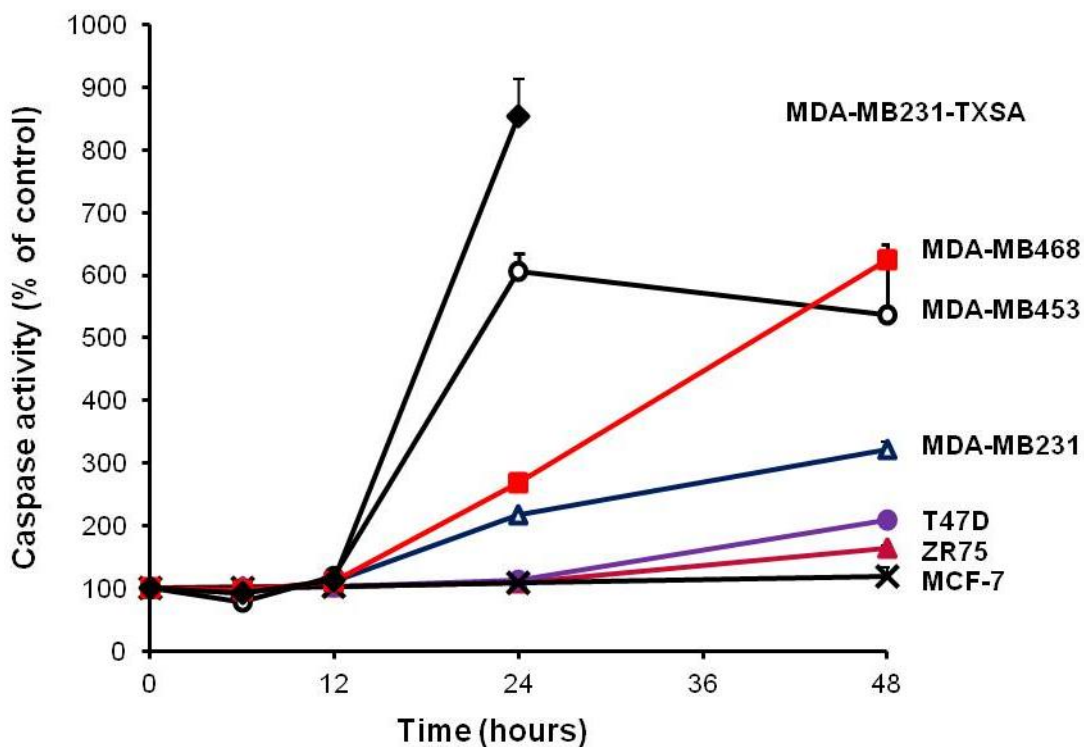
Figure 3-4. Time-dependent caspase-3 activity of human breast cancer cells induced by LBH589. Cells were treated with the IC_{50} of LBH589, as indicated in Table 3-1 for each cell line. Cell lysates were used to determine caspase-3 activity at times 0, 6, 12, 24 and 48 hours. LBH589 induced a time-dependent caspase-3 response in all cell lines tested. Data points ($\pm$ SD) show means of triplicate results from a representative experiment, repeated at least 3 times, and expressed as a percentage of cells isolated at time 0 hour (control). Error bars are within the dimensions of the respective data points.

Further to examining the cytotoxicity of LBH589 in tumour cells, osteoblast-like primary cells derived from human bone (NHB cells) were also treated with LBH589 for 72 hours. This experiment was conducted as it has been shown that a wide variety of HDIs, including inhibitors from the hydroxamate class, have no significant effect on normal cells. Studies using neonatal foreskin fibroblasts (NFF) and normal human melanocytes (NHM), demonstrated that HDIs trigger a G2/M cell-cycle checkpoint response in normal cells, whereas this checkpoint is defective in tumourigenic cells, suggesting that an intact cell-cycle checkpoint is responsible for the resistance observed in normal human cells to HDI treatment (Parsons *et al*., 1997, Qiu *et al*., 2000, Qiu *et al*., 1999). Therefore, in this study, normal human bone cells were chosen for two reasons. Firstly, they were chosen as a prelude to the planned *in vivo* sets of experiments, in which breast cancer cells are transplanted directly into the tibial marrow cavity of mice. Therefore, it was important to determine the response of normal cells to LBH589 treatment. Secondly, while in clinical trials, HDIs are administered systemically, the effect of HDIs, including LBH589, on human osteoblasts has not yet been reported. In this experiment, several normal bone donors were examined for their sensitivity to LBH589. An important attribute of LBH589 is its apparent selectivity in toxicity for cancer cells over normal cells, with a greater than 60% cell survival at a high dose of 250 nM (figure 3-5). When compared to figure 3-1, the IC_{50} doses for tumour cells range between 7 – 250 nM, indicating that the doses that suppress tumour growth do not result in significant growth suppression of normal cells.
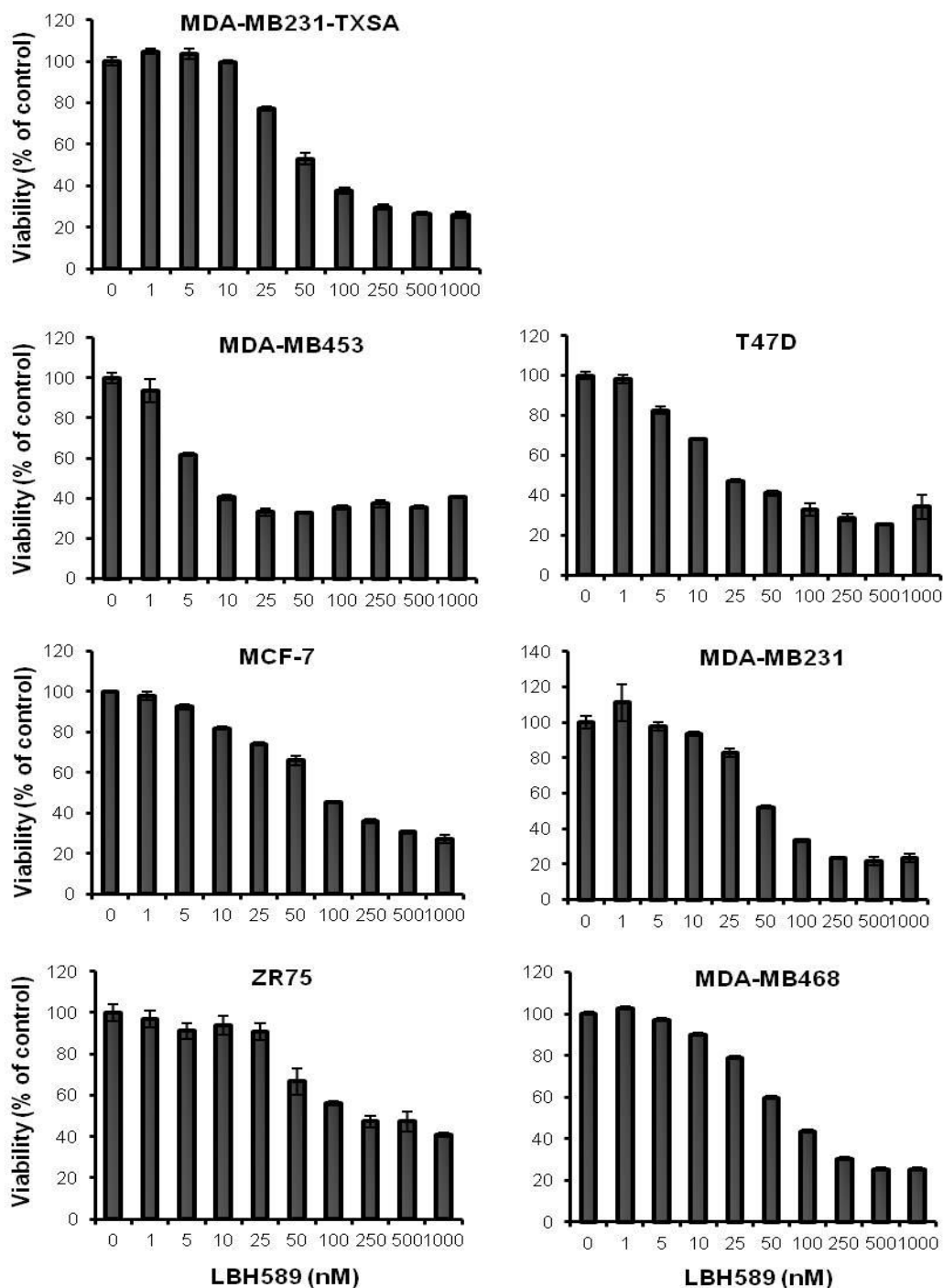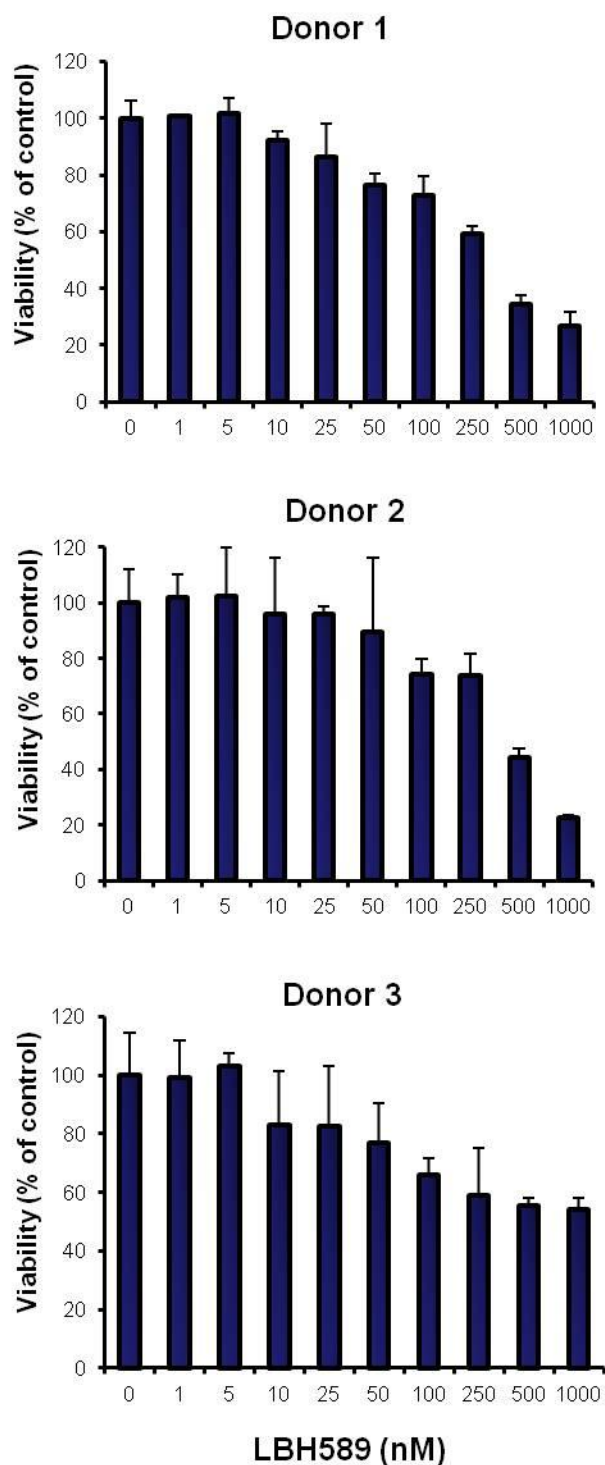
Figure 3-5. The viability of human bone cells against LBH589. Normal human bone cells were seeded into 96-well multiwell plates and treated with increasing doses of LBH589, as indicated. Cell viability was determined with the CellTitre-Blue reagent 72 hours after treatment. Data bars (± SD) show means of quadruplicate results from a representative experiment from 3 independent donors, repeated at least five times.

3.2.2 LBH589 suppresses the growth of MDA-MB231-TXSA breast cancer cells and induces cell death characteristic of apoptosis

As a prelude to the *in vivo* study for testing the anticancer efficacy of LBH589 in breast cancer development and progression, the human MDA-MB231-TXSA breast cancer cell line was selected for a detailed analysis. This cell line forms aggressive, rapidly growing tumours when injected into the orthotopic site of the mammary fat pad of nude mice, and stimulates the formation of osteolytic lesions when injected into the tibial marrow cavity (Thai le *et al*., 2006). Treatment with LBH589 inhibited the growth of MDA-MB231-TXSA breast cancer cells in a dose and time-dependent manner (figure 3-6A and B). Further analysis showed that LBH589 dose-dependently inhibited cell proliferation over a 72 hour period (at concentrations of 1 and 5 nM), as determined by trypan blue dye exclusion assay, with low levels of detectable cell death. However, at concentrations of 25 nM and 50 nM, LBH589 caused complete growth suppression within 24 hours, with continued cell death over the next 48 hours (figure 3-7A and B). Morphological evidence of apoptosis was confirmed by DAPI and Phalloidin staining of cells treated with LBH589. The nuclei and cytoskeletal staining of the MDA-MB231-TXSA breast cancer cells shows morphological changes indicative of apoptosis, including chromatin condensation, nuclear fragmentation and modifications to the cytoskeleton (figure 3-8).
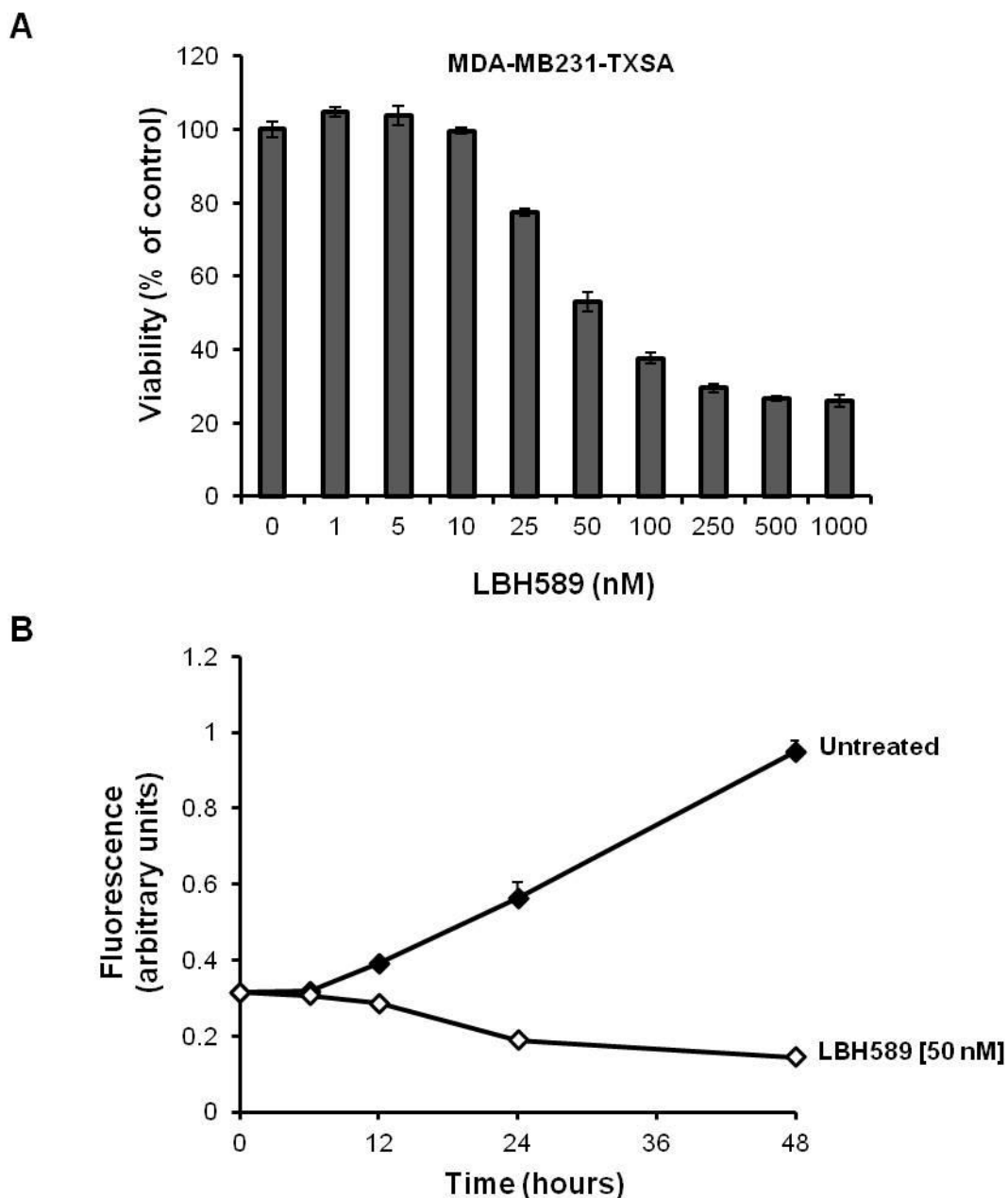
Figure 3-6. Pro-apoptotic activity of LBH589 against MDA-MB231-TXSA breast cancer cells *in vitro*. A). Cells were treated with increasing doses of LBH589, as indicated. Cell viability was determined with the CellTitre-Blue reagent 48hrs after treatment. **B**). Cells were treated with or without 50 nM of LBH589, and viability measured at times 0, 6, 12, 24 and 48 hours. Data points (± SD) show means of triplicate results from a representative experiment, repeated at least 3 times. Error bars are within the dimensions of the respective data points.
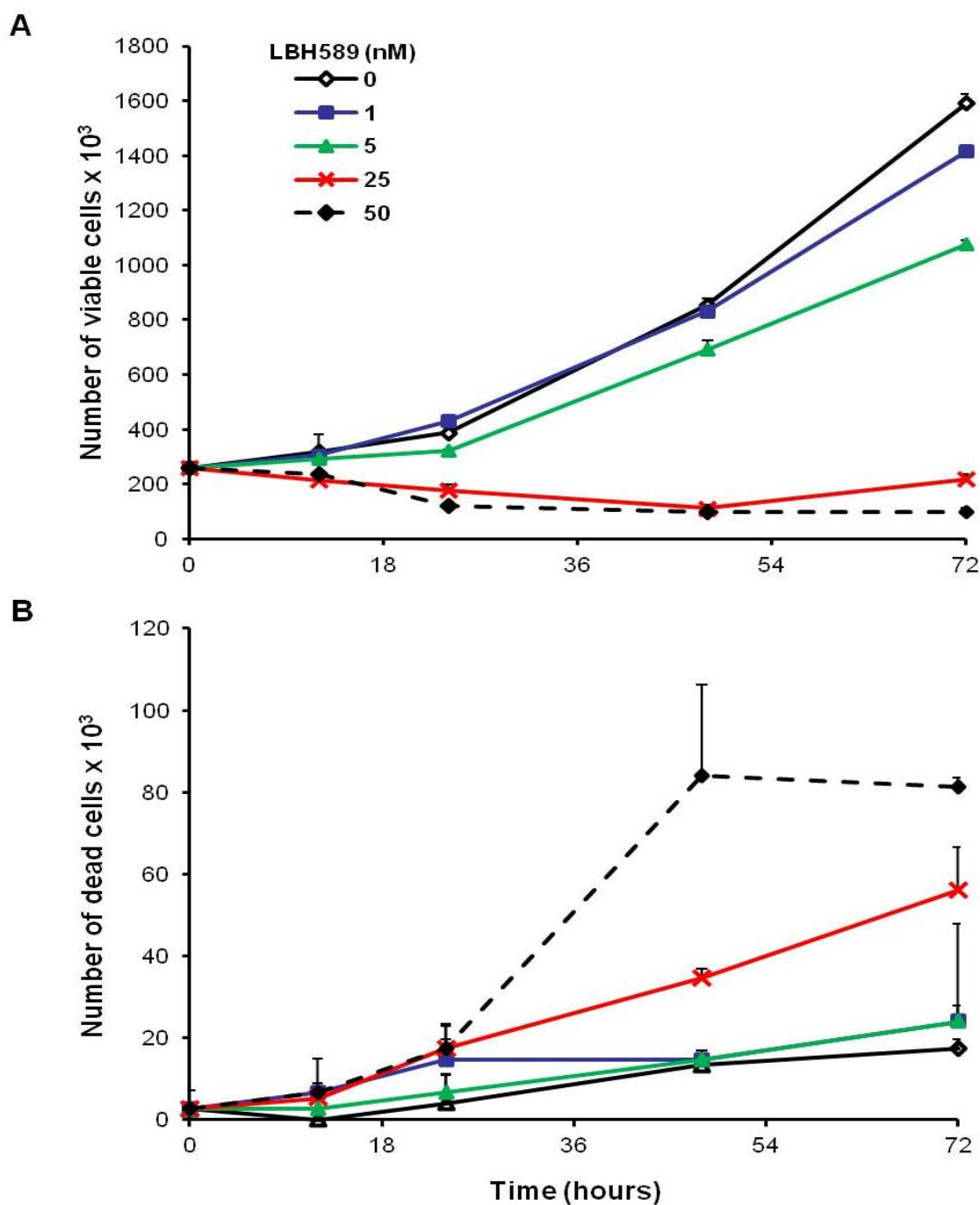
Figure 3-7. The effect of LBH589 on the MDA-MB231-TXSA breast cancer cell proliferation. Cells were seeded in 24-well multiwell plates and treated with LBH589, as indicated. Cells were counted at times 0, 12, 24, 48 and 72 hours after treatment using a hemocytometer, and the number of viable cells was determined by trypan blue exclusion. **A**). Shows the number of viable cells and **B**). Shows the number of dead cells present in each culture. Data points (± SD) show means of triplicate results from a representative experiment, repeated at least 3 times. Error bars are within the dimensions of the respective data points.
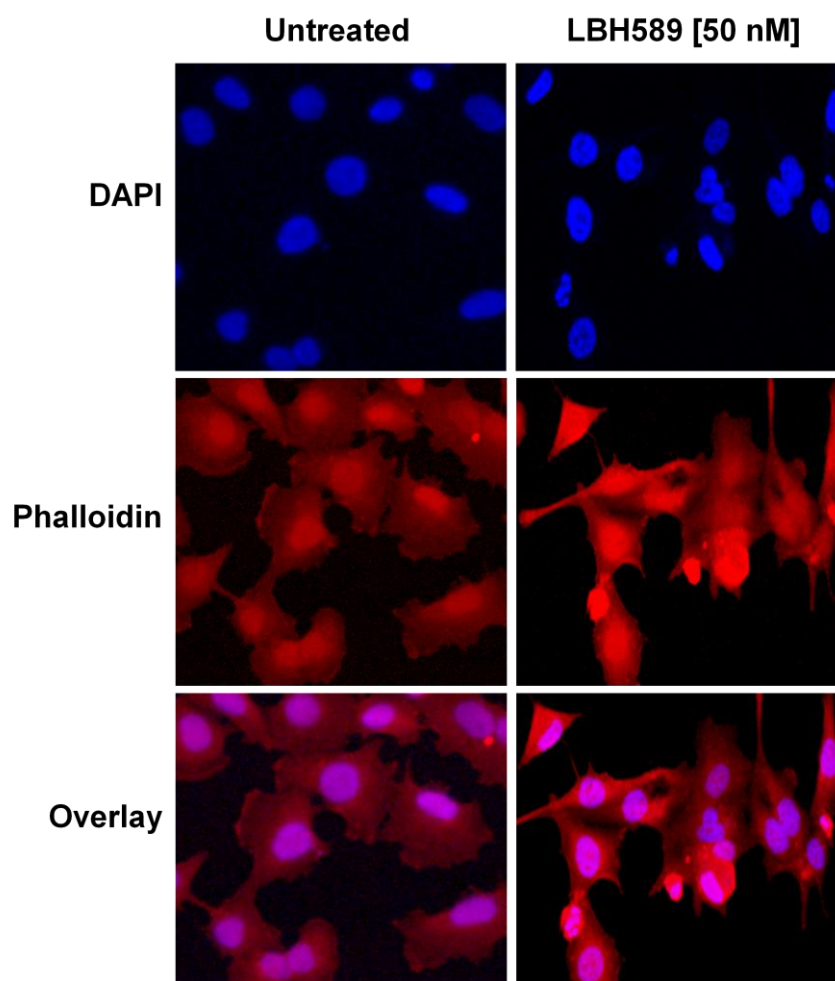
Figure 3-8. LBH589 induces morphological changes in the MDA-MB231-TXSA breast cancer cells. Cells were seeded in chamber slides at 5 x 10^4 cells/chamber, and were treated with 50 nM of LBH589 for 48 hours. Cells were fixed with methanol and incubated with DAPI and Phalloidin staining, as described in the Methods. Cells were visualised by confocal microscopy, using the 20x objective lens.

To further confirm that the reduction in cell viability caused by LBH589 was due to induction of apoptosis and not cellular growth arrest, cells were assayed for DEVD-caspase-3 activity in a time-dependent manner. Figure 3-9 shows the kinetics of DEVD-caspase-3 activity of MDA-MB231-TXSA cells treated with various doses of LBH589, including the IC_{50} (50 nM). The MDA-MB231-TXSA cells showed little induction of caspase-3 activity in the presence of 5 nM LBH589, which is consistent with the lack of cell death observed with trypan blue dye exclusion. There was a moderate increase in caspase-3 activity by 24 hours with a concentration of 25 nM, however at concentrations above, and including the IC_{50} (50 – 250 nM), induced a significant increase in caspase-3 activity. Despite the marked induction in caspase-3 activity, the presence of the pan-caspase inhibitor, zVAD-fmk (50 μM) only marginally protected the cells. There was an approximate 15-30% increase in cell survival at concentrations of 50 – 500 nM (figure 3-10), suggesting the engagement of additional pathways for LBH589-induced cell death.
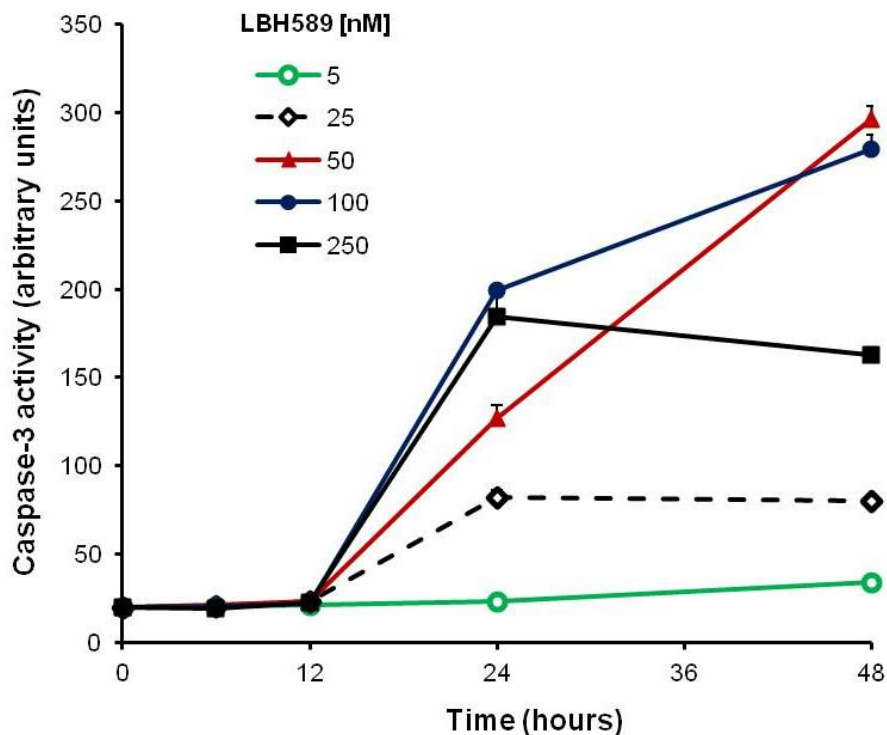
Figure 3-9. Caspase-3 activity of the MDA-MB231-TXSA breast cancer cells induced by LBH589. Cells were seeded in 96-well multiwell plates at 1×10^4 cells/well and treated with LBH589 at the concentrations indicated. Cell lysates were collected at times 0, 6, 12, 24 and 48 hours to determine caspase-3 activity, using the caspase-3 fluorogenic substrate, zDEVD-AFC, as described in the Methods. Data points (± SD) show means of triplicate results from a representative experiment, repeated at least 3 times. Error bars are within the dimensions of the respective data points.
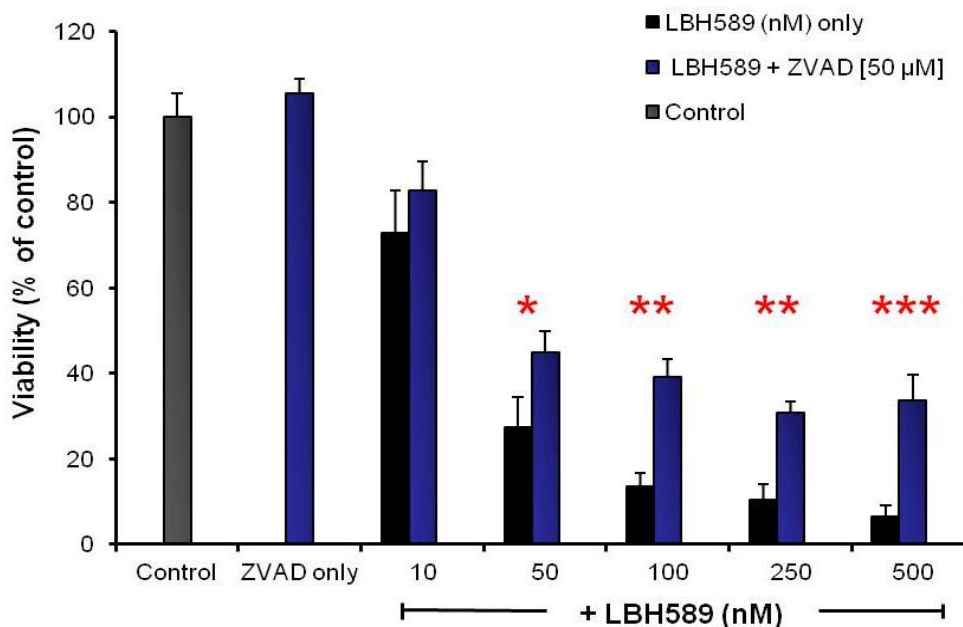
Figure 3-10. LBH589 induces a caspase dependent and independent mechanism of action. Cells were treated with LBH589 alone, or co-incubated with the broad specificity caspase inhibitor; z-ZVAD-fmk (50 μM), as indicated. To exclude possible toxic effects of the inhibitor, cells were also treated with the inhibitor alone. Cell viability was determined using CellTitre-Blue reagent 48 hours after treatment. Data points (± SD) show means of triplicate results from a representative experiment, repeated at least 3 times. Where *control* bar indicates cells with no treatment and, *P < 0.05, **P < 0.005, ***P < 0.0005.

To further clarify the molecular mechanism underlying the LBH589 induced apoptosis, the effects of the HDI on the expression of various proteins known to be involved in the control of apoptosis were investigated by western blot analysis. The primary molecular mechanism of HDI action is to alter the acetylation of the core histone proteins, thus facilitating chromatin remodelling with the subsequent alteration in gene expression for cell differentiation (Bolden *et al*., 2006). In accordance with the actions of HDIs, treatment with LBH589 induced kinetics that showed histone-H3 acetylation as early as 6 hours post treatment and this was sustained for up to 48 hours (figure 3-11). Additionally, p21 induction is a hallmark of HDI-induced cell death, and in agreement with previously published reports (Bolden *et al*., 2006, Johnstone, 2002), LBH589 treatment significantly increased the expression of p21 protein as early as 6 hours after treatment (figure 3-12). Apoptosis induction by LBH589 was also associated with cleavage and activation of the effector caspase-8 (detected starting 12 hours), and the activator caspase-3 (detected at 24 hours), which was concomitant with cleavage of the apoptosis target protein PARP. Evidence of the engagement of the intrinsic apoptotic signalling pathway was demonstrated through the cleavage of the BH-3 domain-only pro-apoptotic protein, Bid, starting at 6 hours post LBH589 treatment. There was no change to the mitochondrial membrane protein VDAC, however, cleavage of the pro-caspase-9 was detected at 12 hours after treatment, illustrating the involvement of the intrinsic mitochondrial apoptotic pathway. Modulation of the anti-apoptotic proteins Bcl_2, Bcl_{xL} and survivin, or the pro-apoptotic proteins Bax, Bmf and AIF was not observed (figure 3-12). Taken together these data demonstrated that LBH589 is a potent cytotoxic drug against breast cancer cells. The mechanisms underlying the effects of LBH589 on cell viability include both apoptosis

induction and a decrease in cell proliferation, as already reported for other HDAC inhibitors (Butler *et al*., 2000, Butler *et al*., 2006).
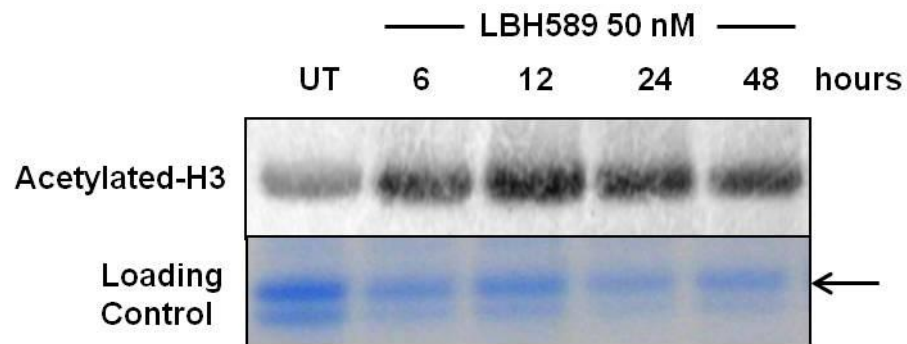
Figure 3-11. LBH589 induces acetylated histone-H3 in the MDA-MB231-TXSA breast cancer cells. MDA-MB231-TXSA cells (1 x 10^6 cells) were treated with 50 nM of LBH589 for the indicated times. Cells were harvested and histones were prepared as described in the Methods. Histone acetylation was detected by western blot using an antibody against acetylated-H3. The *top panel* shows the level of acetylated histone-H3, and the *bottom panel* shows a gelstained polyacrylamide gel of the total histones extracted from the cells. UT = untreated cells.
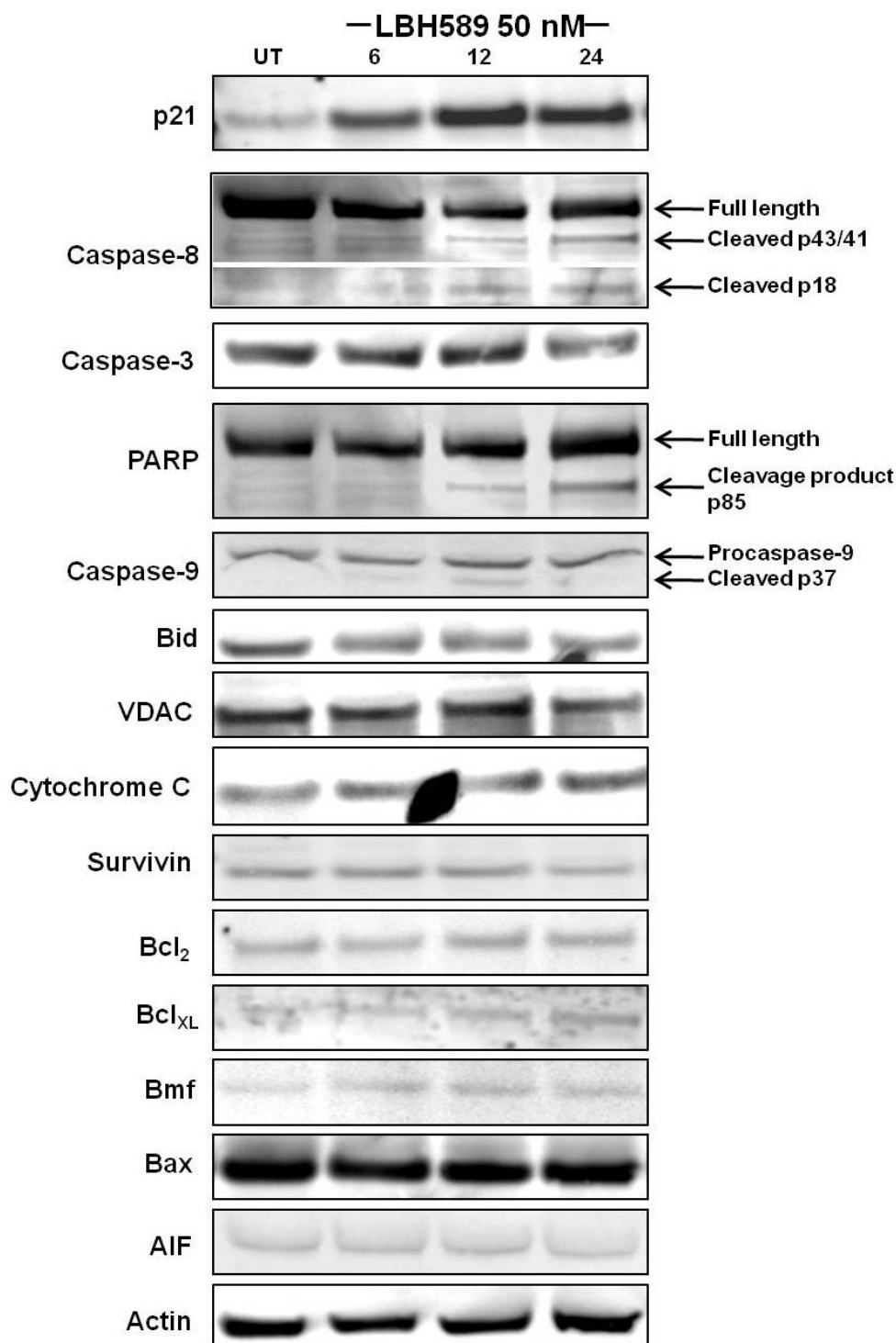
Figure 3-12. Expression of apoptotic and cell cycle regulatory proteins. MDA-MB231-TXSA breast cancer cells were left untreated (UT) or treated with 50 nM of LBH589. Cells were lysed and protein was isolated at 6, 12, and 24 hours after treatment. Cell lysates were analysed by polyacrylamide gel electrophoresis and transferred to PVDF membranes. Each protein was detected using the indicated polyclonal antibodies and HRP-conjugated secondary antibody. The immune complexes were detected using the ECF substrate and visualised using a fluorimager.

3.4 Discussion

The results presented in this chapter demonstrate the potent cytotoxic activity of LBH589 in breast cancer cells, irrespective of ERα status. The mechanisms underlying the effects of LBH589 on cell viability include both apoptosis induction and decrease in cell proliferation as already reported for other HDAC inhibitors (Butler *et al*., 2000, Butler *et al*., 2006). The effect of LBH589 on cell viability was both dose- and time-dependent, and was associated with activation of the caspase cascade. Treatment of the MDA-MB231-TXSA cell line with the IC_{50} concentration of LBH589 (50 nM) induced rapid accumulation of acetylated histone-H3 proteins (within 6 hours), and cell death, in a dose- and time-dependent manner. The observed cell death featured common hallmarks of apoptosis, including, chromatin condensation and/or DNA fragmentation, up-regulation of the pro-apoptotic protein, p21, and induction of caspases; -8, -3 and -9. LBH589-mediated induction of apoptosis was incompletely reversed with the pan-caspase inhibitor ZVAD-fmk, suggesting additional pathways of LBH589-induced cell death may be involved. The rapid accumulation of acetylated histone-H3 following LBH589 treatment is indicative of this being a principal event in the MDA-MB231-TXSA cancer cell apoptotic process.

There are two well-known and functionally separate apoptotic pathways; the 'extrinsic' death receptor pathway and the mitochondrial 'intrinsic' pathway (Johnstone *et al*., 2002, Bolden *et al*., 2006). The extrinsic apoptotic pathway involves the engagement of ligands to their respective death receptors (TNF receptor, TRAIL-DR4/5 receptor), which results in the binding of adaptor proteins (FADD and TRADD) to the intracellular receptor-associated death domain. This in turn recruits and activates proximal membrane 'effector' caspases (8 and 10), which then results in the cleavage of the 'activator' caspases such as caspase-3 and -7. Regulation of these pathways can

be inhibited by c-FLIP, which inhibits effector caspases, while the inhibitor of apoptosis proteins (IAPs), can inhibit both effector and activator caspases. On the other hand, the intrinsic apoptotic pathway involves the disruption of the mitochondrial outer membrane (MOM) permeability, which is activated by stress stimuli such as chemotherapeutic agents, hypoxia and radiation. These agents induce the release of mitochondrial proteins such as cytochrome c, which then interacts with Apaf-1, forming the apoptosome, stimulating the activation of caspase-9. The downstream activator caspases are cleaved by activated caspase-9, resulting in further cleavage of a number of nuclear and cytoplasmic substrates to induce the morphological changes that are characteristic of apoptosis. Figure 3-13 provides a graphical representation of the two apoptotic pathways. Mitochondrial membrane potential is regulated by several anti-apoptotic (Bcl_2 and Bcl_{XL}), and pro-apoptotic (Bak, Bax, Bim, Bad, Bid and Bmf), proteins, which are able to directly inhibit the actions of each other by protein-protein interaction. Even though both pathways are separate in their apoptotic processes, they are also molecularly linked, allowing considerable cross-talk between the two pathways. For example, caspase-8 can cleave Bid to facilitate cytochrome c release from the mitochondria, thereby amplifying the death response given by ligation of death receptors (Green, 2000). Conversely, activators of the intrinsic death pathway can sensitise the cell to extrinsic death ligands, which are well documented for the p53 'master regulator' of the intrinsic apoptotic program (Chipuk and Green, 2006, Pani and Galeotti, 2010, Tomita *et al.*, 2006).
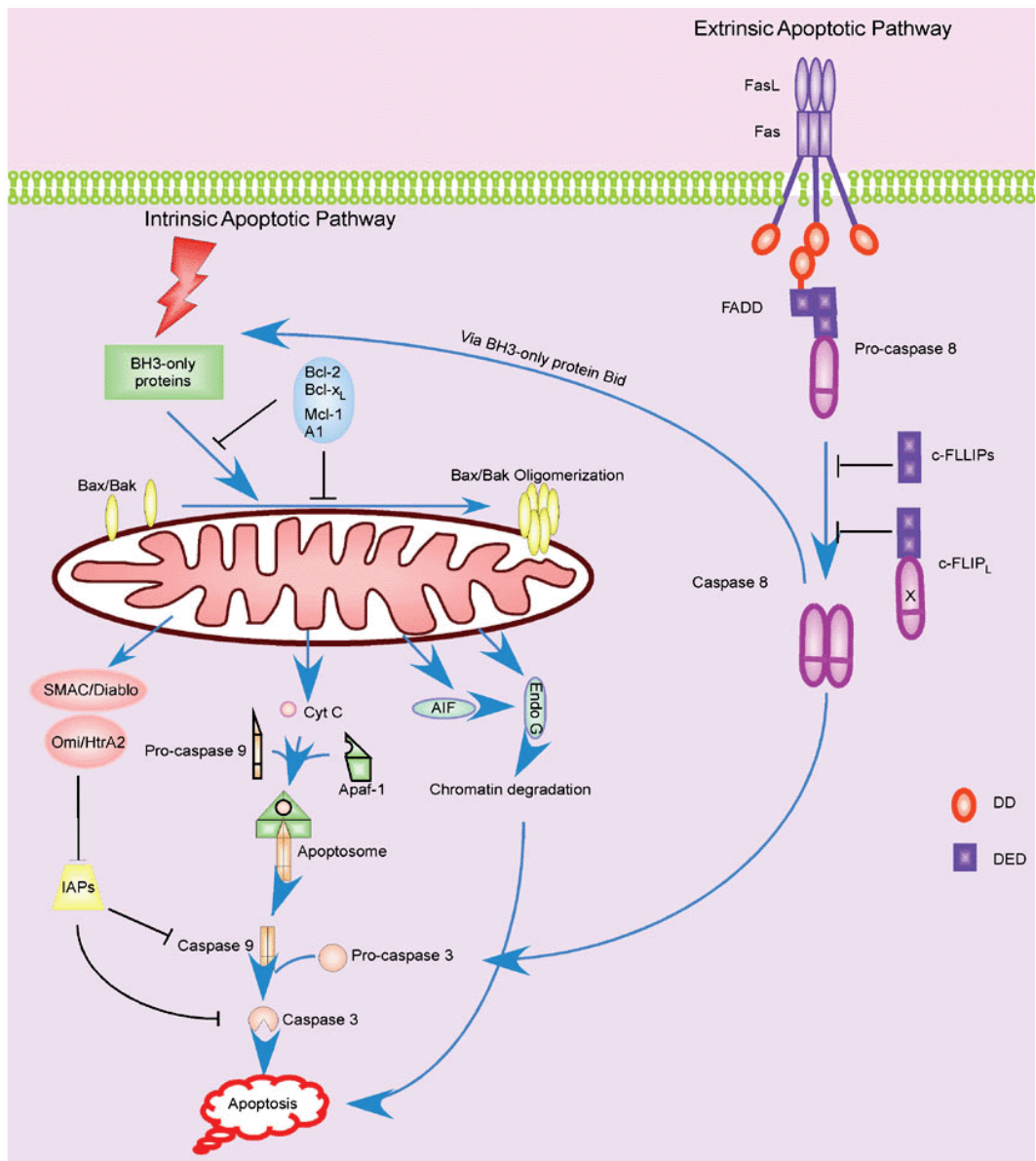
Figure 3-13. Simplified schematic of the two main apoptotic pathways. Taken from (Zhang *et al*., 2005a), showing the extrinsic and intrinsic apoptotic pathways.

Autophagic cell death is another important physiological cell death process that is increasingly recognised in HDI-mediated cytotoxicity of cancer cells. Autophagy is a dynamic process, whereby cytoplasmic materials are degraded by the lysosomal machinery. This process is characterised by vesicle reorganisation and dramatic morphological changes, which have been extensively described (Klionsky and Emr, 2000, Shao *et al.*, 2004). Apoptosis and autophagy have been closely linked in response to cell death (Gorski *et al.*, 2003), and it is believed that autophagy may have even evolved before apoptosis (Schwartz *et al.*, 1993). Early reports have described the role of autophagy in cancer development (Schulte-Hermann *et al.*, 1997, Jia *et al.*, 1997), and in human breast cancer development and progression. Evidence for this comes from the study of *beclin 1* in cancer (Aita *et al.*, 1999). *Beclin 1* is a mammalian tumour suppressor gene and is deleted in 40-75% of human breast and ovarian cancers. This particular gene interacts with the anti-apoptotic protein, Bcl_2, thereby preventing the Bax-dependent release of cytochrome c from the mitochondria. The autophagy-promoting activity of *beclin 1* in MCF-7 human breast cancer cells is associated with its inhibition of cellular proliferation and tumour growth in nude mice. High levels of the *beclin 1* protein are expressed in normal breast epithelia, and its repression has been correlated with breast cancer development and progression (Liang *et al.*, 1999).

In the experiments described in this chapter, treatment of MDA-MB231-TXSA cells with LBH589 resulted in several cellular events characteristic of both apoptosis and autophagy. Involvement of the intrinsic mitochondrial death pathway was demonstrated through the kinetics of the activation of Bid preceding the cleavage of the pro-caspase-9, suggesting compromised mitochondria, contributing to cell death. The cross-talk between the extrinsic and intrinsic pathways involves the effector caspase-8. Along with its commitment to the extrinsic apoptotic signal, caspase-8 may also have

promoted the intrinsic apoptotic signalling by further cleavage of Bid (Green, 2000). Evidence of autophagic mechanisms of cell death was demonstrated through the morphological changes that are hallmarks of apoptosis, including chromatin condensation, and/or DNA fragmentation, and cell phenotypic modifications demonstrated through Phalloidin staining. Furthermore, the addition of the pan-caspase inhibitor zVAD-fmk, did not fully rescue LBH589-induced cell death, suggesting that there may be caspase-independent autophagic mechanisms of cell death. The inhibition of HDAC1, HDAC6 and HDAC7 has been implicated in the role of autophagy (Oh *et al*., 2008, Rodriguez-Gonzalez *et al*., 2008, Hrzenjak *et al*., 2008). It has been reported that knockout of Apaf-1, needed to form a functional apoptosome, or over-expression of Bcl$_{XL}$, as well as pharmacological inhibition of caspase activity, prevented SAHA and sodium butyrate-induced caspase-dependent mechanisms of apoptosis. However, in the same cells, a caspase-independent mechanism of cell death was also reported. This was attributed to a clear morphological transformation, including DNA condensation, leading to a caspase-independent autophagic mechanism of programmed cell death (Shao *et al*., 2004). Furthermore, SAHA-induced autophagy was supported in a recent study, in which *beclin 1* was implicated in the death response (Cao *et al*., 2008). In addition, the nuclear translocation of the apoptosis inducing factor (AIF) corresponded with FK228-meditated autophagy in malignant rhabdoid tumour cells, and siRNA targets of AIF prevented the morphological changes associated with autophagy (Watanabe *et al*., 2009). Moreover, synergistic anti-leukemia effects were observed when SAHA, combined with pro-apoptotic protein mimetics or BH3-mimetics, demonstrated characteristics of both apoptosis and autophagy (Wei *et al*., 2010). In contrast, recent reports have indicated that HDI-mediated autophagy may in fact promote cancer cell survival, which has been documented for ERα^+ breast cancer cells

(Schoenlein *et al*., 2009), and protection of several carcinoma cell lines from hypoxia (Jaakkola and Pursiheimo, 2009). By using chloroquine, a drug that inhibits autophagy, FK228-mediated apoptosis was enhanced (Watanabe *et al*., 2009). Similar results were obtained using the Imatinib-resistant chronic myeloid leukemia (CML) cell lines and PBMCs isolated from CML patients refractory to Imatinib therapy. In this study, Chloroquine enhanced SAHA-induced apoptosis by increasing the levels of reactive oxygen species within the cell (Carew *et al*., 2007). HDAC6 has been directly linked to the aggresome pathway involved in autophagy. This pathway involves the recruitment of motor proteins that transport mis-folded and/or aggregated proteins to chaperones or proteasomes for degradation. Therefore, emerging evidence suggests that inhibition of this pathway leads to an accumulation of mis-folded/aggregated proteins and cell death of tumour cells through autophagy (Rodriguez-Gonzalez *et al*., 2008).

Treatment of the MDA-MB231-TXSA cells with LBH589 was associated with caspase activation and morphological changes characteristic of apoptosis. However, caspase inhibition failed to completely rescue apoptosis induction, suggesting the involvement of caspase-independent mechanisms that are also likely to play a role in this process. Several studies have demonstrated that HDI-induced cell death can also be accomplished independent of apoptosome formation, and by targeting of the aggresome pathway. Even though treatment with LBH589 resulted in morphological changes characteristic of autophagy, including DNA fragmentation and chromatin condensation, additional analysis is required to provide convincing evidence that LBH589 can mediate caspase-independent autophagic cell death. Further investigations into the histone deacetylase enzymes associated with autophagy (Park *et al*., 2008, Rodriguez-Gonzalez *et al*., 2008), and expression of *beclin 1* protein identified in autophagic

pathway signalling (Liang *et al*., 1999), may provide further insight into the mechanisms underlying MDA-MB231-TXSA breast cancer cell death.

In conclusion, the data presented in this chapter demonstrate that the pan-DAC inhibitor, LBH589 acts as a HDAC inhibitor inducing hyperacetylation of histones. Further to its powerful cytotoxic efficacy, LBH589 is also able to induce a caspase-independent mechanism of cell death, associated with morphological changes, including DNA condensation and cytoskeletal augmentation. The data clearly show caspase-dependent and caspase-independent mechanisms of cell death, suggesting that no one pathway is responsible for the efficacy of LBH589. These multiple mechanisms of cell death could possibly explain the potency of LBH589, compared to other reported HDIs. The following chapter describes a translational study from *in vitro* anticancer efficacy to *in vivo* models of breast cancer development and progression.

Chapter 4. The anticancer efficacy of LBH589 in animal models of primary breast cancer and cancer in bone

4.1 Introduction

HDAC inhibitors induce a diverse biological response in a variety of tumour cell lines leading to apoptosis, suppression of proliferation, anti-angiogenesis and activation of cell-cycle checkpoints G2/M or G1/S (Bolden *et al*., 2006, Zhou *et al*., 2011, Ellis *et al*., 2009b). Over the past few years, results obtained from clinical trials and pre-clinical animal experiments demonstrate the ability of HDIs to selectively kill cancer cells with limited or no toxicity to normal tissue and organs. Pre-clinical models have established a link between tumour cell death and therapeutic efficacy (Butler *et al*., 2000, Frew *et al*., 2009), and co-operative activity when combined with standard chemotherapeutics (Frew *et al*., 2009). Therefore, it is clear that HDIs are emerging as an exciting new class of anticancer agents for the treatment of solid and haematological malignancies. Although a number of early-phase clinical trials using different HDIs have demonstrated promising anti-tumour response for a variety of cancer types (Atadja, 2010, de Bono *et al*., 2008), to the best of my knowledge, the effect of HDIs in metastatic bone disease has not been reported

Following the observations of the potent anticancer efficacy of LBH589 *in vitro,* described in chapter 3, it was considered important to determine whether these findings would translate into animal models of primary breast cancer and cancer in bone, the latter being the site of frequent breast cancer metastasis. There are currently no effective treatments for bone metastases, and the treatments that are available are palliative, with minimal improvement in patients' long term survival (Guise *et al*., 2010). Therefore, new therapies are urgently required for this serious disease.

Given the potent *in vitro* cytotoxic activity of LBH589 against breast cancer cells described in chapter 3, the following hypotheses were proposed:

1. LBH589 inhibits tumour growth in the orthotopic site of the mammary glands by direct induction of breast cancer cell apoptosis.

2. LBH589 inhibits breast cancer growth in bone and protects the bone from breast cancer-induced bone destruction, either by direct effects on cancer cells themselves, or indirectly by modulating the interaction between cancer cells and bone cells.

To investigate the anticancer efficacy of LBH589 *in vivo,* the human MDA-MB231-TXSA breast cancer cell line was selected. This bone-seeking variant of the MDA-MB231 human breast cancer cell line forms aggressive, rapidly growing tumours when injected into the orthotopic site of the mammary fat pad of nude mice, and stimulates the formation of osteolytic lesions when injected into the tibial marrow cavity (Thai le *et al*., 2006). For non-invasive monitoring of tumour development and progression, luciferase expressing MDA-MB231-TXSA cells were generated using the retroviral expression vector SFG-NES-TGL, which gives rise to a single fusion protein encoding herpes simplex virus thymidine kinase (TK), green fluorescence protein (GFP) and firefly luciferase (Luc) (figure 4-1A), (Ponomarev *et al*., 2004). After infection, cancer cells were enriched for high level expression of GFP by two rounds of fluorescence-activated cell sorting (FACS), giving rise to the subline designated here as MDA-MB231-TXSA-TGL. This cell line exhibited a 4000-fold induction of luciferase activity when analysed *in vitro* (figure 4-1B).

A

SFG - NES - TGL

B
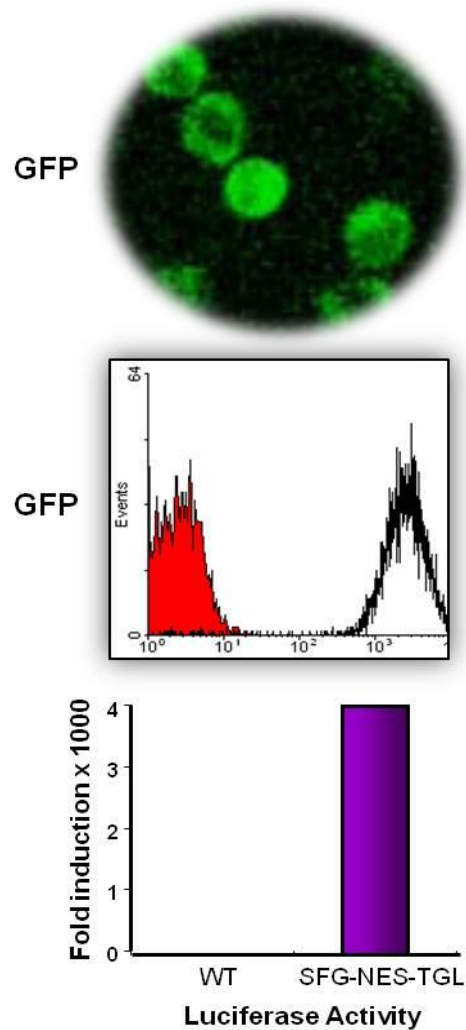
Figure 4-1. Generation of luciferase-expressing cells. MDA-MB231-TXSA breast cancer cells were retrovirally transfected with the SFG-NES-TGL vector (**A**). The retrovirally transduced cells were grown as bulk cultures for 48 hours and subsequently sorted for positive GFP expression. The cells were allowed to proliferate, and the 10% of cells expressing GFP most strongly were obtained by FACS sorting to generate the subline MDA-MB231-TXSA-TGL, as shown to express a 4000-fold increases in luciferase when compared to wild-type (WT) (**B**).

To evaluate the anticancer efficacy of LBH589 against breast cancer development and progression, two murine models were employed, in which MDA-MB231-TXSA-TGL cells were transplanted into the mammary fat pad, or were injected directly into the tibial marrow cavity of athymic female nude mice. Tumour burden was monitored progressively using bioluminescence imaging (BLI), whereas, the development of breast cancer-induced osteolysis was measured using high resolution micro-computed tomography (µ-CT) and histology.

In the experiments described in this chapter, the anticancer efficacy of the HDI, SAHA, which is currently approved by the FDA (U.S.A.), was also tested and compared in both animal models. The anticancer activity of SAHA has been well demonstrated both *in vitro* and in various animal models of cancer (Butler *et al*., 2000, Shi *et al*., 2010), and therefore serves as an appropriate comparison to LBH589.

4.2   Results

4.2.1 Accumulation of acetylated histone-H3 in animal tissues after administration of LBH589

One of the well-characterised biochemical effects of HDAC inhibitors including LBH589 and SAHA is increased accumulation of acetylated histones caused by inhibition of HDAC activity (Atadja, 2010, Bolden *et al*., 2006). Therefore, to confirm the *in vivo* effectiveness of LBH589, the spleen and bone marrow were isolated from mice after administration of the drug for the detection of histone-H3 acetylation. LBH589 at a dose of 15 mg/kg was administered i.p. into athymic nude mice. Four hours after LBH589 administration, the mice were humanely killed. The spleen was isolated and Dounce homogenised, while the bone marrow was flushed from the tibiae, as described in section 2.27. Acetylation of histone-H3 was analysed by western blot using specific antibodies against acetylated histone-H3. The spleen and bone marrow showed significant increases in histone-H3 acetylation following LBH589 treatment when compared to untreated controls (figure 4-2), indicating that i.p. administration of LBH589 could potently inhibit acetylation. The gelstain of the polyacrylamide gel of histone samples extracted from the mouse tissues was used for comparison against protein loading.
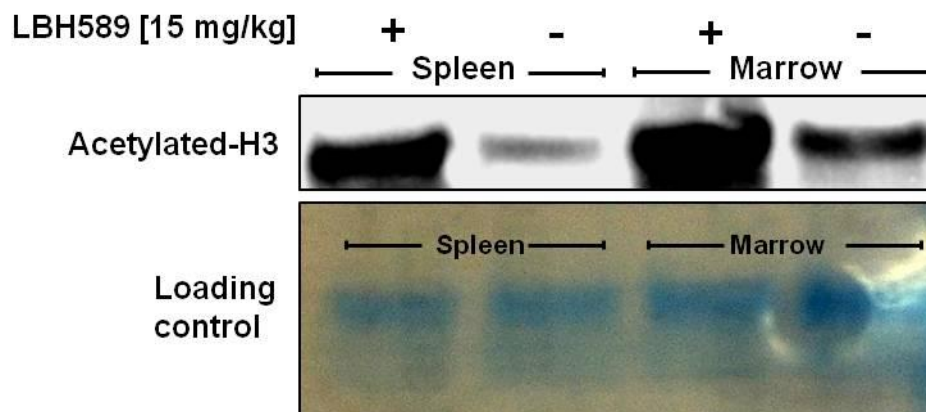
Figure 4-2. The systemic acetylation activities of LBH589 *in vivo*. Mice were injected with LBH589 for 4 hours, and the spleen and bone marrow were isolated and histones were prepared as described in the Methods. Histone-H3 acetylation was detected by western blot using an antibody against acetylated-H3. The *top panel* contains acetylated histone-H3, and the *bottom panel* shows a gelstained polyacrylamide gel of the total histones extracted from the tissues.

4.2.2 The effect of HDIs on the growth of breast cancer xenografts

To investigate the anticancer activity of LBH589 and SAHA against MDA-MB231-TXSA-TGL tumours growing in an orthotopic site, a model in which cells were injected directly into the mammary fat pad of 8 week old athymic female nude mice was used. BLI carried out at days 1 and 7 after cancer cell transplantation confirmed the establishment and growth of tumour in the mammary gland. Treatment was initiated on day 7 after cancer cell transplantation, and BLI of tumour growth was performed once weekly thereafter. No adverse drug effects were noted during the experiment, as assessed by weekly body weight measurements. A slight decrease in mean body weights (not greater than 15% body weight loss) with treatment was noted in the first week, but with the animals recovering thereafter (table 4-1). Animals treated with vehicle alone exhibited an exponential increase in mean photon emission related to an increase in tumour burden. The BLI signal increased significantly from day 7 onwards, and continued to increase until the experiment was terminated on day 28. By this time, the tumour volume exceeded 1000 mm^3 (as measured by calipers), and animals were humanely killed. Animals treated with 15 mg/kg of LBH589 (i.p.), for 5 days/week, for three weeks, demonstrated a trend towards a reduction in tumour growth, but this effect was not statistically significant. Animals treated with 50 mg/kg of SAHA (i.p.), did not show any reduction in tumour growth (figures 4-3A & B). Tumour volume was also measured with calipers (figure 4-4), and was well correlated with the mean photon counts for each group, further substantiating the BLI imaging analysis.

↓ Start drug treatment

Days	1	7	14	21	28
Vehicle	18.1 ± 0.9	19.0 ± 1.2	18.9 ± 1.5	19.4 ± 1.5	19.7 ± 1.5
LBH589 [15mg/kg]	17.5 ± 1.4	18.2 ± 1.6	16.3 ± 1.3	16.6 ± 1.6	17.1 ± 1.8
SAHA [50mg/kg]	17.6 ± 0.8	18.5 ± 1.0	17.3 ± 1.6	18.0 ± 2.4	17.8 ± 2.7

Table 4-1. Body weights of mice bearing orthotopic mammary tumours. Body weights were measured once weekly on days 1 (baseline), 7, 14, 21 and 28 throughout the duration of the experiment, where values; weight (g) ± SD, and n = 10 mice per group.
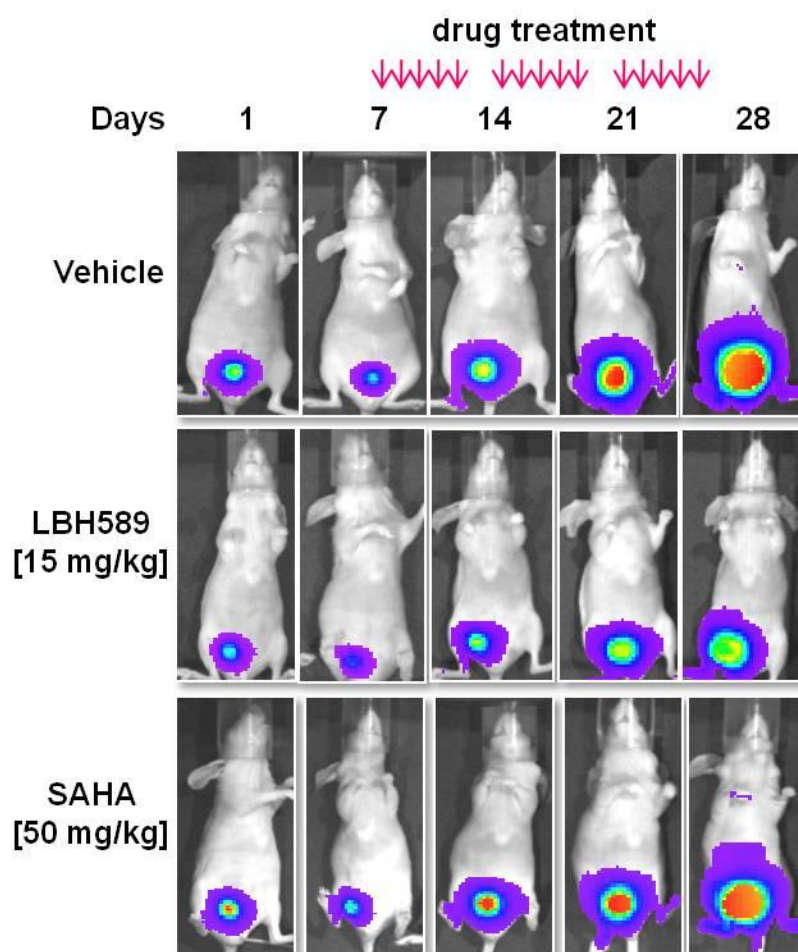
Figure 4-3A. Representative images showing the average mammary tumour volume as determined by BLI. The MDA-MB231-TXSA-TGL breast cancer cell line was transplanted directly into the mammary fat pad of female nude mice. Mice were imaged at days 1 (baseline), 7, 14, 21 and 28, and representative images are depicted. Treatment with either vehicle alone, 15 mg/kg of LBH589, or 50 mg/kg of SAHA, commenced at day 7 when tumour burden was low. Arrows indicate the frequency of treatment.
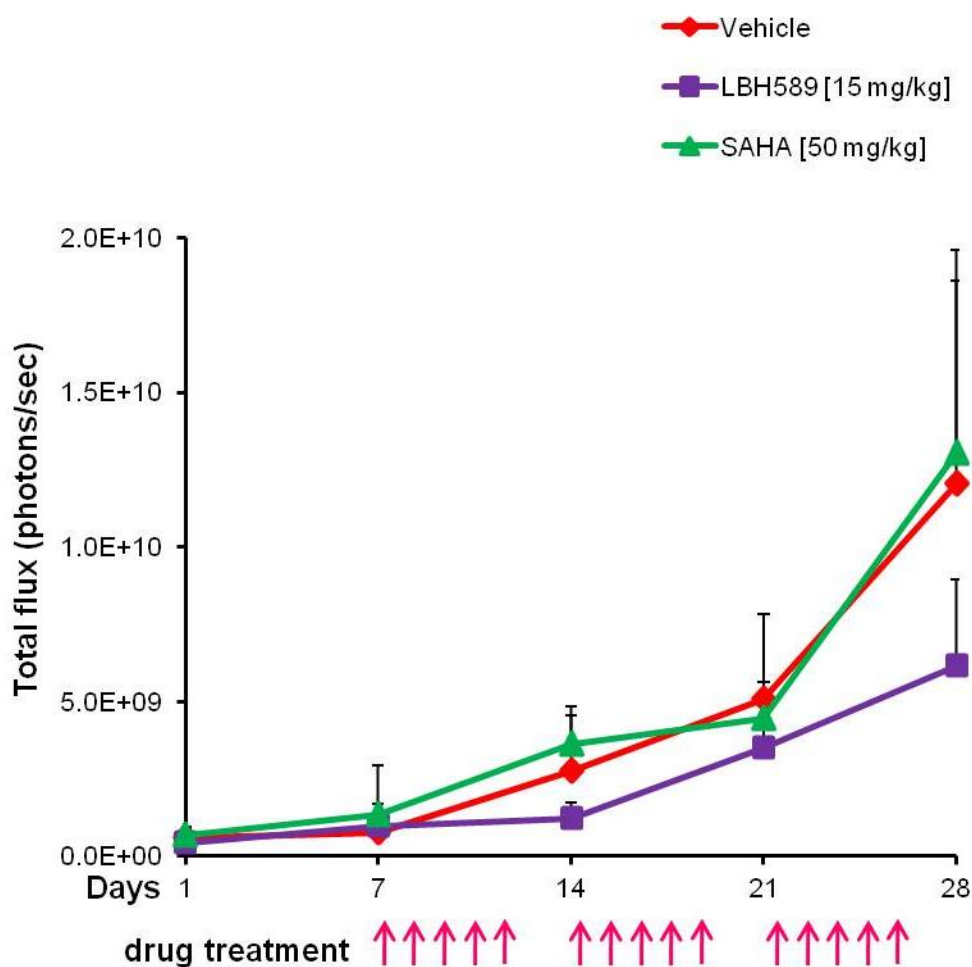
Figure 4-3B. The effect of HDIs on mammary tumours, as determined by BLI. The MDA-MB231-TXSA-TGL breast cancer cell line was transplanted directly into the mammary fat pad of athymic nude mice. Mice were imaged and BLI was measured in photons/second at days 1 (baseline), 7, 14, 21 and 28. Treatment with either vehicle alone (red), 15 mg/kg of LBH589 (purple), or 50 mg/kg of SAHA (green), commenced at day 7 when the tumour burden was low. Arrows indicate the frequency of treatment. No significant differences in tumour size ($\pm$ SD, n = 10), were observed at day 28, when compared between vehicle and LBH589 (p = 0.94).
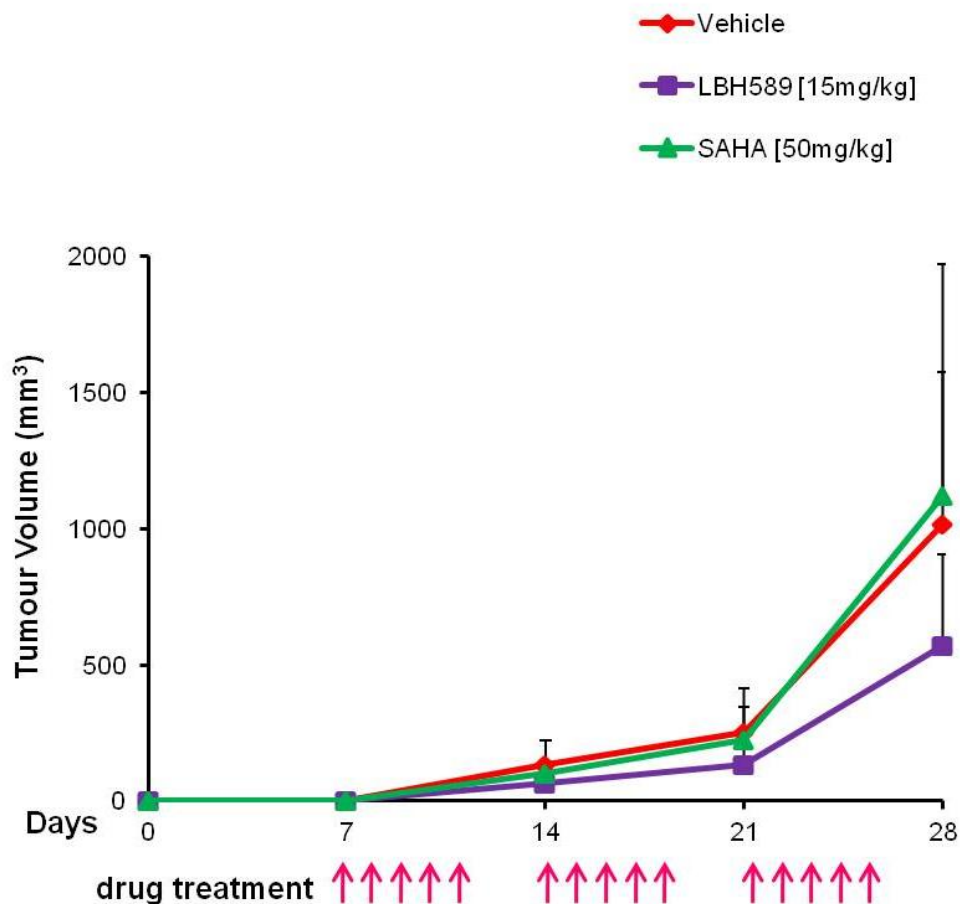
Figure 4-4. The effect of HDIs on mammary tumours, as measured using calipers. The MDA-MB231-TXSA-TGL breast cancer cell line was transplanted directly into the mammary fat pad of female nude mice. Mammary fat pad tumour volume ($\pm$ SD, n = 10) was measured at days 14, 21 and 28. Treatment with either vehicle alone (red), 15 mg/kg of LBH589 (purple), or 50 mg/kg of SAHA (green), commenced at day 7, when the tumour burden was low. Arrows indicate the frequency of treatment. No significant differences in tumour size were observed at day 28, when compared between vehicle and LBH589 (p = 0.17), or SAHA (p = 0.92).

Whilst there was a clear accumulation of acetylated-H3 in various animal tissues, no difference in the acetylated-H3 status was observed in the tumours isolated from the mammary glands (figure 4-5). The lack of anticancer efficacy was further supported when histological examination of mammary tumour sections from representative animals following treatment with either LBH589 or SAHA, showed the absence of apoptotic cells when assessed by TUNEL staining (figure 4-6). In parallel with this study, and as a comparison for the detection of apoptotic cell death *in vivo*, mice bearing the same mammary tumours were also treated with Drozitumab, a fully human agonistic antibody that activates the human Apo2L/TRAIL death receptor DR5 and induces apoptosis of cancer cells both *in vitro* and in various xenograft models of cancer, including breast cancer (Zinonos *et al*., 2009). While LBH589 and SAHA treatment failed to induce apoptosis *in vivo*, Drozitumab induced apoptosis in a substantial proportion of the tumour mass, with intense TUNEL positive staining of tumour cells when compared to vehicle-treated animals.

Figure 4-5. The detection of acetylated-H3 in orthotopic mammary tumours. Mice were transplanted with the MDA-MB231-TXSA-TGL breast cancer cells directly into the mammary gland. Treatment with LBH589 was as indicated in the Methods. Mammary tumours were excised and histones were isolated as indicated in the Methods. Western blot analysis using an antibody against acetylated-H3 was assessed (top panel) against loading control (bottom panel), using a gelstained polyacrylamide gel of the total histones extracted from the tissues. The graph represents the quantification of the western blots, highlighting no difference in band intensity.

Figure 4-6. HDIs do not induce apoptosis of orthotopic mammary tumours. Histological sections were paraffin embedded and stained with H&E or TUNEL. Images were taken using the nanozoom at 40x magnification. Histological examination of representative sections after treatment indicated that the HDIs had no effect on the apoptosis of the tumour cells, with negative TUNEL staining, compared to positive control with Drozitumab.

4.2.3 The effect of HDIs on breast cancer cell growth in bone

To evaluate the anticancer efficacy of LBH589 and SAHA against tumour growth in bone and its effects on cancer-induced bone destruction, the MDA-MB231-TXSA-TGL cells were transplanted directly into the tibial marrow cavity of athymic nude mice. Unlike soft tissue tumours, a limitation in measuring tumour burden in bone is that it is not possible to accurately determine the progression of tumour growth by palpation before the tumours break through the cortical bone. However, non-invasive BLI imaging provided sensitive, real-time *in vivo* assessment of breast cancer growth in the bone marrow, whereas the effect of HDIs on breast cancer-induced bone destruction was determined using high resolution *ex vivo* µ-CT (Skyscan 1072).

In this experiment, MDA-MB231-TXSA-TGL breast cancer cells were transplanted directly into the tibial marrow cavity of athymic female nude mice, and allowed to establish for 4 days prior to commencement of LBH589 or SAHA treatment. Given the lack of anticancer efficacy observed in the orthotopic primary breast cancer model (section 4.2.2), when LBH589 was administered at 15 mg/kg/dose, the dose of LBH589 was increased to 30 mg/kg/dose for the intratibial model. Weekly body weight measurements showed a decrease (not greater than 15% body weight loss), in mean body weights during the second week of treatment, with animals recovering thereafter (table 4-2).

↓ **Start drug treatment**

Days	1	7	14	21	28
Vehicle	17.0 ± 1.1	17.6 ± 1.1	18.3 ± 1.2	18.2 ± 1.2	18.6 ± 1.1
LBH589 [15mg/kg]	17.3 ± 1.0	17.9 ± 1.0	15.3 ± 1.1	15.3 ± 1.1	16.9 ± 1.3
LBH589 [30mg/kg]	17.8 ± 1.1	18.3 ± 1.3	15.0 ± 1.2	15.9 ± 1.0	17.5 ± 1.1
SAHA [50mg/kg]	16.9 ± 1.0	17.8 ± 0.8	16.9 ± 1.4	16.6 ± 1.7	17.7 ± 1.9

Table 4-2. Body weights of mice bearing intratibial tumours. Body weights were measured once weekly on days 1 (baseline), 7, 14, 21 and 28 throughout the duration of the experiment, where values; weight (g) ± SD and n = 10 mice per group.

The non-invasive BLI imaging provided sensitive, real-time *in vivo* assessment of tumour growth within bone, particularly before the tumour had time to break through the cortical bone. All groups showed an increase of mean photon emission associated with an increase in tumour burden, which was evident from day 14 onwards. By day 28, all animals developed large intratibial tumours that penetrated the cortical bone, with the tumour mass invading the surrounding soft tissue. In this model, neither dose of LBH589 or SAHA resulted in a significant reduction of tumour burden compared to vehicle treated animals (figure 4-7A and 4-7B). Similar to the mammary tumours, the accumulation of acetylated-H3 in the tumours isolated from the tibial marrow cavity demonstrated no difference between vehicle-treated and the LBH589 treatment group (figure 4-8). Consistent with the observed lack of anticancer efficacy with treatment, histological sections of intratibial tumours prepared from animals treated with HDIs were also negative for TUNEL staining. This indicates a lack of anticancer efficacy and absence of apoptosis induction (figure 4-9). In contrast animals bearing intratibial tumours and treated with Drozitumab, showed tumour regression and extensive apoptosis as evident by the strong TUNEL staining in the tumour bed. Despite the potent cytotoxic effect of the drugs seen in the *in vitro* experiments described in the previous chapter, it was surprising that this effect could not be translated into *in vivo* anticancer efficacy in the models described here.
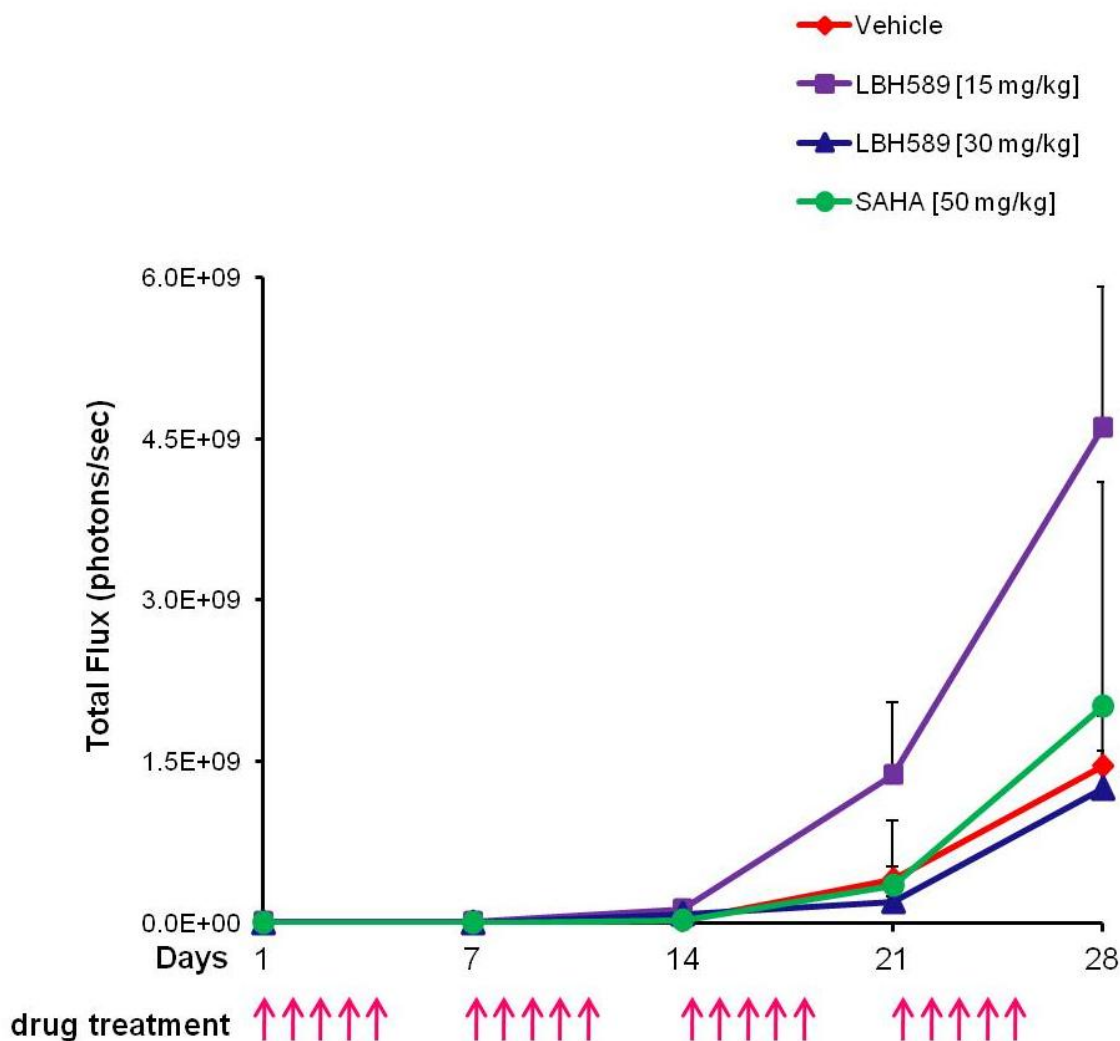
Figure 4-7A. The effects of HDIs on the tumour growth in bone, as determined using BLI. The MDA-MB231-TXSA-TGL breast cancer cell line was transplanted directly into the tibial marrow cavity of athymic nude mice and allowed to establish for 4 days prior to imaging. Mice were imaged and BLI was measured in photons/second at days 1 (baseline), 7, 14, 21 and 28. Treatment with either vehicle alone (red), 15 mg/kg of LBH589 (purple), 30 mg/kg of LBH589 (blue), or 50 mg/kg of SAHA (green), commenced at day 1 after confirmation of tumour establishment. Arrows indicate the frequency of treatment. No significant differences in tumour size ($\pm$ SD, n = 10), were observed at day 28, when compared between vehicle and 15 mg/kg of LBH589 (p = 0.25), or 30 mg/kg of LBH589 (p = 0.73), or SAHA (p = 0.58).

Figure 4-7B. Representative images showing the effect of HDIs on the tumour growth in bone, as determined using BLI. The MDA-MB231-TXSA-TGL breast cancer cell line was transplanted directly into the tibial marrow cavity of female nude mice. Mice were imaged at days 1 (baseline), 7, 14, 21 and 28, and representative images are depicted. Treatment with either vehicle alone, 15 and 30 mg/kg of LBH589, or 50 mg/kg of SAHA, commenced at day 1 when the tumour burden was low. Arrows indicate the frequency of treatment.
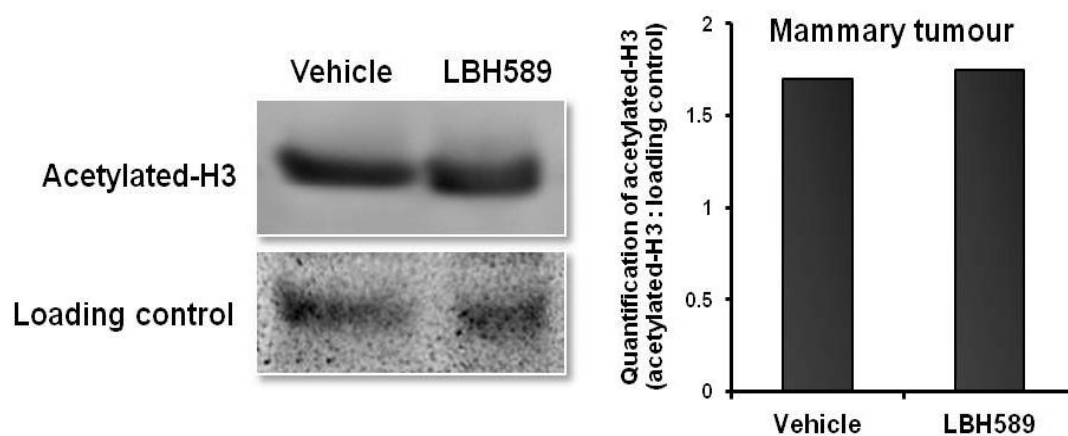
Figure 4-8. The detection of acetylated-H3 in orthotopic bone tumours. Mice were transplanted with the MDA-MB231-TXSA breast cancer cell line directly into the tibial marrow cavity. Treatment with LBH589 was as indicated in the Methods. Intratibial tumours were excised and histones were isolated as indicated in the Methods. Western blot analysis using an antibody against acetylated-H3 was assessed (top panel) against loading control (bottom panel), using a gelstained polyacrylamide gel of the total histones extracted from the tissues. The graph represents the quantification of the western blots, highlighting no difference in band intensity.
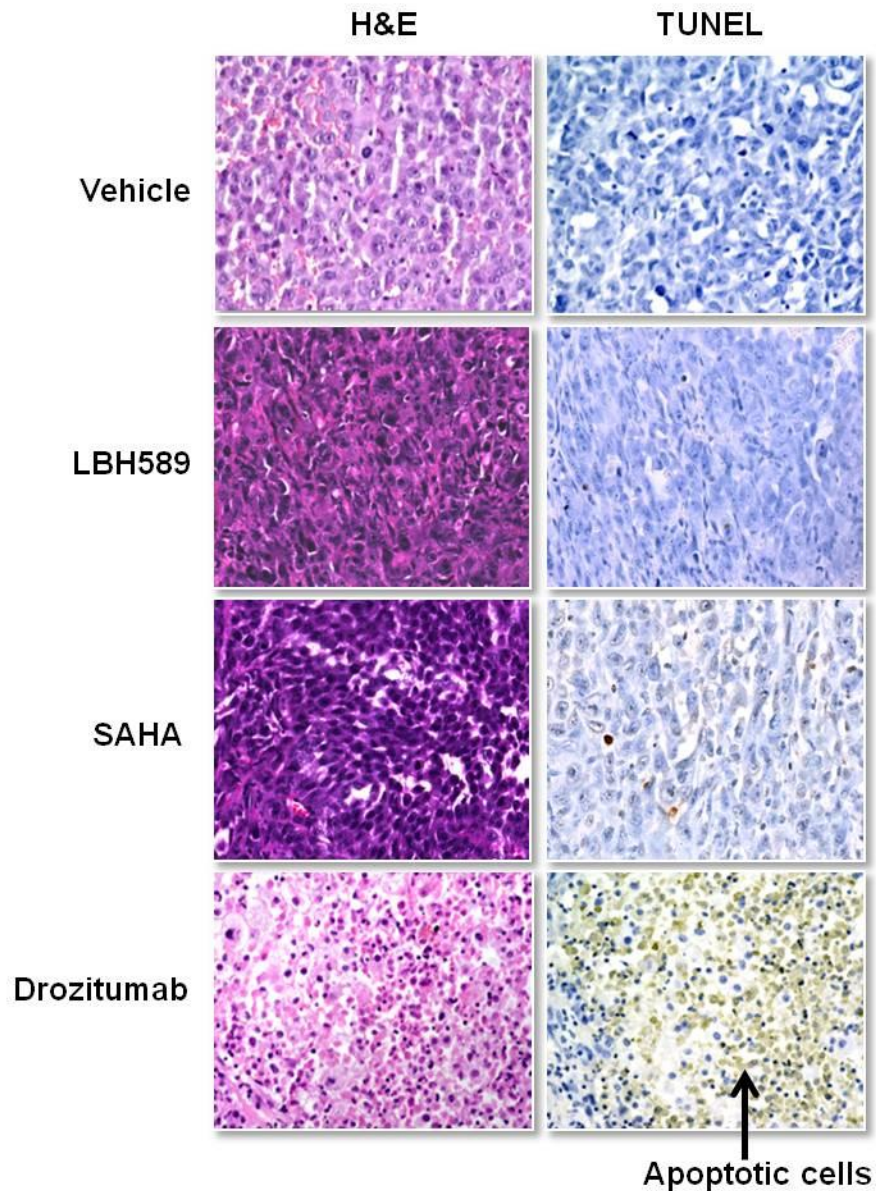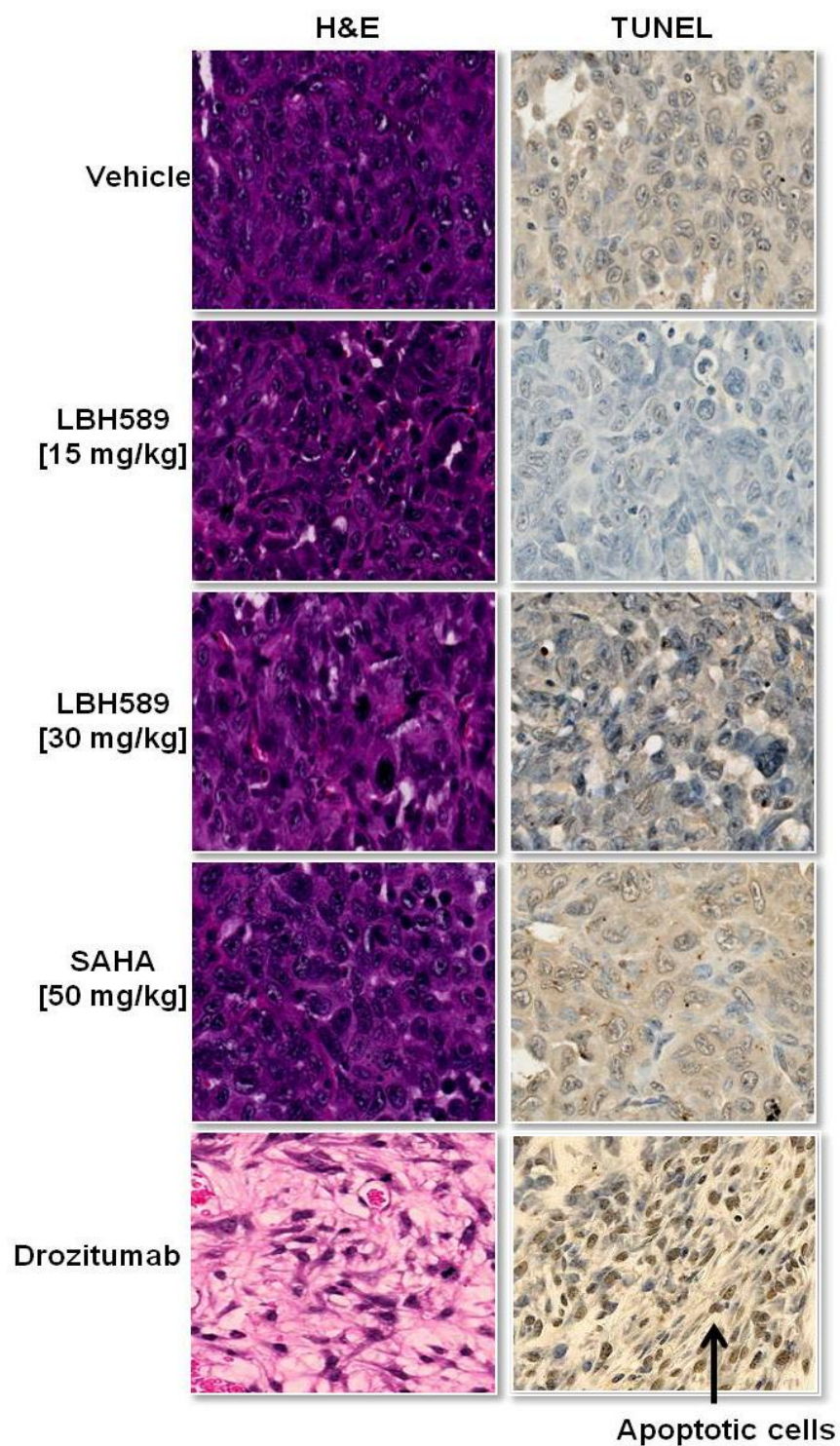
Figure 4-9. HDIs do not induce apoptosis of tumour growth in bone. Histological sections were paraffin embedded and stained with H&E or TUNEL. Images were taken using the nanozoom at 40x magnification. Histological examination of representative sections after treatment indicated that the HDIs had no effect on the apoptosis of the tumour cells, with negative TUNEL staining, compared to positive control with Drozitumab.

4.2.4 The effect of HDIs on cancer-induced bone destruction

To determine the effect of the drugs on cancer-induced bone destruction, isolated tibiae were analysed to determine various bone histomorphometric parameters using *ex vivo* high resolution µ-CT. As expected, quantitative 3D µ-CT analysis demonstrated extensive tumour-induced osteolysis in the vehicle-treated group, with bone volume decreasing to 50% in the tumour-bearing tibiae when compared to the contralateral non-tumour bearing tibiae (figure 4-10). This was consistent with observations in other intratibial animal models using the same cell line (Thai le *et al*., 2006, Zinonos *et al*., 2009). Surprisingly, treatment with LBH589 showed significant protection from cancer-induced osteolysis, despite the drug having no effect on tumour burden. Figures 4-11A and B, represent the mean total bone volume and trabecular bone volume for each of the tumour-bearing tibiae from the LBH589 or SAHA-treated animals. LBH589 dose-dependently protected the bone from cancer-induced osteolysis, while SAHA had no effect.
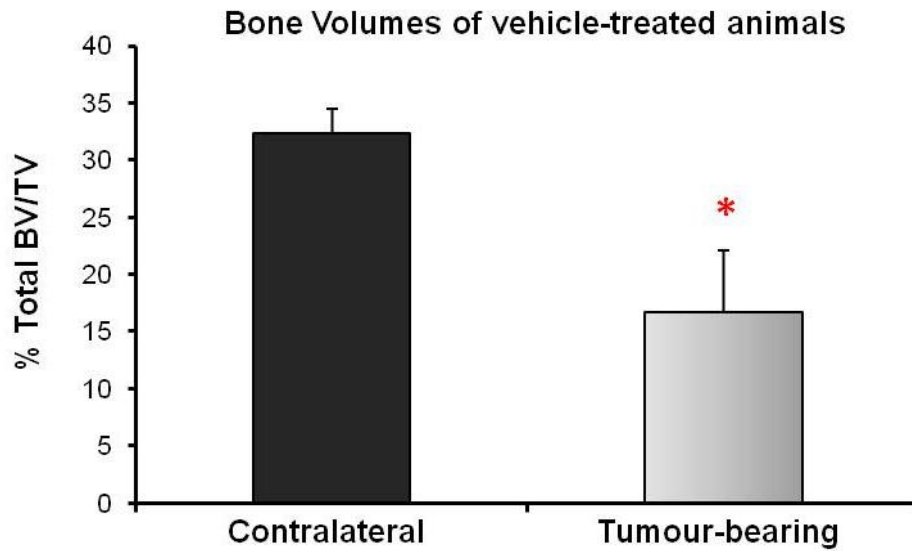
Figure 4-10. Total bone volumes of the vehicle-treated mice. The graph shows the average total bone volume in the vehicle-treated group only, with *P < 0.0001. Bone volume was measured from 730 μ-CT sections of the proximal tibia, starting from the growth plate and using the program CTan. Data shown are the average bone volume from all animals in that group, with bars: mean ± SD (n = 10).

A

B
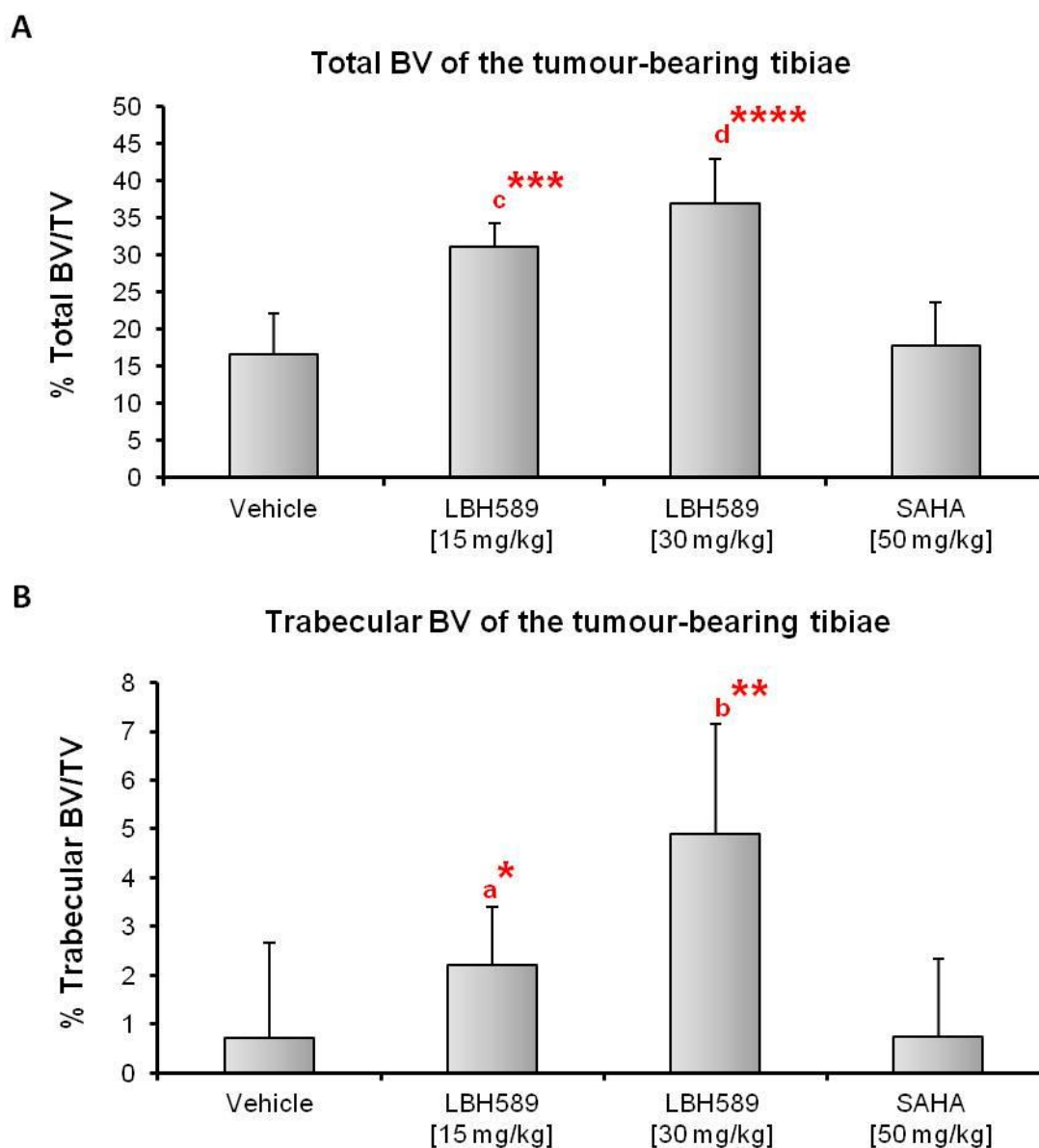
Figure 4-11. LBH589 dose-dependently protects the bone against breast cancer-induced osteolysis. The graph shows the average total bone volume (**A**) and trabecular bone volume (**B**) of the tumour-bearing tibiae in all treatment groups, with:

a* = P < 0.05, b** = P < 0.005, c*** = P < 0.00005, and d**** = P < 0.000005. Bone volume was measured from 730 μ-CT sections of the proximal tibia, starting from the growth plate and using the program CTan. Data shown are the average bone volume from all animals in that group, with bars: mean ± SD (n = 10).

Figure 4-12A shows the total amount of bone lost for each treatment group. While the amount of bone lost in the vehicle-treated group was 50% of the total bone, treatment with low dose LBH589 (15 mg/kg), reduced the amount of bone lost to 20%. This was further reduced to 11% when animals were treated with the higher dose of LBH589 (30 mg/kg), despite comparable tumour burden. Therefore the total amount of bone lost in the vehicle-treated group far exceeded that seen in the LBH589 treatment groups. Animals treated with 50 mg/kg of SAHA demonstrated no protection from cancer-induced bone destruction. Representative tibiae images from 3D µ-CT reconstruction for each treatment group are shown in figure 4-12B.
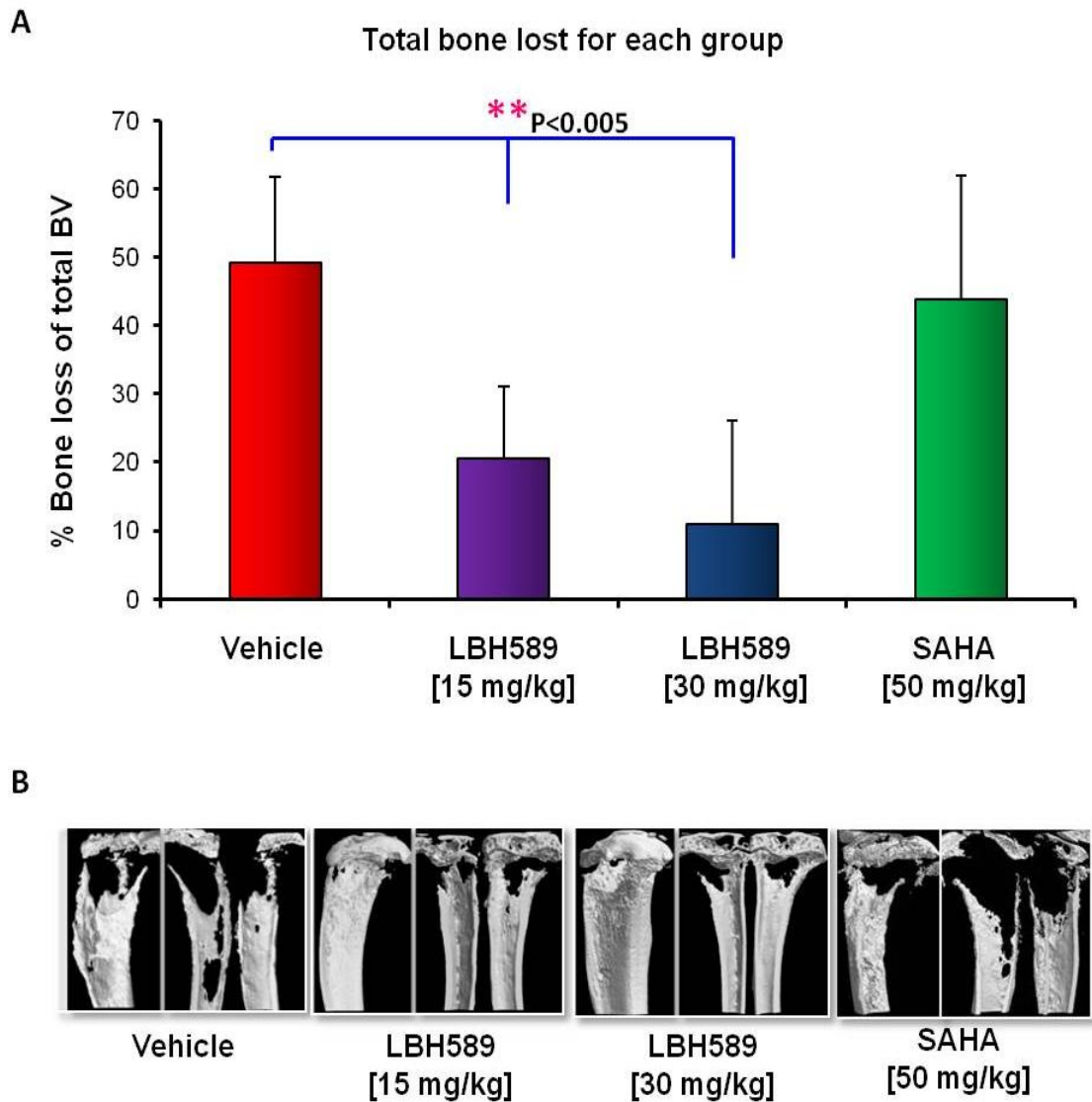
Figure 4-12. LBH589 dose-dependently inhibits bone loss. A). The graph shows the total bone volume that was lost with each treatment group in the tumour-bearing tibiae. This graph demonstrates that the percentage bone loss was reduced with increasing doses of LBH589. Bone volume was measured from 730 μ-CT sections of the proximal tibia, starting from the growth plate and using the program CTan. Data shown are the average bone volume from all animals in that group, with bars: mean ± SD (n = 10). **B**). 3D representative images of the tumour-bearing tibiae in each group, generated using the program ANT.

4.2.5 The effect of LBH589 on the contralateral, non-tumour bearing tibiae in immune deficient mice

The previous μ-CT data demonstrated a surprising protection of cancer-induced osteolysis with LBH589 treatment despite the drug having no effect on tumour burden. This suggested that LBH589 may exert direct effects on bone cells within the bone microenvironment that are independent of its effects on cancer cells. This finding prompted further investigations into the effects of LBH589 treatment on the contralateral, non-tumour bearing tibiae of these animals. This was to determine the direct effects of HDIs on bone cells without the influence of cancer cells. Similar to the observed bone volume increases in the tumour-bearing tibiae, quantitative 3D μ-CT analysis demonstrated a significant dose-dependent increase in bone volume of the non-tumour bearing tibiae of the LBH589 treated animals when compared to the vehicle-treated group (represented in figure 4-13A and B). No changes in bone volume were observed with SAHA treatment. To evaluate the mechanism of LBH589-induced bone volume changes in the context of osteoclast function, histological examination of the non-tumour bearing tibiae demonstrated a dose-dependent decrease in the number of TRAP[+], multinucleated osteoclasts lining the trabecular bone surface. This dose-dependent decrease in the number of TRAP[+], osteoclasts was also evident in histological sections of the tumour-bearing tibiae that showed protection from cancer-induced bone destruction following treatment (figure 4-14A and B).
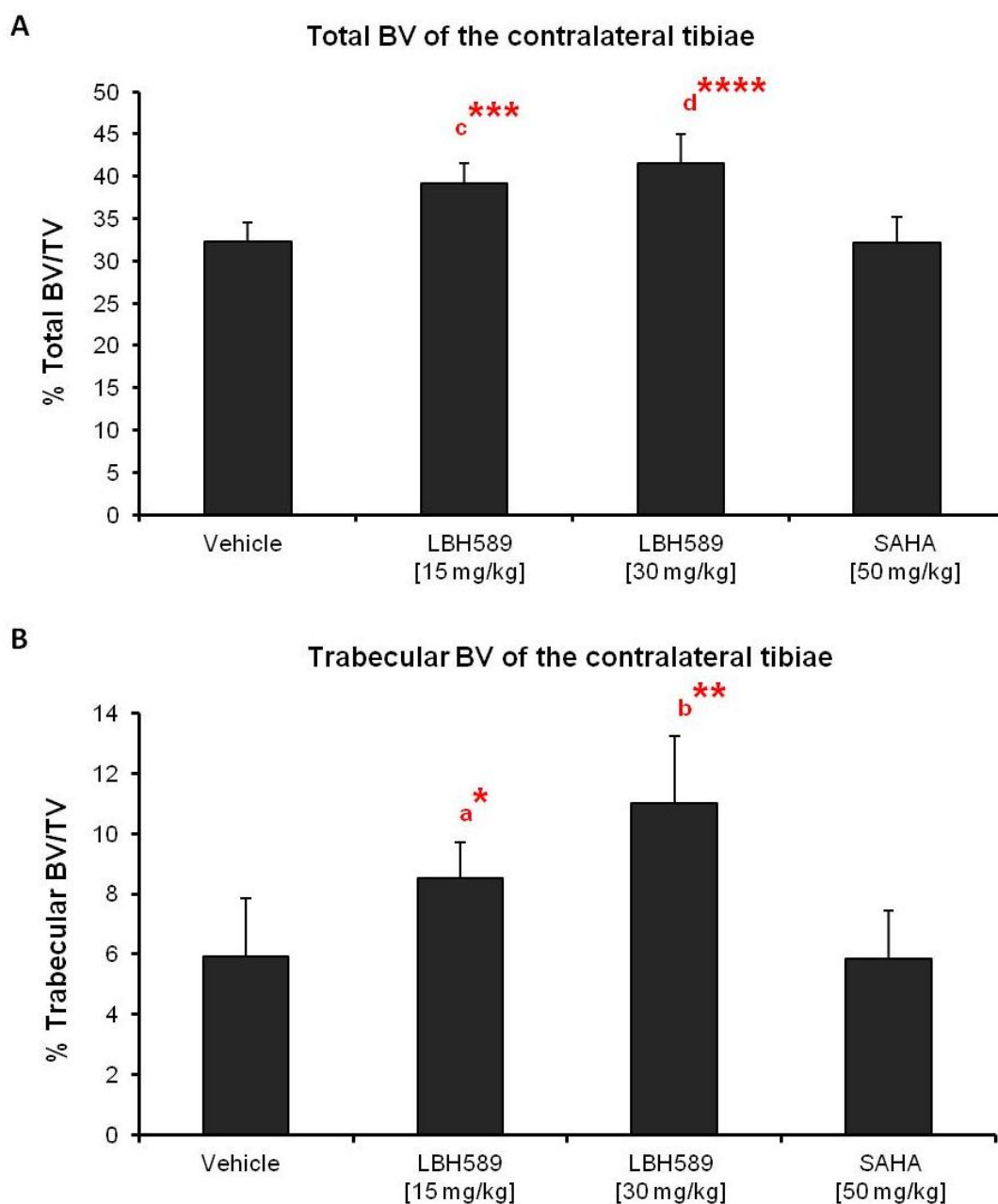
Figure 4-13. LBH589 dose-dependently increases bone volume. The graph shows the average total bone volume (**A**), and trabecular bone volume (**B**) from the contralateral non-tumour bearing tibiae in all treatment groups, with: a* = P < 0.05, b** = P < 0.005, c*** = P < 0.00005 and d**** = P < 0.000005. Bone volume was measured from 730 µ-CT sections of the proximal tibia, starting from the growth plate and using the program CTan. Data shown are the average bone volume from all animals in that group, with bars: mean ± SD (n = 10).
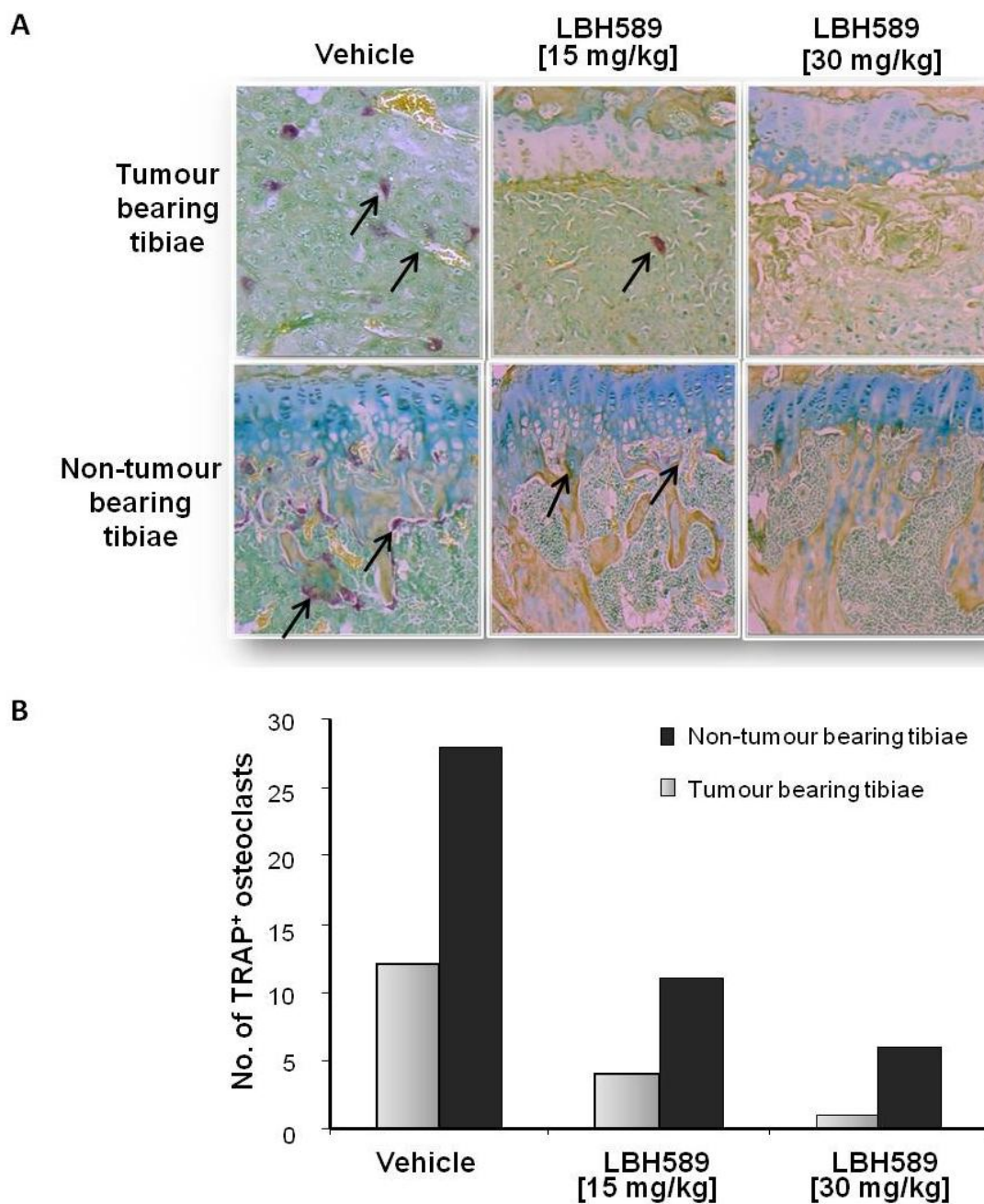
Figure 4-14. LBH589 dose-dependently inhibits the number of TRAP+ osteoclasts, lining the trabecular bone surface. Tibial sections were paraffin embedded, sectioned, and mounted onto glass slides for TRAP staining. The number of purple stained osteoclasts were counted. **A**). Representative sections for each treatment group, with the *top panel* representing the tumour-bearing tibiae and the *bottom panel* representing the contralateral, non-tumour bearing tibiae. Arrows are pointing to examples of purple stained osteoclasts. **B**). Graphical representation of the number of purple stained osteoclasts in each of the sections represented in **A.**

To further corroborate and substantiate these findings, tibiae from the mice bearing mammary tumours that were treated with LBH589 and SAHA as described in section 4.2.2, were also analysed for bone volume changes by μ-CT. It was hypothesised that mice bearing mammary tumours would also demonstrate significant bone volume changes, associated with a direct effect of LBH589 on bone cells. As expected, there were significant increases in both cortical (approx. 2.5%), and trabecular (approx. 0.9%), bone volumes with LBH589 treatment compared to vehicle-treated controls (figure 4-15A and B). Consistent with the previous study, SAHA again did not show any significant changes in bone volume measurements in animals bearing mammary tumours.
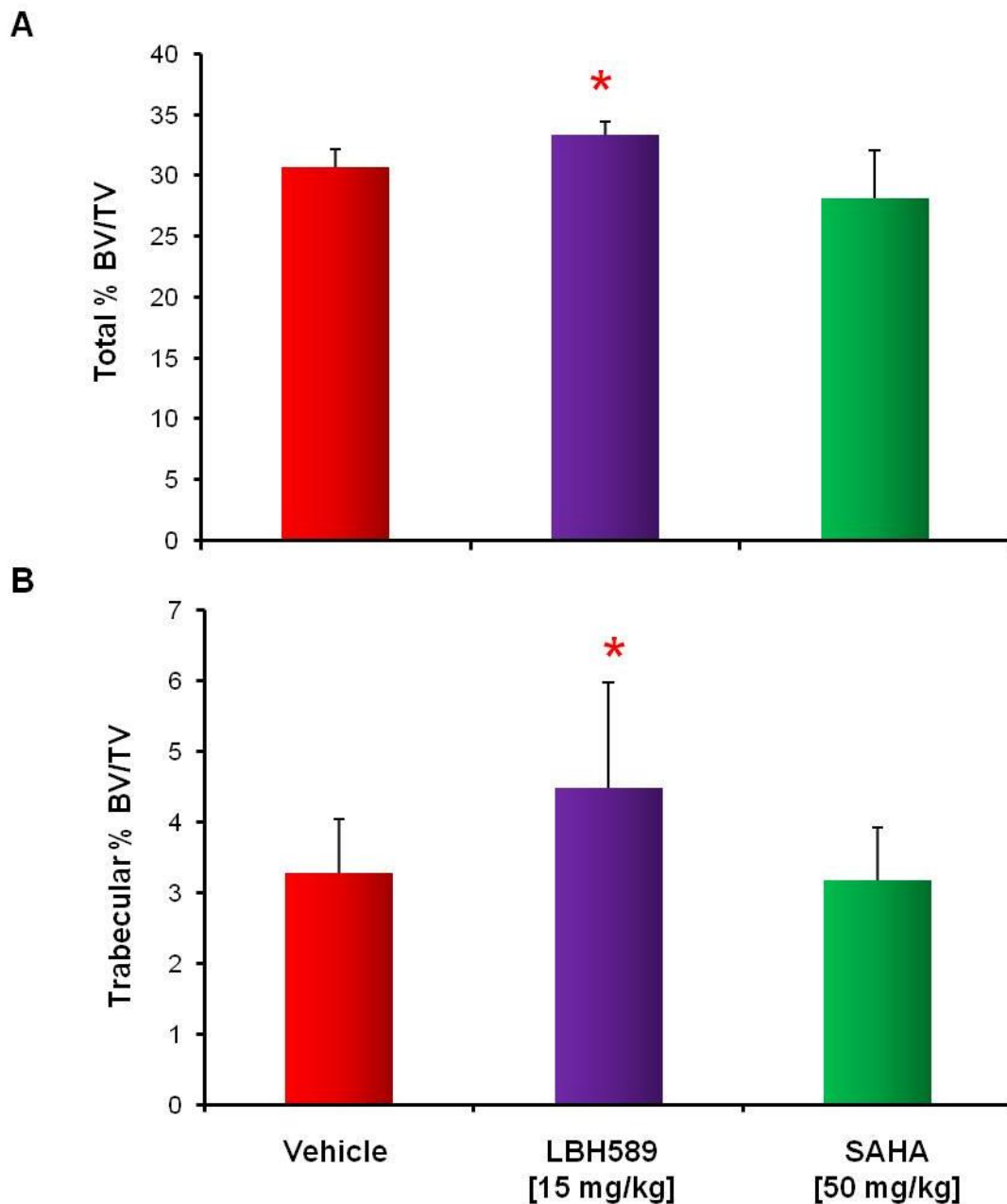
Figure 4-15. LBH589 increases tibial bone volume in athymic nude mice. The graph shows the average total bone volume (**A**), and trabecular bone volume (**B**), from the tibiae of mice bearing primary mammary tumours, with: *$P<0.005$. Treatment with either vehicle, 15 mg/kg of LBH589 or 50 mg/kg SAHA, commenced 7 days after cancer cell inoculation. Bone volume was measured from 730 µ-CT sections of the proximal tibia, starting from the growth plate and using the program CTan. Data shown are the average bone volume from all animals in that group, with bars: mean ± SD (n = 10).

4.3 Discussion

The animal models used in these studies were designed to determine the anticancer efficacy of the HDI LBH589 against the growth of these cells in the primary site of the mammary gland, as well as in a site to which breast cancer preferentially metastasises; the bone marrow. The latter model was also designed to study the interactions between cancer cells and cells of the bone microenvironment, and the effect of LBH589 in modulating the 'vicious cycle' of cancer-induced bone destruction. The bioluminescence, whole body live imaging system provided extremely sensitive tracking of tumour size in real-time.

While previous studies have demonstrated significant anticancer effects of HDIs *in vitro* (Crisanti *et al*., 2009, Haefner *et al*., 2008, Kutko *et al*., 2003) and *in vivo* (Butler *et al*., 2002, Crisanti *et al*., 2009, Floris *et al*., 2009), the data presented in this chapter show that the potent cytotoxic effects of LBH589 on cancer cells observed *in vitro,* did not translate into *in vivo* anticancer efficacy. There are several possible reasons for the observed lack of anticancer efficacy of HDIs in these animal studies. Firstly, HDIs may become unstable *in vivo,* even though they are highly effective on the same cells *in vitro* (Bi and Jiang, 2006). Although LBH589 had minimal effects on cancer growth themselves, the results demonstrating the positive acetylated-H3 within the spleen and bone marrow *in vivo* suggest that active LBH589 levels were achieved systemically in the animals. However, no differences in histone-H3 acetylation were seen in the tumours excised from the mammary glands or from the bone, indicating that LBH589 may have not accumulated at high levels to exert its effects in the tumour mass. One may speculate that the dose and scheduling of treatment may not have been

optimal. Unfortunately the dose of LBH589 could not be scaled upwards as this would have resulted in systemic toxicitiy.

A second possible explanation relates to the epithelial-mesenchymal transition (EMT) phenomena, as this has been implicated in therapeutic resistance (Tomaskovic-Crook *et al*., 2009). Studies on the murine mammary epithelial cell lines, EpH-4 and NMuMG, after EMT induction, have demonstrated acquired resistance to UV-induced apoptosis (Robson *et al*., 2006). Moreover, it has been hypothesised that the resistance of human breast cancer cells to chemotherapy is the result of a population of cells known as "cancer stem cells" or "tumour-initiating cells", forming mammospheres involved in the progression of breast cancer growth. These cells have been shown to have increased EMT-related gene expression profiles, including the downregulation of the *let-7* family of miRNAs, resulting in stem-cell like characteristics and leading to the resistance to chemotherapy (Yu *et al*., 2007). Interestingly, the same authors postulated that these types of cancer cells are characteristic of tumours that can be serially transplanted and cause metastasis when inoculated into mice. More recently, this was supported by another study showing that bone-marrow derived mesenchymal stem cells have the ability to enrich primary mammosphere formation and decrease E-cadherin expression in human breast cancer cell lines both *in vitro* and *in vivo* (Klopp *et al*., 2010), suggesting that the bone micro-environment is critical to the growth and support of cancer metastases. Furthermore, the *in vivo* models that have been investigated previously have been subcutaneous transplantations of cancer cells (Butler *et al*., 2000, Crisanti *et al*., 2009), rather than orthotopic transplant models. Recently, it has been suggested that chemotherapy or total body irradiation to cancer cells in their orthotopic niche may serve as a protective treatment rather than ablative. More specifically to bone cancer models, it was suggested that chemotherapy induces osteoblastic cells to

produce critical growth factors for cancer cell survival within the bone microenvironment, consequently, supplying the cancer cells with vital growth factors for survival (Nilsson, 2009). In the current experiments, the MDA-MB231-TXSA cell line was generated through sequential passages of the parental MDA-MB231 cells (Yoneda *et al*., 2001), therefore according to the literature, these cells may have acquired an EMT-like phenotype. Along with its inoculation into the orthotopic niche, and the lack of distribution of the drug to the cancer cells themselves, these variables may have synergistically contributed to the resistance observed with LBH589 treatment *in vivo.*

In order to assess the activities of LBH589 on breast cancer growth in bone and on cancer-induced bone destruction, the MDA-MB231-TXSA-TGL cells were injected directly into the tibial marrow cavity of nude mice. This model replicates the late stages of the bone metastatic process and enables examination of the effects of LBH589 treatment on the growth of breast cancer cells in the bone microenvironment and on cancer-induced bone destruction. Therefore, to the best of my knowledge, this is the first *in vivo* study of its kind to directly assess the effects of HDIs on cancer growth in bone. This study tested the hypothesis that treatment with LBH589 would abrogate the 'vicious cycle' of cancer-induced bone destruction. While LBH589 treatment failed to reduce tumour load in bone*,* there was however, significant protection of the bone with treatment. In several cancer cell lines, activating the endothelin-1 axis has been suggested to play a crucial role in the progression and survival of cancer cells within the bone microenvironment (Bagnato and Rosano, 2008). This is because β-catenin, an essential regulator of bone formation (Rodda and McMahon, 2006), transcriptionally activates endothelin-1 receptor expression on cancer cells, which is thought to trigger the EMT (Bagnato *et al*., 2004). Also, endothelin-1 can stimulate β-catenin activity

through a P13K-dependent pathway, leading to a futile cycle of cancer progression (Sun *et al*., 2006). Simultaneous functions of endothelin-1 and β-catenin can act together to increase bone formation through decreasing the Dickkopf-1 (Dkk1) inhibition of the Wnt signalling pathway (Clines *et al*., 2007). Furthermore, the expression of endothelin-1 has been implicated in osteoblast bone formation in metastatic cancer models, through the expression of the specific endothelin-1 receptor on osteoblastic cells (Guise *et al*., 2006), therefore indirectly driving the inhibition of osteoclastic bone resorption. Also, it has been suggested that the c-Cbl and Cbl-b family proteins, which are widely expressed mammalian proteins, are implicated in the regulation of osteoclast differentiation and function (Horne *et al*., 2005). Recently it was reported that c-Cbl and Cbl-b act redundantly towards the survival of osteoclastic cells through the displacement of HDAC6, and mice with gene deletions to c-Cbl and Cbl-b are reported to have depleted bone-resorbing activities (Purev *et al*., 2009). HDAC6 has also been implicated in the progression of multiple myeloma, with its constitutive expression playing a critical role in the survival of human PBMCs (Hideshima *et al*., 2005). Therefore, HDAC6 has been implicated in osteoclast formation and function *in vivo*, and the bone preserving activities of LBH589 could, in part, be attributed to the inhibition of HDAC6, therefore inhibiting osteoclast formation and bone resorption.

In addition, osteomimicry, a phenomenon that gives rise to the survival of tumour cells within the bone microenvironment in response to acquired bone cell-like phenotype, has also been explored in the context of metastatic bone disease (Rucci and Teti, 2010). Therefore, further to the findings described herein of HDI-mediated protection of cancer-induced osteolysis, investigations into the pathways involved in the cross-talk between the bone cells and cancer may provide insights into possible

mechanisms involved in the lack of an anticancer response to HDI treatment in its orthotopic niche.

The experiments conducted in this chapter highlight a lack of anticancer efficacy of LBH589 or SAHA against breast cancer growth either in the mammary glands or in bone. However, treatment with LBH589 significantly protected the bone from cancer-induced osteolysis, which was also associated with a drug-induced increase in bone volume of the contralateral, non-tumour bearing tibiae. The increase in bone volume observed in both the tumour-bearing and contralateral, non-tumour bearing tibiae of the LBH589-treated animals was associated with a significant reduction in the number of TRAP$^+$, multinucleated osteoclasts lining the trabecular surface within the bone marrow. This suggests that systemic administration of LBH589 may modulate normal bone metabolism by influencing the function of bone cells independent of its effects on cancer cells, contributing to the protection of cancer-induced bone destruction. While the osteoclasts were identified here as a direct target of LBH589, the observed increase in bone volume may also be attributed to possible effects of LBH589 on the bone forming osteoblasts. These findings have prompted further investigations into the effects of LBH589 on normal bone metabolism in the context of osteoclast and osteoblast function, which will be addressed in the following chapters.

Chapter 5. The effect of LBH589 on osteoclast formation and bone resorption

5.1 Introduction

The data presented in the previous chapter suggested that the protection of breast cancer-induced osteolysis was not the result of direct cytotoxic actions of LBH589 on cancer cells themselves, but rather, was related to LBH589-mediated osteotropism. The number of TRAP$^+$, multinucleated osteoclasts lining the trabecular surface significantly decreased with LBH589 treatment. This effect was not restricted to the tumour-bearing tibiae, but was also observed in the contralateral non-tumour bearing tibiae, in both models tested. This suggests that LBH589 may selectively target osteoclasts within the bone microenvironment. While the actions of several HDIs on cancer cells have been extensively studied, to date no such studies have addressed the role of HDIs on normal bone metabolism in the context of osteoclast or osteoblast function. This highlights an important area of research because cancers that metastasise to bone, often have an osteolytic component, therefore driving a net increase in bone resorption (Body, 2003, Coleman, 1997, Guise *et al*., 2006). Once cancers invade and metastasise into the bone microenvironment, a 'vicious cycle' of cancer-induced bone destruction occurs (Guise *et al*., 2006). Therefore, this chapter will explore the effects of HDIs on the bone cells which drive resorption, the osteoclasts. For these studies, three *in vitro* models of osteoclastogenesis were used. Firstly the RAW264.7 murine monocytic cell line, which differentiates into osteoclast-like cells in the presence of RANKL; secondly, human peripheral blood mononuclear cells (PBMC), which differentiate into osteoclast-like cells in the presence of RANKL and MCS-F, and thirdly, osteoclast-like cells cultured from primary human Giant Cell Tumours (GCT), of bone. All three models were used to investigate the effect of LBH589 treatment on the formation and bone resorptive activity of mature osteoclasts. The effects of LBH589 were also compared to SAHA,

which has been investigated previously by this laboratory (Liapis *et al*., 2006). It was hypothesised that LBH589 inhibits the development and function of osteoclasts.

5.2   Results

5.2.1 LBH589 inhibits osteoclast formation in the murine RAW264.7 monocytic cell line

The formation, function and survival of osteoclasts is largely dependent on two factors, MCS-F and RANKL. While the differentiation of human bone marrow cells into osteoclasts requires both MCS-F and RANKL, mouse RAW264.7 cells require only RANKL. In the first set of experiments, the direct effect of LBH589 and SAHA on RANKL-induced osteoclast differentiation of RAW264.7 murine monocytic cells was investigated. When RAW264.7 cells were cultured for 5 days with RANKL, the number of $TRAP^+$, multinucleated osteoclast-like cells, defined as having greater than 3 nuclei per cell, increased significantly when compared with control cells cultured in the absence of RANKL. When added in combination with RANKL, LBH589 (0.1 – 50 nM), or SAHA (1 – 2000 nM), dose-dependently inhibited RANKL-induced osteoclast differentiation. Figure 5-1 shows that LBH589 was 50 times more potent than SAHA (as shown in figure 5-2), and was able to initiate inhibition of osteoclastogenesis at 1.0 nM vs 50 nM for SAHA (figure 5-2). To determine the viability of RAW264.7 cells treated with LBH589, CellTitre-Blue staining for cell viability demonstrated that this effect was selective for osteoclast differentiation, since the doses of LBH589 that inhibited osteoclast formation did not affect cell viability (figure 5-3).
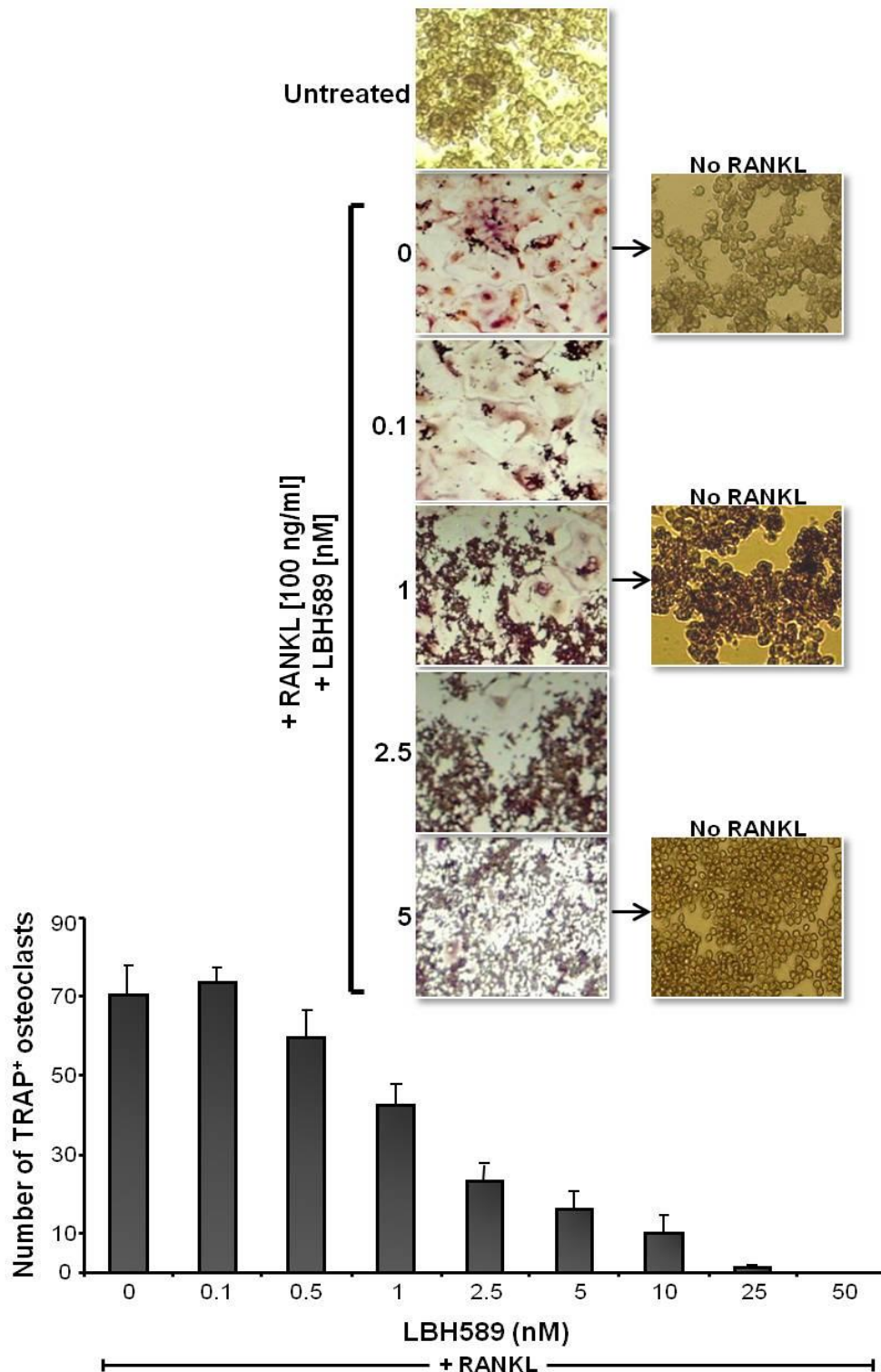
Figure 5-1. The effect of LBH589 on murine RAW264.7 cells. RAW264.7 cells were seeded into 96-well multiwell plates at 1 x 10^4 cells/well, and allowed to adhere overnight. Cells differentiated into TRAP[+], multinucleated osteoclasts when treated with RANKL over 5 days. Addition of LBH589 dose-dependently decreased the number of TRAP[+], multinucleated osteoclasts formed. The graph is a representative experiment, repeated at least 3 times, with bars; mean ± SD.

Figure adapted from *Liapis, et al., 2006*
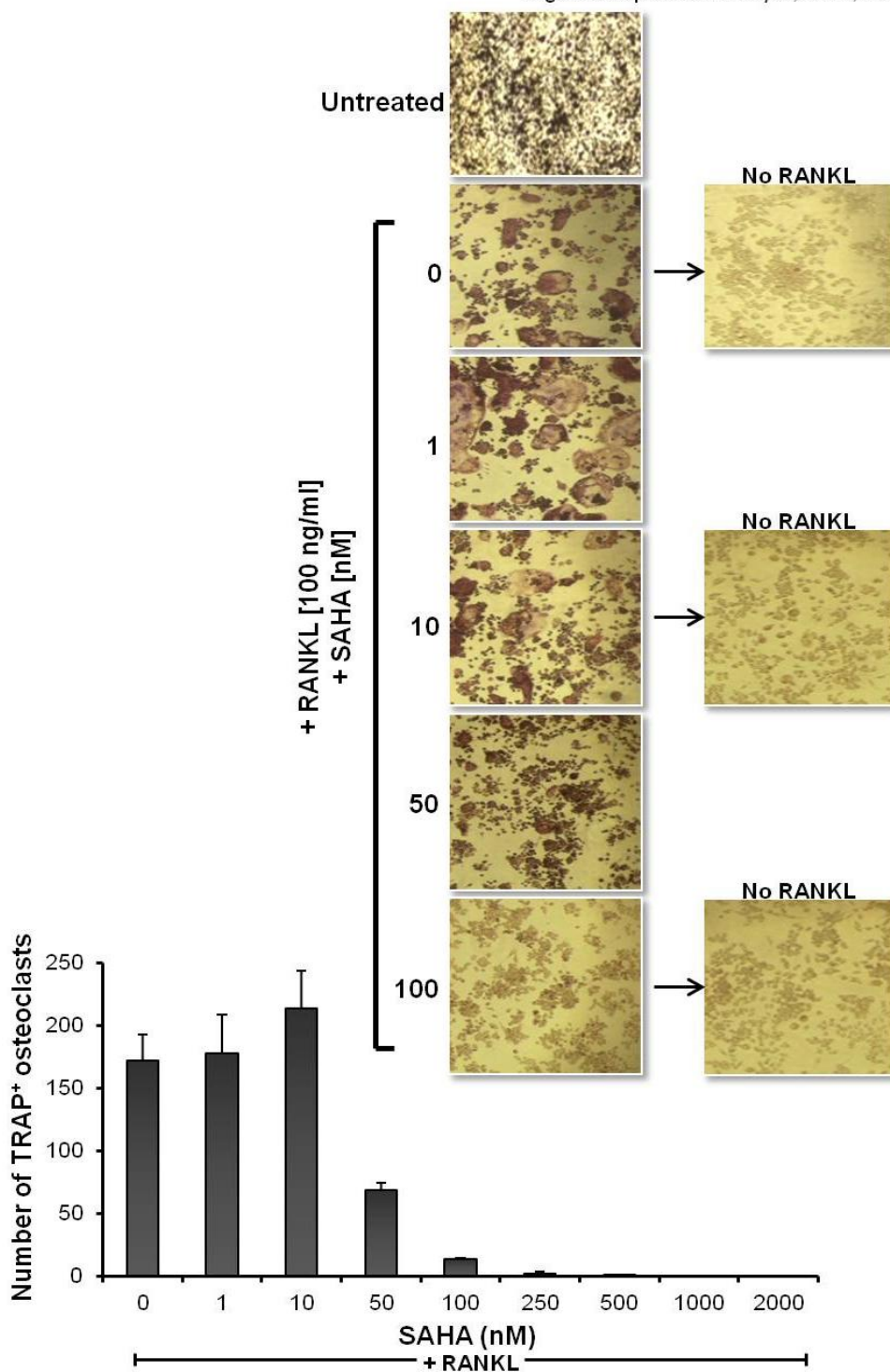
Figure 5-2. The effect of SAHA on murine RAW264.7 cells. RAW264.7 cells were seeded into 96-well multiwell plates at 1×10^4 cells/well, and allowed to adhere overnight. Cells differentiated into TRAP[+], multinucleated osteoclasts when treated with RANKL over 5 days. Addition of SAHA dose-dependently decreased the number of TRAP[+], multinucleated osteoclasts formed. The graph is a representative experiment, repeated at least 3 times, with bars; mean ± SD.
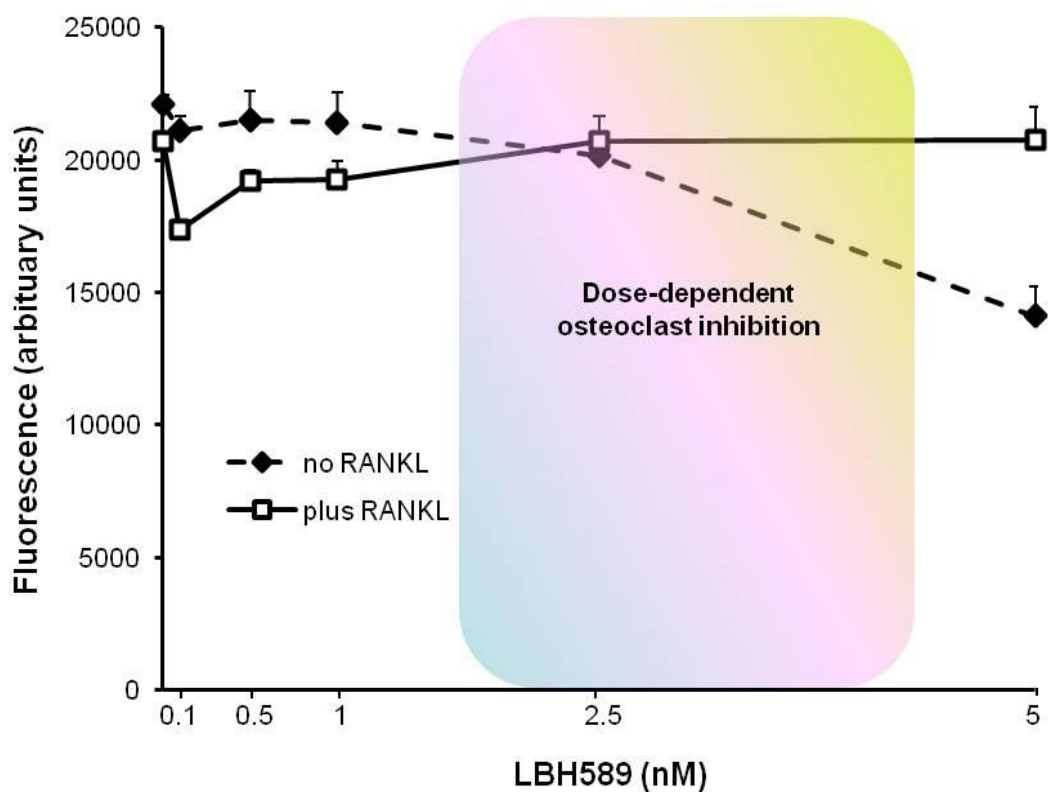
Figure 5-3. LBH589 selectively inhibits osteoclast formation. Cells were cultured with the CellTitre-Blue reagent for 4 hours and fluorescence was measured ($560_{ex}/590_{em}$). The graph demonstrates that there was no difference in cell viability at the LBH589 doses in which osteoclast formation was inhibited (solid line, open squares). The graph is a representative experiment, repeated at least 3 times, with bars; mean ± SD.

5.2.2 LBH589 inhibits osteoclastogenesis and bone resorption by human peripheral blood mononuclear cells (PBMC).

Human peripheral blood mononuclear cells (PBMC) isolated from blood donors were used to investigate the effects of LBH589 in a human model of osteoclastogenesis and bone resorption. In the presence of the key osteoclastic stimulating factors, RANKL and MCS-F, PBMC differentiate into mature, functional osteoclasts over 9 days. PBMC were left untreated or cultured in the presence of increasing concentrations of LBH589 (0.1 – 5 nM), or SAHA (1.0 – 1000 nM), with and without RANKL and MCS-F. LBH589 treatment dose-dependently decreased the number of TRAP$^+$, multinucleated osteoclasts, beginning at a dose as low as 0.1 nM (figure 5-4A). Treatment with SAHA inhibited osteoclast formation only at the highest dose of 1000 nM (figure 5-4B). In parallel with the osteoclastogenesis experiments, PBMC were also seeded directly onto whale dentine slices to assess their bone resorbing activities. The amount of resorption was determined using scanning electron microscopy (SEM). The dose-dependent decrease in the formation of osteoclastic cells observed by TRAP staining was concomitant with a significant inhibition in the number of resorption pits on whale dentine, with complete inhibition of resorption occuring at a concentration as low as 2.5 nM for LBH589 (figure 5-5A). Interestingly, SAHA treatment (at 100 nM) also decreased the number of resorption pits, which is 10-fold lower than the dose which inhibited the formation of TRAP$^+$, multinucleated osteoclasts, suggesting a potent effect on the resorptive function of mature osteoclasts (figure 5-5B).

A

B
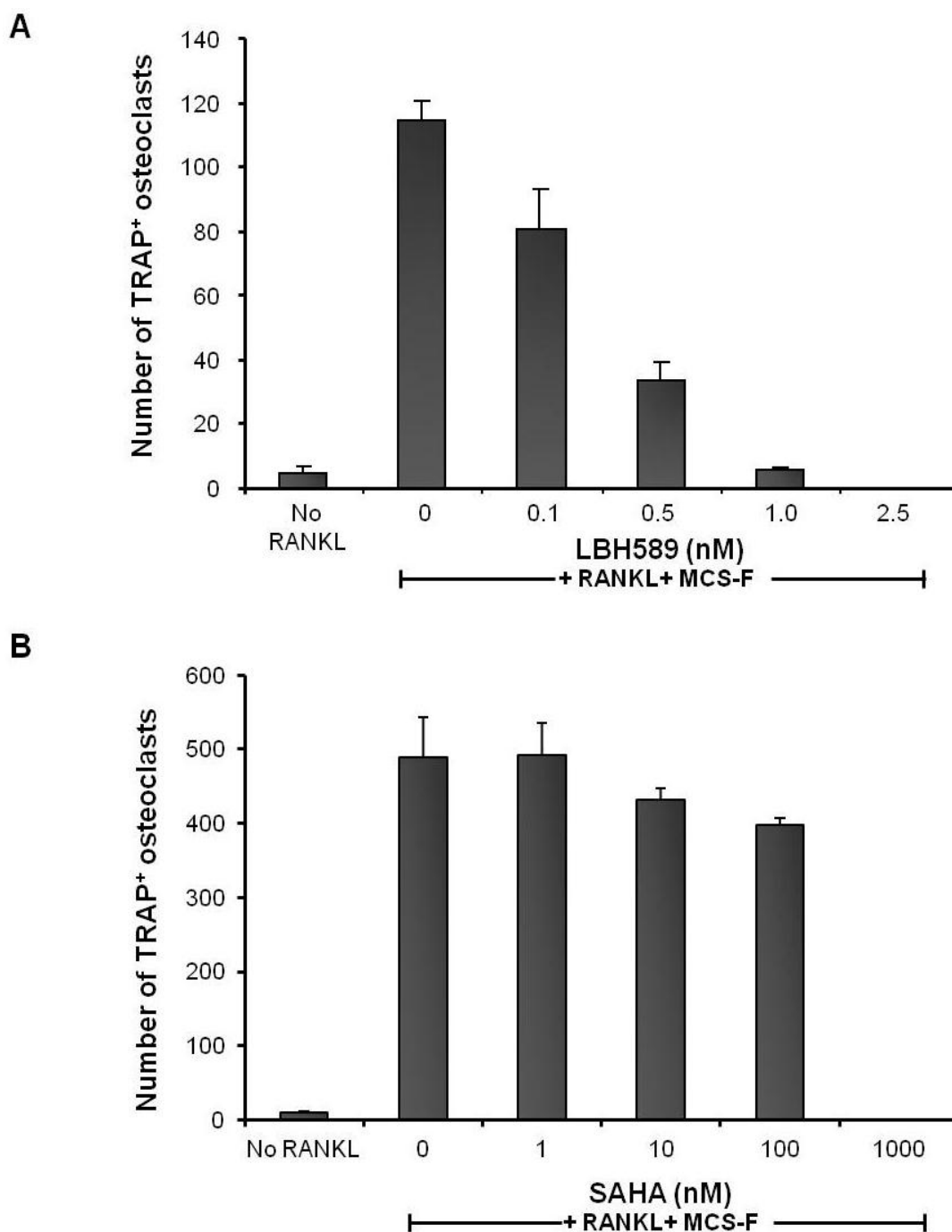
Figure 5-4. The effect of HDIs on the number of TRAP⁺, multinucleated osteoclasts generated from human PBMC. PBMC were seeded into 96-well multiwell plates at 2.5×10^5 cells/well, and allowed to adhere overnight. With the addition of MCS-F and RANKL, PBMC differentiated into TRAP⁺, multinucleated osteoclasts. However, when co-cultured with LBH589 (**A**), or SAHA (**B**), there was a dose-dependent decrease in the number of osteoclasts formed. The graphs are of representative experiments, repeated at least 3 times, with bars; mean ± SD.
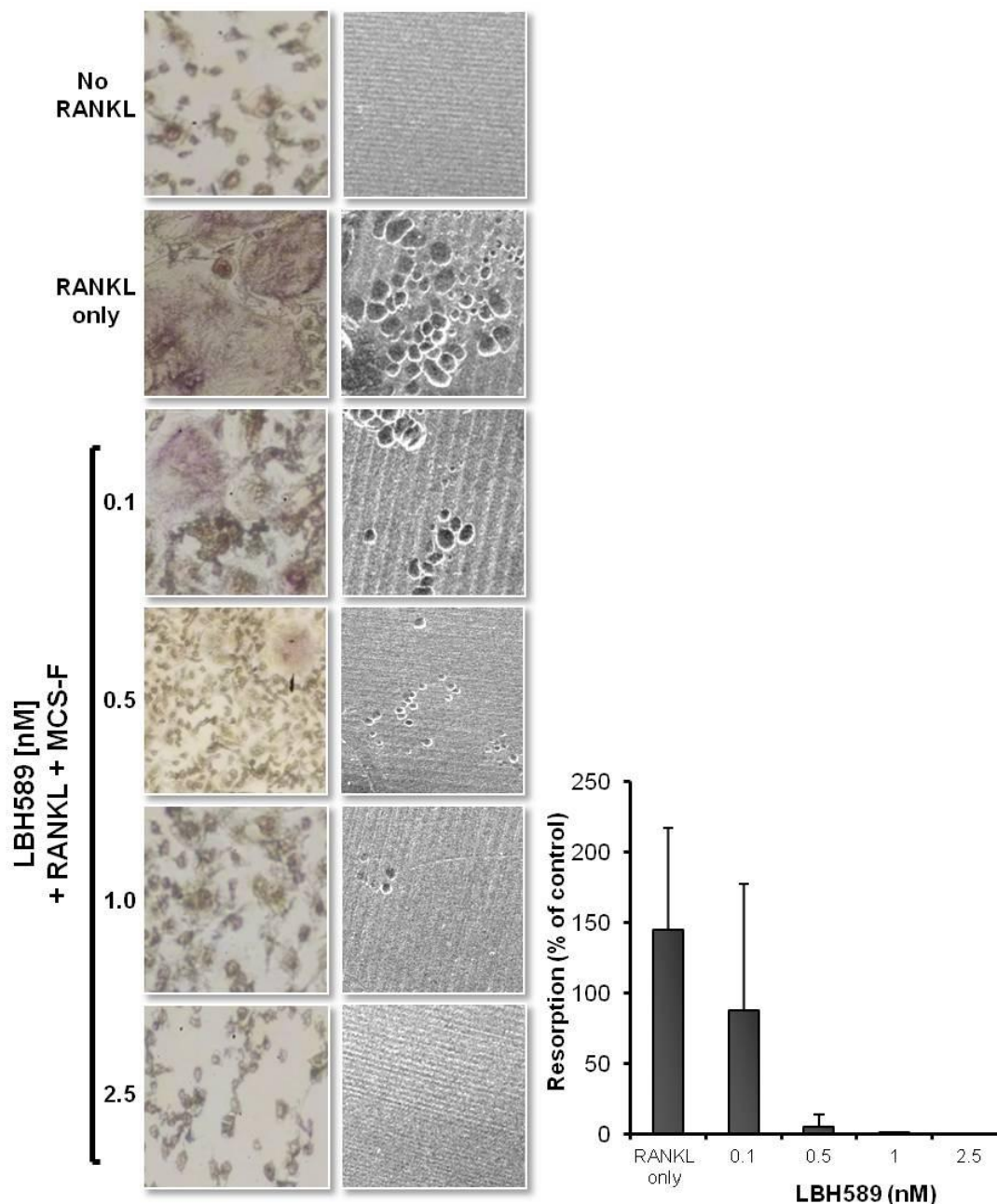
Figure 5-5A. LBH589 inhibits osteoclast formation and bone resorption by human PBMC. Representative images of PBMC treated with LBH589 at the indicated doses, and their resorptive activity on dentine are depicted.

Left panel: cells were co-stained with TRAP and crystal violet and visualised under light microscopy.

Right panel: dentine slices were thoroughly washed and dehydrated as described in the Methods. Resorption pits were visualised under SEM and counted.

The graph represents the quantification of bone resorption, with results expressed as a percentage of control (RANKL only). The experiment was repeated at least 3 times, with bars; mean ± SD.
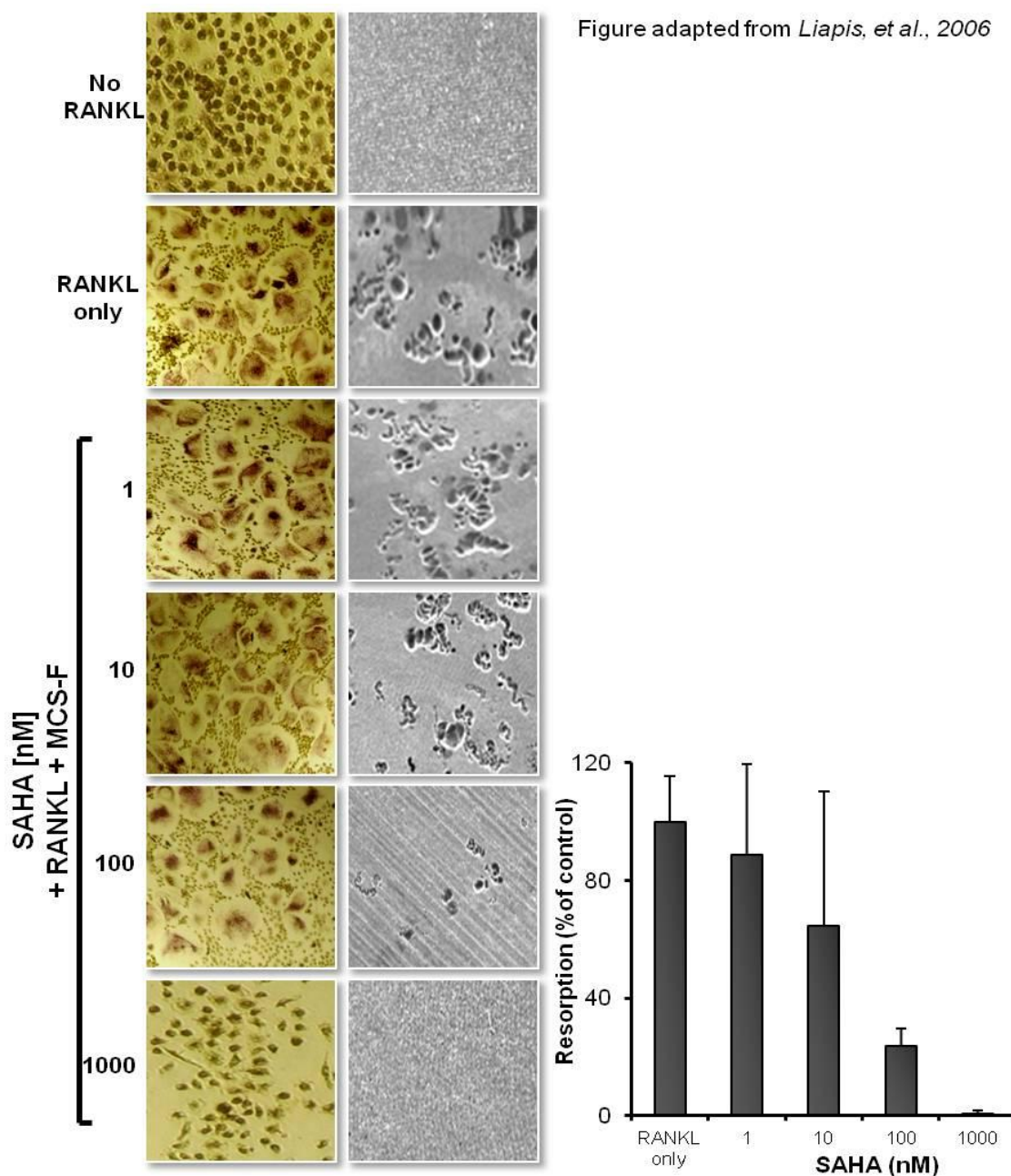
Figure 5-5B. The effect of SAHA on human PBMC. Representative images of PBMC treated with SAHA at the indicated doses, and their resorptive activity on dentine are depicted.

Left panel: cells were co-stained with TRAP and crystal violet and visualised under light microscopy.

Right panel: dentine slices were thoroughly washed and dehydrated as described in the Methods. Resorption pits were visualised under SEM and counted.

The graph represents the quantification of bone resorption, with results expressed as a percentage of control (RANKL only). The experiment was repeated at least 3 times, with bars; mean ± SD.

5.2.3 LBH589 inhibits bone resorption by mature osteoclasts isolated from human giant cell tumours of bone

In this set of experiments the effects of LBH589 on the bone resorbing activity of mature osteoclasts was investigated and also compared to the effects of SAHA. Osteoclast-like cells were isolated from primary human giant cell tumours (GCT) known to contain abundant numbers of mature and active osteoclasts, as described previously by this laboratory (Atkins *et al.*, 2000). When plated on dentine slices for 5 days, GCT-osteoclasts were capable of bone resorption even in the absence of exogenous RANKL. LBH589 (1.0 – 10 nM) dose-dependently decreased bone resorption by mature GCT-osteoclasts (figure 5-6). The concentration of LBH589 required to inhibit resorption was consistently lower (in the nanomolar range), compared to SAHA being in the micromolar (1.0 – 10 μM) range (figure 5-7).
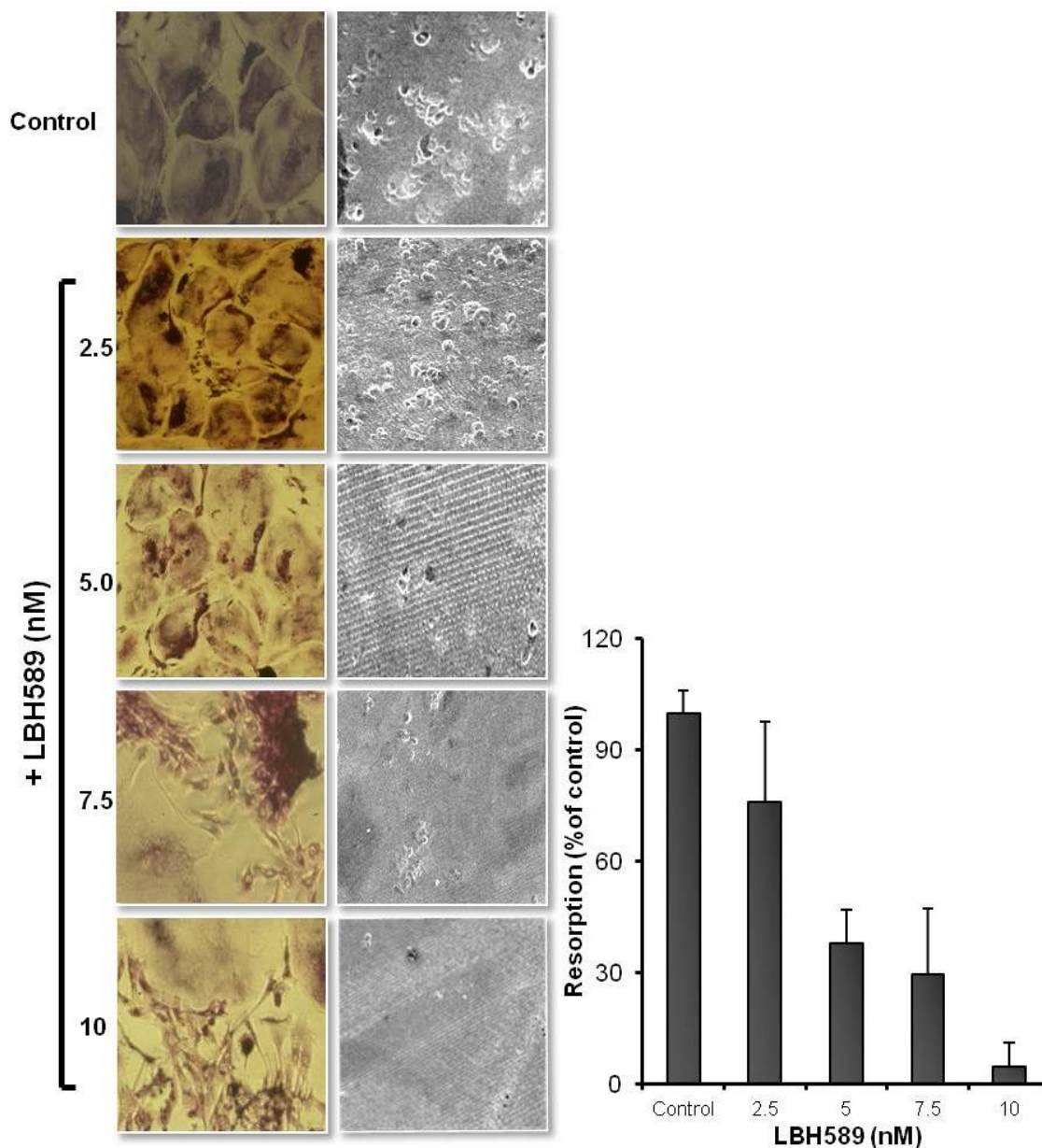
Figure 5-6. The effect of LBH589 on the bone resorbing activities of human GCT. Representative images of GCT treated with LBH589 at the indicated doses, and their resorptive activity on dentine are depicted.

Left panel: cells were co-stained with TRAP and crystal violet and visualised under light microscopy.

Right panel: dentine slices were thoroughly washed and dehydrated as described in the Methods. Resorption pits were visualised under SEM and counted.

The graph represents the quantification of bone resorption, with results expressed as a percentage of control. The experiment was repeated at least 3 times, with bars; mean ± SD.
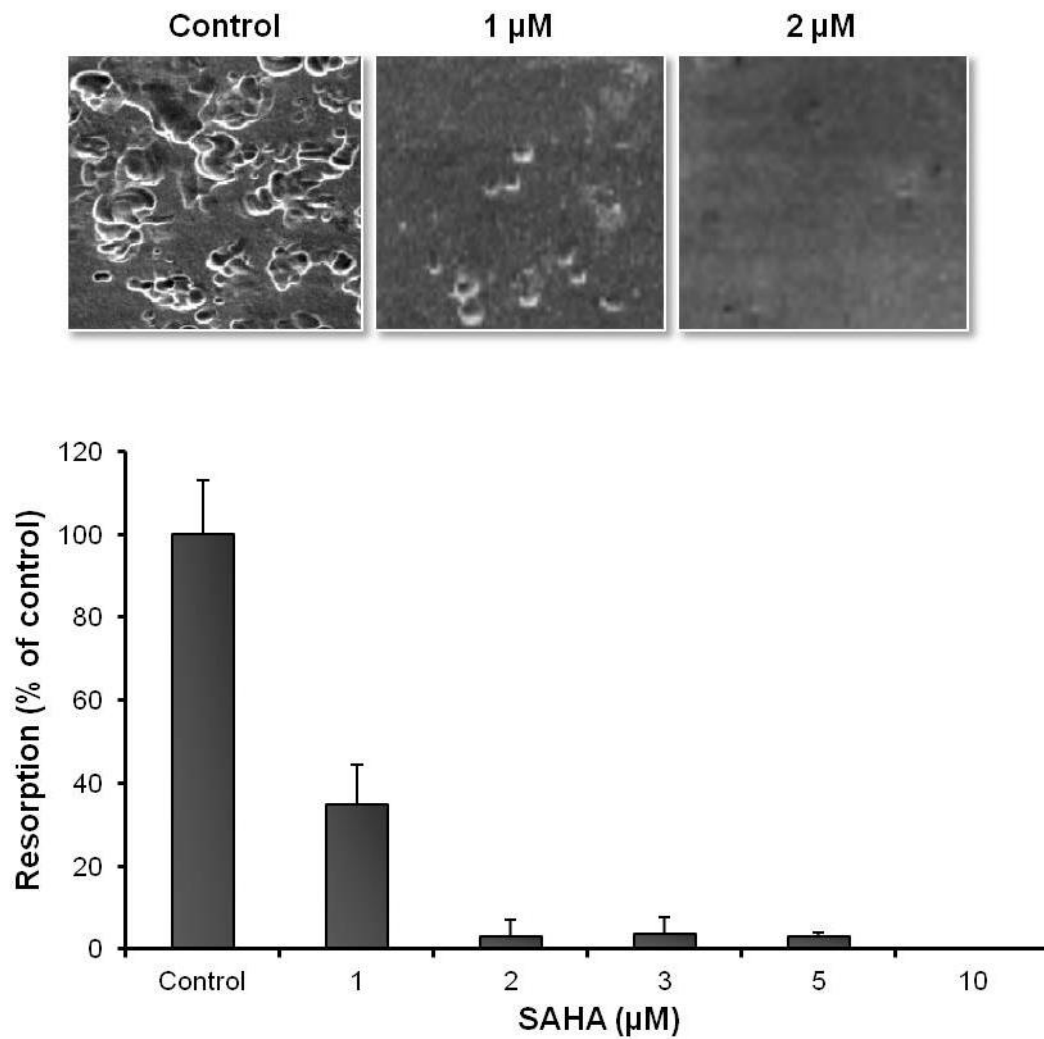
Figure 5-7. The effect of SAHA on the bone resorbing activities of human GCT. Representative images are of dentine slices which were thoroughly washed and dehydrated as indicated in the Methods. Resorption pits were visualised under SEM and counted. The graph represents the quantification of bone resorption, and is expressed as a percentage of the control. The experiment was repeated 3 times, with bars; mean ± SD.

5.2.4 Western blot analyses of the effect of LBH589 on osteoclasts

To investigate a mechanism, by which LBH589 inhibited osteoclastogenesis, western blot analyses of several proteins known to be involved in osteoclast formation was performed. Previous published data have shown that both SAHA and another HDI, LAQ824, suppressed the RANKL-mediated activation of downstream signals, p42/44 MAPK and NF-kB in osteoclasts (Liapis *et al.*, 2006), no such regulation by LBH589 was reported in these studies. While p42/44 MAPK was phosphorylated with RANKL treatment, no changes were observed following LBH589 co-treatment (figure 5-8). The expression of proteins known to be involved in osteoclastogenesis, including, phosphorylated-p38 MAPK, phosphorylated- and total-IκB, p65-NF-κB, and NFATc1, were also examined for regulation following LBH589 treatment. No changes in the expression levels were evident. Furthermore, a hallmark of HDI-induced cell apoptosis is the enhanced expression of the apoptotic protein, p21. Western blot analysis did not show an increase in expression levels following LBH589 treatment, further confirming that LBH589 is likely to exert its effects through osteoclast inhibition, rather than through causing cell death (figure 5-8).
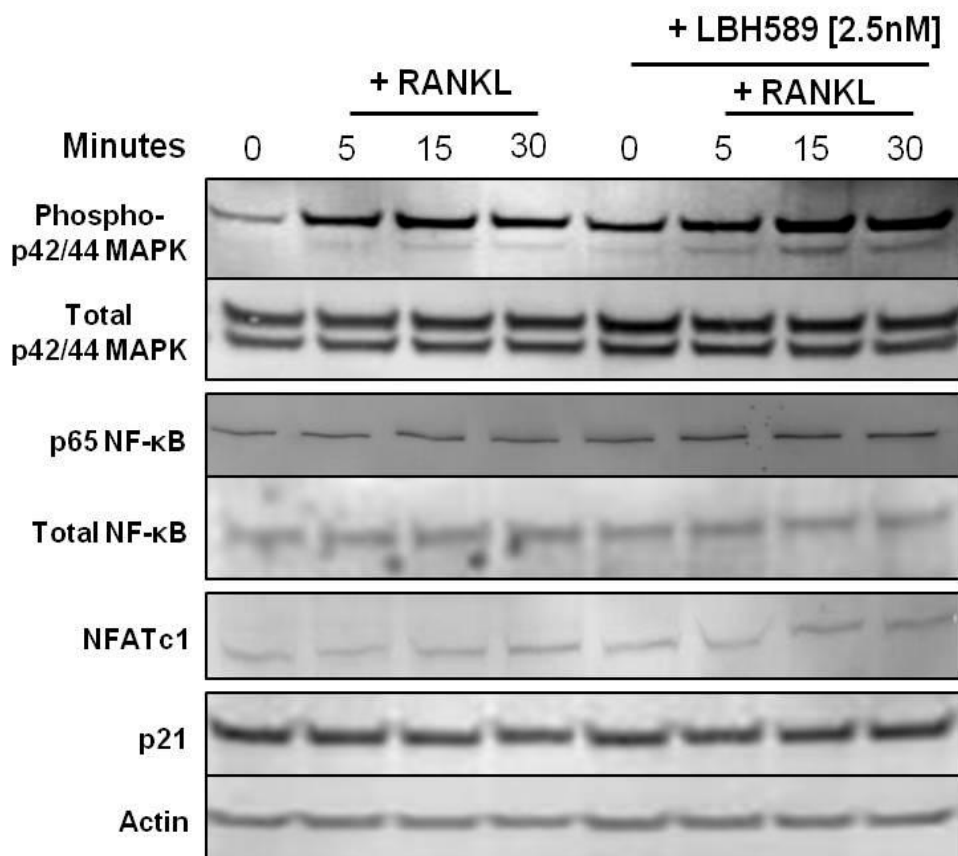
Figure 5-8. Western blot analyses on the effect of LBH589 on osteoclasts. RAW264.7 cells were seeded into T25 flasks at 4 x 10^6 cells/flask and allowed to adhere overnight. Cells were treated with RANKL only, or co-treated with LBH589, as indicated in the Methods. On day 5, after the cells were serum-starved overnight, the cells were isolated for western blot analysis immediately following treatment with and without LBH589, at 5, 15 and 30 minutes.

5.3 Discussion

The experiments described in this chapter clearly demonstrate novel actions of LBH589 with direct effects on osteoclast formation and function. LBH589 exerted its anti-osteoclastogenic actions in the low nanomolar range, which were seen in the three independent model systems of osteoclastogenesis. The inhibition of osteoclastogenesis was associated with a reduction in bone resorption when these cells were cultured on dentine slices. More importantly, this effect was selective for osteoclast function, since the same doses had no effect on cell proliferation and survival.

Tumour-induced bone destruction caused by primary or metastatic cancers are associated with excessive bone resorption due to heightened osteoclast activity. There is also evidence of a strong osteolytic component in 'osteoblastic' lesions (Body, 2003, Labrinidis *et al*., 2009b). Osteoclast precursors express RANK on their surface and are activated to differentiate into functional multinucleated osteoclasts by RANKL, presented on the surface of osteoblasts, osteocytes and stromal cells (Jensen *et al*., 2009, Atkins *et al*., 2009a, Wijenayaka *et al*., 2011). Once mature osteoclasts have performed their function of bone resorption, they undergo apoptosis (Boyle *et al*., 2003). Osteoclast inhibition or apoptosis has been a principal therapeutic target for conditions involving excessive bone loss. However, first line treatments involving high doses of bisphosphonates have been associated with destructive osteonecrosis of the jaw (Bedogni *et al*., 2010), and have also been linked to an increased risk of oesophageal cancer (Cardwell *et al*., 2010), in addition to other unwanted side effects (Mortimer and Pal, 2010). Therefore, there is a need to develop new therapeutic approaches with fewer adverse effects. The concentrations of HDIs that blocked osteoclastogenesis in the studies described in this chapter were comparable and even lower than those reported in the serum of animals in various pre-clinical animal models

of cancer, and in patients from clinical trials (Morita *et al*., 2011, Song *et al*., 2011). Taken together, these results demonstrate that HDIs have a potent and selective inhibitory effect on the differentiation and bone resorbing activity of osteoclasts at doses that are non-toxic and safe. As such, they may be considered as alternative anti-resorptives.

Treatment with HDIs results in hyperacetylation of target genes and proteins, and has been reported to modify their actions either positively or negatively, in a cell-specific manner (Bolden *et al*., 2006). The findings described in this chapter are in support of previous reports demonstrating that HDIs inhibit osteoclastogenesis. However, in contrast, they did not affect the differentiation into macrophages, suggesting the osteotropic-specificity of HDIs as previously reported (Rahman *et al*., 2003). In mouse bone marrow cells, it was reported that the effect of the HDI, TSA, was a potent inducer of osteoclast apoptosis associated with caspase-3 and -9 activation (Yi *et al*., 2007). Other mechanisms proposed to modulate osteoclast differentiation include growth arrest associated with the induction of the p21 cyclin-dependent kinase inhibitor (Sankar *et al*., 2004). This was associated with changes in the promoter-associated proteins, including HDAC1 (Gui *et al*., 2004). The suppression of p21 by knockdown experiments reduced the number of apoptotic osteoclasts (Yi *et al*., 2007). Additionally, several HDIs were shown to inhibit the formation of pre-osteoclast-like cells and multinucleated osteoclasts from cultures of rat bone marrow cells. This effect was associated with a reduction in the mRNA expression of cathepsin K and the calcitonin receptor (Rahman *et al*., 2003). In the present study, novel and selective anti-resorptive activities of LBH589 on human osteoclasts generated from PBMC and mature osteoclasts from GCT of bone were demonstrated.

Previous studies have shown that TSA and sodium butyrate inhibit the activation of p38 MAPK and NF-κB (Rahman *et al*., 2003), and a number of HDIs have been shown to inhibit NF-κB activation (Leoni *et al*., 2002, Yin *et al*., 2001). It is well known that NF-κB activation is required for the initiation of osteoclastogenesis, and osteoclast differentiation from bone marrow precursors was inhibited by the inactivation of NF-κB (Rahman *et al*., 2003, Takada *et al*., 2006). Furthermore, NFATc1, which is activated by RANKL, is a central transcriptional regulator of osteoclastogenesis, and is essential for terminal differentiation of osteoclasts (Takayanagi *et al*., 2002). A previous study by Nakamura and colleagues, (Nakamura *et al*., 2005), found that the HDI, FR901228, strongly inhibited the nuclear translocation of NFATc1, and this was associated with the acetylation state of the IFN-β promoter, thereby inhibiting osteoclastogenesis. In contrast to these findings, the present study failed to show any regulation by LBH589 of key factors previously shown to be involved in RANKL-mediated signalling including, MAPK, NF-κB and NFATc1 signalling. The translocation of NFATc1 to the nucleus is regulated by the calcium/calcineurin-dependent phosphatase pathway (Rao *et al*., 1997), and HDAC inhibition has been reported to negatively affect cellular translocation of the NFATc1 protein, through IL-2 transcription inhibition (Diakos *et al*., 2002). The literature describes only a limited number of studies on the effects of HDIs on osteoclast formation and activity. However, the role of key proteins including NF-κB and NFATc1 is central in the initiation and regulation of osteoclastogenesis (Takayanagi *et al*., 2002, Takada *et al*., 2006).

There are several other mechanisms that may explain the results described here. For example, in a recent study, osteopontin was shown to inhibit NFATc1 translocation and increase the survival of osteoclastic cells isolated from rabbit and rat (Tanabe *et al*.,

2011). In addition, hyaluronan (HA), an extracellular polysaccharide expressed in bone matrices, was shown to inhibit the activity of mature osteoclasts in co-culture with PBMC. This effect was due to a direct interaction with its receptor, CD44, leading to the modulation of osteopontin and matrix metalloproteinase-9 (Pivetta *et al*., 2010). Furthermore, a novel molecule, *Inpp4bα* was identified from an early osteoclast differentiation stage, as a key modulator in NFATc1 translocation and activation. Mice deficient in *Inpp4bα* displayed an increased osteoclast differentiation rate, and more importantly, it was recently recognised as a susceptibility locus in humans for reduced bone mineral density (Ferron *et al*., 2011). As the detailed molecular mechanisms by which LBH589 regulates osteoclastogenesis was not the main scope of this thesis, the above provides further avenues of investigation for elucidating the molecular determinants, by which LBH589 regulates osteoclastogenesis.

It is evident that the mechanisms, by which HDIs inhibit osteoclast differentiation and function, are still not fully understood. However, the findings described in this chapter are consistent with reports that HDIs inhibit osteoclastogenesis and bone resorption, either through the regulation of the expression of known genes in the osteoclastogenesis pathways, or by other mechanisms, yet to be determined. Further investigation into the molecular events that underlie the effects of HDIs in bone may allow the development of new therapeutic approaches in which HDIs will be used either alone, or in combination with other therapies related to cancer in bone. Taken together, the animal experiments described in chapter 4, and the *in vitro* data presented in this chapter, indicate that LBH589 has potent anti-osteoclastogenic activity, and may represent a potential new class of agents useful in the treatment of pathological bone loss associated with cancer-induced bone disease.

Chapter 6. The effect of LBH589 on human primary osteoblasts

6.1 Introduction

The experiments described in this chapter were prompted by the unique findings presented in chapter 4, in which administration of LBH589 to immune-compromised mice resulted in increased bone volume. This effect was associated with a reduction in the number of TRAP$^+$, osteoclasts lining the trabecular bone surface of the tibiae. The possibility that the observed increased bone volume could also be attributed to an increase in bone formation, associated with increased osteoblast number and/or activity, could not be discounted. Therefore the work described here aimed to determine the effects of LBH589 on the maturation and function of osteoblasts *in vitro.* To do this, a well described model system of osteoblast maturation and activity was employed using human-derived normal bone cells (NHB) (Atkins *et al*., 2003, Atkins *et al*., 2005, Atkins *et al*., 2009a).

As mentioned previously, cancer-induced bone destruction is associated with a net increase in osteoclastic activity, and this may be concomitant with suppression of osteoblastic activity, resulting in excessive bone loss (Giuliani *et al*., 2006), The anti-resorptive group of compounds, the bisphosphonates, inhibit the 'vicious cycle' of cancer-induced osteolysis by inhibiting osteoclast function, and have been the standard of care for patients with skeletal malignancies and osteoporosis (Cardwell *et al*., 2010, Mosekilde *et al*., 2011). However, bisphosphonates cannot compensate for the suppression of bone formation by metastatic cancers (Trinkaus *et al*., 2009). While reasonably effective, anti-resorptive treatment is only designed to prevent *further* bone loss and, consequently, anabolic approaches are required to build more bone. Currently, PTH is the main commercially available anabolic therapeutic option to increase bone formation and reduce osteoporotic fractures, but it is relatively expensive and is not recommended for long-term treatment. Sclerostin (SCL) is now also emerging as a

therapeutic target for anabolic bone treatment, with anti-SCL antibodies in early-phase clinical trials (Cejka *et al*., 2011, Mosekilde *et al*., 2011). Therefore, new evidence surrounding the mechanisms and therapeutic advantages of targeting osteogenesis for the treatment of various conditions affecting bone loss is accumulating (Cejka *et al*., 2011, Mosekilde *et al*., 2011, Trivedi *et al*., 2010). Thus, an ideal therapeutic agent for bone-related disorders, including bone cancers, would promote bone formation in addition to inhibiting bone loss. Previous results in this thesis revealed that, while no anticancer effects were observed in animals treated with LBH589, there was nonetheless a treatment-induced increase in tibial bone volume. This increase in bone volume was associated with a significant reduction in the number of TRAP$^+$, osteoclasts lining the trabecular bone surface. However, it remains unclear as to whether LBH589 also affects osteoblast function.

There have been few studies into the effects of HDIs on osteoblastic cells, and the studies that have been reported are limited to the use of the pre-osteoblastic MC3T3-E1 mouse cell line. It was previously reported that sodium butyrate induced ALP expression in the pre-osteoblastic MC3T3-E1 mouse cell line, but not in mature osteoblasts (Iwami and Moriyama, 1993). More recently, HDAC3 inhibition by HDIs, or HDAC3-specific short hairpin RNAs in the same cells, was shown to accelerate mineralisation and induced expression of osteocalcin, osteopontin and bone sialoprotein (Schroeder et al., 2004b). The same authors then showed that HDIs promoted mouse osteoblast maturation, at least in part, by enhancing Runx2-dependent transcriptional activation (Schroeder and Westendorf, 2005). There are currently no reports of the effects of HDIs, and in particular, LBH589, on human primary osteoblasts.

The normal human bone (NHB) cells used for the experiments in this chapter have been described extensively. Briefly, these cells were derived from trabecular bone

fragments obtained from normal patients, aged between 58-80 years, during joint replacement surgery (Royal Adelaide Hospital, SA, Australia). The monoclonal antibody, STRO-1, identifies several maturation stages of NHB cells (Gronthos *et al*., 1999), and when cultured under osteogenic conditions, these cells are able to develop into mature functional osteoblasts associated with gene expression and matrix mineralisation (Atkins *et al*., 2009a). It has also been shown that, when cultured under osteogenic conditions, NHB cells are able to further differentiate into mature osteoblasts that lay down a collagen-rich mineralised matrix, express specific genes, and ultimately adopt a morphology consistent with osteocytes (Atkins *et al*., 2009a, Atkins *et al*., 2009b). Therefore, these NHB cells are an appropriate and accepted *in vitro* surrogate model of *in vivo* bone formation. The aim of the experiments described here was to investigate the effects of LBH589 on human osteoblast maturation and function. The hypothesis was that LBH589 promotes human osteoblast maturation and activity.

6.2 Results

6.2.1 Normal human bone (NHB) cells are resistant to the cytotoxic effects of LBH589

A panel of NHB cell lines, isolated from 8 different donors, was screened using long-term (21 day) cultures of NHB cells under standard osteo-inductive conditions. From this panel, cultures from 4 donors were selected for further experiments, based on their ability to predominate under long-term cultre conditions, and their ability to lay down mineral (rationale as described by (Atkins *et al*., 2009a, Gronthos *et al*., 1999)). NHB cells were treated for 72 hours with LBH589 at doses ranging from $1.0 - 1000$ nM. Using the CellTitre-Blue reagent, cell viability was determined 72 hours after treatment. This reagent directly measures the metabolic activity of live cells by reducing a dye to its fluorescent counterpart, therefore directly correlating the activity of cells to cell viability (as described in section 2.4). Figure 6-1 represents the results obtained for 2 representative donors. LBH589 treatment at doses of 1 and 5 nM did not reduce the number of viable NHB cells. However, viability reduced progressively at higher concentrations of the drug, with an IC_{50} of approximately 350 nM for donor 1. This compares to an IC_{50} of approximately 50 nM for the breast cancer cell line MDA-MB231-TXSA (refer to section 3.2.1), consistent with an increased resistance of non-transformed NHB cells, in terms of cell viability with LBH589, compared with the breast cancer cells. Cells from two donors were chosen to characterise in detail the effect of LBH589 under long-term, osteo-inductive conditions. To test the effects of LBH589 on mineralisation and gene expression, a concentration of 2.5 nM was chosen. This dose was well within the range where no loss of cell viability could be detected (as evident from figure 6-1).
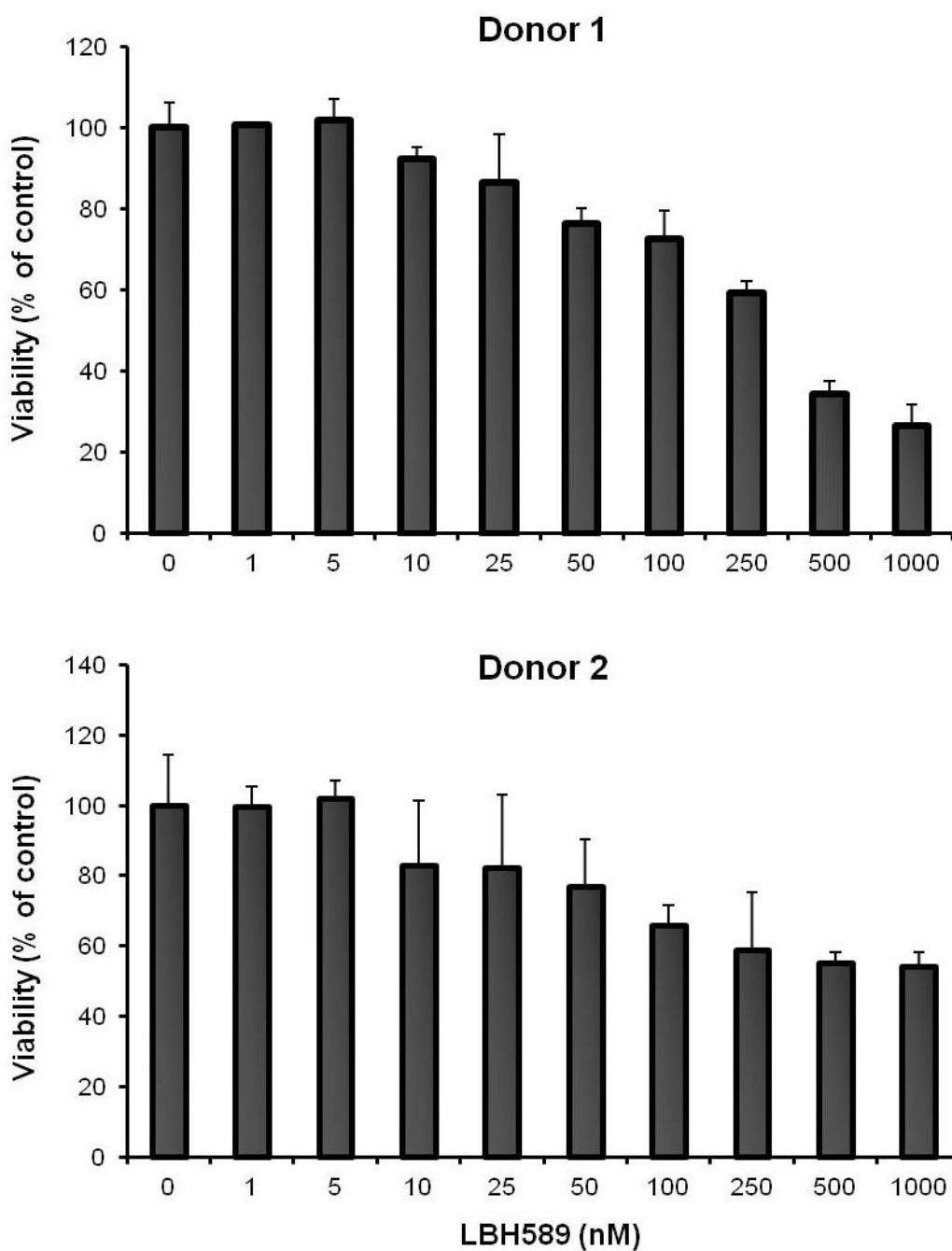
Figure 6-1. NHB cells are resistant to the cytotoxic effects of LBH589. NHB cells were treated over 72 hours with LBH589. CellTitre-Blue reagent was added to each well and incubated for 4 hours before fluorescence reading ($560_{ex}/590_{em}$). The graphs are representative of two independent donors, with each data point presented as a mean of quadruplicate measures ± SD. The data are expressed as percentage relative to untreated (0 nM).

6.2.2 LBH589 enhances human osteoblast mineralisation

To determine the effect of LBH589 on calcium deposition by NHB cells, mineralisation in the cell layer was measured in the presence or absence of LBH589 at 2.5 nM at days 0 (baseline), 1, 3, 7, 14 and 21. Cells from two representative donors demonstrated that treatment with LBH589 under standard osteo-inductive conditions significantly enhanced the calcium deposition by these cells at days 14 and 21, with no changes at earlier times (figure 6-2 = donor 1; figure 6-3 = donor 2). Staining of the cells with crystal violet at each time point showed no significant changes ($p > 0.05$) in cell density when comparing the two treatment conditions (figure 6-4). As a comparison to LBH589, this laboratory has previously examined the effect of SAHA on the same cell type (unpublished data; Evdokiou, *et al*., 2006). Similar observations were noted with SAHA treatment (500 nM), with a significant enhancement of calcium deposition apparent from day 21, with no significant difference ($p > 0.05$) in cell density (figure 6-5A and B). Although the effects of the inhibitors appear to elicit similar responses, LBH589 appears to have an earlier and more potent effect than SAHA.
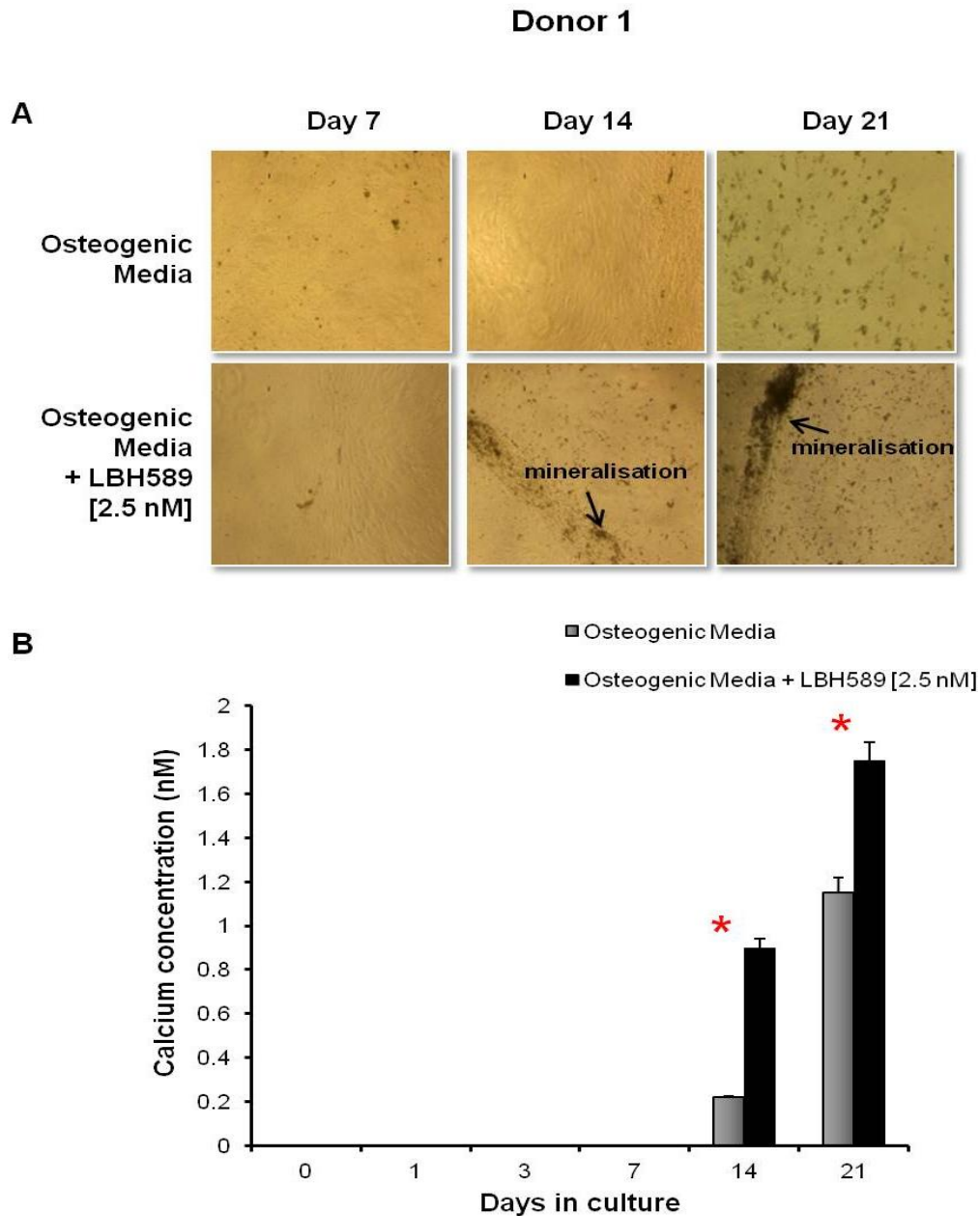
Figure 6-2. LBH589 enhances mineralisation by NHB cells; representative donor 1. NHB cells were cultured under standard osteo-inductive media over 21 days, and calcium quantification and images were taken at days 0, 1, 3, 7, 14 and 21, as outlined in the Methods. **A**). Representative images taken at days 7, 14 and 21. *Top panel*; images showing mineralisation for NHB cells treated under osteo-inductive media only, and *bottom panel;* images showing mineralisation for NHB cells treated with the addition of 2.5 nM of LBH589. **B**). Quantification of cell layer calcium levels with LBH589 treatment, with *$p < 0.005$. Bars are mean of quadruplicate measures $\pm$ SD.

Donor 2

A

B
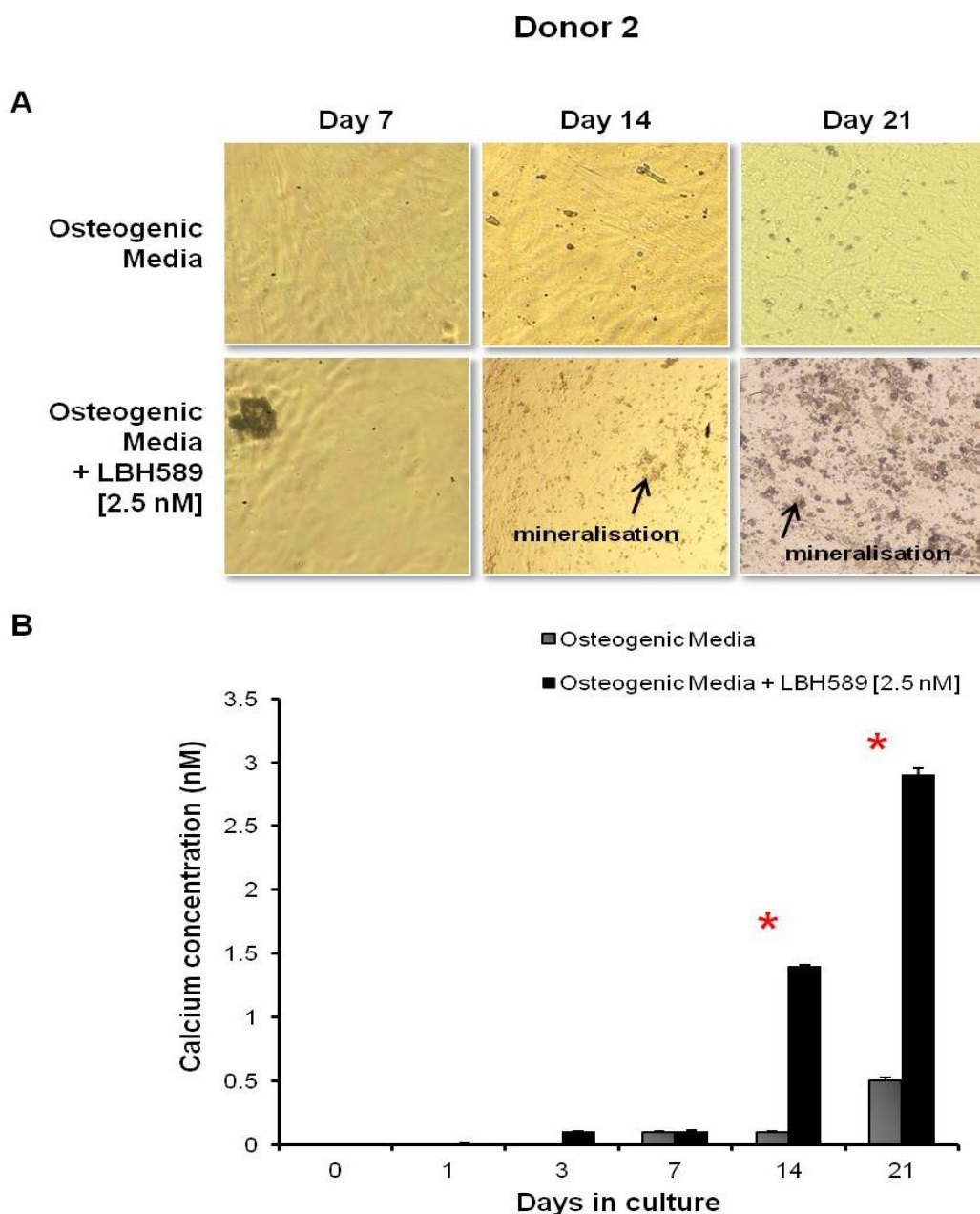
Figure 6-3. LBH589 enhances mineralisation by NHB cells; representative donor 2. NHB cells were cultured under standard osteo-inductive media over 21 days, and calcium quantification and images were taken at days 0, 1, 3, 7, 14 and 21, as outlined in the Methods. **A**). Representative images taken at days 7, 14 and 21. *Top panel*; images showing mineralisation for NHB cells treated under osteo-inductive media only, and *bottom panel;* images showing mineralisation for NHB cells treated with the addition of 2.5 nM of LBH589. **B**). Quantification of cell layer calcium levels following LBH589 treatment, with *p < 0.0001. Bars are mean of quadruplicate measures ± SD.
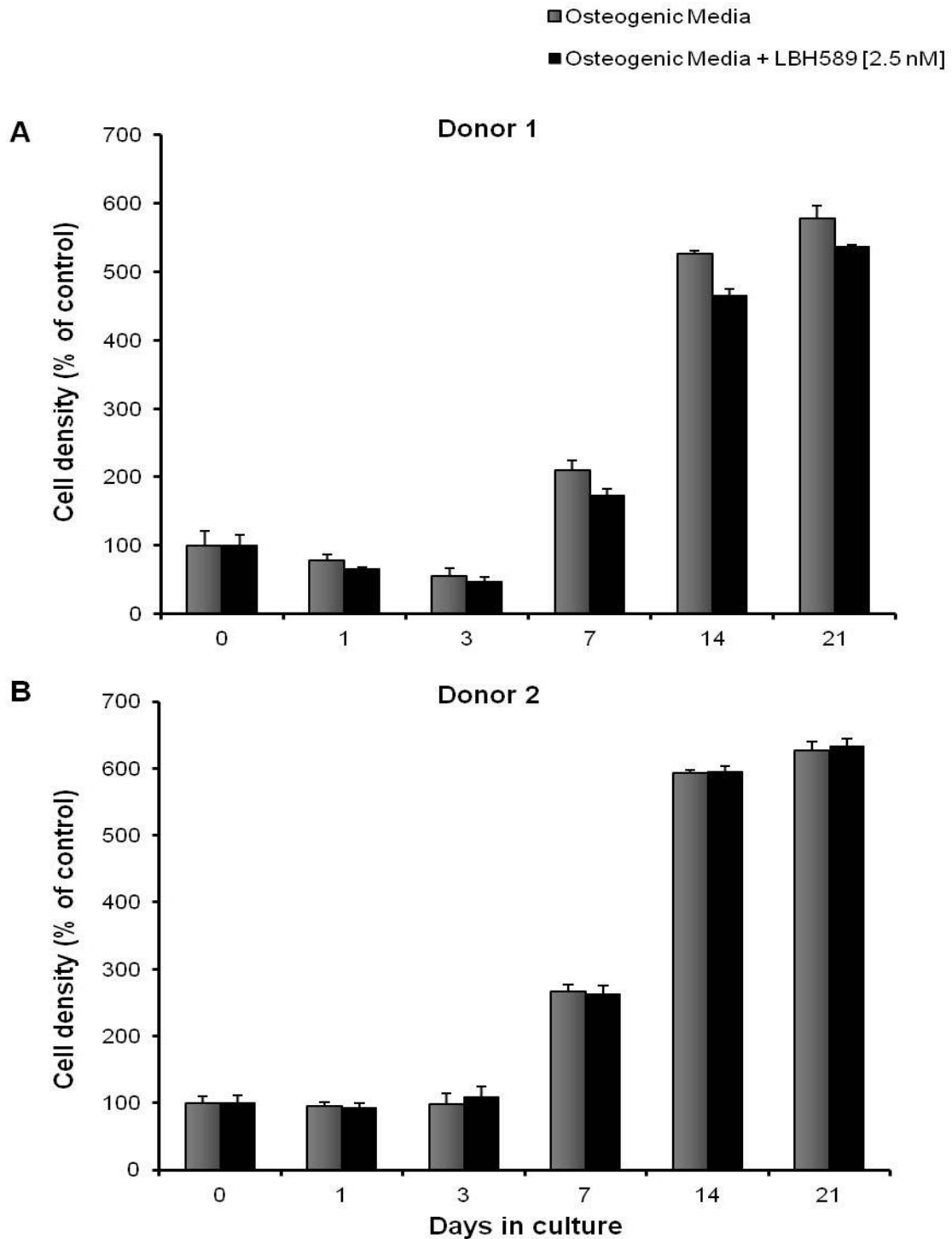
Figure 6-4. The effect of LBH589 on the viability of NHB cells in long-term mineralisation cultures. NHB cells from 2 representative donors were simultaneously assessed for calcium mineralisation (figure 6-2B and 6-3B), and viability using crystal violet at days 0 (baseline), 1, 3, 7, 14 and 21. Graphs are presented as a percentage of control (defined as, baseline-day 0). Bars are the mean of triplicate measures ± SD. P > 0.05.
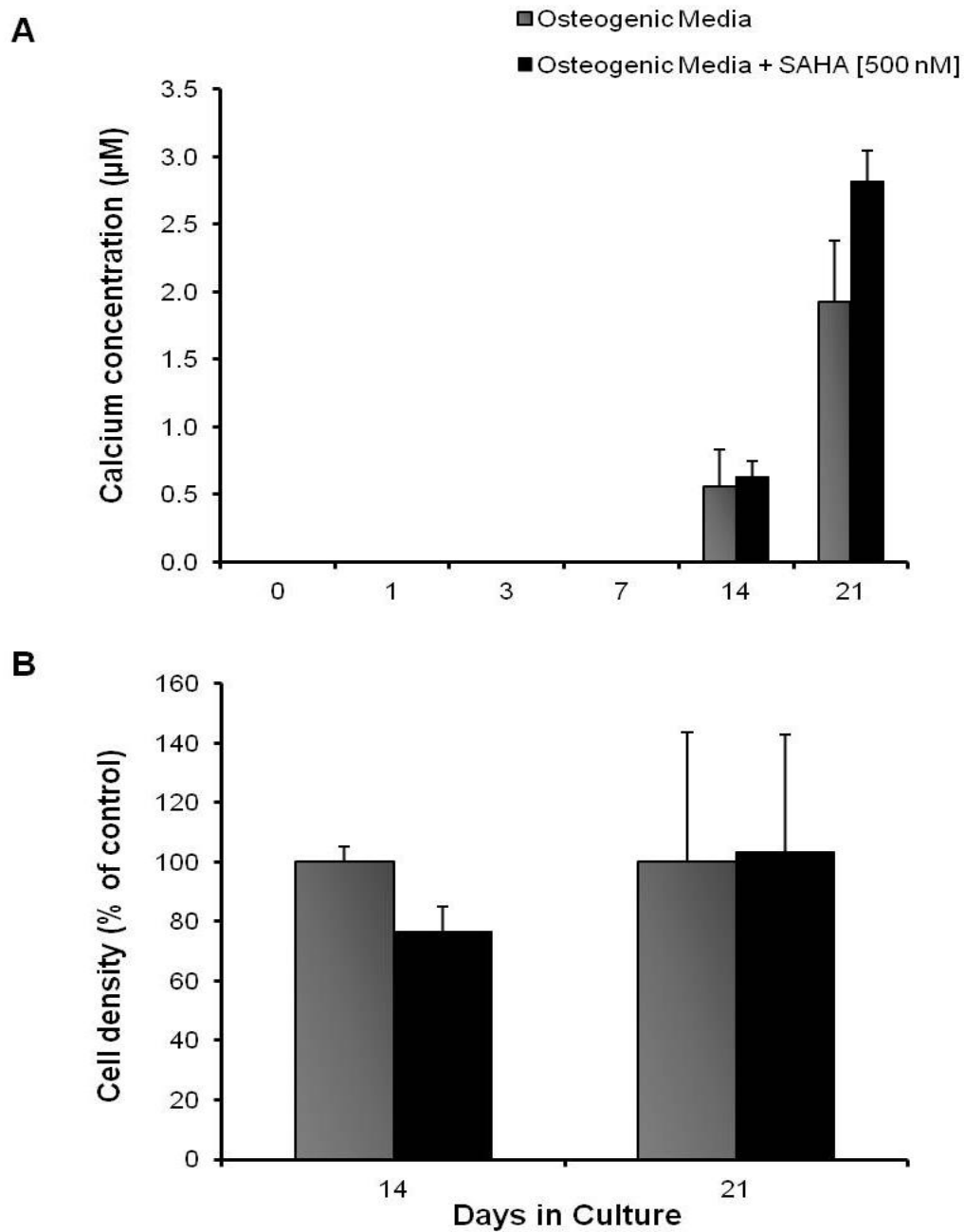
Figure 6-5. The effect of SAHA on NHB cell mineralisation and viability. Data previously investigated by this laboratory (*Evdokiou, et al., 2006)* were compared to the effects of LBH589, using the same NHB cells isolated from human donors. **A**). Calcium mineralisation was determined at days 0, 1, 3, 7, 14 and 21, with the data bars presented as the mean of quadruplicate measures, ± SD. **B**). Cell viability (crystal violet) was measured at days 14 and 21, with the data bars presented as the mean of triplicate measures ± SD, and expressed as a percentage of the control. P > 0.05.

6.2.3 LBH589 promotes osteogenic gene expression

To investigate the expression of genes known to be involved in osteoblast activity, total RNA was isolated from these cells at days 0 (baseline), 1, 3, 7, 14 and 21. Using real-time PCR analysis, the mRNA expression profiles of ALP, Type I collagen, RANKL, osteocalcin, Runx2, and osteoprotegerin (OPG) were determined. Cells from two donors were cultured for 21 days in the presence or absence of LBH589 under both osteo-inductive and non-osteo-inductive conditions. While the mRNA expression profile for ALP, Type I collagen and osteocalcin remained unchanged, with the addition of LBH589, RANKL, Runx2 and OPG expression was highly regulated with LBH589 treatment under osteo-inductive conditions. Figure 6-6 shows a representative experiment from donor 1. The data demonstrate that cells cultured under standard, non-osteogenic α-MEM (control media), with (closed triangles), or without (open triangles), LBH589 showed no changes to the mRNA gene expression profile of Runx2, OPG or RANKL. Under osteo-inductive conditions, the gene expression profile for Runx2 and OPG changed in that, both showed an increase in mRNA expression at day 14, whereas RANKL significantly increased at day 21 (closed squares). In contrast, the addition of LBH589 (open squares), significantly enhanced the expression of both Runx2 and OPG, when compared to osteogenic medium alone ($p < 0.05$). Interestingly, RANKL was significantly enhanced at an earlier time point, at day 1 ($p < 0.05$), and peaked again at day 21. Figure 6-7 describes the mRNA expression of RANKL, Runx2 and OPG for donor 2. Similar to donor 1, treatment with LBH589 under osteogenic conditions, significantly enhanced Runx2 gene expression at day 21 and OPG at day 14, when compared to osteogenic medium alone ($p < 0.05$). LBH589 also significantly increased the mRNA expression of RANKL at day 1 ($p < 0.05$). Therefore the enhanced mineral deposition by NHB cells following LBH589 treatment was

associated with a significant increase in gene expression for Runx2, OPG and RANKL, indicating that key osteogenic genes were tightly regulated by LBH589. In addition, the resulting RANKL-OPG mRNA ratio implied that treatment with LBH589 can promote an anti-osteoclastic phenotype in NHB-like cells. The results demonstrate for the first time that LBH589 may promote maturation and activity of human osteoblasts by mechanisms likely to involve the regulation of genes playing key roles in osteogenesis.
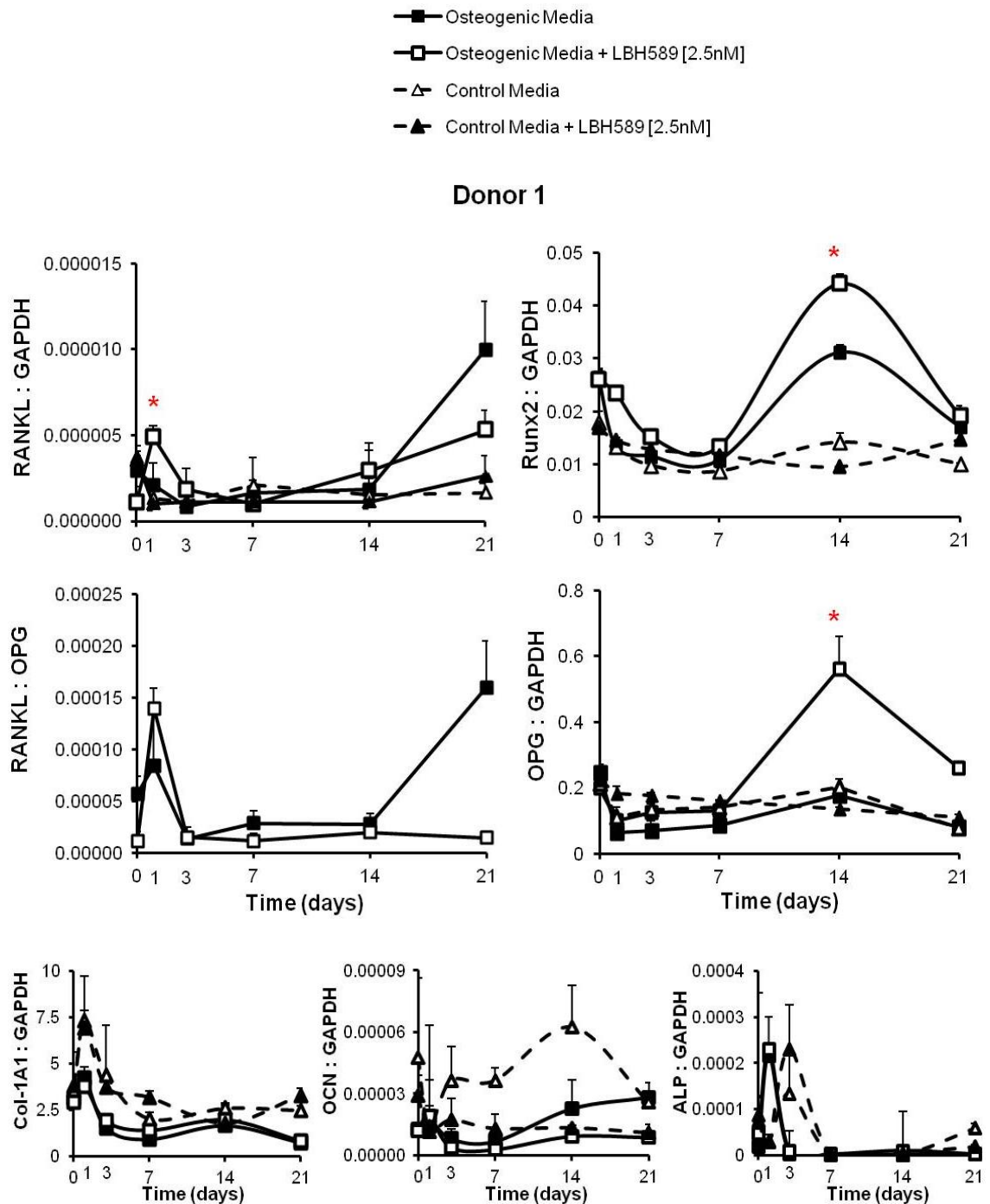
Figure 6-6. LBH589 promotes osteogenic gene expression (donor 1). NHB cells were cultured under standard osteo-inductive media over 21 days, and total RNA was isolated using the Trizole method, as outlined in the Methods. The mRNA expression for Runx2, OPG, RANKL, Col-1A1, OCN and ALP, normalised against GAPDH are shown for donor 1. The resulting RANKL-OPG mRNA ratio is expressed for cells treated under osteogenic media, with or without LBH589. Significance is defined between cells treated with osteogenic media alone and with the addition of LBH589, where $*P < 0.05$. The data points are presented as the mean of triplicate measures $\pm$ SD.
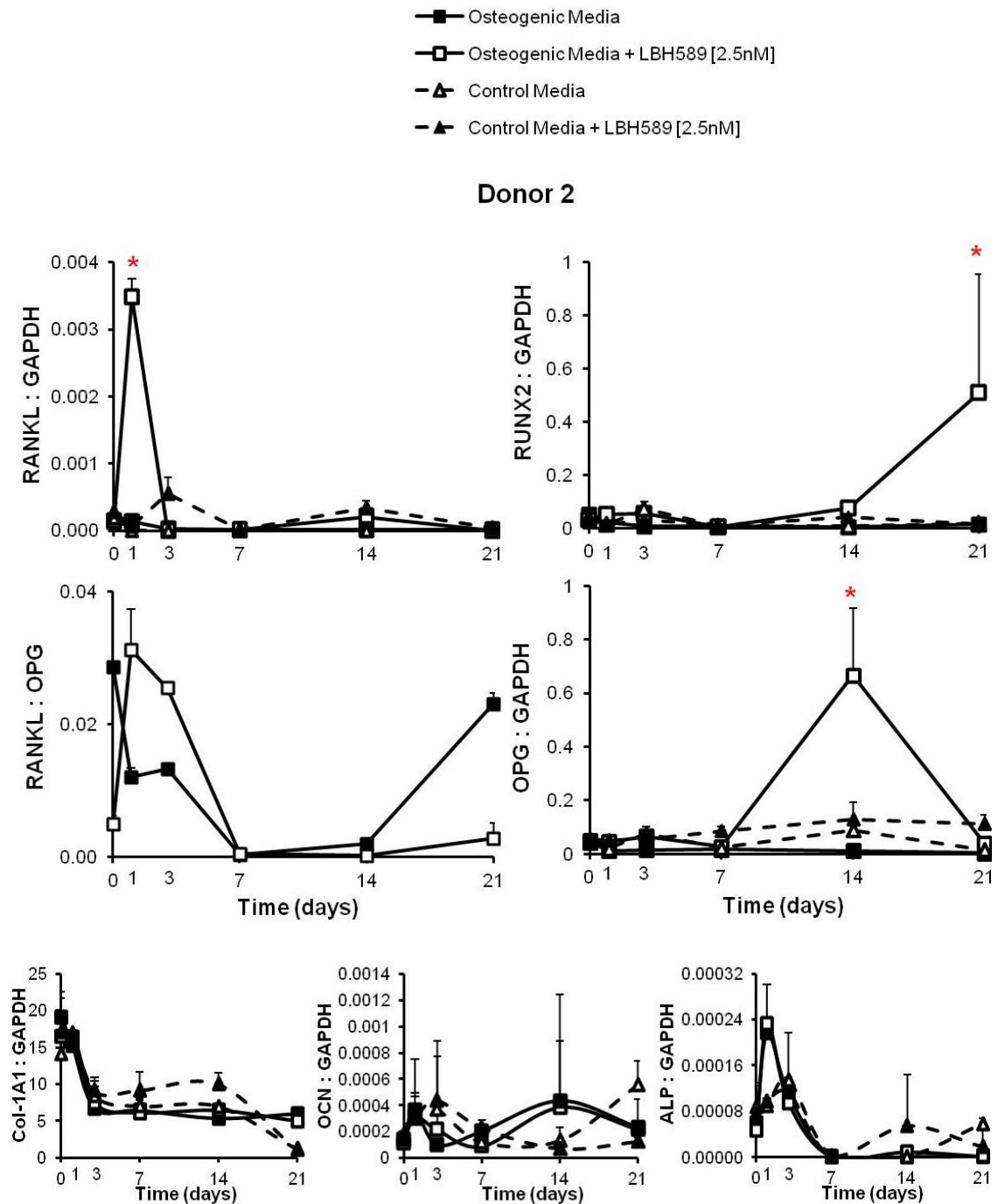
Figure 6-7. LBH589 promotes osteogenic gene expression (donor 2). NHB cells were cultured under standard osteo-inductive media over 21 days, and total RNA was isolated using the Trizole method, as outlined in the Methods. The mRNA expression for Runx2, OPG, RANKL, Col-1A1, OCN and ALP, normalised against GAPDH are shown for donor 2. The resulting RANKL-OPG mRNA ratio is expressed for cells treated under osteogenic media, with or without LBH589. Significance is defined between cells treated with osteogenic media alone and with the addition of LBH589, where *P < 0.05. The data points are presented as the mean of triplicate measures ± SD.

6.3 Discussion

HDIs are administered systemically to patients and therefore it is of paramount importance to understand their effects on normal cells. The osteotropic actions of LBH589 observed in the animal models described in the previous chapters, suggest that LBH589-mediated inhibition of osteoclast function is a contributing factor to the observed increase in bone volume. This notion is further supported by the data presented in chapter 5, demonstrating potent inhibitory effects of HDIs on osteoclastogenesis and function. The set of experiments described in this chapter aimed to determine the effects of LBH589 on the bone forming osteoblastic cells.

Long-term culture of NHB cells under osteo-inductive conditions showed that LBH589 promoted osteoblast mineralisation, which is an accepted *in vitro* surrogate model of *in vivo* bone formation. This effect was concomitant with enhanced mRNA expression of Runx2 and OPG, which is consistent with progression towards a more mature osteoblast phenotype (Schroeder *et al*., 2005). Specifically, the RANKL-OPG mRNA relationship was tightly regulated and with these genes expressed in opposition to one another, perhaps also suggesting a potential regulation in osteoclast formation and function, with implications for osteoclast inhibition (Piedra *et al*., 2011). Earlier studies focussed on the use of mouse primary osteoblasts, specifically MC3T3-E1 cells (Schroeder et al., 2004b, Schroeder et al., 2007, Schroeder and Westendorf, 2005). The results presented in this chapter represent the first study to examine the effects of LBH589, or indeed any other HDI, on normal human osteoblastic cells. Consistent with the results reported in this chapter, a study on MC3T3-E1 osteoblastic cells reported that the HDIs, sodium butyrate and TSA, enhanced the differentiation of these cells, indicated by enhanced expression of osteoblast specific genes, including ALP, osteocalcin and Runx2 (Jung *et al*., 2010). Furthermore, in the same study, the authors

hypothesised that the combination of these HDIs and α-calcium sulphate (αCS) could have a potential role for bone regeneration therapy. αCS is a biomaterial used for bone regeneration therapy, and is completely resorbed without inducing significant host adverse responses (Park *et al*., 2011). Using a rat model with critical calvarial bone defects, the authors injected a combination of αCS and sodium butyrate into the affected area and calvarial bone volume was determined using μ-CT. This combination resulted in approximately 2 times more bone formation than αCS-filled defects alone, suggesting the potential use of HDIs for bone regeneration therapy (Jung *et al*., 2010).

While the molecular mechanisms, by which HDIs affect skeletal cells, are not fully understood, some have been proposed. For example, it was shown that the class II HDAC4 is a central regulator of chondrocyte hypertrophy and skeletal bone formation, and that the suppression or over-expression of HDAC4 resulted in the activation or repression of Runx2 targeted genes (Vega *et al*., 2004). In more recent studies, HDAC4 was shown to suppress MMP-13 gene expression by competing with the HAT, p300, for Runx2, consequently leading to a disruption in osteoblast development and differentiation (Boumah *et al*., 2009, Shimizu *et al*., 2010). The Wnt signalling pathway is well documented as playing a critical role in the regulation of bone mass (Trivedi *et al*., 2010). Wnts appear to have 3 major functions in osteoblasts. Firstly, to promote specification of osteoblasts from progenitor cells, secondly, to stimulate osteoblast proliferation, and thirdly, to prolong survival of osteoblasts and osteocytes (Westendorf *et al*., 2004). Furthermore, the expression of Wnt in mesenchymal progenitor cells induced the expression of osteoblast transcription factors such as Runx2, osterix (Bennett *et al*., 2005), ALP and BMP2 (Rawadi *et al*., 2003), to stimulate osteoblast maturation. LRP5/6 and frizzled receptor form a complex that transduces signals for canonical Wnt signalling. Inactivating mutations to LRP5 were associated with low

bone mass resulting in an osteoporosis-like syndrome in humans and osteopenia in mice (Gong *et al*., 2001). In contrast, an activating G171V mutation in the LRP5 gene (Ai *et al*., 2005), and over-expression of β-catenin in osteoblastic cells (Kato *et al*., 2002), resulted in an excessively high bone mass phenotype. Several inhibitors of the Wnt pathway have been identified, including Dkk and sclerostin. The Dkk family are Wnt antagonists that bind to the LRP5/6 receptors to inhibit canonical Wnt signalling. Deletion of the Dkk1 gene in mice results in the development of a phenotype with increased bone mass, whereas over-expression of Dkk1 is associated with a reduced osteoblast activity, and cancer-induced osteolytic lesions (Yaccoby *et al*., 2007). Sclerostin is the product of the SOST gene, and is a key negative regulator of bone formation (Findlay and Atkins, 2011). In adult bone, sclerostin is constitutively expressed by osteocytes, which is the final differentiated cell of the osteoblast lineage (Lin *et al*., 2009). Its physiological importance was further supported by the high bone mass phenotype found in sclerostin-null mice (Li *et al*., 2008a).

Little is known regarding the effects of HDIs on the canonical Wnt pathway in the context of bone, although acetylation of β-catenin by HATs has been reported to positively influence osteoblast transcriptional activity (Levy *et al*., 2004). An early study reported that the pan-DAC inhibitor, TSA, completely reversed the inhibition by dexamethasone of osteoblast differentiation associated with an inhibition of HDAC1, thereby reversing the reduction in β-catenin levels (Smith and Frenkel, 2005). A recent study demonstrated the novel involvement of the class IV HDAC, Sirt1, in the regulation of bone mass. By comparing Sirt1, haplo-insufficient mice (Sirt1$^{+/-}$), to wild-type, the authors reported that there was a reduction in bone mass characterised by decreased bone formation. This effect was directly correlated with deacetylation of histone-H3 at the SOST promoter, leading to a decrease in SOST gene transcription

(Cohen-Kfir *et al*., 2011). It is also documented that an intact Wnt signalling pathway is necessary for osteoblast mineralisation and maturation in mouse MC3T3-E1 cells (Rawadi *et al*., 2003). Importantly, this laboratory recently reported the involvement of the Wnt signalling pathway in the same NHB cell type used in this study (Vincent *et al*., 2009). Treatment of NHB cells with sclerostin suppressed Runx2 and osteocalcin expression and altered the active levels of β-catenin, which were associated with a reduction in mineralisation. Therefore, in light of recent reviews (Cohen-Kfir *et al*., 2011, Vincent *et al*., 2009), and taking in together with the observations in this chapter describing the effects of HDIs on osteoblasts, it will be instructive to conduct further research into the involvement of sclerostin and the Wnt signalling in HDI-mediated osteoblast maturation and function.

In contrast to treatments that target increased bone resorption in disease, there appears to have been relatively little exploration into treatments that are able to target factors that lead to an aberrant increase in bone formation. Such diseases include osteoblastic lesions arising from metastatic prostate cancer, or from primary cancers originating in the bone, such as osteosarcoma. Underlying these diseases, some factors thought to be involved in promoting osteoblastic lesions, for example are, Dkk1 and ligands of the Wnt family (Logothetis and Lin, 2005, Chen *et al*., 2004a, Haaber *et al*., 2008), bone morphogenic proteins (Autzen *et al*., 1998), and fibroblast growth factors (Li *et al*., 2008b). Current literature has described a potential therapeutic option to target osteoblastic lesions. The HDI TSA, and other class I HDAC inhibitors have been shown to increase the gene expression of the antagonist Dkk1 in metastatic colon cancer cells (Sikandar *et al*., 2010), suggesting a role for Dkk1 in suppressing the progression of osteoblastic tumours. Recently, a pilot study performed by this laboratory examined the effects of LBH589 in athymic nude mice bearing the

osteosarcoma cell line, KHOS. When injected into the bone marrow, KHOS produced

mixed osteolytic/osteoblastic lesions were (the same dose and schedule of LBH589 was

applied, as in chapter 4). Remarkably, LBH589 was able to significantly inhibit the

extra bony growth caused by the cancer within the bone, independent of tumour burden

(see figure 6-8). These preliminary data (ongoing investigation), further demonstrate

the potential use of HDAC inhibitors in the context of cancer-induced osteolytic and

osteoblastic bone lesions.
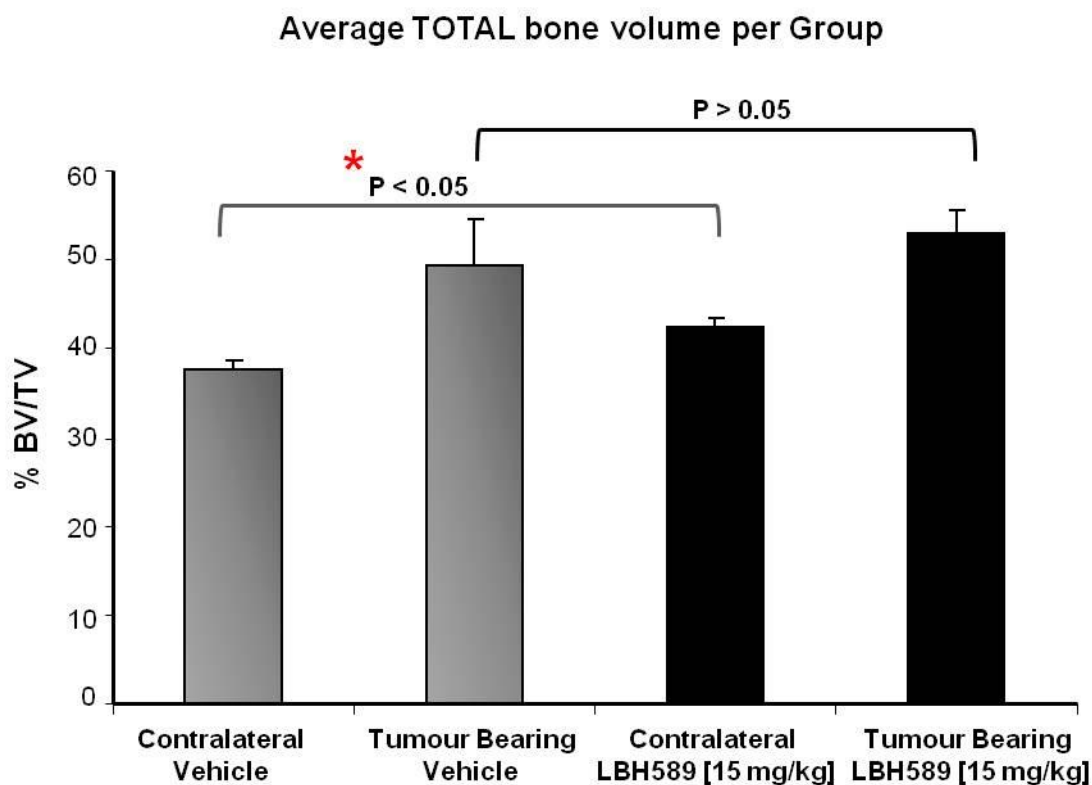
Figure 6-8. LBH589 increases total BV, and protects the bone from osteosarcoma-induced bone destruction. Bone volume was measured from 730 μ-CT sections of the proximal tibia, starting from the growth plate and using the program CTan. This graph represents the TOTAL bone volume of the tumour-bearing and contralateral tibiae per treatment group. Grey bars represent the vehicle-treated control group, and the black bars represent the LBH589-treated group. Data shown are the average bone volume from all animals in that group, with bars: mean ± SD (n = 10).

*P < 0.05. Total BV from the contralateral tibiae of the LBH589-treated group is significantly increased when compared to the contralateral tibiae of the vehicle-treated group.

There is no difference between the total BV of the tumour-bearing tibiae from the LBH589-treated group and the vehicle-treated group (p > 0.05).

The data presented here show for the first time, that LBH589 enhanced osteoblast maturation, in addition to promoting an anti-osteoclastic phenotype in NHB-like cells. This further supports the suggestion that LBH589, or HDIs in general, may be useful for promoting bone formation. These data warrant further investigations into the biological effects of HDIs on human osteoblast cells and suggest the potential use of this class of drugs in various conditions associated with bone loss. It is also important to consider the long-term effects of HDI administration on bone strength. Clinical studies showed that the long-term administration (6 months) of the HDI, VPA, was associated with decreased bone mineral density, osteopenia and osteoporosis in children and adults, leading to an increased fracture risk (Oner *et al*., 2004, Boluk *et al*., 2004). Therefore, additional studies examining the prolonged exposure to HDIs on bone formation are required. The osteotropic properties of LBH589 demonstrated in this thesis, have prompted further investigations into the translational efficacy of LBH589 into animals with an intact immune system and normal bone physiology. Chapter 7 discusses the efficacy of systemic administration of LBH589 in normal mice with an intact immune system and without the influence of cancer, to determine its direct effects on normal bone metabolism *in vivo*.

Chapter 7. The effect of LBH589 on normal bone metabolism *in vivo*

7.1 Introduction

The tumour xenograft experiments performed using immune-compromised animals described in chapter 4 provided an opportunity to determine the effects of LBH589 treatment on normal bone remodelling by analysing the contralateral non-tumour bearing tibiae. However, an important limitation of the immune-compromised mouse models was that it did not take into account the role of the immune system. Therefore, in the current study it was important to investigate the effects of LBH589 on normal bone remodelling in immune competent animals, without tumours. The work described in chapters 5 and 6 are in support of the findings reported in the literature on the effects of HDAC inhibition on osteoclastogenesis and promotion of murine osteoblast maturation and function (Schroeder *et al*., 2007, Schroeder and Westendorf, 2005). Furthermore, these data demonstrated novel actions of the HDI, LBH589 on human osteoclast and osteoblast function. The studies described in this chapter aimed to provide further insight into the effect of LBH589 on normal bone metabolism. The hypothesis was that animals treated with LBH589 exhibit increased bone volume associated with:

1. Inhibition of osteoclast formation and bone resorption,

2. Enhanced osteogenic activity by osteoblasts

Together, these two parameters would drive bone metabolism to a net increase of bone formation. To address this hypothesis, groups of six immune-competent balb/c mice were treated i.p. with 30 mg/kg of LBH589, 5 days/week for 4 weeks, this being the same dose and schedule used in the tumour xenograft experiments described in chapter 4. Longitudinal changes in architectural bone parameters were determined using *in vivo* μ-CT analysis, at the mid-point of 2 weeks after treatment. To determine

the effects of LBH589 on the rate of new bone formation and bone remodelling *in vivo*, the fluorescent calcium binding dye, calcein, was injected i.p. into mice 6 and 2 days prior to sacrifice.

7.2 Results

7.2.1 The effects of LBH589 on quantitative bone parameters

Normal 8 week old balb/c mice were treated with LBH589 at a dose of 30 mg/kg. This dose produced the greatest change in bone volume observed in the previous study without causing significant toxicity. LBH589 was administered i.p. for 5 days/week over 4 weeks. Baseline and longitudinal changes in tibial bone volume were monitored using live μ-CT scans (Skyscan 1076 live μ-CT scanner). A mid-point scan at 2 weeks into the experiment revealed a significant increase in total bone volume from baseline in LBH589-treated mice compared to vehicle-treated mice. There was an approximate 13% increase compared to a 6% increase in total bone volume in the vehicle-treated mice. The trabecular bone volume increased significantly in mice treated with LBH589 by approximately 5%, with only a 0.4% increase in the vehicle-treated mice (figure 7-1A & B). At the mid-point scan, LBH589 treatment increased trabecular thickness (Tb.Th), trabecular number (Tb.N) and trabecular separation (Tb.Sp). However, when compared to vehicle-treated mice, Tb.N significantly increased from 0.014 mm^{-1} to 0.019 mm^{-1} (p = 0.01) after 2 weeks of treatment. At the completion of treatment at 4 weeks of treatment, the animals were humanely killed, and the hind legs were collected for high resolution *ex-vivo* μ-CT (Skyscan 1072 X-ray μ-CT scanner) analysis, using comparable scanning parameters. Additional, but only minimal increases in bone parameters were observed with LBH589 treatment, suggesting that the major changes in altered bone metabolism occurred in the first 2 weeks of LBH589 treatment. Table 7-1 summarises the quantitative μ-CT analyses, including percent bone volume (% BV/TV), Tb.Th, Tb.N and Tb.Sp at baseline, 2 weeks and at 4 weeks. P values were defined between the values at 2 or 4 weeks of treatment, and baseline.
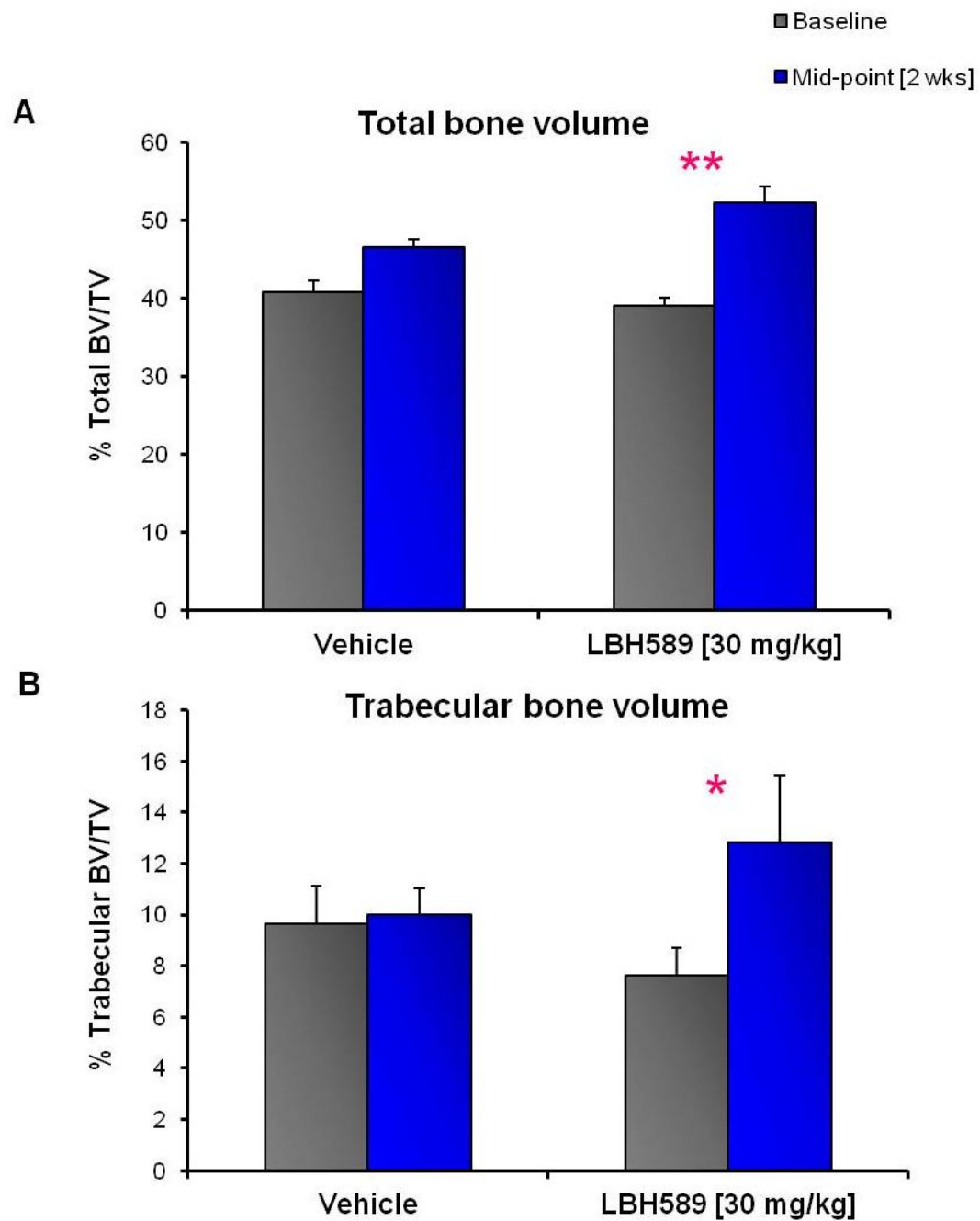
Figure 7-1. The longitudinal bone volume effects of LBH589 on physiological bone turnover. Normal balb/c mice were treated with either vehicle or LBH589 as indicated in the Methods. Baseline (grey bars), and longitudinal mid-point (blue bars), scans were obtained using the 1076 live μ-CT. **A**). Represents the percentage total BV/TV, with **p = 0.0002. **B**). Represents the percentage trabecular BV/TV, with *P = 0.008. Graphs are represented as bars; mean ± SD (n = 6).

μ-CT Parameters			Vehicle	Significance $p =$	LBH589 [30 mg/kg]	Significance $p =$
TOTAL Bone Volume	Baseline	% BV/TV ± SD	40.8 ± 1.5	-	39.1 ± 1.0	-
	2 week	% BV/TV ± SD	46.5 ± 0.9	0.002	52.3 ± 2.0	**0.0002** *
	4 week	% BV/TV ± SD	51.0 ± 0.6	0.00002	54.0 ± 1.5	**0.00001** *
TRABECULAR Bone Volume	Baseline	% BV/TV ± SD	9.6 ± 1.5	-	7.6 ± 1.1	-
		Tb.Th (μm)	5.3	-	5.4	-
		Tb.N (mm⁻¹)	0.018	-	0.014	-
		Tb.Sp (mm)	18.0	-	19.3	-
	2 week	% BV/TV ± SD	10.0 ± 1.0	0.67	12.8 ± 2.6	**0.008** *
		Tb.Th (μm)	6.0	0.001	6.7	0.003
		Tb.N (mm⁻¹)	0.017	0.15	0.019	**0.01** *
		Tb.Sp (mm)	24.4	0.0007	25.4	0.0007
	4 week	% BV/TV ± SD	11.9 ± 0.6	0.02	13.9 ± 1.9	0.002
		Tb.Th (μm)	6.4	0.0005	7.0	0.001
		Tb.N (mm⁻¹)	0.019	0.8	0.02	**0.01** *
		Tb.Sp (mm)	24.8	0.0006	24.7	0.02

Table 7-1. Quantitative tibial bone parameters on physiologocial bone turnover. The parameters for percentage total BV/TV, percentage trabecular BV/TV, trabecular thickness (Tb.Th), trabecular number (Tb.N) and trabecular separation (Tb.Sp), were determined for each animal in all treatment groups at the following times: Baseline, 2 week mid-point, and at 4 weeks following treatment. Values are expressed as the mean ± SD, (n = 6). * indicate significant p < 0.05, where significance was defined between 2- or 4-weeks of treatment and baseline values.

Figure 7-2 shows the total bone volume changes during the course of treatment, confirming that the major changes occur within the first 2 weeks of treatment. No adverse effects were noted with treatment of animals with LBH589, in terms of the body weight measurements throughout the duration of the experiment, as shown in table 7-2. Similar to the previous xenografts models, an initial drop in body weights occurred in the first week of treatment, with animals recovering thereafter. This study demonstrated that the effects of LBH589 on bone turnover seen in immune-compromised animals could be translated to immune-competent animals.
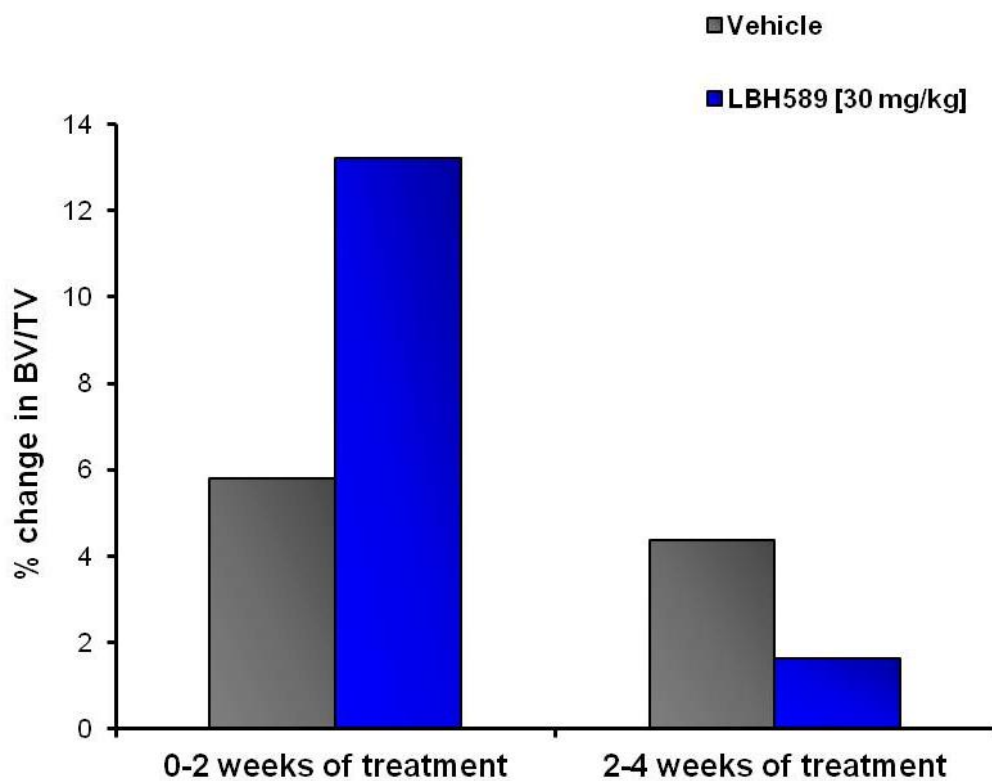
Figure 7-2. Total bone volume changes during the course of LBH589 treatment on physiological bone turnover. This graph demonstrates the percentage change in bone volume in mice treated with either vehicle, or LBH589. *Left side bars;* represent the change in bone volume during the first 2 weeks of treatment, while the *right side bars;* show the bone volume changes during the last 2 weeks of treatment.

↓ Start drug treatment

Group	Day 1	Day 7	Day 14	Day 21	Day 28
Vehicle	20.4 ± 0.9	20.6 ± 0.9	20.9 ± 1.0	21.2 ± 1.0	22.8 ± 0.9
LBH589 [30 mg/kg]	19.7 ± 1.2	17.8 ± 0.8	18.0 ± 1.1	18.2 ± 0.8	19.2 ± 1.0

Table 7-2. Body weights of normal balb/c mice treated with LBH589. Weekly body weight measurements at days 1 (baseline), 7, 14, 21 and 28, where values; weight (g) ± SD, and n = 6 mice per group.

7.2.2 The effect of LBH589 on osteoclasts

The data described in chapters 4 and 5 suggested that LBH589 exerted its actions by reducing the number of TRAP$^+$, multinucleated osteoclasts lining the trabecular bone surface, concomitant with inhibition of osteoclast differentiation and bone resorption. In this experiment, the tibiae and femurs were excised for histomorphometric analysis, in which the number of TRAP$^+$ osteoclasts lining the trabecular bone surfaces was quantified. TRAP$^+$ osteoclasts were readily visible and quantifiable in the untreated sections (figure 7-3A-top panel). In contrast, osteoclasts lining the trabecular surfaces of LBH589 treated animals were significantly reduced or more often undetectable (figure 7-3A-bottom panel). Figure 7-3B represents the mean number of TRAP$^+$ osteoclasts counted in a defined 1mm^2 trabecular section within the tibiae and femurs. The data demonstrated that LBH589 inhibited bone resorption through reducing the number of osteoclasts, in animals with physiological bone remodelling (p = 0.03).
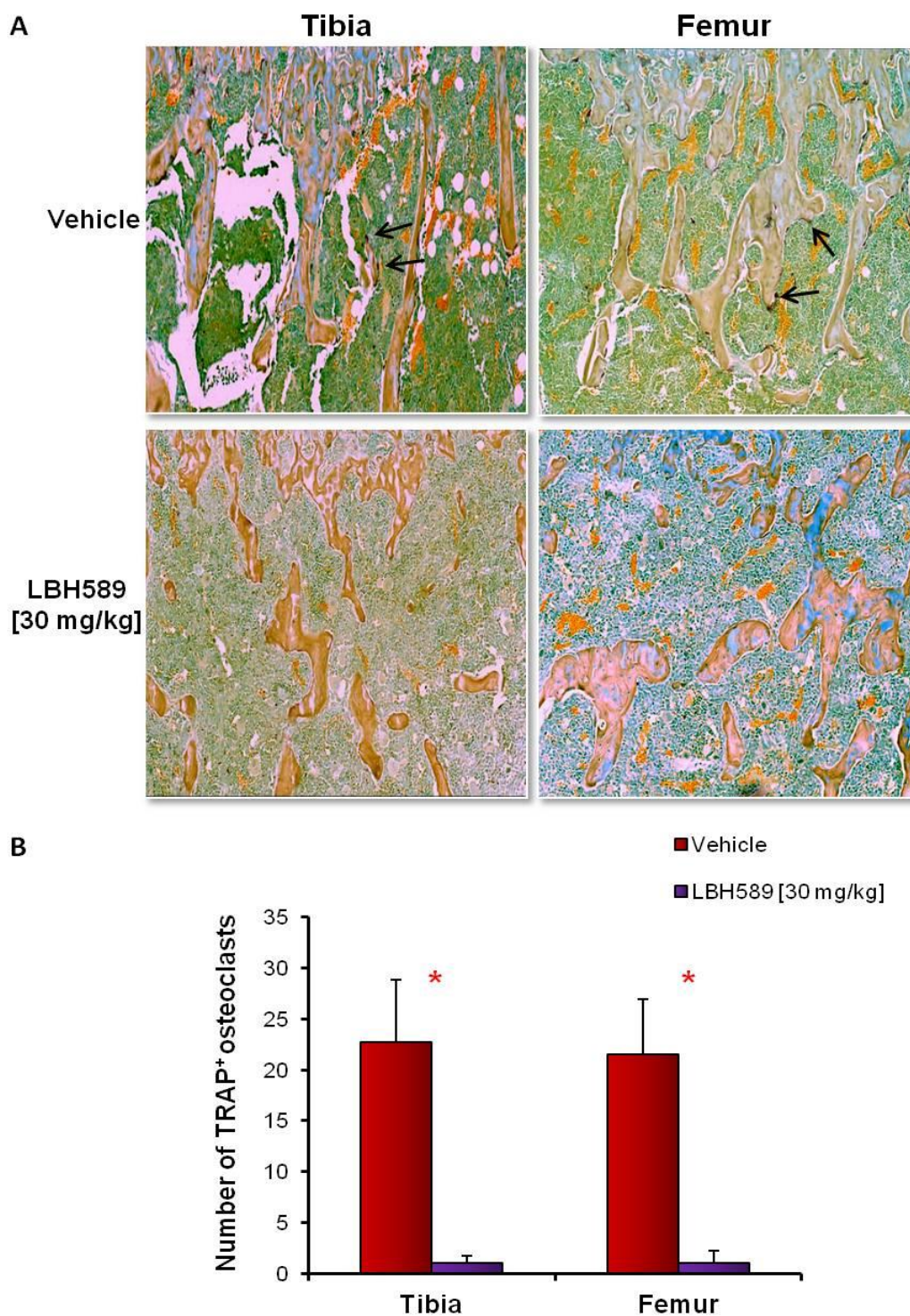
Figure 7-3. The effect of LBH589 on the osteoclasts, as determined by histological examination. A). Histological sections of the tibiae and femurs were stained for TRAP$^+$ cells. A 1mm^2 area was counted for purple-stained osteoclasts, in each of the image inserts. Arrows indicate an example of a TRAP$^+$ osteoclast. B). The graph shows the average number of osteoclasts counted in the tibiae and femurs within each treatment group, $\pm$ SD (n = 6), where * p = 0.03.

7.2.3 The effects of LBH589 on the rate of new bone formation

To investigate the action of LBH589 on bone formation in normal balb/c mice, histomorphometric analyses of osteoblasts was examined by the fluorescent calcein double-labelling technique. The calcium-binding, double-label, calcein was administered to the animals at 6 and 2 days prior to euthanasia. Figure 7-4 shows a fluorescent double-labelled section of trabecular bone in mice treated with either vehicle or LBH589. Using this technique, the measures of <u>M</u>ineralising <u>S</u>urface (MS), <u>M</u>ineral <u>A</u>pposition <u>R</u>ate (MAR), and <u>B</u>one <u>F</u>ormation <u>R</u>ate (BFR), could be calculated. These three histomorphometric parameters quantitatively describe osteoblastic bone formation. The terminology and nomenclature have been comprehensively described by the ASBMR nomenclature committee (Parfitt *et al*., 1987), and is accepted as the international standard for describing histomorphometric analyses of bone. MS (standard abbreviation/symbol: Md.Pm/B.Pm), is directly related to the number of active osteoblasts on a given surface area expressed as a percentage, whilst MAR (standard abbreviation/symbol: MAR), is correlated to the rate at which these active osteoblasts lay down mineral, expressed as µm/day. Together, these 2 parameters give rise to the BFR (standard abbreviation/symbol: BFR/B.Pm) across the whole bone, using the formula:

$$\text{BFR/B.Pm} = \text{MAR} \times \text{Md.Pm/B.Pm} \qquad \text{units: } \mu m^2/\mu m/day$$

The study described in this chapter is the first to examine the effects of LBH589 on normal bone remodelling *in vivo*. The measurements of MS, MAR and BFR collectively revealed an increase in osteogenic activity associated with HDAC inhibition. The BFR across the whole tibiae and femurs were significantly increased by treatment with LBH589 compared to vehicle-treated animals ($p = 0.03$). This was

attributed to an increase in MAR ($p = 0.01$), with a minimal increase in MS area with LBH589 treatment (figures 7-5A – C). These results indicate that the increase in BFR could be most readily attributed to an increase in the activity of existing osteoblasts.
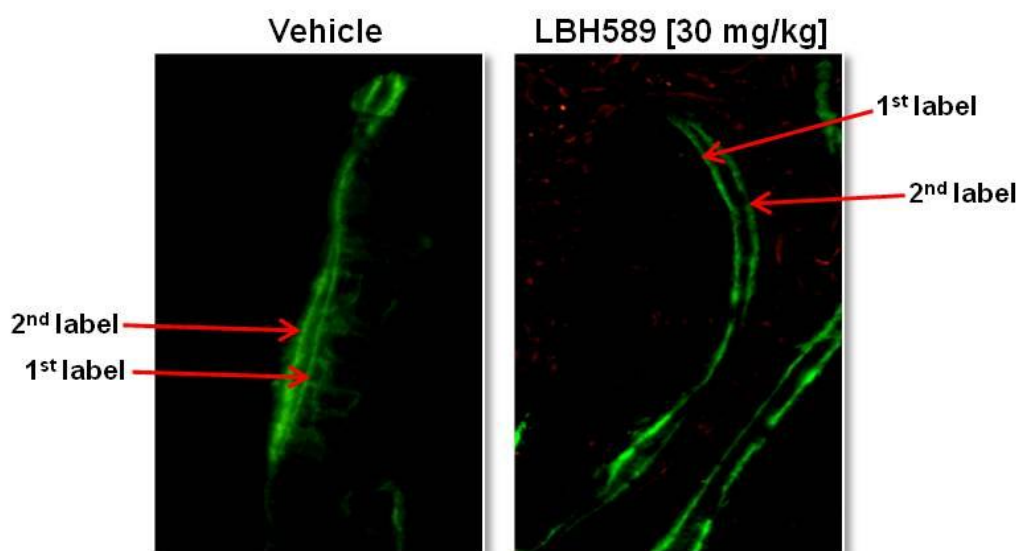
Figure 7-4. The effect of LBH589 on the osteoblasts, as determined by histological examination. Representative images of mice injected with the green-fluorescent calcein dye at 6 (1st label), and 2 (2nd label), days prior to histomorphometric examination of osteoblastic bone formation. Representative images were taken on the UV-fluorescence microscope at 40x magnification.
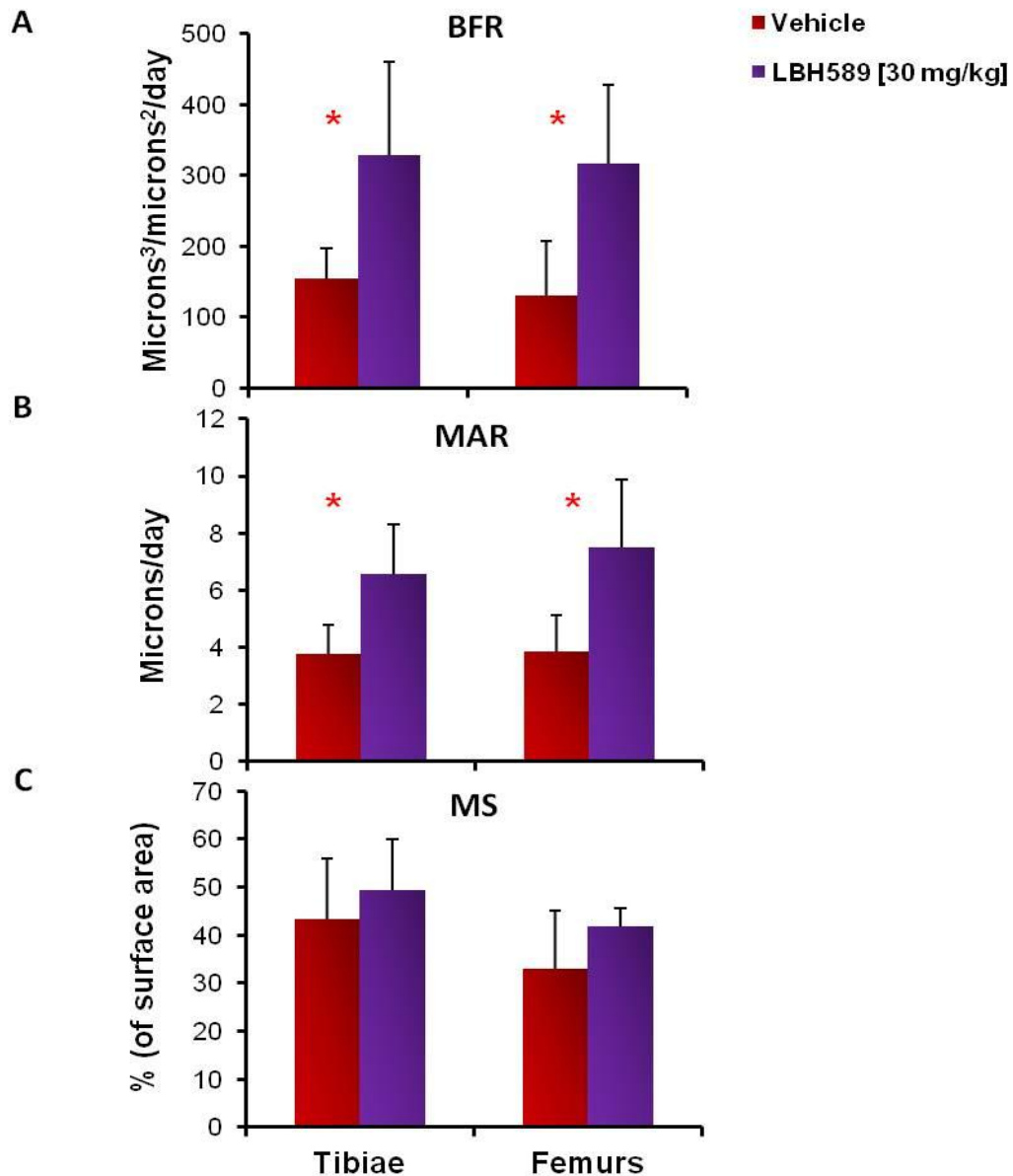
Figure 7-5. The effect of LBH589 on bone formation rate. Mice were injected with the green-fluorescence calcein dye at 6 and 2 days prior to euthanasia to determine osteoblastic bone formation. Tibiae and femurs were resected, and the required section of each bone was cut using a diamond-edge, slow-speed saw. Bones were then prepared accordingly into resin blocks, as indicated in the Methods. Sections were cut into 5 micron sections using the polycut instrument, and placed onto glass slides. Visualisation of UV-fluorescent, double-labelled sections, were imaged at 40x magnification, and each double-labelled section was manually counted. **A, B and C**, represent the average measures of bone formation rate (BFR), mineral apposition rate (MAR), and mineralising surface (MS), of all animals (n = 6), in each treatment group for the tibiae and femurs, with bars; mean ± SD. Significance is *P < 0.05.

7.3 Discussion

To the best of my knowledge, the work described in this chapter is the first to demonstrate that *in vivo*, LBH589 has dual effects on bone, by decreasing the number of TRAP[+], osteoclasts, while simultaneously enhancing the bone forming activity of osteoblasts. The dual effects seen with this HDI indicates a readjustment of the balance of bone turnover to favour bone formation, where in a typical setting, bone turnover is tightly regulated to maintain a net balance close to zero (Trinkaus *et al*., 2009, Boyce and Xing, 2008). Taken together with the findings from chapters 4-6 on the effects of LBH589 on the protection of cancer-induced bone destruction, and on the potent effects on osteoclasts and osteoblasts, these results suggest that the increase in bone volume seen in immune-competent animals can be attributed to both an increase in osteoblastic activity as well a decrease in osteoclastic activity.

The observed decrease in the number of osteoclasts with LBH589 treatment in tumour-bearing nude mice was also evident in immune competent animals. In addition, fluorescent double-labelling introduced to the animals 6 and 2 days prior to euthanasia, demonstrated a significant increase in the rate of new bone formation with LBH589 treatment. In the last two decades, bone histomorphometric techniques have evolved and have been applied to various assessments of bone architecture in determining the cellular pathophysiology of different forms of bone diseases, and in defining mechanisms by which drugs affect bone. For example, some early studies on the effects of anti-resorptive agents on normal rat bones (Pataki *et al*., 1997), and osteoporosis and ageing in clinical studies (Balena *et al*., 1998, Shih *et al*., 1993), have employed the use of the double-label histomorphometric techniques to examine bone growth. In this study, the results demonstrated for the first time that the increase in bone volume, seen in animals with physiological bone remodelling, is associated with an increase in the

activity of osteoblasts. The significant increase in MAR, suggest that the increase in BFR was due to the maturation of existing osteoblastic cells, rather than increasing the number of active osteoblasts. Data from the µ-CT analysis showed that trabecular thickness was significantly increased, whilst trabecular number remained unchanged, further corroborating the anabolic effects of LBH589 treatment. Therefore, when combining MAR and the data from the µ-CT analysis, the data suggest that no new trabeculae were formed, hence the LBH589-induced bone formation *in vivo* was most likely appositional.

Importantly, the findings arising from the animal studies described in chapters 4 and 7 showed that the actions of LBH589 extend beyond the protection from cancer-induced bone destruction. The uncoupling of bone formation and resorption is a key factor in the pathogenesis of several debilitating non-cancerous skeletal diseases. Such diseases include, childhood rickets (Mellanby, 1976), adult osteomalacia (Amling *et al*., 1999), osteogenesis imperfecta (Huber, 2007) and osteoporosis (Hosoi, 2010). Both rickets and osteomalacia have been well-characterised in their aetiology by an inability to form mineralised bone, largely due to a low vitamin D status, and sufficient dietary intake of both calcium and vitamin D has been highly recommended to prevent the onset of these diseases (Aaron *et al*., 1974, Allgrove, 2009). Osteogenesis imperfecta (OI) is a group of diseases often caused by mutation of the COL1A1 and/or COL1A2 genes, and displays varying severity (Steiner *et al*., 1993). The current treatment for X-linked autosomal dominant OI involves the use of the anti-resorptive bisphosphonates (Edouard *et al*., 2011). In the above diseases, there is a dysregulation of osteoblast function, leading to an impairment of mineralised bone. Therefore, patients with any of these diseases are prone to bone fragility and fractures.

On the other hand, osteoporosis is classified as having compromised bone strength due to low bone mass and a decline of bone micro-architecture, resulting in an increased risk of fracture (Deeks and Dhillon, 2010). Several lines of investigation have associated osteoporosis with various gene polymorphisms, including RANK/RANKL, matrix proteins and hormone related molecules (Sano *et al*., 1995, Tsukamoto *et al*., 2000, Ohmori *et al*., 2002). In recent years, low-bone mass mutations of the low-density lipoprotein receptor-related protein 5 (LRP5) gene have been linked to the increased susceptibility to osteoporosis (Cui *et al*., 2011). Deletion of LRP5 specifically in osteocytes, generated mice with significantly reduced bone mass (Cui *et al*., 2011). On the other hand, mutations to LRP5, causing high-bone mass, have also been explored in the context of osteoporosis. It was found that this particular mutation to LRP5 alters or inactivates the action of the Wnt antagonist, Dkk, thus, increasing Wnt signalling, and bone density (Boyden *et al*., 2002). Therefore, depending on the type of LRP5 mutation, by increasing LRP5 signalling in bone cells, or pharmacologic antagonism of Dkk action, either through the inhibition of binding or action at the LRP5, may have a role in the prevention or treatment of osteoporosis.

For many years, the main approach to targeting osteoporosis has been with the use of anti-resorptives, such as bisphosphonates (Dalle Carbonare *et al*., 2009). However, a limitation to the use of bisphosphonates has emerged in the clinical toxic side-effects, including the most common, osteonecrosis of the jaw in patients receiving high-dose, and long-term bisphosphonates (Cardwell *et al*., 2010, Dalle Carbonare *et al*., 2009, Pazianas *et al*., 2010, Wutzl *et al*., 2006), as well as the reduced renewal of bone tissue (Huja *et al*., 2009). In recent years, pharmacological agents for osteoporosis with potential anabolic activities have become available (Girotra *et al*., 2006, Marie, 2006). One such agent is strontium ranelate (SR), which comprises two molecules of

strontium and one molecule of ranelic acid (Marie *et al*., 2011). SR is now in clinical use for the treatment of postmenopausal osteoporosis to reduce the risk of vertebral and hip fractures. It has been described as a bone-seeking agent capable of rebalancing bone turnover by increasing bone formation and reducing bone resorption (Deeks and Dhillon, 2010). There are *in vitro*, *in vivo* and clinical lines of evidence for dual effects of SR on bone cells (Brennan *et al*., 2009), ovariectomised rats (Bain *et al*., 2009) and in women receiving long term SR for osteoporosis (Arlot *et al*., 2008).

Other anabolic drugs available for the treatment of osteoporosis are Parathyroid hormone (PTH) and anti-sclerostin antibodies. PTH is available as either the N-terminal fragment teriparatide (1-34), or the full length PTH (1-84) (Rachner *et al*., 2011), while anti-sclerostin antibodies are an emerging approach to increase bone mass (Roux, 2010). PTH is currently the only anabolic agent approved in the U.S.A. for the treatment of osteoporosis, and has been shown to reduce fracture risk and improve bone mineral density, making it an attractive therapy for severe osteoporotic patients (Mosekilde *et al*., 2011). However, in part, because of its daily subcutaneous dosing regimen, PTH is limited in its long term use (Greenblatt, 2005). Pre-clinical trials with anti-sclerostin antibodies have demonstrated a marked improvement in bone mass and bone strength (Mosekilde *et al*., 2011). Sclerostin is a soluble secreted protein that is responsible for the negative regulation of osteoblast-mediated bone formation, through antagonising the Wnt signalling pathway (van Bezooijen *et al*., 2007). Inhibition of sclerostin protein or its gene results in a high bone mass phenotype in mice (Li *et al*., 2008a), rats (Li *et al*., 2010), cynomolgus monkeys (Ominsky *et al*., 2010), and increased bone formation in humans (Cejka *et al*., 2011, Padhi *et al*., 2011). The only clinical trial on anti-sclerostin antibodies in normal male subjects and postmenopausal women reported only mild, non-serious adverse effects, including dizziness,

constipation and erythema, and one patient was reported to have serious non-specific hepatitis (Padhi *et al*., 2011). Currently, there is a plethora of research into possible treatment avenues for osteoporosis, as outlined in the review by Rachner and colleagues (Rachner *et al*., 2011). Although therapeutic strategies to treat patients with osteoporosis have been positive, limitations to these uses are as a result of the occurrence of rare but late complications, as well as restrictions for its use with co-existing diseases or treatment duration may be limited (Mosekilde *et al*., 2011, Rachner *et al*., 2011). To date there is no one drug that is safe, well-tolerated and able to address both the increased osteoclast activity and reduced bone formation in non-cancerous conditions affecting altered bone homeostasis.

Therefore the novel osteogenic effects of LBH589 described in this chapter may potentially be compared to the effects of other anabolic agents, such as strontium ranelate. However, more in-depth research into the actions of LBH589, including long term exposure, pharmacokinetics and assessment of bone tissue quality and strength after exposure, will provide a stronger rationale for the potential use of HDIs in bone diseases, in which altered bone homeostasis plays a significant role.

Chapter 8. General discussions and conclusions

Concluding remarks

Although the HDI field is still in its infancy, HDIs have emerged as an exciting new class of anticancer agents that can induce cellular death against a wide variety of malignancies. While some HDIs have successfully progressed into early-phase clinical trials for the treatment of certain cancers, the mechanisms underlying their anticancer activities are still not fully understood. Furthermore, the treatment options for secondary or metastatic bone cancers are limited to the use of anti-resorptive therapeutic strategies, which aim to alleviate further symptoms and often do not translate to a greater survival outcome. Once cancers invade the bone microenvironment, the 'vicious cycle' of cancer-induced bone destruction appears inevitable, and to date, there have been no *in vivo* investigations into the potential benefits of using HDIs in the treatment of cancer-induced bone disease.

In this thesis, the use of the intratibial breast cancer bone model is representative of the latter stages of advanced breast cancer. This model describes a simple technique, in which cancer cells are transplanted directly into the marrow cavity of tibiae of athymic mice, producing local lesions in the area of transplantation. An added advantage of this model is that the contralateral tibia in the same animal can be used as a control. Furthermore, the intratibial bone cancer model results in localised tumour growth at a single bony site and allows for a consistent measurable outcome, in which the efficacy of HDI treatment can be accurately determined. Therefore, not only did this model allow the direct investigation of the effect of LBH589 on cancer growth in bone, but it also allowed the evaluation of its osteotropic properties.

The studies in this thesis adopted a systematic approach to illustrate the overall responses of breast cancer cells, osteoclasts and osteoblasts to the therapeutic activity of LBH589. To investigate these effects, the bone-seeking MDA-MB231-TXSA breast cancer cell line was initially screened and subsequently, the apoptotic pathways were defined for their sensitivity to LBH589. Apoptosis induction was associated with the cleavage and subsequent activation of both 'activator' and 'effector' caspases, as well as engagement of the intrinsic pathway, exemplified by the cleavage of Bid and caspase-9 to further amplify apoptosis. However, these cells could not be fully rescued from LBH589-induced apoptosis with co-culture with caspase inhibitors, suggesting caspase independent mechanisms of action, such as autophagy.

Whilst a large number of reports have demonstrated the anticancer therapeutic efficacy of HDIs *in vivo*, the data presented in this thesis showed that, no such translation from *in vitro* to *in vivo* efficacy was apparent. Systemic treatment with LBH589 significantly protected the bone from the effects of breast cancer-induced osteolysis and this was correlated to a reduction in the number of TRAP$^+$ osteoclasts lining the trabecular bone surface. Despite the observed bone protection, LBH589 had no effect on tumour load in bone. This suggests a direct effect of LBH589 on the bone resorbing cells, independent of tumour burden. However, the lack of anticancer efficacy shown in this study raises further questions regarding the potential resistance of cancer cells within the bone microenvironment following LBH589 therapy. This highlights the importance for a better understanding of the interactions between cancer cells and of the cells within its immediate environment. While systemic administration of LBH589 or SAHA induced histone-H3 acetylation in the spleen and bone marrow, no such acetylation was detected in the tumour-bed either in the primary site, or in bone. Reasons for this remain unclear, but it is likely that the dose and schedule of treatment

may not have been optimum in this setting. Further escalation of drug dose could not be attempted due to the likely onset of systemic toxicity. Therefore further investigations into the pharmaco-kinetics of LBH589 would highlight potential clinically-relevant limitations to its use in patients with solid tumours.

Further *in vitro* investigations into the activity of LBH589 on normal bone cells elucidated a number of novel pathways. For instance, the effect of HDIs have not been correlated to human-derived osteoclasts and osteoblasts. Therefore, in the investigations reported in this thesis, treatment with LBH589 inhibited RANKL-induced osteoclastogenesis and bone resorption, while promoting mineralisation by normal human osteoblasts, which was associated with the induction of osteogenic genes. Therefore, treatment with LBH589 induced a shift towards an anti-osteoclastic phenotype in NHB-like cells, contributing to the altered balance of bone homeostasis, to favour bone formation. The osteotropic actions of LBH589 seen *in vitro* were further corroborated with supporting evidence from the *in vivo* experiments. The resulting increase in LBH589-mediated bone formation was most likely attributed to an increase in appositional rate.

Several HDIs were reported to have synergistic and/or additive effects when combined with conventional therapeutics. In this thesis, the effect of LBH589 and SAHA on the anticancer efficacy *in vivo* was compared to the monoclonal antibody, Drozitumab. In collaboration with colleagues from the Breast Cancer Research Unit, Drozitumab was compared using the same *in vivo* models of breast cancer and cancer-induced bone destruction, outlined in this thesis. These data indicated that Drozitumab was highly efficacious in reducing breast cancer growth in, both the primary site, and in bone, which suggest a potential therapeutic strategy using this combinatorial approach. Furthermore the osteotropic properties of LBH589 demonstrated in this thesis may have

potential significance in clinically-relevant bone conditions, in which bone loss is indicated, such as osteoporosis. For example, for patients receiving long-term bisphosphonates have developed an increased bone fragility, as well as little compensatory bone formation. Therefore, combination treatment with LBH589 may have potential in compensating for the lack of bone formation and increased bone fragility, observed in patients receiving bisphosphonate alone. Therefore, investigations into the combinatorial activities of HDIs, in particular, LBH589, with current treatment modalities, may be informative in further detailing this drug's combined effects on the 'vicious cycle' of cancer-induced bone destruction. Moreover, combinatorial studies may also provide indications for increasing bone formation in diseases, in which bone loss is significant.

The work presented in this thesis demonstrate that LBH589 and SAHA, used as single agent therapies, exhibit positive *in vitro* anti-tumour activities, however, the results at present do not translate into *in vivo* anticancer efficacy. However, previously unrecognised osteotropic properties of LBH589 were demonstrated through the regulation of osteoclast and osteoblast functions, leading towards an increased bone formation. The cross-talk between the cancer cells and cells of the bone microenvironment has been proposed as providing a protective environment against treatment with LBH589. Therefore, future investigations into this affect would benefit in facilitating the improvement and potential novel treatment avenues for patients with skeletal malignancies.

Chapter 9. Bibliography

AARON, J. E., GALLAGHER, J. C., ANDERSON, J., STASIAK, L., LONGTON, E. B., NORDIN, B. E. & NICHOLSON, M. (1974) Frequency of osteomalacia and osteoporosis in fractures of the proximal femur. *Lancet,* 1**,** 229-33.

ABO-TOUK, N. A., SAKR, H. A. & ABD EL-LATTEF, A. (2010) Switching to letrozole versus continued tamoxifen therapy in treatment of postmenopausal women with early breast cancer. *J Egypt Natl Canc Inst,* 22**,** 79-85.

ADIMOOLAM, S., SIRISAWAD, M., CHEN, J., THIEMANN, P., FORD, J. M. & BUGGY, J. J. (2007) HDAC inhibitor PCI-24781 decreases RAD51 expression and inhibits homologous recombination. *Proc Natl Acad Sci U S A,* 104**,** 19482-7.

AFT, R., PEREZ, J. R., RAJE, N., HIRSH, V. & SAAD, F. (2011) Could targeting bone delay cancer progression? Potential mechanisms of action of bisphosphonates. *Crit Rev Oncol Hematol,* 82**,** 233-48.

AI, M., HOLMEN, S. L., VAN HUL, W., WILLIAMS, B. O. & WARMAN, M. L. (2005) Reduced affinity to and inhibition by DKK1 form a common mechanism by which high bone mass-associated missense mutations in LRP5 affect canonical Wnt signaling. *Mol Cell Biol,* 25**,** 4946-55.

AITA, V. M., LIANG, X. H., MURTY, V. V., PINCUS, D. L., YU, W., CAYANIS, E., KALACHIKOV, S., GILLIAM, T. C. & LEVINE, B. (1999) Cloning and genomic organization of beclin 1, a candidate tumor suppressor gene on chromosome 17q21. *Genomics,* 59**,** 59-65.

ALLGROVE, J. (2009) A practical approach to rickets. *Endocr Dev,* 16**,** 115-32.

AMLING, M., PRIEMEL, M., HOLZMANN, T., CHAPIN, K., RUEGER, J. M., BARON, R. & DEMAY, M. B. (1999) Rescue of the skeletal phenotype of vitamin D receptor-ablated mice in the setting of normal mineral ion homeostasis: formal histomorphometric and biomechanical analyses. *Endocrinology,* 140**,** 4982-7.

ANTONIUCCI, D. M., SELLMEYER, D. E., BILEZIKIAN, J. P., PALERMO, L., ENSRUD, K. E., GREENSPAN, S. L. & BLACK, D. M. (2007) Elevations in serum and urinary calcium with parathyroid hormone (1-84) with and without alendronate for osteoporosis. *J Clin Endocrinol Metab,* 92**,** 942-7.

ANZICK, S. L., KONONEN, J., WALKER, R. L., AZORSA, D. O., TANNER, M. M., GUAN, X. Y., SAUTER, G., KALLIONIEMI, O. P., TRENT, J. M. & MELTZER, P. S. (1997) AIB1, a steroid receptor coactivator amplified in breast and ovarian cancer. *Science,* 277**,** 965-8.

ARANY, Z., SELLERS, W. R., LIVINGSTON, D. M. & ECKNER, R. (1994) E1A-associated p300 and CREB-associated CBP belong to a conserved family of coactivators. *Cell,* 77**,** 799-800.

ARAUJO, J. & LOGOTHETIS, C. (2008) Targeting Src signaling in metastatic bone disease. *Int J Cancer,* 124**,** 1-6.

ARLOT, M. E., JIANG, Y., GENANT, H. K., ZHAO, J., BURT-PICHAT, B., ROUX, J. P., DELMAS, P. D. & MEUNIER, P. J. (2008) Histomorphometric and microCT analysis of bone biopsies from postmenopausal osteoporotic women treated with strontium ranelate. *J Bone Miner Res,* 23**,** 215-22.

ARNOLD, M. A., KIM, Y., CZUBRYT, M. P., PHAN, D., MCANALLY, J., QI, X., SHELTON, J. M., RICHARDSON, J. A., BASSEL-DUBY, R. & OLSON, E. N. (2007) MEF2C transcription factor controls chondrocyte hypertrophy and bone development. *Dev Cell,* 12**,** 377-89.

ATADJA, P. (2010) Development of the pan-DAC inhibitor panobinostat (LBH589): Successes and challenges. *Cancer Letters,* 280**,** 233-241.

ATKINS, G. J., ANDERSON, P. H., FINDLAY, D. M., WELLDON, K. J., VINCENT, C., ZANNETTINO, A. C., O'LOUGHLIN, P. D. & MORRIS, H. A. (2007) Metabolism of vitamin D3 in human osteoblasts: evidence for autocrine and paracrine activities of 1 alpha,25-dihydroxyvitamin D3. *Bone,* 40**,** 1517-28.

ATKINS, G. J., HAYNES, D. R., GRAVES, S. E., EVDOKIOU, A., HAY, S., BOURALEXIS, S. & FINDLAY, D. M. (2000) Expression of osteoclast differentiation signals by stromal elements of giant cell tumors. *J Bone Miner Res,* 15**,** 640-9.

ATKINS, G. J., KOSTAKIS, P., PAN, B., FARRUGIA, A., GRONTHOS, S., EVDOKIOU, A., HARRISON, K., FINDLAY, D. M. & ZANNETTINO, A. C. (2003) RANKL expression is related to the differentiation state of human osteoblasts. *J Bone Miner Res,* 18**,** 1088-98.

ATKINS, G. J., KOSTAKIS, P., WELLDON, K. J., VINCENT, C., FINDLAY, D. M. & ZANNETTINO, A. C. (2005) Human trabecular bone-derived osteoblasts support human osteoclast formation in vitro in a defined, serum-free medium. *J Cell Physiol,* 203**,** 573-82.

ATKINS, G. J., WELLDON, K. J., HALBOUT, P. & FINDLAY, D. M. (2009a) Strontium ranelate treatment of human primary osteoblasts promotes an osteocyte-like phenotype while eliciting an osteoprotegerin response. *Osteoporos Int,* 20**,** 653-64.

ATKINS, G. J., WELLDON, K. J., HOLDING, C. A., HAYNES, D. R., HOWIE, D. W. & FINDLAY, D. M. (2009b) The induction of a catabolic phenotype in human primary osteoblasts and osteocytes by polyethylene particles. *Biomaterials,* 30**,** 3672-81.

AUTZEN, P., ROBSON, C. N., BJARTELL, A., MALCOLM, A. J., JOHNSON, M. I., NEAL, D. E. & HAMDY, F. C. (1998) Bone morphogenetic protein 6 in skeletal metastases from prostate cancer and other common human malignancies. *Br J Cancer,* 78**,** 1219-23.

AYTON, P. M. & CLEARY, M. L. (2001) Molecular mechanisms of leukemogenesis mediated by MLL fusion proteins. *Oncogene,* 20**,** 5695-707.

BAGNATO, A. & ROSANO, L. (2008) The endothelin axis in cancer. *Int J Biochem Cell Biol,* 40**,** 1443-51.

BAGNATO, A., ROSANO, L., SPINELLA, F., DI CASTRO, V., TECCE, R. & NATALI, P. G. (2004) Endothelin B receptor blockade inhibits dynamics of cell interactions and communications in melanoma cell progression. *Cancer Res,* 64**,** 1436-43.

BAIN, S. D., JEROME, C., SHEN, V., DUPIN-ROGER, I. & AMMANN, P. (2009) Strontium ranelate improves bone strength in ovariectomized rat by positively influencing bone resistance determinants. *Osteoporos Int,* 20**,** 1417-28.

BAKKENIST, C. J. & KASTAN, M. B. (2003) DNA damage activates ATM through intermolecular autophosphorylation and dimer dissociation. *Nature,* 421**,** 499-506.

BALENA, R., KLEEREKOPER, M., FOLDES, J. A., SHIH, M. S., RAO, D. S., SCHOBER, H. C. & PARFITT, A. M. (1998) Effects of different regimens of sodium fluoride treatment for osteoporosis on the structure, remodeling and mineralization of bone. *Osteoporos Int,* 8**,** 428-35.

BALI, P., PRANPAT, M., SWABY, R., FISKUS, W., YAMAGUCHI, H., BALASIS, M., ROCHA, K., WANG, H. G., RICHON, V. & BHALLA, K. (2005) Activity of suberoylanilide hydroxamic Acid against human breast cancer cells with amplification of her-2. *Clin Cancer Res,* 11**,** 6382-9.

BALLA, B., VASZILKO, M., KOSA, J., PODANI, J., TAKACS, I., TOBIAS, B., NAGY, Z., LAZARY, A. & LAKATOS, P. (2012) New approach to analyze genetic and clinical data in bisphosphonate-induced osteonecrosis of the jaw. *Oral Dis.*

BARDOU, V. J., ARPINO, G., ELLEDGE, R. M., OSBORNE, C. K. & CLARK, G. M. (2003) Progesterone receptor status significantly improves outcome prediction over estrogen receptor status alone for adjuvant endocrine therapy in two large breast cancer databases. *J Clin Oncol,* 21**,** 1973-9.

BATSON, O. V. (1942) The role of the vertebral veins in the metastatic process. *Ann Intern Med,* 16**,** 1588-1594.

BAYLIN, S. B. & OHM, J. E. (2006) Epigenetic gene silencing in cancer - a mechanism for early oncogenic pathway addiction? *Nat Rev Cancer,* 6**,** 107-16.

BCS (2011) www.breastcancer.org.au.

BECKERS, T., BURKHARDT, C., WIELAND, H., GIMMNICH, P., CIOSSEK, T., MAIER, T. & SANDERS, K. (2007) Distinct pharmacological properties of second generation HDAC inhibitors with the benzamide or hydroxamate head group. *Int J Cancer,* 121**,** 1138-1148.

BEDOGNI, A., BETTINI, G., TOTOLA, A., SAIA, G. & NOCINI, P. F. (2010) Oral bisphosphonate-associated osteonecrosis of the jaw after implant surgery: a case report and literature review. *J Oral Maxillofac Surg,* 68**,** 1662-6.

BENNETT, C. N., LONGO, K. A., WRIGHT, W. S., SUVA, L. J., LANE, T. F., HANKENSON, K. D. & MACDOUGALD, O. A. (2005) Regulation of osteoblastogenesis and bone mass by Wnt10b. *Proc Natl Acad Sci U S A,* 102**,** 3324-9.

BERRUTI, A., DOGLIOTTI, L., BITOSSI, R., FASOLIS, G., GORZEGNO, G., BELLINA, M., TORTA, M., PORPIGLIA, F., FONTANA, D. & ANGELI, A. (2000) Incidence of skeletal complications in patients with bone metastatic prostate cancer and hormone refractory disease: predictive role of bone resorption and formation markers evaluated at baseline. *J Urol,* 164**,** 1248-53.

BI, G. & JIANG, G. (2006) The molecular mechanism of HDAC inhibitors in anticancer effects. *Cell Mol Immunol,* 3**,** 285-90.

BIELIAUSKAS, A. V. & PFLUM, M. K. (2008) Isoform-selective histone deacetylase inhibitors. *Chem Soc Rev,* 37**,** 1402-13.

BODY, J. J. (2003) Rationale for the use of bisphosphonates in osteoblastic and osteolytic bone lesions. *Breast,* 12 Suppl 2**,** S37-44.

BODY, J. J., BARTL, R., BURCKHARDT, P., DELMAS, P. D., DIEL, I. J., FLEISCH, H., KANIS, J. A., KYLE, R. A., MUNDY, G. R., PATERSON, A. H. & RUBENS, R. D. (1998) Current use of bisphosphonates in oncology. International Bone and Cancer Study Group. *J Clin Oncol,* 16**,** 3890-9.

BOLDEN, J. E., PEART, M. J. & JOHNSTONE, R. W. (2006) Anticancer activities of histone deacetylase inhibitors. *Nat Rev Drug Discov,* 5**,** 769-84.

BOLUK, A., GUZELIPEK, M., SAVLI, H., TEMEL, I., OZISIK, H. I. & KAYGUSUZ, A. (2004) The effect of valproate on bone mineral density in adult epileptic patients. *Pharmacol Res,* 50**,** 93-7.

BOUMAH, C. E., LEE, M., SELVAMURUGAN, N., SHIMIZU, E. & PARTRIDGE, N. C. (2009) Runx2 recruits p300 to mediate parathyroid hormone's effects on histone acetylation and transcriptional activation of the matrix metalloproteinase-13 gene. *Mol Endocrinol,* 23**,** 1255-63.

BOUMBER, Y. & ISSA, J. P. (2011) Epigenetics in cancer: what's the future? *Oncology (Williston Park),* 25**,** 220-6, 228.

BOYCE, B. F. & XING, L. (2008) Functions of RANKL/RANK/OPG in bone modeling and remodeling. *Arch Biochem Biophys,* 473**,** 139-46.

BOYDEN, L. M., MAO, J., BELSKY, J., MITZNER, L., FARHI, A., MITNICK, M. A., WU, D., INSOGNA, K. & LIFTON, R. P. (2002) High bone density due to a mutation in LDL-receptor-related protein 5. *N Engl J Med,* 346**,** 1513-21.

BOYES, J., BYFIELD, P., NAKATANI, Y. & OGRYZKO, V. (1998) Regulation of activity of the transcription factor GATA-1 by acetylation. *Nature,* 396**,** 594-8.

BOYLE, W. J., SIMONET, W. S. & LACEY, D. L. (2003) Osteoclast differentiation and activation. *Nature,* 423**,** 337-42.

BRENNAN, T. C., RYBCHYN, M. S., GREEN, W., ATWA, S., CONIGRAVE, A. D. & MASON, R. S. (2009) Osteoblasts play key roles in the mechanisms of action of strontium ranelate. *Br J Pharmacol,* 157**,** 1291-300.

BRETSCHER, A., CHAMBERS, D., NGUYEN, R. & RECZEK, D. (2000) ERM-Merlin and EBP50 protein families in plasma membrane organization and function. *Annu Rev Cell Dev Biol,* 16**,** 113-43.

BRODIE, A. & SABNIS, G. (2011) Adaptive changes result in activation of alternate signaling pathways and acquisition of resistance to aromatase inhibitors. *Clin Cancer Res,* 17**,** 4208-13.

BROWNELL, J. E. & ALLIS, C. D. (1996) Special HATs for special occasions: linking histone acetylation to chromatin assembly and gene activation. *Curr Opin Genet Dev,* 6**,** 176-84.

BRYDEN, A. A., HOYLAND, J. A., FREEMONT, A. J., CLARKE, N. W. & GEORGE, N. J. (2002) Parathyroid hormone related peptide and receptor expression in paired primary prostate cancer and bone metastases. *Br J Cancer,* 86**,** 322-5.

BUGLIO, D. & YOUNES, A. (2010) Histone deacetylase inhibitors in Hodgkin lymphoma. *Invest New Drugs,* 28 Suppl 1**,** S21-7.

BUTLER, L. M., AGUS, D. B., SCHER, H. I., HIGGINS, B., ROSE, A., CORDON-CARDO, C., THALER, H. T., RIFKIND, R. A., MARKS, P. A. & RICHON, V. M. (2000) Suberoylanilide Hydroxamic Acid, an inihibitor of histone deacetylase, suppresses the growth of prostate cancer cells in Vitro and in Vivo. *Cancer Research,* 60**,** 5165-5170.

BUTLER, L. M., LIAPIS, V., BOURALEXIS, S., WELLDON, K., HAY, S., LABRINIDIS, A., TILLEY, W. D., FINDLAY, D. M. & EVDOKIOUS, A. (2006) The histone deacetylase inhibitor, suberoylanilide hydroxamic acid, overcomes resistance of human breast cancer cells to Apo2L/TRAIL. *Int. J. Cancer,* 119**,** 1-10.

BUTLER, L. M., ZHOU, X., XU, W. S., SCHER, H. I., RIFKIND, R. A., MARKS, P. A. & RICHON, V. M. (2002) The histone deacetylase inhibitor SAHA arrests cancer cell growth, up-regulates thioredoxin-binding protein-2, and down-regulates thioredoxin. *Proc Natl Acad Sci U S A,* 99**,** 11700-5.

CAO, Q., YU, C., XUE, R., HSUEH, W., PAN, P., CHEN, Z., WANG, S., MCNUTT, M. & GU, J. (2008) Autophagy induced by suberoylanilide hydroxamic acid in Hela S3 cells involves inhibition of protein kinase B and up-regulation of Beclin 1. *Int J Biochem Cell Biol,* 40**,** 272-83.

CARAFA, V., NEBBIOSO, A. & ALTUCCI, L. (2010) Histone deacetylase inhibitors: recent insights from basic to clinical knowledge & patenting of anti-cancer actions. *Recent Pat Anticancer Drug Discov,* 6**,** 131-45.

CARAPETI, M., AGUIAR, R. C., WATMORE, A. E., GOLDMAN, J. M. & CROSS, N. C. (1999) Consistent fusion of MOZ and TIF2 in AML with inv(8)(p11q13). *Cancer Genet Cytogenet,* 113**,** 70-2.

CARDWELL, C. R., ABNET, C. C., CANTWELL, M. M. & MURRAY, L. J. (2010) Exposure to oral bisphosphonates and risk of esophageal cancer. *JAMA,* 304**,** 657-63.

CAREW, J. S., NAWROCKI, S. T., KAHUE, C. N., ZHANG, H., YANG, C., CHUNG, L., HOUGHTON, J. A., HUANG, P., GILES, F. J. & CLEVELAND, J. L. (2007) Targeting autophagy augments the anticancer activity of the histone deacetylase inhibitor SAHA to overcome Bcr-Abl-mediated drug resistance. *Blood,* 110**,** 313-22.

CATLEY, L., WEISBERG, E., KIZILTEPE, T., TAI, Y. T., HIDESHIMA, T., NERI, P., TASSONE, P., ATADJA, P., CHAUHAN, D., MUNSHI, N. C. & ANDERSON, K. C. (2006) Aggresome induction by proteasome inhibitor bortezomib and alpha-tubulin hyperacetylation by tubulin deacetylase (TDAC) inhibitor LBH589 are synergistic in myeloma cells. *Blood,* 108**,** 3441-9.

CEJKA, D., JAGER-LANSKY, A., KIEWEG, H., WEBER, M., BIEGLMAYER, C., HAIDER, D. G., DIARRA, D., PATSCH, J., KAINBERGER, F., BOHLE, B. & HAAS, M. (2011) Sclerostin serum levels correlate positively with bone mineral density and microarchitecture in haemodialysis patients. *Nephrol Dial Transplant,* 27**,** 226-230.

CHEN, G., SHUKEIR, N., POTTI, A., SIRCAR, K., APRIKIAN, A., GOLTZMAN, D. & RABBANI, S. A. (2004a) Up-regulation of Wnt-1 and beta-catenin production in patients with advanced metastatic prostate carcinoma: potential pathogenetic and prognostic implications. *Cancer,* 101**,** 1345-56.

CHEN, S., YE, J., KIJIMA, I. & EVANS, D. (2010) The HDAC inhibitor LBH589 (panobinostat) is an inhibitory modulator of aromatase gene expression. *Proc Natl Acad Sci U S A,* 107**,** 11032-7.

CHEN, W. K., CHEN, Y., GU, J. X. & CUI, G. H. (2004b) Effect of trichostatin A on histone acetylation level and apoptosis in HL-60 cells. *Zhongguo Shi Yan Xue Ye Xue Za Zhi,* 12**,** 324-8.

CHERIYATH, V., KUHNS, M. A., KALAYCIO, M. E. & BORDEN, E. C. (2011) Potentiation of apoptosis by histone deacetylase inhibitors and doxorubicin combination: cytoplasmic cathepsin B as a mediator of apoptosis in multiple myeloma. *Br J Cancer,* 104**,** 957-67.

CHIPUK, J. E. & GREEN, D. R. (2006) Dissecting p53-dependent apoptosis. *Cell Death Differ,* 13**,** 994-1002.

CHO, K. S., ELIZONDO, L. I. & BOERKOEL, C. F. (2004) Advances in chromatin remodeling and human disease. *Curr Opin Genet Dev,* 14**,** 308-15.

CHOI, J. H., KWON, H. J., YOON, B. I., KIM, J. H., HAN, S. U., JOO, H. J. & KIM, D. Y. (2001) Expression profile of histone deacetylase 1 in gastric cancer tissues. *Jpn J Cancer Res,* 92**,** 1300-4.

CHOPIN, V., SLOMIANNY, C., HONDERMARCK, H. & LE BOURHIS, X. (2004) Synergistic induction of apoptosis in breast cancer cells by cotreatment with butyrate and TNF-alpha, TRAIL, or anti-Fas agonist antibody involves enhancement of death receptors' signaling and requires P21(waf1). *Exp Cell Res,* 298**,** 560-73.

CLINES, G. A., MOHAMMAD, K. S., BAO, Y., STEPHENS, O. W., SUVA, L. J., SHAUGHNESSY, J. D., JR., FOX, J. W., CHIRGWIN, J. M. & GUISE, T. A. (2007) Dickkopf homolog 1 mediates endothelin-1-stimulated new bone formation. *Mol Endocrinol,* 21**,** 486-98.

COHEN-KFIR, E., ARTSI, H., LEVIN, A., ABRAMOWITZ, E., BAJAYO, A., GURT, I., ZHONG, L., D'URSO, A., TOIBER, D., MOSTOSLAVSKY, R. &

DRESNER-POLLAK, R. (2011) Sirt1 Is a Regulator of Bone Mass and a Repressor of Sost Encoding for Sclerostin: A Bone Formation Inhibitor. *Endocrinology,* 152**,** 4514-4524.

COLEMAN, R. E. (1997) Skeletal complications of malignancy. *Cancer,* 80**,** 1588-94.

COLEMAN, R. E. (2001) Metastatic bone disease: clinical features, pathophysiology and treatment strategies. *Cancer Treat Rev,* 27**,** 165-76.

COLEMAN, R. E. (2004a) Bisphosphonates: clinical experience. *Oncologist,* 9 Suppl 4**,** 14-27.

COLEMAN, R. E. (2004b) The role of bisphosphonates in breast cancer. *Breast,* 13 Suppl 1**,** S19-28.

COLEMAN, R. E. & RUBENS, R. D. (1987) The clinical course of bone metastases from breast cancer. *Br J Cancer,* 55**,** 61-6.

COXON, F. P. & ROGERS, M. J. (2003) The role of prenylated small GTP-binding proteins in the regulation of osteoclast function. *Calcif Tissue Int,* 72**,** 80-4.

COXON, F. P., THOMPSON, K. & ROGERS, M. J. (2006) Recent advances in understanding the mechanism of action of bisphosphonates. *Curr Opin Pharmacol,* 6**,** 307-12.

CRAMER, J. A., GOLD, D. T., SILVERMAN, S. L. & LEWIECKI, E. M. (2007) A systematic review of persistence and compliance with bisphosphonates for osteoporosis. *Osteoporos Int,* 18**,** 1023-31.

CRAZZOLARA, R., JOHRER, K., JOHNSTONE, R. W., GREIL, R., KOFLER, R., MEISTER, B. & BERNHARD, D. (2002) Histone deacetylase inhibitors potently repress CXCR4 chemokine receptor expression and function in acute lymphoblastic leukaemia. *Br J Haematol,* 119**,** 965-9.

CRISANTI, M. C., WALLACE, A. F., KAPOOR, V., VANDERMEERS, F., DOWLING, M. L., PEREIRA, L. P., COLEMAN, K., CAMPLING, B. G., FRIDLENDER, Z. G., KAO, G. D. & ALBELDA, S. M. (2009) The HDAC inhibitor panobinostat (LBH589) inhibits mesothelioma and lung cancer cells in vitro and in vivo with particular efficacy for small cell lung cancer. *Mol Cancer Ther,* 8**,** 2221-2231.

CROESE, J. W., VAN DEN ENDEN-VIEVEEN, M. H. & RADL, J. (1991) Immune regulation of 5T2 mouse multiple myeloma. II. Immunological treatment of 5T2 MM residual disease. *Neoplasma,* 38**,** 467-74.

CUI, Y., NIZIOLEK, P. J., MACDONALD, B. T., ZYLSTRA, C. R., ALENINA, N., ROBINSON, D. R., ZHONG, Z., MATTHES, S., JACOBSEN, C. M., CONLON, R. A., BROMMAGE, R., LIU, Q., MSEEH, F., POWELL, D. R., YANG, Q. M., ZAMBROWICZ, B., GERRITS, H., GOSSEN, J. A., HE, X., BADER, M., WILLIAMS, B. O., WARMAN, M. L. & ROBLING, A. G. (2011) Lrp5 functions in bone to regulate bone mass. *Nat Med,* 17**,** 684-691.

DALLE CARBONARE, L., BERTOLDO, F. & LO CASCIO, V. (2009) Evidences of safety and tolerability of the zoledronic acid 5 mg yearly in the post-menopausal osteoporosis: the HORIZON project. *Reumatismo,* 61**,** 54-64.

DASS, C. R. & CHOONG, P. F. (2007) Zoledronic acid inhibits osteosarcoma growth in an orthotopic model. *Mol Cancer Ther,* 6**,** 3263-70.

DAVIE, J. R., SAMUEL, S. K., SPENCER, V. A., HOLTH, L. T., CHADEE, D. N., PELTIER, C. P., SUN, J. M., CHEN, H. Y. & WRIGHT, J. A. (1999) Organization of chromatin in cancer cells: role of signalling pathways. *Biochem Cell Biol,* 77**,** 265-75.

DAVIS, P. K. & BRACKMANN, R. K. (2003) Chromatin remodeling and cancer. *Cancer Biol Ther,* 2**,** 22-9.

DE BONO, J. S., KRISTELEIT, R., TOLCHER, A., FONG, P., PACEY, S., KARAVASILIS, V., MITA, M., SHAW, H., WORKMAN, P., KAYE, S., ROWINSKY, E. K., AHERNE, W., ATADJA, P., SCOTT, J. W. & PATNAIK, A. (2008) Phase I Pharmacokinetic and Pharmacodynamic Study of LAQ824, a Hydroxamate Histone Deacetylase Inhibitor with a Heat Shock Protein-90 Inhibitory Profile, in Patients with Advanced Solid Tumors. *Clin Cancer Res,* 14**,** 6663-73.

DEEKS, E. D. & DHILLON, S. (2010) Strontium ranelate: a review of its use in the treatment of postmenopausal osteoporosis. *Drugs,* 70**,** 733-59.

DELEU, S., LEMAIRE, M., ARTS, J., MENU, E., VAN VALCKENBORGH, E., VANDE BROEK, I., DE RAEVE, H., COULTON, L., VAN CAMP, B., CROUCHER, P. & VANDERKERKEN, K. (2009) Bortezomib Alone or in Combination with the Histone Deacetylase Inhibitor JNJ-26481585: Effect on Myeloma Bone Disease in the 5T2MM Murine Model of Myeloma. *Cancer Res,* 16**,** 16.

DEMERS, L. M., COSTA, L. & LIPTON, A. (2003) Biochemical markers and skeletal metastases. *Clin Orthop Relat Res***,** S138-47.

DIAKOS, C., PRIESCHL, E. E., SAEMANN, M., NOVOTNY, V., BOHMIG, G., CSONGA, R., BAUMRUKER, T. & ZLABINGER, G. J. (2002) Novel mode of interference with nuclear factor of activated T-cells regulation in T-cells by the bacterial metabolite n-butyrate. *J Biol Chem,* 277**,** 24243-51.

DORFMAN, H. D. & CZERNIAK, B. (1995) Bone cancers. *Cancer,* 75**,** 203-10.

DOWNEY, S. E., HOYLAND, J., FREEMONT, A. J., KNOX, F., WALLS, J. & BUNDRED, N. J. (1997) Expression of the receptor for parathyroid hormone-related protein in normal and malignant breast tissue. *J Pathol,* 183**,** 212-7.

DRABSCH, Y. & TEN DIJKE, P. (2011) TGF-beta Signaling in Breast Cancer Cell Invasion and Bone Metastasis. *J Mammary Gland Biol Neoplasia,* 16**,** 97-108.

DUNFORD, J. E., THOMPSON, K., COXON, F. P., LUCKMAN, S. P., HAHN, F. M., POULTER, C. D., EBETINO, F. H. & ROGERS, M. J. (2001) Structure-activity relationships for inhibition of farnesyl diphosphate synthase in vitro and inhibition of bone resorption in vivo by nitrogen-containing bisphosphonates. *J Pharmacol Exp Ther,* 296**,** 235-42.

DUONG, V., BRET, C., ALTUCCI, L., MAI, A., DURAFFOURD, C., LOUBERSAC, J., HARMAND, P. O., BONNET, S., VALENTE, S., MAUDELONDE, T., CAVAILLES, V. & BOULLE, N. (2008) Specific activity of class II histone deacetylases in human breast cancer cells. *Mol Cancer Res,* 6**,** 1908-19.

DUVIC, M., TALPUR, R., NI, X., ZHANG, C., HAZARIKA, P., KELLY, C., CHIAO, J. H., REILLY, J. F., RICKER, J. L., RICHON, V. M. & FRANKEL, S. R. (2007) Phase 2 trial of oral vorinostat (suberoylanilide hydroxamic acid, SAHA) for refractory cutaneous T-cell lymphoma (CTCL). *Blood,* 109**,** 31-9.

EBCTCG (2001) Tamoxifen for early breast cancer. *Cochrane Database Syst Rev.* 2001/11/09 ed.

ECKNER, R., EWEN, M. E., NEWSOME, D., GERDES, M., DECAPRIO, J. A., LAWRENCE, J. B. & LIVINGSTON, D. M. (1994) Molecular cloning and functional analysis of the adenovirus E1A-associated 300-kD protein (p300) reveals a protein with properties of a transcriptional adaptor. *Genes Dev,* 8**,** 869-84.

EDOUARD, T., GLORIEUX, F. H. & RAUCH, F. (2011) Relationship between Vitamin D status and bone mineralization, mass and metabolism in children with Osteogenesis imperfecta: Histomorphometric study. *J Bone Miner Res,* 26**,** 2245-2251.

ELLIS, L., ATADJA, P. W. & JOHNSTONE, R. W. (2009a) Epigenetics in cancer: targeting chromatin modifications. *Mol Cancer Ther,* 8**,** 1409-20.

ELLIS, L., HAMMERS, H. & PILI, R. (2009b) Targeting tumor angiogenesis with histone deacetylase inhibitors. *Cancer Lett,* 280**,** 145-53.

ELLIS, L., PAN, Y., SMYTH, G. K., GEORGE, D. J., MCCORMACK, C., WILLIAMS-TRUAX, R., MITA, M., BECK, J., BURRIS, H., RYAN, G.,

ATADJA, P., BUTTERFOSS, D., DUGAN, M., CULVER, K., JOHNSTONE, R. W. & PRINCE, H. M. (2008) Histone deacetylase inhibitor panobinostat induces clinical responses with associated alterations in gene expression profiles in cutaneous T-cell lymphoma. *Clin Cancer Res,* 14**,** 4500-10.

FERRON, M., BOUDIFFA, M., ARSENAULT, M., RACHED, M., PATA, M., GIROUX, S., ELFASSIHI, L., KISSELEVA, M., MAJERUS, P. W., ROUSSEAU, F. & VACHER, J. (2011) Inositol polyphosphate 4-phosphatase B as a regulator of bone mass in mice and humans. *Cell Metab,* 14**,** 466-77.

FINDLAY, D. M. & ATKINS, G. J. (2011) TWEAK and TNF regulation of sclerostin: a novel pathway for the regulation of bone remodelling. *Adv Exp Med Biol,* 691**,** 337-48.

FINNIN, M. S., DONIGIAN, J. R., COHEN, A., RICHON, V. M., RIFKIND, R. A., MARKS, P. A., BRESLOW, R. & PAVLETICH, N. P. (1999) Structures of a histone deacetylase homologue bound to the TSA and SAHA inhibitors. *Nature,* 401**,** 188-93.

FISKUS, W., BUCKLEY, K., RAO, R., MANDAWAT, A., YANG, Y., JOSHI, R., WANG, Y., BALUSU, R., CHEN, J., KOUL, S., JOSHI, A., UPADHYAY, S., ATADJA, P. & BHALLA, K. N. (2009) Panobinostat treatment depletes EZH2 and DNMT1 levels and enhances decitabine mediated de-repression of JunB and loss of survival of human acute leukemia cells. *Cancer Biol Ther,* 8**,** 10.

FISKUS, W., REN, Y., MOHAPATRA, A., BALI, P., MANDAWAT, A., RAO, R., HERGER, B., YANG, Y., ATADJA, P., WU, J. & BHALLA, K. (2007) Hydroxamic acid analogue histone deacetylase inhibitors attenuate estrogen receptor-alpha levels and transcriptional activity: a result of hyperacetylation and inhibition of chaperone function of heat shock protein 90. *Clin Cancer Res,* 13**,** 4882-90.

FLEISCH, H. (2002) Development of bisphosphonates. *Breast Cancer Res,* 4**,** 30-4.

FLEISCH, H., RUSSELL, R. G., BISAZ, S., CASEY, P. A. & MUHLBAUER, R. C. (1968) The influence of pyrophosphate analogues (diphosphonates) on the precipitation and dissolution. *Calcif Tissue Res***,** Suppl:10-10a.

FLORIS, G., DEBIEC-RYCHTER, M., SCIOT, R., STEFAN, C., FIEUWS, S., MACHIELS, K., ATADJA, P., WOZNIAK, A., FAA, G. & SCHOFFSKI, P. (2009) High Efficacy of Panobinostat Towards Human Gastrointestinal Stromal Tumors in a Xenograft Mouse Model. *Clin Cancer Res,* 9**,** 9.

FORTUNATI, N., BERTINO, S., COSTANTINO, L., DE BORTOLI, M., COMPAGNONE, A., BANDINO, A., CATALANO, M. G. & BOCCUZZI, G. (2010) Valproic acid restores ER alpha and antiestrogen sensitivity to ER alpha-negative breast cancer cells. *Mol Cell Endocrinol,* 314**,** 17-22.

FREW, A. J., JOHNSTONE, R. W. & BOLDEN, J. E. (2009) Enhancing the apoptotic and therapeutic effects of HDAC inhibitors. *Cancer Lett,* 280**,** 125-33.

FREW, A. J., LINDEMANN, R. K., MARTIN, B. P., CLARKE, C. J., SHARKEY, J., ANTHONY, D. A., BANKS, K. M., HAYNES, N. M., GANGATIRKAR, P., STANLEY, K., BOLDEN, J. E., TAKEDA, K., YAGITA, H., SECRIST, J. P., SMYTH, M. J. & JOHNSTONE, R. W. (2008) Combination therapy of established cancer using a histone deacetylase inhibitor and a TRAIL receptor agonist. *Proc Natl Acad Sci U S A,* 105**,** 11317-22.

FUKUTOMI, A., HATAKE, K., MATSUI, K., SAKAJIRI, S., HIRASHIMA, T., TANII, H., KOBAYASHI, K. & YAMAMOTO, N. (2011) A phase I study of oral panobinostat (LBH589) in Japanese patients with advanced solid tumors. *Invest New Drugs*.

FUSS, I. J., KANOF, M. E., SMITH, P. D. & ZOLA, H. (2009) Isolation of whole mononuclear cells from peripheral blood and cord blood. *Curr Protoc Immunol,* Chapter 7**,** Unit7 1.

GAYTHER, S. A., BATLEY, S. J., LINGER, L., BANNISTER, A., THORPE, K., CHIN, S. F., DAIGO, Y., RUSSELL, P., WILSON, A., SOWTER, H. M., DELHANTY, J. D., PONDER, B. A., KOUZARIDES, T. & CALDAS, C. (2000) Mutations truncating the EP300 acetylase in human cancers. *Nat Genet,* 24**,** 300-3.

GEORGE, P., BALI, P., ANNAVARAPU, S., SCUTO, A., FISKUS, W., GUO, F., SIGUA, C., SONDARVA, G., MOSCINSKI, L., ATADJA, P. & BHALLA, K. (2005) Combination of the histone deacetylase inhibitor LBH589 and the hsp90 inhibitor 17-AAG is highly active against human CML-BC cells and AML cells with activating mutation of FLT-3. *Blood,* 105**,** 1768-76.

GILES, F., FISCHER, T., CORTES, J., GARCIA-MANERO, G., BECK, J., RAVANDI, F., MASSON, E., RAE, P., LAIRD, G., SHARMA, S., KANTARJIAN, H., DUGAN, M., ALBITAR, M. & BHALLA, K. (2006) A phase I study of intravenous LBH589, a novel cinnamic hydroxamic acid analogue histone deacetylase inhibitor, in patients with refractory hematologic malignancies. *Clin Cancer Res,* 12**,** 4628-35.

GIROTRA, M., RUBIN, M. R. & BILEZIKIAN, J. P. (2006) Anabolic skeletal therapy for osteoporosis. *Arq Bras Endocrinol Metabol,* 50**,** 745-54.

GIULIANI, N., RIZZOLI, V. & ROODMAN, G. D. (2006) Multiple myeloma bone disease: Pathophysiology of osteoblast inhibition. *Blood,* 108**,** 3992-6.

GONG, Y., SLEE, R. B., FUKAI, N., RAWADI, G., ROMAN-ROMAN, S., REGINATO, A. M., WANG, H., CUNDY, T., GLORIEUX, F. H., LEV, D., ZACHARIN, M., OEXLE, K., MARCELINO, J., SUWAIRI, W., HEEGER, S.,

SABATAKOS, G., APTE, S., ADKINS, W. N., ALLGROVE, J., ARSLAN-KIRCHNER, M., BATCH, J. A., BEIGHTON, P., BLACK, G. C., BOLES, R. G., BOON, L. M., BORRONE, C., BRUNNER, H. G., CARLE, G. F., DALLAPICCOLA, B., DE PAEPE, A., FLOEGE, B., HALFHIDE, M. L., HALL, B., HENNEKAM, R. C., HIROSE, T., JANS, A., JUPPNER, H., KIM, C. A., KEPPLER-NOREUIL, K., KOHLSCHUETTER, A., LACOMBE, D., LAMBERT, M., LEMYRE, E., LETTEBOER, T., PELTONEN, L., RAMESAR, R. S., ROMANENGO, M., SOMER, H., STEICHEN-GERSDORF, E., STEINMANN, B., SULLIVAN, B., SUPERTI-FURGA, A., SWOBODA, W., VAN DEN BOOGAARD, M. J., VAN HUL, W., VIKKULA, M., VOTRUBA, M., ZABEL, B., GARCIA, T., BARON, R., OLSEN, B. R. & WARMAN, M. L. (2001) LDL receptor-related protein 5 (LRP5) affects bone accrual and eye development. *Cell,* 107**,** 513-23.

GONZALEZ-SUAREZ, E. (2011) RANKL inhibition: a promising novel strategy for breast cancer treatment. *Clin Transl Oncol,* 13**,** 222-8.

GORSKI, S. M., CHITTARANJAN, S., PLEASANCE, E. D., FREEMAN, J. D., ANDERSON, C. L., VARHOL, R. J., COUGHLIN, S. M., ZUYDERDUYN, S. D., JONES, S. J. & MARRA, M. A. (2003) A SAGE approach to discovery of genes involved in autophagic cell death. *Curr Biol,* 13**,** 358-63.

GREEN, D. R. (2000) Apoptotic pathways: paper wraps stone blunts scissors. *Cell,* 102**,** 1-4.

GREEN, J. R. & GUENTHER, A. (2011) The backbone of progress--preclinical studies and innovations with zoledronic acid. *Crit Rev Oncol Hematol,* 77 Suppl 1**,** S3-S12.

GREENBLATT, D. (2005) Treatment of postmenopausal osteoporosis. *Pharmacotherapy,* 25**,** 574-84.

GRONTHOS, S., ZANNETTINO, A. C., GRAVES, S. E., OHTA, S., HAY, S. J. & SIMMONS, P. J. (1999) Differential cell surface expression of the STRO-1 and alkaline phosphatase antigens on discrete developmental stages in primary cultures of human bone cells. *J Bone Miner Res,* 14**,** 47-56.

GRUNSTEIN, M. (1997) Histone acetylation in chromatin structure and transcription. *Nature,* 389**,** 349-52.

GU, W. & ROEDER, R. G. (1997) Activation of p53 sequence-specific DNA binding by acetylation of the p53 C-terminal domain. *Cell,* 90**,** 595-606.

GUI, C. Y., NGO, L., XU, W. S., RICHON, V. M. & MARKS, P. A. (2004) Histone deacetylase (HDAC) inhibitor activation of p21WAF1 involves changes in promoter-associated proteins, including HDAC1. *Proc Natl Acad Sci U S A,* 101**,** 1241-6.

GUISE, T. A., BRUFSKY, A. & COLEMAN, R. E. (2010) Understanding and optimizing bone health in breast cancer. *Curr Med Res Opin,* 26 Suppl 3**,** 3-20.

GUISE, T. A., MOHAMMAD, K. S., CLINES, G., STEBBINS, E. G., WONG, D. H., HIGGINS, L. S., VESSELLA, R., COREY, E., PADALECKI, S., SUVA, L. & CHIRGWIN, J. M. (2006) Basic mechanisms responsible for osteolytic and osteoblastic bone metastases. *Clin Cancer Res,* 12**,** 6213s-6216s.

GUPTA, M., ANSELL, S. M., NOVAK, A. J., KUMAR, S., KAUFMANN, S. H. & WITZIG, T. E. (2009) Inhibition of histone deacetylase overcomes rapamycin-mediated resistance in diffuse large B cell lymphoma by inhibiting Akt signaling through mTORC2. *Blood,* 114**,** 2926-2935.

HAABER, J., ABILDGAARD, N., KNUDSEN, L. M., DAHL, I. M., LODAHL, M., THOMASSEN, M., KERNDRUP, G. B. & RASMUSSEN, T. (2008) Myeloma cell expression of 10 candidate genes for osteolytic bone disease. Only overexpression of DKK1 correlates with clinical bone involvement at diagnosis. *Br J Haematol,* 140**,** 25-35.

HABERLAND, M., MOKALLED, M. H., MONTGOMERY, R. L. & OLSON, E. N. (2009) Epigenetic control of skull morphogenesis by histone deacetylase 8. *Genes Dev,* 23**,** 1625-30.

HAEFNER, M., BLUETHNER, T., NIEDERHAGEN, M., MOEBIUS, C., WITTEKIND, C., MOSSNER, J., CACA, K. & WIEDMANN, M. (2008) Experimental treatment of pancreatic cancer with two novel histone deacetylase inhibitors. *World J Gastroenterol,* 14**,** 3681-92.

HALKIDOU, K., GAUGHAN, L., COOK, S., LEUNG, H. Y., NEAL, D. E. & ROBSON, C. N. (2004) Upregulation and nuclear recruitment of HDAC1 in hormone refractory prostate cancer. *Prostate,* 59**,** 177-89.

HEYMANN, D., ORY, B., BLANCHARD, F., HEYMANN, M. F., COIPEAU, P., CHARRIER, C., COUILLAUD, S., THIERY, J. P., GOUIN, F. & REDINI, F. (2005) Enhanced tumor regression and tissue repair when zoledronic acid is combined with ifosfamide in rat osteosarcoma. *Bone,* 37**,** 74-86.

HIDESHIMA, T., BRADNER, J. E., WONG, J., CHAUHAN, D., RICHARDSON, P., SCHREIBER, S. L. & ANDERSON, K. C. (2005) Small-molecule inhibition of proteasome and aggresome function induces synergistic antitumor activity in multiple myeloma. *Proc Natl Acad Sci U S A,* 102**,** 8567-72.

HILLNER, B. E., INGLE, J. N., CHLEBOWSKI, R. T., GRALOW, J., YEE, G. C., JANJAN, N. A., CAULEY, J. A., BLUMENSTEIN, B. A., ALBAIN, K. S., LIPTON, A. & BROWN, S. (2003) American Society of Clinical Oncology 2003 update on the role of bisphosphonates and bone health issues in women with breast cancer. *J Clin Oncol,* 21**,** 4042-57.

HORNE, W. C., SANJAY, A., BRUZZANITI, A. & BARON, R. (2005) The role(s) of Src kinase and Cbl proteins in the regulation of osteoclast differentiation and function. *Immunol Rev,* 208**,** 106-25.

HOSKINS, J. M., CAREY, L. A. & MCLEOD, H. L. (2009) CYP2D6 and tamoxifen: DNA matters in breast cancer. *Nat Rev Cancer,* 9**,** 576-86.

HOSOI, T. (2010) Genetic aspects of osteoporosis. *J Bone Miner Metab,* 28**,** 601-607.

HRZENJAK, A., KREMSER, M. L., STROHMEIER, B., MOINFAR, F., ZATLOUKAL, K. & DENK, H. (2008) SAHA induces caspase-independent, autophagic cell death of endometrial stromal sarcoma cells by influencing the mTOR pathway. *J Pathol,* 216**,** 495-504.

HUANG, B. H., LABAN, M., LEUNG, C. H., LEE, L., LEE, C. K., SALTO-TELLEZ, M., RAJU, G. C. & HOOI, S. C. (2005) Inhibition of histone deacetylase 2 increases apoptosis and p21Cip1/WAF1 expression, independent of histone deacetylase 1. *Cell Death Differ,* 12**,** 395-404.

HUBER, M. A. (2007) Osteogenesis imperfecta. *Oral Surg Oral Med Oral Pathol Oral Radiol Endod,* 103**,** 314-20.

HUJA, S. S., FERNANDEZ, S. A., PHILLIPS, C. & LI, Y. (2009) Zoledronic acid decreases bone formation without causing osteocyte death in mice. *Arch Oral Biol,* 54**,** 851-6.

HULTBORN, R., GUNDERSEN, S., RYDEN, S., HOLMBERG, E., CARSTENSEN, J., WALLGREN, U. B., KILLANY, S., ANDREASSEN, L., CARLSSON, G., FAHL, N., HATSCHEK, T., SOMMER, H. H., HESSMAN, Y., HORNMARK-STENSTAM, B., JOHNSBORG, S., KLEPP, R., LAINO, R., NIKLASSON, L. G., RUDENSTAM, C. M., SUNDBECK, A., SODERBERG, M. & TEJLER, G. (1999) Efficacy of pamidronate in breast cancer with bone metastases: a randomized, double-blind placebo-controlled multicenter study. *Anticancer Res,* 19**,** 3383-92.

IMAI, T., ADACHI, S., NISHIJO, K., OHGUSHI, M., OKADA, M., YASUMI, T., WATANABE, K., NISHIKOMORI, R., NAKAYAMA, T., YONEHARA, S., TOGUCHIDA, J. & NAKAHATA, T. (2003) FR901228 induces tumor regression associated with induction of Fas ligand and activation of Fas signaling in human osteosarcoma cells. *Oncogene,* 22**,** 9231-42.

INOUE, S., RILEY, J., GANT, T. W., DYER, M. J. & COHEN, G. M. (2007) Apoptosis induced by histone deacetylase inhibitors in leukemic cells is mediated by Bim and Noxa. *Leukemia,* 21**,** 1773-82.

INSINGA, A., MONESTIROLI, S., RONZONI, S., GELMETTI, V., MARCHESI, F., VIALE, A., ALTUCCI, L., NERVI, C., MINUCCI, S. & PELICCI, P. G. (2005)

Inhibitors of histone deacetylases induce tumor-selective apoptosis through activation of the death receptor pathway. *Nat Med,* 11**,** 71-6.

IWAMI, K. & MORIYAMA, T. (1993) Effects of short chain fatty acid, sodium butyrate, on osteoblastic cells and osteoclastic cells. *Int J Biochem,* 25**,** 1631-5.

IWATA, H. (2011) Future treatment strategies for metastatic breast cancer: curable or incurable? *Breast Cancer.*

JAAKKOLA, P. M. & PURSIHEIMO, J. P. (2009) p62 degradation by autophagy: another way for cancer cells to survive under hypoxia. *Autophagy,* 5**,** 410-2.

JAKOB, F., SEEFRIED, L. & EBERT, R. (2008) Pathophysiology of bone metabolism. *Internist (Berl),* 24**,** 24.

JENSEN, E. D., GOPALAKRISHNAN, R. & WESTENDORF, J. J. (2009) Bone morphogenic protein 2 activates protein kinase D to regulate histone deacetylase 7 localization and repression of Runx2. *J Biol Chem,* 284**,** 2225-34.

JENUWEIN, T. & ALLIS, C. D. (2001) Translating the histone code. *Science,* 293**,** 1074-80.

JIA, L., DOURMASHKIN, R. R., ALLEN, P. D., GRAY, A. B., NEWLAND, A. C. & KELSEY, S. M. (1997) Inhibition of autophagy abrogates tumour necrosis factor alpha induced apoptosis in human T-lymphoblastic leukaemic cells. *Br J Haematol,* 98**,** 673-85.

JIANG, Y., WANG, Y., SU, Z., YANG, L., GUO, W., LIU, W. & ZUO, J. (2010) Synergistic induction of apoptosis in HeLa cells by the proteasome inhibitor bortezomib and histone deacetylase inhibitor SAHA. *Mol Med Report,* 3**,** 613-9.

JIMI, E., AOKI, K., SAITO, H., D'ACQUISTO, F., MAY, M. J., NAKAMURA, I., SUDO, T., KOJIMA, T., OKAMOTO, F., FUKUSHIMA, H., OKABE, K., OHYA, K. & GHOSH, S. (2004) Selective inhibition of NF-kappa B blocks osteoclastogenesis and prevents inflammatory bone destruction in vivo. *Nat Med,* 10**,** 617-24.

JOHNSTONE, R. W. (2002) Histone-deacetylase inhibitors: novel drugs for the treatment of cancer. *Nat Rev Drug Discov,* 1**,** 287-99.

JOHNSTONE, R. W., FREW, A. J. & SMYTH, M. J. (2008) The TRAIL apoptotic pathway in cancer onset, progression and therapy. *Nat Rev Cancer,* 8**,** 782-98.

JOHNSTONE, R. W. & LICHT, J. D. (2003) Histone deacetylase inhibitors in cancer therapy: is transcription the primary target? *Cancer Cell,* 4**,** 13-8.

JOHNSTONE, R. W., RUEFLI, A. A. & LOWE, S. W. (2002) Apoptosis: a link between cancer genetics and chemotherapy. *Cell,* 108**,** 153-64.

JONES, S. F., BENDELL, J. C., INFANTE, J. R., SPIGEL, D. R., THOMPSON, D. S., YARDLEY, D. A., GRECO, F. A., MURPHY, P. B. & BURRIS, H. A., 3RD (2011) A phase I study of panobinostat in combination with gemcitabine in the treatment of solid tumors. *Clin Adv Hematol Oncol,* 9**,** 225-30.

JOSEPH, J., WAJAPEYEE, N. & SOMASUNDARAM, K. (2005) Role of p53 status in chemosensitivity determination of cancer cells against histone deacetylase inhibitor sodium butyrate. *Int J Cancer,* 115**,** 11-8.

JUNG, H. M., SONG, G. A., LEE, Y. K., BAEK, J. H., RYOO, H. M., KIM, G. S., CHOUNG, P. H. & WOO, K. M. (2010) Modulation of the resorption and osteoconductivity of alpha-calcium sulfate by histone deacetylase inhibitors. *Biomaterials,* 31**,** 29-37.

KANIS, J. A., MCCLOSKEY, E. V., TAUBE, T. & O'ROURKE, N. (1991) Rationale for the use of bisphosphonates in bone metastases. *Bone,* 12 Suppl 1**,** S13-8.

KATO, M., PATEL, M. S., LEVASSEUR, R., LOBOV, I., CHANG, B. H., GLASS, D. A., 2ND, HARTMANN, C., LI, L., HWANG, T. H., BRAYTON, C. F., LANG, R. A., KARSENTY, G. & CHAN, L. (2002) Cbfa1-independent decrease in osteoblast proliferation, osteopenia, and persistent embryonic eye vascularization in mice deficient in Lrp5, a Wnt coreceptor. *J Cell Biol,* 157**,** 303-14.

KIRIYAMA, T., GILLESPIE, M. T., GLATZ, J. A., FUKUMOTO, S., MOSELEY, J. M. & MARTIN, T. J. (1993) Transforming growth factor beta stimulation of parathyroid hormone-related protein (PTHrP): a paracrine regulator? *Mol Cell Endocrinol,* 92**,** 55-62.

KLIONSKY, D. J. & EMR, S. D. (2000) Autophagy as a regulated pathway of cellular degradation. *Science,* 290**,** 1717-21.

KLOPP, A. H., LACERDA, L., GUPTA, A., DEBEB, B. G., SOLLEY, T., LI, L., SPAETH, E., XU, W., ZHANG, X., LEWIS, M. T., REUBEN, J. M., KRISHNAMURTHY, S., FERRARI, M., GASPAR, R., BUCHHOLZ, T. A., CRISTOFANILLI, M., MARINI, F., ANDREEFF, M. & WOODWARD, W. A. (2010) Mesenchymal stem cells promote mammosphere formation and decrease E-cadherin in normal and malignant breast cells. *PLoS One,* 5**,** e12180.

KOMATSU, Y., TOMIZAKI, K. Y., TSUKAMOTO, M., KATO, T., NISHINO, N., SATO, S., YAMORI, T., TSURUO, T., FURUMAI, R., YOSHIDA, M., HORINOUCHI, S. & HAYASHI, H. (2001) Cyclic hydroxamic-acid-containing peptide 31, a potent synthetic histone deacetylase inhibitor with antitumor activity. *Cancer Res,* 61**,** 4459-66.

KORNBERG, R. D. & LORCH, Y. (1999) Twenty-five years of the nucleosome, fundamental particle of the eukaryote chromosome. *Cell,* 98**,** 285-94.

KOSHIBA, T., HOSOTANI, R., MIYAMOTO, Y., IDA, J., TSUJI, S., NAKAJIMA, S., KAWAGUCHI, M., KOBAYASHI, H., DOI, R., HORI, T., FUJII, N. & IMAMURA, M. (2000) Expression of stromal cell-derived factor 1 and CXCR4 ligand receptor system in pancreatic cancer: a possible role for tumor progression. *Clin Cancer Res,* 6**,** 3530-5.

KOURAKLIS, G. A. & THEOCHARIS, S. (2006) Histone Deacetylase Inhibitors: A novel target of anticancer therapy (Review). *Oncology Reports.* Athens, University of Athens.

KOUTSILIERIS, M., RABBANI, S. A., BENNETT, H. P. & GOLTZMAN, D. (1987) Characteristics of prostate-derived growth factors for cells of the osteoblast phenotype. *J Clin Invest,* 80**,** 941-6.

KRUSCHE, C. A., WULFING, P., KERSTING, C., VLOET, A., BOCKER, W., KIESEL, L., BEIER, H. M. & ALFER, J. (2005) Histone deacetylase-1 and -3 protein expression in human breast cancer: a tissue microarray analysis. *Breast Cancer Res Treat,* 90**,** 15-23.

KUNG, A. L., REBEL, V. I., BRONSON, R. T., CH'NG, L. E., SIEFF, C. A., LIVINGSTON, D. M. & YAO, T. P. (2000) Gene dose-dependent control of hematopoiesis and hematologic tumor suppression by CBP. *Genes Dev,* 14**,** 272-7.

KUTKO, M. C., GLICK, R. D., BUTLER, L. M., COFFEY, D. C., RIFKIND, R. A., MARKS, P. A., RICHON, V. M. & LAQUAGLIA, M. P. (2003) Histone deacetylase inhibitors induce growth suppression and cell death in human rhabdomyosarcoma in vitro. *Clin Cancer Res,* 9**,** 5749-55.

LABRINIDIS, A., DIAMOND, P., MARTIN, S., HAY, S., LIAPIS, V., ZINONOS, I., SIMS, N. A., ATKINS, G. J., VINCENT, C., PONOMAREV, V., FINDLAY, D. M., ZANNETTINO, A. C. & EVDOKIOU, A. (2009a) Apo2L/TRAIL inhibits tumor growth and bone destruction in a murine model of multiple myeloma. *Clin Cancer Res,* 15**,** 1998-2009.

LABRINIDIS, A., HAY, S., LIAPIS, V., FINDLAY, D. M. & EVDOKIOU, A. (2010) Zoledronic acid protects against osteosarcoma-induced bone destruction but lacks efficacy against pulmonary metastases in a syngeneic rat model. *Int J Cancer,* 127**,** 345-354.

LABRINIDIS, A., HAY, S., LIAPIS, V., PONOMAREV, V., FINDLAY, D. M. & EVDOKIOU, A. (2009b) Zoledronic acid inhibits both the osteolytic and osteoblastic components of osteosarcoma lesions in a mouse model. *Clin Cancer Res,* 15**,** 3451-61.

LEE, J. K., RYU, J. K., YANG, K. Y., WOO, S. M., PARK, J. K., YOON, W. J., LEE, S. H., JEONG, K. S., KIM, Y. T. & YOON, Y. B. (2011) Effects and mechanisms of the combination of suberoylanilide hydroxamic Acid and bortezomib on the anticancer property of gemcitabine in pancreatic cancer. *Pancreas,* 40**,** 966-73.

LEHENKARI, P. P., KELLINSALMI, M., NAPANKANGAS, J. P., YLITALO, K. V., MONKKONEN, J., ROGERS, M. J., AZHAYEV, A., VAANANEN, H. K. & HASSINEN, I. E. (2002) Further insight into mechanism of action of clodronate: inhibition of mitochondrial ADP/ATP translocase by a nonhydrolyzable, adenine-containing metabolite. *Mol Pharmacol,* 61**,** 1255-62.

LEONI, F., ZALIANI, A., BERTOLINI, G., PORRO, G., PAGANI, P., POZZI, P., DONA, G., FOSSATI, G., SOZZANI, S., AZAM, T., BUFLER, P., FANTUZZI, G., GONCHAROV, I., KIM, S. H., POMERANTZ, B. J., REZNIKOV, L. L., SIEGMUND, B., DINARELLO, C. A. & MASCAGNI, P. (2002) The antitumor histone deacetylase inhibitor suberoylanilide hydroxamic acid exhibits antiinflammatory properties via suppression of cytokines. *Proc Natl Acad Sci U S A,* 99**,** 2995-3000.

LEVY, L., WEI, Y., LABALETTE, C., WU, Y., RENARD, C. A., BUENDIA, M. A. & NEUVEUT, C. (2004) Acetylation of beta-catenin by p300 regulates beta-catenin-Tcf4 interaction. *Mol Cell Biol,* 24**,** 3404-14.

LI, X., OMINSKY, M. S., NIU, Q. T., SUN, N., DAUGHERTY, B., D'AGOSTIN, D., KURAHARA, C., GAO, Y., CAO, J., GONG, J., ASUNCION, F., BARRERO, M., WARMINGTON, K., DWYER, D., STOLINA, M., MORONY, S., SAROSI, I., KOSTENUIK, P. J., LACEY, D. L., SIMONET, W. S., KE, H. Z. & PASZTY, C. (2008a) Targeted deletion of the sclerostin gene in mice results in increased bone formation and bone strength. *J Bone Miner Res,* 23**,** 860-9.

LI, X., WARMINGTON, K. S., NIU, Q. T., ASUNCION, F. J., BARRERO, M., GRISANTI, M., DWYER, D., STOUCH, B., THWAY, T. M., STOLINA, M., OMINSKY, M. S., KOSTENUIK, P. J., SIMONET, W. S., PASZTY, C. & KE, H. Z. (2010) Inhibition of sclerostin by monoclonal antibody increases bone formation, bone mass, and bone strength in aged male rats. *J Bone Miner Res,* 25**,** 2647-56.

LI, Z. G., MATHEW, P., YANG, J., STARBUCK, M. W., ZURITA, A. J., LIU, J., SIKES, C., MULTANI, A. S., EFSTATHIOU, E., LOPEZ, A., WANG, J., FANNING, T. V., PRIETO, V. G., KUNDRA, V., VAZQUEZ, E. S., TRONCOSO, P., RAYMOND, A. K., LOGOTHETIS, C. J., LIN, S. H., MAITY, S. & NAVONE, N. M. (2008b) Androgen receptor-negative human prostate cancer cells induce osteogenesis in mice through FGF9-mediated mechanisms. *J Clin Invest,* 118**,** 2697-710.

LIANG, X. H., JACKSON, S., SEAMAN, M., BROWN, K., KEMPKES, B., HIBSHOOSH, H. & LEVINE, B. (1999) Induction of autophagy and inhibition of tumorigenesis by beclin 1. *Nature,* 402**,** 672-6.

LIAO, J. & MCCAULEY, L. K. (2006) Skeletal metastasis: Established and emerging roles of parathyroid hormone related protein (PTHrP). *Cancer Metastasis Rev,* 25**,** 559-71.

LIAPIS, V., HAY, S., VINCENT, C., ATKINS, G. J., BUTLER, L. M., FINDLAY, D. M. & EVDOKIOU, A. (2006) The histone deacetylase inhibitor, Suberoylanilide hydroxamic acid (SAHA) blocks osteoclastogenesis. *IOF & ANZBMS combined meeting.* Port Douglas, Queensland, Australia.

LIBURA, J., DRUKALA, J., MAJKA, M., TOMESCU, O., NAVENOT, J. M., KUCIA, M., MARQUEZ, L., PEIPER, S. C., BARR, F. G., JANOWSKA-WIECZOREK, A. & RATAJCZAK, M. Z. (2002) CXCR4-SDF-1 signaling is active in rhabdomyosarcoma cells and regulates locomotion, chemotaxis, and adhesion. *Blood,* 100**,** 2597-606.

LIN, C., JIANG, X., DAI, Z., GUO, X., WENG, T., WANG, J., LI, Y., FENG, G., GAO, X. & HE, L. (2009) Sclerostin mediates bone response to mechanical unloading through antagonizing Wnt/beta-catenin signaling. *J Bone Miner Res,* 24**,** 1651-61.

LIN, R. J., STERNSDORF, T., TINI, M. & EVANS, R. M. (2001) Transcriptional regulation in acute promyelocytic leukemia. *Oncogene,* 20**,** 7204-15.

LIN, W., ZHANG, Z., CHEN, C. H., BEHRINGER, R. R. & DENT, S. Y. (2008) Proper Gcn5 histone acetyltransferase expression is required for normal anteroposterior patterning of the mouse skeleton. *Dev Growth Differ,* 50**,** 321-30.

LINARES, A., DALENC, F., BALAGUER, P., BOULLE, N. & CAVAILLES, V. (2011) Manipulating protein acetylation in breast cancer: a promising approach in combination with hormonal therapies? *J Biomed Biotechnol,* 2011**,** 856985.

LINDEMANN, R. K., NEWBOLD, A., WHITECROSS, K. F., CLUSE, L. A., FREW, A. J., ELLIS, L., WILLIAMS, S., WIEGMANS, A. P., DEAR, A. E., SCOTT, C. L., PELLEGRINI, M., WEI, A., RICHON, V. M., MARKS, P. A., LOWE, S. W., SMYTH, M. J. & JOHNSTONE, R. W. (2007) Analysis of the apoptotic and therapeutic activities of histone deacetylase inhibitors by using a mouse model of B cell lymphoma. *Proc Natl Acad Sci U S A,* 104**,** 8071-6.

LIPTON, A., THERIAULT, R. L., HORTOBAGYI, G. N., SIMEONE, J., KNIGHT, R. D., MELLARS, K., REITSMA, D. J., HEFFERNAN, M. & SEAMAN, J. J. (2000) Pamidronate prevents skeletal complications and is effective palliative treatment in women with breast carcinoma and osteolytic bone metastases: long term follow-up of two randomized, placebo-controlled trials. *Cancer,* 88**,** 1082-90.

LIU, T., KULJACA, S., TEE, A. & MARSHALL, G. M. (2006) Histone deacetylase inhibitors: multifunctional anticancer agents. *Cancer Treat Rev,* 32**,** 157-65. Epub 2006 Mar 3.

LLOYD, S. A., TRAVIS, N. D., LU, T. & BATEMAN, T. A. (2008) Development of a low-dose anti-resorptive drug regimen reveals synergistic suppression of bone formation when coupled with disuse. *J Appl Physiol,* 104**,** 729-38.

LOGOTHETIS, C. J. & LIN, S. H. (2005) Osteoblasts in prostate cancer metastasis to bone. *Nat Rev Cancer,* 5**,** 21-8.

LUGER, K., MADER, A. W., RICHMOND, R. K., SARGENT, D. F. & RICHMOND, T. J. (1997) Crystal structure of the nucleosome core particle at 2.8 A resolution. *Nature,* 389**,** 251-60.

LUND, A. H. & VAN LOHUIZEN, M. (2004) Epigenetics and cancer. *Genes Dev,* 18**,** 2315-35.

MACRAE, T. H. (1997) Tubulin post-translational modifications--enzymes and their mechanisms of action. *Eur J Biochem,* 244**,** 265-78.

MAISO, P., CARVAJAL-VERGARA, X., OCIO, E. M., LOPEZ-PEREZ, R., MATEO, G., GUTIERREZ, N., ATADJA, P., PANDIELLA, A. & SAN MIGUEL, J. F. (2006) The histone deacetylase inhibitor LBH589 is a potent antimyeloma agent that overcomes drug resistance. *Cancer Res,* 66**,** 5781-9.

MANN, B. S., JOHNSON, J. R., COHEN, M. H., JUSTICE, R. & PAZDUR, R. (2007) FDA approval summary: vorinostat for treatment of advanced primary cutaneous T-cell lymphoma. *Oncologist,* 12**,** 1247-52.

MANOLAGAS, S. C. & JILKA, R. L. (1995) Bone marrow, cytokines, and bone remodeling. Emerging insights into the pathophysiology of osteoporosis. *N Engl J Med,* 332**,** 305-11.

MARGUERON, R., DUONG, V., CASTET, A. & CAVAILLES, V. (2004) Histone deacetylase inhibition and estrogen signalling in human breast cancer cells. *Biochem Pharmacol,* 68**,** 1239-46.

MARIE, P. J. (2006) Strontium ranelate: a dual mode of action rebalancing bone turnover in favour of bone formation. *Curr Opin Rheumatol,* 18 Suppl 1**,** S11-5.

MARIE, P. J., FELSENBERG, D. & BRANDI, M. L. (2011) How strontium ranelate, via opposite effects on bone resorption and formation, prevents osteoporosis. *Osteoporos Int,* 22**,** 1659-67.

MARKS, P., RIFKIND, R. A., RICHON, V. M., BRESLOW, R., MILLER, T. & KELLY, W. K. (2001) Histone deacetylases and cancer: causes and therapies. *Nat Rev Cancer,* 1**,** 194-202.

MARROCCO, D. L., TILLEY, W. D., BIANCO-MIOTTO, T., EVDOKIOU, A., SCHER, H. I., RIFKIND, R. A., MARKS, P. A., RICHON, V. M. & BUTLER, L. M. (2007) Suberoylanilide hydroxamic acid (vorinostat) represses androgen receptor expression and acts synergistically with an androgen receptor antagonist to inhibit prostate cancer cell proliferation. *Mol Cancer Ther,* 6**,** 51-60.

MARTIN, T. J. (2002) Manipulating the environment of cancer cells in bone: a novel therapeutic approach. *J Clin Invest,* 110**,** 1399-401.

MASSARWEH, S. & SCHIFF, R. (2007) Unraveling the mechanisms of endocrine resistance in breast cancer: new therapeutic opportunities. *Clin Cancer Res,* 13**,** 1950-4.

MATSUMOTO, M., SUDO, T., MARUYAMA, M., OSADA, H. & TSUJIMOTO, M. (2000) Activation of p38 mitogen-activated protein kinase is crucial in osteoclastogenesis induced by tumor necrosis factor. *FEBS Lett,* 486**,** 23-8.

MATSUMOTO, S., KIMURA, S., SEGAWA, H., KURODA, J., YUASA, T., SATO, K., NOGAWA, M., TANAKA, F., MAEKAWA, T. & WADA, H. (2005) Efficacy of the third-generation bisphosphonate, zoledronic acid alone and combined with anti-cancer agents against small cell lung cancer cell lines. *Lung Cancer,* 47**,** 31-9.

MELLANBY, E. (1976) Nutrition Classics. The Lancet 1:407-12, 1919. An experimental investigation of rickets. Edward Mellanby. *Nutr Rev,* 34**,** 338-40.

MERCADANTE, S. (1997) Malignant bone pain: pathophysiology and treatment. *Pain,* 69**,** 1-18.

MORITA, S., OIZUMI, S., MINAMI, H., KITAGAWA, K., KOMATSU, Y., FUJIWARA, Y., INADA, M., YUKI, S., KIYOTA, N., MITSUMA, A., SAWAKI, M., TANII, H., KIMURA, J. & ANDO, Y. (2011) Phase I dose-escalating study of panobinostat (LBH589) Administered intravenously to Japanese patients with advanced solid tumors. *Invest New Drugs.*

MORTIMER, J. E. & PAL, S. K. (2010) Safety considerations for use of bone-targeted agents in patients with cancer. *Semin Oncol,* 37 Suppl 1**,** S66-72.

MOSEKILDE, L., TORRING, O. & REJNMARK, L. (2011) Emerging anabolic treatments in osteoporosis. *Curr Drug Saf,* 6**,** 62-74.

MUNDY, G. R. (1987) Bone resorption and turnover in health and disease. *Bone,* 8 Suppl 1**,** S9-16.

MUNDY, G. R. (1991) Mechanisms of osteolytic bone destruction. *Bone,* 12 Suppl 1**,** S1-6.

MUSGROVE, E. A. & SUTHERLAND, R. L. (2009) Biological determinants of endocrine resistance in breast cancer. *Nat Rev Cancer,* 9**,** 631-43.

NAKAMURA, T., KUKITA, T., SHOBUIKE, T., NAGATA, K., WU, Z., OGAWA, K., HOTOKEBUCHI, T., KOHASHI, O. & KUKITA, A. (2005) Inhibition of histone deacetylase suppresses osteoclastogenesis and bone destruction by inducing IFN-beta production. *J Immunol,* 175**,** 5809-16.

NAKATA, S., YOSHIDA, T., HORINAKA, M., SHIRAISHI, T., WAKADA, M. & SAKAI, T. (2004) Histone deacetylase inhibitors upregulate death receptor 5/TRAIL-R2 and sensitize apoptosis induced by TRAIL/APO2-L in human malignant tumor cells. *Oncogene,* 23**,** 6261-71.

NANES, M. S. & KALLEN, C. B. (2009) Clinical assessment of fracture risk and novel therapeutic strategies to combat osteoporosis. *Fertil Steril,* 92**,** 403-12.

NEBBIOSO, A., CLARKE, N., VOLTZ, E., GERMAIN, E., AMBROSINO, C., BONTEMPO, P., ALVAREZ, R., SCHIAVONE, E. M., FERRARA, F., BRESCIANI, F., WEISZ, A., DE LERA, A. R., GRONEMEYER, H. & ALTUCCI, L. (2005) Tumor-selective action of HDAC inhibitors involves TRAIL induction in acute myeloid leukemia cells. *Nat Med,* 11**,** 77-84.

NEWBOLD, A., LINDEMANN, R. K., CLUSE, L. A., WHITECROSS, K. F., DEAR, A. E. & JOHNSTONE, R. W. (2008) Characterisation of the novel apoptotic and therapeutic activities of the histone deacetylase inhibitor romidepsin. *Mol Cancer Ther,* 7**,** 1066-79.

NILSSON, S. (2009) The osteoblastic niche following TBI. *Blood,* 114**,** 2210-1.

OCKER, M. & SCHNEIDER-STOCK, R. (2007) Histone deacetylase inhibitors: signalling towards p21cip1/waf1. *Int J Biochem Cell Biol,* 39**,** 1367-74.

OEHME, I., DEUBZER, H. E., WEGENER, D., PICKERT, D., LINKE, J. P., HERO, B., KOPP-SCHNEIDER, A., WESTERMANN, F., ULRICH, S. M., VON DEIMLING, A., FISCHER, M. & WITT, O. (2009) Histone deacetylase 8 in neuroblastoma tumorigenesis. *Clin Cancer Res,* 15**,** 91-9.

OH, M., CHOI, I. K. & KWON, H. J. (2008) Inhibition of histone deacetylase1 induces autophagy. *Biochem Biophys Res Commun,* 369**,** 1179-83.

OHMORI, H., MAKITA, Y., FUNAMIZU, M., HIROOKA, K., HOSOI, T., ORIMO, H., SUZUKI, T., IKARI, K., NAKAJIMA, T., INOUE, I. & HATA, A. (2002) Linkage and association analyses of the osteoprotegerin gene locus with human osteoporosis. *J Hum Genet,* 47**,** 400-6.

OMINSKY, M. S., VLASSEROS, F., JOLETTE, J., SMITH, S. Y., STOUCH, B., DOELLGAST, G., GONG, J., GAO, Y., CAO, J., GRAHAM, K., TIPTON, B., CAI, J., DESHPANDE, R., ZHOU, L., HALE, M. D., LIGHTWOOD, D. J., HENRY, A. J., POPPLEWELL, A. G., MOORE, A. R., ROBINSON, M. K., LACEY, D. L., SIMONET, W. S. & PASZTY, C. (2010) Two doses of sclerostin antibody in cynomolgus monkeys increases bone formation, bone mineral density, and bone strength. *J Bone Miner Res,* 25**,** 948-59.

ONER, N., KAYA, M., KARASALIHOGLU, S., KARACA, H., CELTIK, C. & TUTUNCULER, F. (2004) Bone mineral metabolism changes in epileptic children receiving valproic acid. *J Paediatr Child Health,* 40**,** 470-3.

OTTEWELL, P. D., WOODWARD, J. K., LEFLEY, D. V., EVANS, C. A., COLEMAN, R. E. & HOLEN, I. (2009) Anticancer mechanisms of doxorubicin and zoledronic acid in breast cancer tumor growth in bone. *Mol Cancer Ther,* 8**,** 2821-32.

PADHI, D., JANG, G., STOUCH, B., FANG, L. & POSVAR, E. (2011) Single-dose, placebo-controlled, randomized study of AMG 785, a sclerostin monoclonal antibody. *J Bone Miner Res,* 26**,** 19-26.

PANDOLFI, P. P. (2001) Histone deacetylases and transcriptional therapy with their inhibitors. *Cancer Chemother Pharmacol,* 48 Suppl 1**,** S17-9.

PANI, G. & GALEOTTI, T. (2010) ROLE OF MnSOD AND P66SHC IN MITOCHONDRIAL RESPONSE TO P53. *Antioxid Redox Signal,* 15**,** 1715-1727.

PARFITT, A. M., DREZNER, M. K., GLORIEUX, F. H., KANIS, J. A., MALLUCHE, H., MEUNIER, P. J., OTT, S. M. & RECKER, R. R. (1987) Bone histomorphometry: standardization of nomenclature, symbols, and units. Report of the ASBMR Histomorphometry Nomenclature Committee. *J Bone Miner Res,* 2**,** 595-610.

PARK, J. H., KIM, S. H., CHOI, M. C., LEE, J., OH, D. Y., IM, S. A., BANG, Y. J. & KIM, T. Y. (2008) Class II histone deacetylases play pivotal roles in heat shock protein 90-mediated proteasomal degradation of vascular endothelial growth factor receptors. *Biochem Biophys Res Commun,* 368**,** 318-22.

PARK, Y. B., MOHAN, K., AL-SANOUSI, A., ALMAGHRABI, B., GENCO, R. J., SWIHART, M. T. & DZIAK, R. (2011) Synthesis and characterization of nanocrystalline calcium sulfate for use in osseous regeneration. *Biomed Mater,* 6**,** 1-11.

PARSONS, P. G., HANSEN, C., FAIRLIE, D. P., WEST, M. L., DANOY, P. A., STURM, R. A., DUNN, I. S., PEDLEY, J. & ABLETT, E. M. (1997) Tumor

selectivity and transcriptional activation by azelaic bishydroxamic acid in human melanocytic cells. *Biochem Pharmacol,* 53**,** 1719-24.

PASQUALUCCI, L., BERESCHENKO, O., NIU, H., KLEIN, U., BASSO, K., GUGLIELMINO, R., CATTORETTI, G. & DALLA-FAVERA, R. (2003) Molecular pathogenesis of non-Hodgkin's lymphoma: the role of Bcl-6. *Leuk Lymphoma,* 44 Suppl 3**,** S5-12.

PATAKI, A., MULLER, K., GREEN, J. R., MA, Y. F., LI, Q. N. & JEE, W. S. (1997) Effects of short-term treatment with the bisphosphonates zoledronate and pamidronate on rat bone: a comparative histomorphometric study on the cancellous bone formed before, during, and after treatment. *Anat Rec,* 249**,** 458-68.

PAZIANAS, M., COMPSTON, J. & HUANG, C. L. (2010) Atrial fibrillation and bisphosphonate therapy. *J Bone Miner Res,* 25**,** 2-10.

PENG, H., SOHARA, Y., MOATS, R. A., NELSON, M. D., JR., GROSHEN, S. G., YE, W., REYNOLDS, C. P. & DECLERCK, Y. A. (2007) The activity of zoledronic Acid on neuroblastoma bone metastasis involves inhibition of osteoclasts and tumor cell survival and proliferation. *Cancer Res,* 67**,** 9346-55.

PERISSINOTTO, E., CAVALLONI, G., LEONE, F., FONSATO, V., MITOLA, S., GRIGNANI, G., SURRENTI, N., SANGIOLO, D., BUSSOLINO, F., PIACIBELLO, W. & AGLIETTA, M. (2005) Involvement of chemokine receptor 4/stromal cell-derived factor 1 system during osteosarcoma tumor progression. *Clin Cancer Res,* 11**,** 490-7.

PHIEL, C. J., ZHANG, F., HUANG, E. Y., GUENTHER, M. G., LAZAR, M. A. & KLEIN, P. S. (2001) Histone deacetylase is a direct target of valproic acid, a potent anticonvulsant, mood stabilizer, and teratogen. *J Biol Chem,* 276**,** 36734-41.

PIEDRA, M., GARCIA-UNZUETA, M. T., BERJA, A., PAULE, B., LAVIN, B. A., VALERO, C., RIANCHO, J. A. & AMADO, J. A. (2011) "Single nucleotide polymorphisms of the OPG/RANKL system genes in primary hyperparathyroidism and their relationship with bone mineral density". *BMC Med Genet,* 12**,** 168.

PIVETTA, E., SCAPOLAN, M., WASSERMANN, B., STEFFAN, A., COLOMBATTI, A. & SPESSOTTO, P. (2010) Blood-derived human osteoclast resorption activity is impaired by hyaluronan-CD44 engagement via a p38-dependent mechanism. *J Cell Physiol,* 226**,** 769-779.

PONOMAREV, V., DOUBROVIN, M., SERGANOVA, I., VIDER, J., SHAVRIN, A., BERESTEN, T., IVANOVA, A., AGEYEVA, L., TOURKOVA, V., BALATONI, J., BORNMANN, W., BLASBERG, R. & GELOVANI

TJUVAJEV, J. (2004) A novel triple-modality reporter gene for whole-body fluorescent, bioluminescent, and nuclear noninvasive imaging. *Eur J Nucl Med Mol Imaging,* 31**,** 740-51.

PRINCE, H. M., BISHTON, M. J. & HARRISON, S. J. (2009) Clinical studies of histone deacetylase inhibitors. *Clin Cancer Res,* 15**,** 3958-69.

PRYSTOWSKY, M. B., ADOMAKO, A., SMITH, R. V., KAWACHI, N., MCKIMPSON, W., ATADJA, P., CHEN, Q., SCHLECHT, N. F., PARISH, J. L., CHILDS, G. & BELBIN, T. J. (2009) The histone deacetylase inhibitor LBH589 inhibits expression of mitotic genes causing G2/M arrest and cell death in head and neck squamous cell carcinoma cell lines. *J Pathol,* 218**,** 467-477.

PUREV, E., NEFF, L., HORNE, W. C. & BARON, R. (2009) c-Cbl and Cbl-b act redundantly to protect osteoclasts from apoptosis and to displace HDAC6 from beta-tubulin, stabilizing microtubules and podosomes. *Mol Biol Cell,* 20**,** 4021-30.

QIAN, D. Z., KATO, Y., SHABBEER, S., WEI, Y., VERHEUL, H. M. W., SALUMBIDES, B., SANNI, T., ATADJA, P. & PILI, R. (2006) Targeting Tumour Angiogenesis with Histone deacetylase Inhibitors: the Hydroxamic Acid Derivative LBH589. *Clin Cancer Res,* 12**,** 634-642.

QIAN, D. Z., KATO, Y., SHABBEER, S., WEI, Y., VERHEUL, H. M., SALUMBIDES, B., SANNI, T., ATADJA, P. AND PILI, R. (2006) Targeting tumor angiogenesis with histone deacetylase inhibitors: the hydroxamic acid derivative LBH589. *Clin Cancer Res,* 12**,** 634-42.

QIAN, D. Z., WANG, X., KACHHAP, S. K., KATO, Y., WEI, Y., ZHANG, L., ATADJA, P. & PILI, R. (2004) The histone deacetylase inhibitor NVP-LAQ824 inhibits angiogenesis and has a greater antitumor effect in combination with the vascular endothelial growth factor receptor tyrosine kinase inhibitor PTK787/ZK222584. *Cancer Res,* 64**,** 6626-34.

QIU, L., BURGESS, A., FAIRLIE, D. P., LEONARD, H., PARSONS, P. G. & GABRIELLI, B. G. (2000) Histone deacetylase inhibitors trigger a G2 checkpoint in normal cells that is defective in tumor cells. *Mol Biol Cell,* 11**,** 2069-83.

QIU, L., KELSO, M. J., HANSEN, C., WEST, M. L., FAIRLIE, D. P. & PARSONS, P. G. (1999) Anti-tumour activity in vitro and in vivo of selective differentiating agents containing hydroxamate. *Br J Cancer,* 80**,** 1252-8.

RACHNER, T. D., KHOSLA, S. & HOFBAUER, L. C. (2011) Osteoporosis: now and the future. *Lancet,* 377**,** 1276-87.

RADL, J., CROESE, J. W., ZURCHER, C., VAN DEN ENDEN-VIEVEEN, M. H., BRONDIJK, R. J., KAZIL, M., HAAIJMAN, J. J., REITSMA, P. H. &

BIJVOET, O. L. (1985) Influence of treatment with APD-bisphosphonate on the bone lesions in the mouse 5T2 multiple myeloma. *Cancer,* 55**,** 1030-40.

RAHMAN, M. M., KUKITA, A., KUKITA, T., SHOBUIKE, T., NAKAMURA, T. & KOHASHI, O. (2003) Two histone deacetylase inhibitors, trichostatin A and sodium butyrate, suppress differentiation into osteoclasts but not into macrophages. *Blood,* 101**,** 3451-9.

RANNEY, M. K., AHMED, I. S., POTTS, K. R. & CRAVEN, R. J. (2007) Multiple pathways regulating the anti-apoptotic protein clusterin in breast cancer. *Biochim Biophys Acta,* 1772**,** 1103-11.

RAO, A., LUO, C. & HOGAN, P. G. (1997) Transcription factors of the NFAT family: regulation and function. *Annu Rev Immunol,* 15**,** 707-47.

RAO, R., FISKUS, W., YANG, Y., LEE, P., JOSHI, R., FERNANDEZ, P., MANDAWAT, A., ATADJA, P., BRADNER, J. E. & BHALLA, K. (2008) HDAC6 inhibition enhances 17-AAG--mediated abrogation of hsp90 chaperone function in human leukemia cells. *Blood,* 112**,** 1886-93.

RAO, R., NALLURI, S., KOLHE, R., YANG, Y., FISKUS, W., CHEN, J., HA, K., BUCKLEY, K. M., BALUSU, R., COOTHANKANDASWAMY, V., JOSHI, A., ATADJA, P. & BHALLA, K. N. (2010) Treatment with panobinostat induces glucose-regulated protein 78 acetylation and endoplasmic reticulum stress in breast cancer cells. *Mol Cancer Ther,* 9**,** 942-52.

RAWADI, G., VAYSSIERE, B., DUNN, F., BARON, R. & ROMAN-ROMAN, S. (2003) BMP-2 controls alkaline phosphatase expression and osteoblast mineralization by a Wnt autocrine loop. *J Bone Miner Res,* 18**,** 1842-53.

RICHARDS, J. B., RIVADENEIRA, F., INOUYE, M., PASTINEN, T. M., SORANZO, N., WILSON, S. G., ANDREW, T., FALCHI, M., GWILLIAM, R., AHMADI, K. R., VALDES, A. M., ARP, P., WHITTAKER, P., VERLAAN, D. J., JHAMAI, M., KUMANDURI, V., MOORHOUSE, M., VAN MEURS, J. B., HOFMAN, A., POLS, H. A., HART, D., ZHAI, G., KATO, B. S., MULLIN, B. H., ZHANG, F., DELOUKAS, P., UITTERLINDEN, A. G. & SPECTOR, T. D. (2008) Bone mineral density, osteoporosis, and osteoporotic fractures: a genome-wide association study. *Lancet,* 371**,** 1505-12.

RIGGINS, R. B., SCHRECENGOST, R. S., GUERRERO, M. S. & BOUTON, A. H. (2007) Pathways to tamoxifen resistance. *Cancer Lett,* 256**,** 1-24.

RING, A. & DOWSETT, M. (2004) Mechanisms of tamoxifen resistance. *Endocr Relat Cancer,* 11**,** 643-58.

ROBSON, E. J., KHALED, W. T., ABELL, K. & WATSON, C. J. (2006) Epithelial-to-mesenchymal transition confers resistance to apoptosis in three murine mammary epithelial cell lines. *Differentiation,* 74**,** 254-64.

RODDA, S. J. & MCMAHON, A. P. (2006) Distinct roles for Hedgehog and canonical Wnt signaling in specification, differentiation and maintenance of osteoblast progenitors. *Development,* 133**,** 3231-44.

RODRIGUEZ-GONZALEZ, A., LIN, T., IKEDA, A. K., SIMMS-WALDRIP, T., FU, C. & SAKAMOTO, K. M. (2008) Role of the aggresome pathway in cancer: targeting histone deacetylase 6-dependent protein degradation. *Cancer Res,* 68**,** 2557-60.

ROGERS, M. J. (2003) New insights into the molecular mechanisms of action of bisphosphonates. *Curr Pharm Des,* 9**,** 2643-58.

ROSEN, L. S., GORDON, D., KAMINSKI, M., HOWELL, A., BELCH, A., MACKEY, J., APFFELSTAEDT, J., HUSSEIN, M. A., COLEMAN, R. E., REITSMA, D. J., CHEN, B. L. & SEAMAN, J. J. (2003) Long-term efficacy and safety of zoledronic acid compared with pamidronate disodium in the treatment of skeletal complications in patients with advanced multiple myeloma or breast carcinoma: a randomized, double-blind, multicenter, comparative trial. *Cancer,* 98**,** 1735-44.

ROSEN, L. S., GORDON, D. H., DUGAN, W., JR., MAJOR, P., EISENBERG, P. D., PROVENCHER, L., KAMINSKI, M., SIMEONE, J., SEAMAN, J., CHEN, B. L. & COLEMAN, R. E. (2004) Zoledronic acid is superior to pamidronate for the treatment of bone metastases in breast carcinoma patients with at least one osteolytic lesion. *Cancer,* 100**,** 36-43.

ROSSOUW, J. E., ANDERSON, G. L., PRENTICE, R. L., LACROIX, A. Z., KOOPERBERG, C., STEFANICK, M. L., JACKSON, R. D., BERESFORD, S. A., HOWARD, B. V., JOHNSON, K. C., KOTCHEN, J. M. & OCKENE, J. (2002) Risks and benefits of estrogen plus progestin in healthy postmenopausal women: principal results From the Women's Health Initiative randomized controlled trial. *JAMA,* 288**,** 321-33.

ROTH, S. Y., DENU, J. M. & ALLIS, C. D. (2001) Histone acetyltransferases. *Annu Rev Biochem,* 70**,** 81-120.

ROUX, S. (2010) New treatment targets in osteoporosis. *Joint Bone Spine,* 77**,** 222-8.

RUCCI, N. & TETI, A. (2010) Osteomimicry: how tumor cells try to deceive the bone. *Front Biosci (Schol Ed),* 2**,** 907-15.

RUIZ-CARRILLO, A., WANGH, L. J. & ALLFREY, V. G. (1975) Processing of newly synthesized histone molecules. *Science,* 190**,** 117-28.

SAAD, F. (2002) Treatment of bone complications in advanced prostate cancer: rationale for bisphosphonate use and results of a phase III trial with zoledronic acid. *Semin Oncol,* 29**,** 19-27.

SALARI SHARIF, P., ABDOLLAHI, M. & LARIJANI, B. (2010) Current, new and future treatments of osteoporosis. *Rheumatol Int,* 31**,** 289-300.

SANKAR, U., PATEL, K., ROSOL, T. J. & OSTROWSKI, M. C. (2004) RANKL coordinates cell cycle withdrawal and differentiation in osteoclasts through the cyclin-dependent kinase inhibitors p27KIP1 and p21CIP1. *J Bone Miner Res,* 19**,** 1339-48.

SANO, M., INOUE, S., HOSOI, T., OUCHI, Y., EMI, M., SHIRAKI, M. & ORIMO, H. (1995) Association of estrogen receptor dinucleotide repeat polymorphism with osteoporosis. *Biochem Biophys Res Commun,* 217**,** 378-83.

SATO, A., ASANO, T., HORIGUCHI, A., ITO, K. & SUMITOMO, M. (2011) Antitumor effect of suberoylanilide hydroxamic acid and topotecan in renal cancer cells. *Oncol Res,* 19**,** 217-23.

SAWADA, K., MORISHIGE, K., TAHARA, M., KAWAGISHI, R., IKEBUCHI, Y., TASAKA, K. & MURATA, Y. (2002) Alendronate inhibits lysophosphatidic acid-induced migration of human ovarian cancer cells by attenuating the activation of rho. *Cancer Res,* 62**,** 6015-20.

SCHOENLEIN, P. V., PERIYASAMY-THANDAVAN, S., SAMADDAR, J. S., JACKSON, W. H. & BARRETT, J. T. (2009) Autophagy facilitates the progression of ERalpha-positive breast cancer cells to antiestrogen resistance. *Autophagy,* 5**,** 400-3.

SCHROEDER, T. M., JENSEN, E. D. & WESTENDORF, J. J. (2005) Runx2: a master organizer of gene transcription in developing and maturing osteoblasts. *Birth Defects Res C Embryo Today,* 75**,** 213-25.

SCHROEDER, T. M., KAHLER, R. A., LI, X. & WESTENDORF, J. J. (2004a) Histone Deacetylase 3 Interacts with Runx2 to Repress the Osteocalcin Promoter and Regulate Osteoblast Differentiation. *Journal of Biological Chemistry,* 279**,** 41998-42007.

SCHROEDER, T. M., KAHLER, R. A., LI, X. & WESTENDORF, J. J. (2004b) Histone deacetylase 3 interacts with runx2 to repress the osteocalcin promoter and regulate osteoblast differentiation. *J Biol Chem,* 279**,** 41998-42007.

SCHROEDER, T. M., NAIR, A. K., STAGGS, R., LAMBLIN, A. F. & WESTENDORF, J. J. (2007) Gene profile analysis of osteoblast genes differentially regulated by histone deacetylase inhibitors. *BMC Genomics,* 8**,** 362.

SCHROEDER, T. M. A. & WESTENDORF, J. J. (2005) Histone Deacetylase Inhibitors Promote Osteoblast Maturation. *J of Bone and Mineral Research,* 20**,** 2254-2263.

SCHULTE-HERMANN, R., BURSCH, W., GRASL-KRAUPP, B., MARIAN, B., TOROK, L., KAHL-RAINER, P. & ELLINGER, A. (1997) Concepts of cell death and application to carcinogenesis. *Toxicol Pathol,* 25**,** 89-93.

SCHWARTZ, L. M., SMITH, S. W., JONES, M. E. & OSBORNE, B. A. (1993) Do all programmed cell deaths occur via apoptosis? *Proc Natl Acad Sci U S A,* 90**,** 980-4.

SEMENZA, G. L. (2003) Targeting HIF-1 for cancer therapy. *Nat Rev Cancer,* 3**,** 721-32.

SENARATNE, S. G. & COLSTON, K. W. (2002) Direct effects of bisphosphonates on breast cancer cells. *Breast Cancer Res,* 4**,** 18-23.

SHAO, W., GROWNEY, J. D., FENG, Y., WANG, P., YAN-NEALE, G. & O'CONNOR, G. (2008) Potent anticancer activity of the pan-deacetylase inhibitor panobinostat (LBH589) as a single agent in in vitro and in vivo tumour models. *99th AACR Annual Meeting.* San Diego, CA.

SHAO, Y., GAO, Z., MARKS, P. A. & JIANG, X. (2004) Apoptotic and autophagic cell death induced by histone deacetylase inhibitors. *Proc Natl Acad Sci U S A,* 101**,** 18030-5.

SHENOLIKAR, S., VOLTZ, J. W., MINKOFF, C. M., WADE, J. B. & WEINMAN, E. J. (2002) Targeted disruption of the mouse NHERF-1 gene promotes internalization of proximal tubule sodium-phosphate cotransporter type IIa and renal phosphate wasting. *Proc Natl Acad Sci U S A,* 99**,** 11470-5.

SHI, Y. K., LI, Z. H., HAN, X. Q., YI, J. H., WANG, Z. H., HOU, J. L., FENG, C. R., FANG, Q. H., WANG, H. H., ZHANG, P. F., WANG, F. S., SHEN, J. & WANG, P. (2010) The histone deacetylase inhibitor suberoylanilide hydroxamic acid induces growth inhibition and enhances taxol-induced cell death in breast cancer. *Cancer Chemother Pharmacol,* 66**,** 1131-40.

SHIH, M. S., COOK, M. A., SPENCE, C. A., PALNITKAR, S., MCELROY, H. & PARFITT, A. M. (1993) Relationship between bone formation rate and osteoblast surface on different subdivisions of the endosteal envelope in aging & osteoporosis. *Bone,* 14**,** 519-21.

SHIMIZU, E., SELVAMURUGAN, N., WESTENDORF, J. J., OLSON, E. N. & PARTRIDGE, N. C. (2010) HDAC4 represses matrix metalloproteinase-13 transcription in osteoblastic cells, and parathyroid hormone controls this repression. *J Biol Chem,* 285**,** 9616-26.

SHIPMAN, C. M., VANDERKERKEN, K., ROGERS, M. J., LIPPITT, J. M., ASOSINGH, K., HUGHES, D. E., VAN CAMP, B., RUSSELL, R. G. & CROUCHER, P. I. (2000) The potent bisphosphonate ibandronate does not induce myeloma cell apoptosis in a murine model of established multiple myeloma. *Br J Haematol,* 111**,** 283-6.

SIKANDAR, S., DIZON, D., SHEN, X., LI, Z., BESTERMAN, J. & LIPKIN, S. M. (2010) The class I HDAC inhibitor MGCD0103 induces cell cycle arrest and apoptosis in colon cancer initiating cells by upregulating Dickkopf-1 and non-canonical Wnt signaling. *Oncotarget,* 1**,** 596-605.

SINGH, S. K., DOBES, S., SINGH, G., KOENIG, A. O., REUTLINGER, K., HOFBAUER, L. C., BARTH, P., GRESS, T. M., LOMBERK, G., URRUTIA, R., FERNANDEZ-ZAPICO, M. E. & ELLENRIEDER, V. (2011) Disruption of a nuclear NFATc2 stabilization loop confers breast and pancreatic cancer growth supression by zoledronic acid. *J Biol Chem,* 286**,** 28761-28771.

SMITH, E. & FRENKEL, B. (2005) Glucocorticoids inhibit the transcriptional activity of LEF/TCF in differentiating osteoblasts in a glycogen synthase kinase-3beta-dependent and -independent manner. *J Biol Chem,* 280**,** 2388-94.

SONG, W., TAI, Y. T., TIAN, Z., HIDESHIMA, T., CHAUHAN, D., NANJAPPA, P., EXLEY, M. A., ANDERSON, K. C. & MUNSHI, N. C. (2011) HDAC inhibition by LBH589 affects the phenotype and function of human myeloid dendritic cells. *Leukemia,* 25**,** 161-8.

STEINER, R. D., PEPIN, M. G. & BYERS, P. H. (1993) Osteogenesis Imperfecta. *GeneReviews (Internet),* University of Washington, Seattle.

STYRKARSDOTTIR, U., HALLDORSSON, B. V., GRETARSDOTTIR, S., GUDBJARTSSON, D. F., WALTERS, G. B., INGVARSSON, T., JONSDOTTIR, T., SAEMUNDSDOTTIR, J., CENTER, J. R., NGUYEN, T. V., BAGGER, Y., GULCHER, J. R., EISMAN, J. A., CHRISTIANSEN, C., SIGURDSSON, G., KONG, A., THORSTEINSDOTTIR, U. & STEFANSSON, K. (2008) Multiple genetic loci for bone mineral density and fractures. *N Engl J Med,* 358**,** 2355-65.

SUN, P., XIONG, H., KIM, T. H., REN, B. & ZHANG, Z. (2006) Positive inter-regulation between beta-catenin/T cell factor-4 signaling and endothelin-1 signaling potentiates proliferation and survival of prostate cancer cells. *Mol Pharmacol,* 69**,** 520-31.

SUZUKI, J., CHEN, Y. Y., SCOTT, G. K., DEVRIES, S., CHIN, K., BENZ, C. C., WALDMAN, F. M. & HWANG, E. S. (2009) Protein acetylation and histone deacetylase expression associated with malignant breast cancer progression. *Clin Cancer Res,* 15**,** 3163-71.

TAICHMAN, R. S., COOPER, C., KELLER, E. T., PIENTA, K. J., TAICHMAN, N. S. & MCCAULEY, L. K. (2002) Use of the stromal cell-derived factor-1/CXCR4 pathway in prostate cancer metastasis to bone. *Cancer Res,* 62**,** 1832-7.

TAKADA, Y., GILLENWATER, A., ICHIKAWA, H. & AGGARWAL, B. B. (2006) Suberoylanilide Hydroxamic Acid Potentiates Apoptosis, Inhibits Invasion, and Abolishes Osteoclastogenesis by Suppressing Nuclear Factor-kB Activation. *J of Biological Chemistry,* 281**,** 5612-5622.

TAKAYANAGI, H., KIM, S., KOGA, T., NISHINA, H., ISSHIKI, M., YOSHIDA, H., SAIURA, A., ISOBE, M., YOKOCHI, T., INOUE, J., WAGNER, E. F., MAK, T. W., KODAMA, T. & TANIGUCHI, T. (2002) Induction and activation of the transcription factor NFATc1 (NFAT2) integrate RANKL signaling in terminal differentiation of osteoclasts. *Dev Cell,* 3**,** 889-901.

TANABE, N., WHEAL, B. D., KWON, J., CHEN, H. H., SHUGG, R. P., SIMS, S. M., GOLDBERG, H. A. & DIXON, S. J. (2011) Osteopontin signals through Calcium-NFAT in osteoclasts: A novel RGD-dependent pathway promoting cell survival. *J Biol Chem,* 286**,** 39871-39881.

THAI LE, M., LABRINIDIS, A., HAY, S., LIAPIS, V., BOURALEXIS, S., WELLDON, K., COVENTRY, B. J., FINDLAY, D. M. & EVDOKIOU, A. (2006) Apo2l/Tumor necrosis factor-related apoptosis-inducing ligand prevents breast cancer-induced bone destruction in a mouse model. *Cancer Res,* 66**,** 5363-70.

THERIAULT, R. L., LIPTON, A., HORTOBAGYI, G. N., LEFF, R., GLUCK, S., STEWART, J. F., COSTELLO, S., KENNEDY, I., SIMEONE, J., SEAMAN, J. J., KNIGHT, R. D., MELLARS, K., HEFFERNAN, M. & REITSMA, D. J. (1999) Pamidronate reduces skeletal morbidity in women with advanced breast cancer and lytic bone lesions: a randomized, placebo-controlled trial. Protocol 18 Aredia Breast Cancer Study Group. *J Clin Oncol,* 17**,** 846-54.

THIAGALINGAM, S., CHENG, K. H., LEE, H. J., MINEVA, N., THIAGALINGAM, A. & PONTE, J. F. (2003) Histone deacetylases: unique players in shaping the epigenetic histone code. *Ann N Y Acad Sci,* 983**,** 84-100.

TOMAO, F., SPINELLI, G., VICI, P., PISANELLI, G. C., CASCIALLI, G., FRATI, L., PANICI, P. B. & TOMAO, S. (2011) Current role and safety profile of aromatase inhibitors in early breast cancer. *Expert Rev Anticancer Ther,* 11**,** 1253-63.

TOMASKOVIC-CROOK, E., THOMPSON, E. W. & THIERY, J. P. (2009) Epithelial to mesenchymal transition and breast cancer. *Breast Cancer Res,* 11**,** 213.

TOMITA, Y., MARCHENKO, N., ERSTER, S., NEMAJEROVA, A., DEHNER, A., KLEIN, C., PAN, H., KESSLER, H., PANCOSKA, P. & MOLL, U. M. (2006)

WT p53, but not tumor-derived mutants, bind to Bcl2 via the DNA binding domain and induce mitochondrial permeabilization. *J Biol Chem,* 281**,** 8600-6.

TRINKAUS, M., OOI, W. S., AMIR, E., POPOVIC, S., KALINA, M., KAHN, H., SINGH, G., GAINFORD, M. C. & CLEMONS, M. (2009) Examination of the mechanisms of osteolysis in patients with metastatic breast cancer. *Oncol Rep,* 21**,** 1153-9.

TRIVEDI, R., GOSWAMI, R. & CHATTOPADHYAY, N. (2010) Investigational anabolic therapies for osteoporosis. *Expert Opin Investig Drugs,* 19**,** 995-1005.

TSE, C., SERA, T., WOLFFE, A. P. & HANSEN, J. C. (1998) Disruption of higher-order folding by core histone acetylation dramatically enhances transcription of nucleosomal arrays by RNA polymerase III. *Mol Cell Biol,* 18**,** 4629-38.

TSUKAMOTO, K., ORIMO, H., HOSOI, T., MIYAO, M., YOSHIDA, H., WATANABE, S., SUZUKI, T. & EMI, M. (2000) Association of bone mineral density with polymorphism of the human matrix Gla protein locus in elderly women. *J Bone Miner Metab,* 18**,** 27-30.

VAN BEEK, E., PIETERMAN, E., COHEN, L., LOWIK, C. & PAPAPOULOS, S. (1999) Farnesyl pyrophosphate synthase is the molecular target of nitrogen-containing bisphosphonates. *Biochem Biophys Res Commun,* 264**,** 108-11.

VAN BEZOOIJEN, R. L., SVENSSON, J. P., EEFTING, D., VISSER, A., VAN DER HORST, G., KARPERIEN, M., QUAX, P. H., VRIELING, H., PAPAPOULOS, S. E., TEN DIJKE, P. & LOWIK, C. W. (2007) Wnt but not BMP signaling is involved in the inhibitory action of sclerostin on BMP-stimulated bone formation. *J Bone Miner Res,* 22**,** 19-28.

VAN POZNAK, C. H., TEMIN, S., YEE, G. C., JANJAN, N. A., BARLOW, W. E., BIERMANN, J. S., BOSSERMAN, L. D., GEOGHEGAN, C., HILLNER, B. E., THERIAULT, R. L., ZUCKERMAN, D. S. & VON ROENN, J. H. (2011) American Society of Clinical Oncology executive summary of the clinical practice guideline update on the role of bone-modifying agents in metastatic breast cancer. *J Clin Oncol,* 29**,** 1221-7.

VEGA, R. B., MATSUDA, K., OH, J., BARBOSA, A. C., YANG, X., MEADOWS, E., MCANALLY, J., POMAJZL, C., SHELTON, J. M., RICHARDSON, J. A., KARSENTY, G. & OLSON, E. N. (2004) Histone deacetylase 4 controls chondrocyte hypertrophy during skeletogenesis. *Cell,* 119**,** 555-66.

VIGUSHIN, D. M., ALI, S., PACE, P. E., MIRSAIDI, N., ITO, K., ADCOCK, I. & COOMBES, R. C. (2001) Trichostatin A is a histone deacetylase inhibitor with potent antitumor activity against breast cancer in vivo. *Clin Cancer Res,* 7**,** 971-6.

VINCENT, C., FINDLAY, D. M., WELLDON, K. J., WIJENAYAKA, A. R., ZHENG, T. S., HAYNES, D. R., FAZZALARI, N. L., EVDOKIOU, A. & ATKINS, G. J. (2009) Pro-inflammatory cytokines TNF-related weak inducer of apoptosis (TWEAK) and TNFalpha induce the mitogen-activated protein kinase (MAPK)-dependent expression of sclerostin in human osteoblasts. *J Bone Miner Res,* 24**,** 1434-49.

VOELTER-MAHLKNECHT, S., HO, A. D. & MAHLKNECHT, U. (2005) Chromosomal organization and localization of the novel class IV human histone deacetylase 11 gene. *Int J Mol Med,* 16**,** 589-98.

WANG, C., FU, M., MANI, S., WADLER, S., SENDEROWICZ, A. M. & PESTELL, R. G. (2001) Histone acetylation and the cell-cycle in cancer. *Front Biosci,* 6**,** D610-29.

WATANABE, M., ADACHI, S., MATSUBARA, H., IMAI, T., YUI, Y., MIZUSHIMA, Y., HIRAUMI, Y., WATANABE, K., KAMITSUJI, Y., TOYOKUNI, S. Y., HOSOI, H., SUGIMOTO, T., TOGUCHIDA, J. & NAKAHATA, T. (2009) Induction of autophagy in malignant rhabdoid tumor cells by the histone deacetylase inhibitor FK228 through AIF translocation. *Int J Cancer,* 124**,** 55-67.

WEI, Y., KADIA, T., TONG, W., ZHANG, M., JIA, Y., YANG, H., HU, Y., VIALLET, J., O'BRIEN, S. & GARCIA-MANERO, G. (2010) The combination of a histone deacetylase inhibitor with the BH3-mimetic GX15-070 has synergistic antileukemia activity by activating both apoptosis and autophagy. *Autophagy,* 6.

WESTENDORF, J. J., KAHLER, R. A. & SCHROEDER, T. M. (2004) Wnt signaling in osteoblasts and bone diseases. *Gene,* 341**,** 19-39.

WHO http://www.who.int/en/.

WIJENAYAKA, A. R., KOGAWA, M., LIM, H. P., BONEWALD, L. F., FINDLAY, D. M. & ATKINS, G. J. (2011) Sclerostin stimulates osteocyte support of osteoclast activity by a RANKL-dependent pathway. *PLoS One,* 6**,** e25900.

WILSON, A. J., BYUN, D. S., POPOVA, N., MURRAY, L. B., L'ITALIEN, K., SOWA, Y., ARANGO, D., VELCICH, A., AUGENLICHT, L. H. & MARIADASON, J. M. (2006) Histone deacetylase 3 (HDAC3) and other class I HDACs regulate colon cell maturation and p21 expression and are deregulated in human colon cancer. *J Biol Chem,* 281**,** 13548-58.

WON, J., YIM, J. & KIM, T. K. (2002) Sp1 and Sp3 recruit histone deacetylase to repress transcription of human telomerase reverse transcriptase (hTERT) promoter in normal human somatic cells. *J Biol Chem,* 277**,** 38230-8.

WU, P., TIAN, Y., CHEN, G., WANG, B., GUI, L., XI, L., MA, X., FANG, Y., ZHU, T., WANG, D., MENG, L., XU, G., WANG, S., MA, D. & ZHOU, J. (2009) Ubiquitin B: an essential mediator of trichostatin A-induced tumor-selective killing in human cancer cells. *Cell Death Differ,* 17**,** 109-118.

WUTZL, A., EISENMENGER, G., HOFFMANN, M., CZERNY, C., MOSER, D., PIETSCHMANN, P., EWERS, R. & BAUMANN, A. (2006) Osteonecrosis of the jaws and bisphosphonate treatment in cancer patients. *Wien Klin Wochenschr,* 118**,** 473-8.

YACCOBY, S., LING, W., ZHAN, F., WALKER, R., BARLOGIE, B. & SHAUGHNESSY, J. D., JR. (2007) Antibody-based inhibition of DKK1 suppresses tumor-induced bone resorption and multiple myeloma growth in vivo. *Blood,* 109**,** 2106-11.

YANG, Y., RAO, R., SHEN, J., TANG, Y., FISKUS, W., NECHTMAN, J., ATADJA, P. & BHALLA, K. (2008) Role of acetylation and extracellular location of heat shock protein 90alpha in tumor cell invasion. *Cancer Res,* 68**,** 4833-42.

YI, T., BAEK, J. H., KIM, H. J., CHOI, M. H., SEO, S. B., RYOO, H. M., KIM, G. S. & WOO, K. M. (2007) Trichostatin A-mediated upregulation of p21(WAF1) contributes to osteoclast apoptosis. *Exp Mol Med,* 39**,** 213-21.

YIN, L., LAEVSKY, G. & GIARDINA, C. (2001) Butyrate suppression of colonocyte NF-kappa B activation and cellular proteasome activity. *J Biol Chem,* 276**,** 44641-6.

YONEDA, T., WILLIAMS, P. J., HIRAGA, T., NIEWOLNA, M. & NISHIMURA, R. (2001) A bone-seeking clone exhibits different biological properties from the MDA-MB-231 parental human breast cancer cells and a brain-seeking clone in vivo and in vitro. *J Bone Miner Res,* 16**,** 1486-95.

YOSHIDA, M., KIJIMA, M., AKITA, M. & BEPPU, T. (1990) Potent and specific inhibition of mammalian histone deacetylase both in vivo and in vitro by trichostatin A. *J Biol Chem,* 265**,** 17174-9.

YOSHIDA, M., NOMURA, S. & BEPPU, T. (1987) Effects of trichostatins on differentiation of murine erythroleukemia cells. *Cancer Res,* 47**,** 3688-91.

YU, F., YAO, H., ZHU, P., ZHANG, X., PAN, Q., GONG, C., HUANG, Y., HU, X., SU, F., LIEBERMAN, J. & SONG, E. (2007) let-7 regulates self renewal and tumorigenicity of breast cancer cells. *Cell,* 131**,** 1109-23.

YUE, W., FAN, P., WANG, J., LI, Y. & SANTEN, R. J. (2007) Mechanisms of acquired resistance to endocrine therapy in hormone-dependent breast cancer cells. *J Steroid Biochem Mol Biol,* 106**,** 102-10.

ZANNETTINO, A. C., RAYNER, J. R., ASHMAN, L. K., GONDA, T. J. & SIMMONS, P. J. (1996) A powerful new technique for isolating genes encoding cell surface antigens using retroviral expression cloning. *J Immunol,* 156**,** 611-20.

ZHANG, L., WANG, G., WANG, L., SONG, C., LENG, Y., WANG, X. & KANG, J. (2011) VPA inhibits breast cancer cell migration by specifically targeting HDAC2 and down-regulating Survivin. *Mol Cell Biochem,* 361**,** 39-45.

ZHANG, N., HARTIG, H., DZHAGALOV, I., DRAPER, D. & HE, Y. W. (2005a) The role of apoptosis in the development and function of T lymphocytes. *Cell Res,* 15**,** 749-69.

ZHANG, Y., ADACHI, M., KAWAMURA, R. & IMAI, K. (2006a) Bmf is a possible mediator in histone deacetylase inhibitors FK228 and CBHA-induced apoptosis. *Cell Death Differ,* 13**,** 129-40.

ZHANG, Y., ADACHI, M., KAWAMURA, R., ZOU, H. C., IMAI, K., HAREYAMA, M. & SHINOMURA, Y. (2006b) Bmf contributes to histone deacetylase inhibitor-mediated enhancing effects on apoptosis after ionizing radiation. *Apoptosis,* 11**,** 1349-57.

ZHANG, Z., YAMASHITA, H., TOYAMA, T., SUGIURA, H., ANDO, Y., MITA, K., HAMAGUCHI, M., HARA, Y., KOBAYASHI, S. & IWASE, H. (2005b) Quantitation of HDAC1 mRNA expression in invasive carcinoma of the breast*. *Breast Cancer Res Treat,* 94**,** 11-6.

ZHANG, Z., YAMASHITA, H., TOYAMA, T., SUGIURA, H., OMOTO, Y., ANDO, Y., MITA, K., HAMAGUCHI, M., HAYASHI, S. & IWASE, H. (2004) HDAC6 expression is correlated with better survival in breast cancer. *Clin Cancer Res,* 10**,** 6962-8.

ZHANG, Z. K., DAVIES, K. P., ALLEN, J., ZHU, L., PESTELL, R. G., ZAGZAG, D. & KALPANA, G. V. (2002) Cell cycle arrest and repression of cyclin D1 transcription by INI1/hSNF5. *Mol Cell Biol,* 22**,** 5975-88.

ZHAO, Y., TAN, J., ZHUANG, L., JIANG, X., LIU, E. T. & YU, Q. (2005) Inhibitors of histone deacetylases target the Rb-E2F1 pathway for apoptosis induction through activation of proapoptotic protein Bim. *Proc Natl Acad Sci U S A,* 102**,** 16090-5.

ZHOU, Q., AGOSTON, A. T., ATADJA, P., NELSON, W. G. & DAVIDSON, N. E. (2008) Inhibition of histone deacetylases promotes ubiquitin-dependent proteasomal degradation of DNA methyltransferase 1 in human breast cancer cells. *Mol Cancer Res,* 6**,** 873-83.

ZHOU, Q., ATADJA, P. & DAVIDSON, N. E. (2007a) Histone Deacetylase Inhibitor LBH589 Reactivates Silenced Estrogen Receptor Alpha (ER) Gene Expression without Loss of DNA Hypermethylation. *Cancer Biol Ther,* 6**,** 64-69.

ZHOU, Q., DALGARD, C. L., WYNDER, C. & DOUGHTY, M. L. (2011) Histone deacetylase inhibitors SAHA and sodium butyrate block G1-to-S cell cycle progression in neurosphere formation by adult subventricular cells. *BMC Neurosci,* 12**,** 50.

ZHOU, Y., YAU, C., GRAY, J. W., CHEW, K., DAIRKEE, S. H., MOORE, D. H., EPPENBERGER, U., EPPENBERGER-CASTORI, S. & BENZ, C. C. (2007b) Enhanced NF kappa B and AP-1 transcriptional activity associated with antiestrogen resistant breast cancer. *BMC Cancer,* 7**,** 59.

ZINONOS, I., LABRINIDIS, A., LEE, M., LIAPIS, V., HAY, S., PONOMAREV, V., DIAMOND, P., ZANNETTINO, A. C., FINDLAY, D. M. & EVDOKIOU, A. (2009) Apomab, a fully human agonistic antibody to DR5, exhibits potent antitumor activity against primary and metastatic breast cancer. *Mol Cancer Ther,* 8**,** 2969-80.